Bogdan Ovidiu Varga
Calin Iclodean
Florin Mariasiu

Electric and Hybrid Buses for Urban Transport

Energy Efficiency Strategies

Springer

Green Energy and Technology

Bogdan Ovidiu Varga · Calin Iclodean
Florin Mariasiu

Electric and Hybrid Buses for Urban Transport

Energy Efficiency Strategies

Bogdan Ovidiu Varga
Department of Automotive Engineering
  and Transports
Technical University of Cluj-Napoca
Cluj-Napoca
Romania

Calin Iclodean
Department of Automotive Engineering
  and Transports
Technical University of Cluj-Napoca
Cluj-Napoca
Romania

Florin Mariasiu
Department of Automotive Engineering
  and Transports
Technical University of Cluj-Napoca
Cluj-Napoca
Romania

Foreword

Nowadays, the urban transport is one of the most challenging areas of research in terms of timing, efficiency, transport capacity, and nevertheless pollution reduction.

Electrification of the urban transport is not a new approach, but the technologies used these days are. Electric urban transport without the limitation of the tram tracks and the electric lines of the trolleybus becomes one of the most attractive present solution in terms of efficiency, coverage, and versatility taking into account the fixed specific tracks of the urban transport.

The solutions presented in this book in terms of strategies for usage of the electric and hybrid urban buses for designated urban arrears, it is based on a complete approach that there is on the scientific agenda nowadays.

I dare to say that by using the solution of energetic efficiency for specific electric and hybrid urban buses any local community can develop its own solution taking into account the fact that the authors have provided a virtual solution for specific road infrastructure development, for electric and hybrid power train configuration, and for various charging and load capacities.

The amount of technicalities in this book will offer automotive and road traffic engineers a clear perspective of what is expected to take into consideration in case of making a decision in terms of electrification of their specific coordinated transport infrastructure.

All the data represented by the specific study of the book is presented in terms of charts and graphs as common language for all engineers. The language is clear and concise giving to the reader a simple and concise answer to the questions resulting for the studied topic.

I recommend this book to all those to find a proper solution related to the topic of reliability of the electric urban transport supported by urban buses.

April 2016

Felix Pfister
Product and Business Development Manager
Department of Instrumentation and Test Systems
AVL LIST GMBH

Acknowledgments

The writing process of this book consumed huge amount of work, research and documentation, but in the end, the effort is dedicated to those who are interested (students, researchers, professional engineers) in applicative use of advanced modeling and simulation technologies for the optimization of energy efficiency in automotive electric and hybrid power trains.

First of all we are deeply grateful to AVL LIST GmbH, A-8020 Graz, Hans-List-Platz 1 (www.avl.com) for their essential logistic support, availability, and also for provision of their high-level professional expertise and technical support in the writing process of the book. Their advices definitively increase the scientific and applicative quality of book.

Nevertheless, we would like to thank IPG Automotive GmbH, D-76185 Karlsruhe, Bannwaldallee 60, (www.ipg-automotive.com) for their essential logistic support, availability, and also for provision of their high-level professional expertise and technical support in the writing process of the book.

At the end but not last, we would like to express our gratitude toward our families for their support, understanding and encouragement, which helped us permanently throughout the preparation of the book.

<div align="right">

Bogdan Ovidiu Varga
Calin Iclodean
Florin Mariasiu

</div>

Contents

Abbreviations

4WD	Four Wheel Drive
ABS	Anti-lock Braking System
AC	Alternating Current
ACC	Autonomous Cruise Control
ADAS	Advanced Driver Assistance Systems
AMT	Automated Manual Transmission
ARB	Anti-Roll Bar
ASC	Anti-Slip Control
ASM	Asynchronous Motor
AVL	Anstalt für Verbrennungskraftmaschinen List
BEV	Battery Electric Vehicle
BMEP	Brake Mean Effective Pressure
CACSD	Computer-Aided Control Systems Design
CIT	CarMaker Interface Toolbox
CNG	Compressed Natural Gas
CTF	Concerto Transport File
CTP	Compania de Transport Public (in Roumanian)
DAS	Driving Assistance Sensor
DC	Direct Current
DLL	Dynamic Link Library
DVA	Direct Variable Access
EC	European Commission
ECU	Electronic Control Unit
EPS	Electric Power Steering
ESC	Electronic Stability Control
ESP	Electronic Stability Program
EU	European Union
EV	Electric Vehicle
FDU	Final Drive Unit
FMEP	Friction Mean Effective Pressure

FSS	Free-Space Sensor
FWD	Front Wheel Drive
GHG	GreenHouse Gas emissions
GIS	Geographic Information System
GPS	Global Positioning System
GPX	GPS eXchange Format
GUI	Graphic User Interface
HEV	Hybrid Electric Vehicle
HIL	Hardware in the Loop
HTML	HyperText Markup Language
ICE	Internal Combustion Engine
iFD	Ratio of Final Drive
iTR	Ratio of Final Transmission
KML	Keyhole Markup Language
LCC	Life Cost Cycle
OSM	OpenStreetMap
PHEV	Plug-in Hybrid Electric Vehicle
PID	Proportional Integral Derivative
PM	Particulate Matter
PNG	Portable Network Graphics
PSM	Permanent Synchronous Motor
REV	Range Extender Vehicle
RT	Real Time
SAM	System Analysis Mode
SIL	Software in the Loop
SOC	State of Charge
SRM	Switched Reluctance Motor
SRT	Single Ratio Transmission
TC	TurboCharger
TFM	Transversal Flux Motor
TIT	TruckMaker Interface Toolbox
TSS	Traffic Sign Sensor
UTM	Universal Time Measurement
VD	Virtual Driver
VE	Vehicle Editor
VR	Virtual Road
VV	Virtual Vehicle
VVE	Virtual Vehicle Environment
XML	eXtensible Markup Language

Chapter 1
Introduction

In the contemporary period of the development of human society the migration process of the people towards the urban environment is a dynamic one, recording increases from year to year. Thus appears a tendency of metropolitanization of urban centers with known advantages and disadvantages [1–5]. The public transportation system is an important component in maintaining the sustainable character of the urban development, because it represents the main means of transport for citizens. Besides the main function of assuring the mobility, the urban transportation system must also offer efficiency, versatility, intermodality, comfort, etc.

A great percentage of the common means of transport which compose the urban transport system use as main energy source the internal combustion engine. The internal combustion engine offers easiness and versatility while operating, but because of the specific processes of fuel combustion and transformation of chemical energy contained by it in mechanical work, it also emits pollutant gases into the atmosphere [6, 7].

The pollutant gases have a negative effect on the environment and the health of the people (citizens). It is well known that the transportation domain is (generally) responsible for the emission of approximately 13 % of the greenhouse gases (GHG) at a European level [8]. Because of this major cause, laws and norms regarding the reduction of pollutant emissions (EURO pollution norms) are permanently adopted across the European Union.

Within the urban transportation system there are means of transport which use as energy source the internal combustion engine. They have the generic name of "buses" and are destined to either transport people on relatively short distances within the urban traffic or for creating the necessary connections with the peripheries of the metropolitan areas or with other metropolitan areas.

Even though for a short period one of the solutions for reducing the pollutant gases emitted in the atmosphere by the buses is the usage of biofuel mixes (because of their renewable character), there are numerous limitations regarding the harmful effects of using these biofuels [9, 10].

From this point of view there are many studies that prove that using a mix of fossil fuels and a higher percentage of biofuels leads to an increase of NO_x emissions. Although in this case there is a reduction of particle emissions (PM), the latter can cause serious health issues [11–13].

Moreover there are studies which have emphasized that the PM emissions can contain toxic compounds with a cancerous character [14].

From this point of view, the classic buses which exist and are operated in urban traffic do not meet the more and more strict criteria, which are:

- to reduce the levels of noise and to improve the air quality, according to the obligations imposed through the EU directives;
- to reduce the CO_2 emissions created by the classic buses with internal combustion engines;
- to reduce the exploitation of conventional energy resources obtained from fossil fuels.

The replacement of classic diesel engine buses with hybrid and electric buses is necessary on the strength of the legislation promoted by the EU, more precisely the 443/23rd of April 2009 Regulation which regards the reduction of emission coming from vehicles and which imposes limitations for CO_2 emissions (130 g CO_2/km up until 2015, respectively 95 g CO_2/km up until 2020, as opposed to 150 g CO_2/km which is imposed for the present) [15].

A technological method which is at hand is replacing the energy source of the means of transportation for people, which is based on using an internal combustion engine, with an energy source which uses electric energy. Thus at a local level of utilization of these sources, the pollution with pollutant emissions can be completely eliminated.

However, due to some market factors there is still little availability of integrating these means of transport in the urban transportation system. Some of the penetration barriers for the auto market [16] are: the initial investment cost, the travel autonomy, the problems regarding the duration of exploitation of the electric battery, the global benefit over the environment, the insufficiently developed technologies for efficient reconditioning of the batteries and the insufficient support measures for the authorities.

Despite the arguments presented previously, globally many researches and trials to implement electric buses in the urban transport system have started and the main reason is eliminating the pollutant emissions and increasing the safety and health level of the citizens.

Globally there are towns which have started using electric and/or hybrid buses. The New York, Beijing, Winchester, Vienna and Madrid public passenger transportation systems use these modern and nonpolluting means of transport on one or more transport routes.

Because presently the costs associated with the integration of electric buses within the urban transport system are relatively high it is necessary to perform studies and researches to offer the best solution in relation to their optimal usage,

taking into consideration the particularities required by the characteristics of the transport infrastructure (the length of routes, the flux of passengers, the creation of a specific loading infrastructure, road gradient, traffic volume, temperature of the environment, seasonality and loading degree).

Thus the performance in exploitation of an electric bus is different from case to case, depending on the particularities of the urban transport system, specific for each city.

An important factor which directly influences the (servicing) travelling autonomy of the electric bus is its weight. This exploitation parameter is made of two well-defined sub-ensembles: the weight of the transported passengers (variable) and the weight of the batteries which are the energy source (constant). If the weight of the passengers can be determined through experimental studies (analysis regarding the density of passenger flow depending on the exploitation seasonality), the weight of the batteries remains a constant value, being a factor imposed (predetermined) by the version chosen by the manufacturer and the beneficiary.

Up until recently the acquisition and utilization prices of a battery which can offer a high energetic efficiency in the exploitation of an urban bus were relatively high. In a recent study made by Nykvist and Nilsson, published in 2015, the authors analyzed the production prices of a battery with Li-ion accumulators. The presented fact is that the prices of these batteries have fallen from over 1.000 $/kWh to almost 410 $/kWh (the period taken into consideration for the study was between the years 2007–2014) [17]. Moreover, one of the conclusions of the study demonstrated that the production costs for such an accumulator (Li-ion technology) would rise to 150 $/kWh, this value is considered to be the turning point for large-scale commercialization of electric battery vehicles and their successful integration in the contemporary transport system.

This book presents a research study accomplished in the particular case of integration optimization for electric buses in the urban passenger transport system of Cluj-Napoca municipality (Transylvania region, Romania).

According to the data from the Public Transport Company (Compania de Transport Public S.A.—CTP) from Cluj-Napoca, presently within the company auto park there are approximately 252 buses, from which 120 of them are used within a working day (respectively only 60 buses within a weekend day). These buses use 42 routes with a total length of 100 km and assure the transportation of 60 % of the total passenger number [18].

The buses used in Cluj-Napoca municipality within the public transport system are equipped with classic engines which respect the pollution norms: EURO 0, EURO 2, EURO 3 and EURO 5.

The necessity and opportunity of making this research study has resulted in the following considerations:

- an optimized integration of the electric buses from the point of view of the energetic efficiency and of the costs associated with them within the urban passenger transportation system;

- the insurance of the lowest possible values for pollutant emissions (locally zero), according to the norms regarding these values;
- the assurance of comfort for the transported passengers;
- the implementation of new innovative solutions in the urban passenger transportation domain;
- a decreased level of CO_2 emissions generated by the urban public transportation, on the strength of a high efficiency via a suitable energetic management specific for hybrid and electric vehicles, as opposed to the ones with a classic drive system;
- a decreased level of noise, vibrations and an improvement in air quality, to meet the obligations imposed through the present EU norms and regulations;
- a decreased national dependency to primary energy resources and resources obtained from fossil fuels.

The general objective of the research is to identify ideal routes to be followed by the buses equipped with the hybrid Plug-in energy source and the electric ones, in order to save a maximum of energy and to retrieve energy (with respect to the specific running conditions), to expand the travelled distance and to make these vehicles equipped with alternative drive systems more energetically efficient [19].

The routes presently identified as being the most economic ones referring to the vehicles equipped with classic drive systems are significantly different from the exploitation concept in a maximum energetic efficiency regime, corroborated with the recovery of kinetic energy, which is one of the basic principles for the concepts of a hybrid or electric drive group implicitly supporting their autonomy.

In general the algorithm for conducting such a study consists of the following general steps:

- identification of the current state of knowledge in the field of energetic efficiency management of vehicles equipped with hybrid and electric drive systems for the urban public passenger transportation;
- deign and simulation of different drive systems depending on the characteristics of the urban passenger transportation routes;
- verification and validation of the results;
- identification of the optimal solution for the drive system and route on which the determination will be locally made;
- determination of the impact over the local environment from an economical-social point of view;
- presentation of the general conclusions drawn after analyzing the results.

To achieve the target objectives of this research study, the used methodology takes into consideration three important general courses of action:

- establishing the complete architecture of the hybrid drive system based on the eligible cinematic drafts;
- choosing the type of electric motor and its characteristics based on the design, modeling and simulation studies;

- creating a simulation route in the AVL CRUISE and AVL CONCERTO™ with AVL Road Importer application pack, based on the type of drive system chosen and the real/specific conditions of Cluj-Napoca municipality;
- developing and optimizing the route based on the studies regarding the developed energy flows.

The methodology of the experimental research will be based on a system made of methods, procedures, techniques, principles and instruments used within the process of achieving the desiderata pursued through the research study. The manner of organization and planning of the study according to the proposed objectives implies organizing the scientific research in many unitary structured steps (from the premise up until the achievement of the desired goals) by going through the intermediary phases of concept, modelling, simulation, optimization and implementation of the hybrid and electric drive system.

One of the main components of the research methodology is the modeling-simulation software application pack AVL CRUISE and AVL CONCERTO^{TM} with the AVL Road Importer interface. This flexible application pack can simulate any type of hybrid or electric drive system architecture in conditions of real traffic. Based on the strategies developed and analyzed through computer simulation for obtaining the proposed goals, eligible technical solution sets will be obtained which will be used in the hybrid and electric drive system architecture implementation. The modeling-simulation software pack will use the capacities of each application to analyze unitarily each architecture model eligible for designing and dimensioning the hybrid and electric drive systems.

Another important chapter of the research methodology is represented by a multi and inter-disciplinary approach within the domain regarding the control and management characteristics of the hybrid and electric drive systems for the integration of the control algorithms within the design, and respectively the simulation and implementation of these algorithms in the management system of the hybrid and electric vehicle.

The final pursued objective is to determine based on the conducted simulations which is the technical solution eligible for the implementation in real traffic conditions of the urban route established and studied within the research.

Consequently, the studies and researches will have as objective the design, development and implementation of an integrated management system for hybrid and electric drives in order to command and control the parts which compose the powertrain (thermal engine, electric vehicle, generator, transmission etc.).

The results obtained from implementing this study in real and energetically efficient exploitation conditions of the electric buses within the urban passenger transportation system will bring the following valid results for the economic environment:

- the usage of the studied algorithm as an initial solution for updating the coordination applications for the routes of hybrid and electric vehicles afferent to the economic road function;

- the efficiency and stringency in choosing the type and location of the fast loading stations, by identifying the best algorithm and by applying it locally;
- the future development of applications for using the best routes, for smartphones and digital tablets.

The researches results in accordance with the research objectives, on short or long term, are based on the strategic decisions, plans and reports regarding a solution for a durable urban transportation made by local and/or national authorities which represent a request for the present tendencies to replace the transport vehicles equipped with classic engines with transport vehicles equipped with hybrid and electric drive systems in order to reduce the pollutant emissions.

The development of a solution for urban public passenger transportation based on vehicles equipped with hybrid and electric drive systems encourages the usage of public transportation and the development of the public transportation infrastructure in order to reduce greenhouse gas emissions. In this regard the present research study aims to contribute directly in immediately identifying the most sustainable solutions for replacing the old buses equipped with diesel engine drive systems with hybrid and electric buses.

The development of new hybrid and electric drive systems and of the infrastructure needed for implementing the study brings an added value for the urban public transportation and will guide the society towards a solution for modern and sustainable mobility, compatible with the present requirements regarding environmental protection.

Implementing the new drive system proposed by this book will offer a tendency of increase for the public transportation dynamic, in relation to the individual transport based on personal vehicles, which in an urban agglomeration contributes in maintaining and improving the qualitative parameters of the state of the environment by reducing the air pollution and by minimizing the CO_2 emissions.

References

1. Rose, E. A. (1992). A Europe of regions—the West Midlands of England: Planning for metropolitan change in Birmingham. *Landscape and Urban Planning, 22*(2–4), 229–242.
2. Scott, A. J. (2008). Resurgent metropolis: Economy. *Society and Urbanization in an Interconnected World, International Journal of Urban and Regional Research, 32*(3), 548–564.
3. International Federation Of Surveyors (FIG), (2010). Rapid urbanization and mega cities: The need for spatial information management, research study by FIG Commission 3. Retrieved Oct 8 2015 from http://www.fig.net/resources/publications/figpub/pub48/figpub48.pdf
4. Mishra, R. K., Parida, M., & Rangnekar, S. (2012). Urban transport system: An environmentally sustainable approach. *Journal of Environmental Research and Development, 6*(3), 500–506.
5. Wu, J. (2014). Urban ecology and sustainability: The state-of-the-science and future directions. *Landscape and Urban Planning, 125*, 209–221.
6. Tomic, M., et al. (2013). Effects of fossil diesel and biodiesel blends on the performances and emissions of agricultural tractor engines. *Thermal Science, 17*(1), 263–278.

7. Heywood, J. B. (1988). *Internal combustion engines fundamentals*. Singapore: McGraw-Hill International Editions.
8. Dodman, D. (2009). Blaming cities for climate change? *An analysis of urban greenhouse gas emissions inventories, Environment and Urbanization, 21*, 185–201.
9. Moldovanu, D., & Burnete, N. (2013). Computational fluid dynamics simulation of a single cylinder research engine working with biodiesel. *Thermal Science, 17*(1), 195–203.
10. European Biofuels Technology Platform, Bioethanol use in Europe and Globally, (2015). Retrieved May 9 2015 from http://www.biofuelstp.eu
11. Crouse, D. L., Goldberg, M. S., Ross, N., Chen, H., & Labreche, F. (2010). Postmenopausal breast cancer is associated with exposure to traffic-related air pollution in Montreal, Canada: A case-control study. *Environment and Health Perspective, 118*, 1578–1583.
12. Manzetti, S. (2012). Eco toxicity of polycyclic aromatic hydrocarbons, aromatic amines and nitroarenes from molecular properties. *Environmental Chemistry Letter, 10*, 349–361.
13. Manzetti, S. (2013). Polycyclic aromatic hydrocarbons in the environment: Environmental fate and transformation. *Polycyclic Aromatic Compounds, 33*, 311–330.
14. Hung, L. J., Tsai, S., Chen, P., Yang, Y., Liou, S., & Yang, C. (2011). Traffic air pollution and risk of death from breast cancer in Taiwan: Fine particulate matter (PM 2.5) as a proxy marker. *Aerosol and Air Quality Research, 12*, 275–282.
15. Regulation (EC) No 443/2009 of the European Parliament and of the Council of 23 April 2009 setting emission performance standards for new passenger cars as part of the Community's integrated approach to reduce CO_2 emissions from light-duty vehicles. Retrieved Mar 11 2015 from http://eur-lex.europa.eu/legal-content/RO/TXT/?uri=CELEX%3A32009R0443
16. Mariasiu, F. (2012). Energy sources management and future automotive technologies: Environmental impact. *International Journal of Energy Economics and Policy, 2*(4), 342–347.
17. Nykvist, B., & Nilsson, M. (2015). Rapidly falling costs of battery packs for electric vehicles. *Nature Climate Change, 5*, 329–332.
18. Retrieved Dec 9 2015 from http://ctpcj.ro/index.php/ro/, (in Romanian).
19. Varga, B.O., (2015). Energy efficiency of vehicles equipped with hybrid or electrical powertrain for urban public transport (in Romanian), Habilitation thesis, Technical University of Cluj-Napoca, Romania, 18th of September 2015.

Chapter 2
Energetic Efficiency of Vehicles Equipped with Hybrid and Electric Drive Systems

2.1 The Hybrid Drive System

Hybrid Electric Vehicle (HEV) are equipped with both an internal combustion engine and an electric motor, thus using two different sources of energy. Each of these engines can transmit the torque to the wheels through a parallel and/or mixed series system.

A hybrid vehicle uses two or more different power sources to get started. The hybrid vehicle combines a conventional drive system with a system which stocks recoverable energy in order to obtain a better yield, a lower fuel consumption and a lower emissions level.

The hybrid drive system has the following main elements [1]:

- electric batteries;
- electric motor;
- internal combustion engine;
- electric current generator;
- coupling elements to connect the mechanical system with the electric system;
- management system for the two drive systems.

The batteries or supercapacitors used by the electric motor are recharged by the internal combustion engine and/or from the energy generated during braking. Plug-in Hybrid Electric Vehicles (PHEV) have the particularity of allowing the electric batteries to charge by connecting the to an electricity network. This constructive model assures a greater autonomy for travelling in the electric mode.

The combination between the internal combustion engine and the electric motor is based on a perfect interaction between the modern command system and the optimized hybrid components. The management systems integrated in the hybrid vehicles assure the commutation between the electric, hybrid and internal combustion drive systems without affecting the comfort of the passengers.

In this regard, the electronic command system has permanent access to the data coming from the sensors of the internal combustion engine, the electronic control unit, the batteries recharge state etc. The management system analyzes, regulates and commands in real time the interaction between the two drive systems [1].

An essential component is the adaptive clutch which allows a smooth commutation between gears. The clutch aims to assure that the electric motor and the internal combustion engine have the same speed at the time of the functioning mode change so that the vehicle movement should not be affected by the drive source change.

Presently a hybrid drive system consisting of an internal combustion engine and an electric motor, equipped with the Plug-in technology may be considered as a transitory solution towards the new technology based on an electric vehicle equipped with a Range Extender unit (REV), namely a vehicle equipped with an internal combustion engine which serves exclusively in recharging the accumulator and not for driving the vehicle.

This concept assures the usage of the electric energy on medium distances, within the conditions of using a minimum quantity of fossil fuel and implicitly producing lesser pollutant emissions. Unlike the serial hybrid vehicle, where the internal combustion engine assures the necessary power for the electric motor during almost 90 % of the functioning time, the electric vehicle with Range Extender functions exclusively based on the energy provided by the accumulator and the internal combustion engine only starts when the level of energy from within the accumulators drops under a certain level.

A functional cycle of a hybrid vehicle consists of an acceleration period, a period of driving at a constant velocity and a deceleration period (Fig. 2.1), from which one can observe that the power necessary for the first phase is much greater than the power necessary for driving at a constant velocity [2].
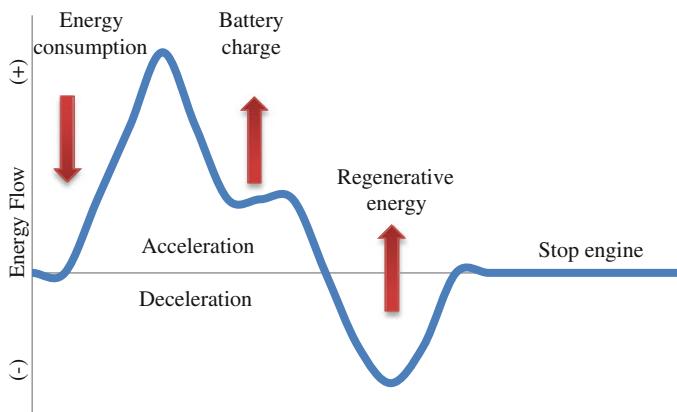
Fig. 2.1 Functioning cycle of an hybrid vehicle [2]

By braking the vehicle, the internal combustion engine functions at idle speed and the kinetic energy obtained at deceleration is recovered and used to recharge the batteries. In the case of a hybrid vehicle the brakes take over the braking kinetic energy and the electric motor is used as generator and recharges the batteries. To maximize the power of the recuperative braking it is important for the stopping to be smooth and gradual—a sudden braking can lead to the activation of the anti-blocking system (ABS) and the loss of kinetic energy [3].

The drive systems which have besides an internal combustion engine in their composition at least another system which provides traction coupling for the wheels of the vehicle and which recovers some of the kinetic energy obtained at deceleration are also known as regenerative hybrid drive system [4].

The advantages of using hybrid vehicles are [5]:

- pollutant emissions (CO, NO_x, HC, PM, CO_2 etc.) under the values imposed by the EURO 6 norm and a reduced exposure of the passengers and pedestrians to these emissions;
- a decrease of pollutant emissions which have a negative impact on the surface of the historical buildings from the central areas;
- a decrease of vibrations which are harmful to the urban infrastructure and the historical buildings from the central areas;
- the assurance of a higher comfort for the passengers and the traffic participants through the lack of vibrations generated by high capacity internal combustion engines;
- the possibility of creating central areas with a more reduced pollution;
- lower maintenance costs due to the lack of internal combustion engine specific systems;
- reduced exploitation costs due to a lower price of electric energy compared to the classic fuel, taking into account the traveled distance.

The disadvantages of using hybrid vehicles [5]:

- during the cold season the lower temperatures affect the stocking capacity of the batteries and also the loading time, which limits the traveled distance and also extends the loading time;
- diminished transport capacity because of the mass of the batteries used to fuel the electric motor;
- for the Plug-in hybrid system, investments are necessary for acquisitioning charging stations for the batteries;
- the acquisition price for hybrid buses is approximately double the classic buses price.

2.2   Classification of Hybrid Drive Systems

Hybrid drive systems can be classified in two categories: serial and parallel, which can themselves be combined in many subcategories according to the constructive architecture.

The serial hybrid drive system relies on two energy sources which power a sole electric motor, called the propulsion motor. The internal combustion engine is coupled with an electric generator which fuels the electric motor through a rectifier. The internal combustion engine functions in the maximum efficiency area because it is coupled to the motor wheels; this allows the usage of an internal combustion engine with high speed and low coupling.

Because the electric motors have an almost ideal coupling-velocity characteristic they do not need transmissions with multiple gears; also more electric motors can be used to operate each wheel individually. This configuration allows the mechanical coupling between the wheels, thus assuring the control of the vehicle traction individually on each motor wheel.

The management of the transmission is simplified because there is a mechanical decoupling between the motor wheels and the internal combustion engine.

The disadvantages of the serial hybrid system are [5]:

- the mechanical energy generated by the internal combustion engine is transformed in electric energy by the generator, which fuels the electric motor and transforming it again in traction mechanical energy, thus resulting a lower efficiency for the vehicle;
- the electric generator used increases the weight and costs of the vehicle;
- the electric motor must have a sufficiently high power to assure the propulsion of the vehicle in maximum performance conditions.

The parallel hybrid drive system assures a parallel distribution of the power flow generated by the internal combustion engine and the electric motor to start the motor wheels. Because the two motors are coupled to the axel of the wheels via two gearboxes, the power flow can be provided by the internal combustion engine, by the electric motor or by both. The coupling of the two motors is made through a velocity summing device.

The electric motors used for hybrid vehicles are three-phase machines of alternative current, divided in the following categories [6]:

- asynchronous motors (ASM);
- synchronous motors with permanent magnets (PSM—Permanent Synchronous Motor);
- transversal flux motors (TFM);
- motors with reversed magnetic resistance (SRM—Switched Reluctance Motor).

Another method of classifying the hybrid vehicles is according to the power characteristics of different types of hybrid vehicles (Table 2.1).The classification of hybrid systems from the point of view of the transmission is presented in Fig. 2.2.

Table 2.1 Power characteristics of hybrid vehicles

Type	Micro hybrid	Medium hybrid	Total hybrid
Electric motor power	2…10 kW	4…20 kW	>20 kW
Electric motor coupling	<90 Nm	<500 Nm	<500 Nm
Tension	14…42 V	≥42 V	100…650 V
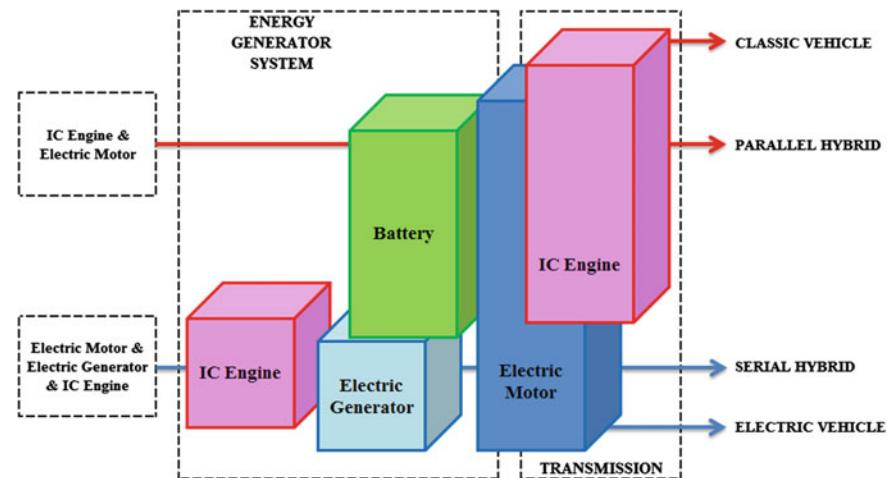
Fig. 2.2 Hybrid drive structure

Hybrid vehicles can also be classified according to the type of fuel used to power the internal combustion engine. This classification is as it follows:

- compression ignition engine fueled with diesel fossil fuel;
- compression ignition engine fueled with biodiesel blend;
- spark-ignition engine fueled with gasoline fossil fuel;
- spark-ignition engine powered by a bioethanol based blend;
- compression ignition engine fueled with CNG.

The connection between the components through which the energy flow of the hybrid vehicle passes and the control part is called constructive architecture. From the point of view of the constructive architecture, the hybrid vehicles can be divided in two big categories: the ones with serial transmission and the ones with parallel transmission [7].

The hybrid vehicles with a serial transmission of the energy flow or Serial Hybrid (Fig. 2.3) have no mechanical connection between the internal combustion engine and wheel drive shaft, and the propulsion is assured by the electric motor.

The internal combustion engine stimulates a generator and the electric motor uses the generated electric current to start the wheels of the vehicle. This model is called the serial hybrid system because the power flow to the wheels of the vehicle
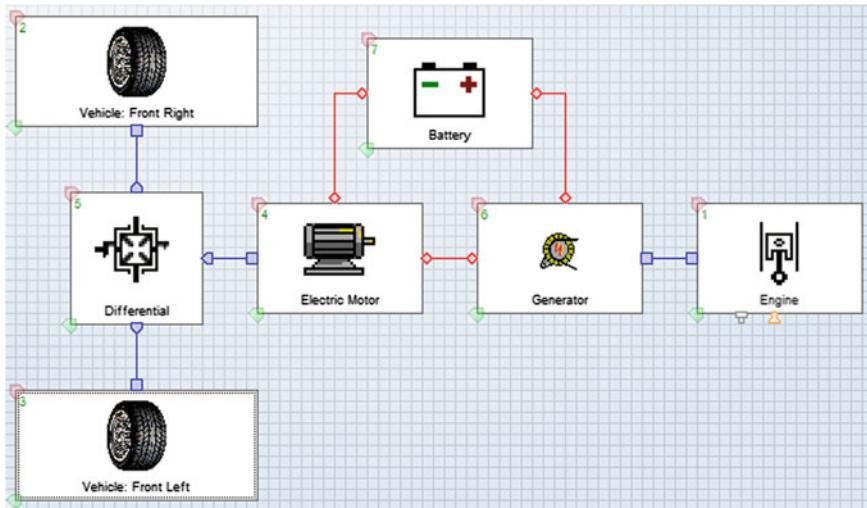
Fig. 2.3 Serial hybrid architecture

acts like a system in series. A serial hybrid system can be used in the case of an electric motor which can be easily maintained in a stable domain of its functioning and which is also capable of providing an energy surplus to the electric motor which, in turn, can charge the battery [5, 8].

The power transmitted from the internal combustion engine must go through the generator towards the electric motor, thus reducing the energetic efficiency of the system because each transformation has an energy loss effect.

The efficiency of the motor-transmission group is approximatively 70–80 % lower than the efficiency of a conventional mechanical clutch which has an efficiency of almost 98 %. In the case of a long distance drive the internal combustion engine must compensate the energy losses, thus the serial hybrid system is 20–30 % less efficient than the parallel hybrid system. The use of a motor for each motor wheel leads to the elimination of mechanical transmission elements (gearbox, differential) and can eliminate the flexible couplings. The advantage of motors placed on each wheel includes a more simplified traction control with gearing in all wheels which also allows the use of lower access ramps—in the case of buses.

Hybrid vehicles with a parallel transmission of the energy flow or Parallel Hybrid (Fig. 2.4) have an internal combustion engine connected to the wheel drive shaft, but also a generator with the role of charging the batteries system. The system is called parallel because the power flow is transmitted towards the motor wheels in parallel [7].

The electric motor is mechanically connected to the internal combustion engine through a clutch. This system can assure an extra coupling, which leads to higher dynamic performances. Furthermore, the torque of the internal combustion engine can be transmitted directly to the axels no matter the state of the electric motor [1].
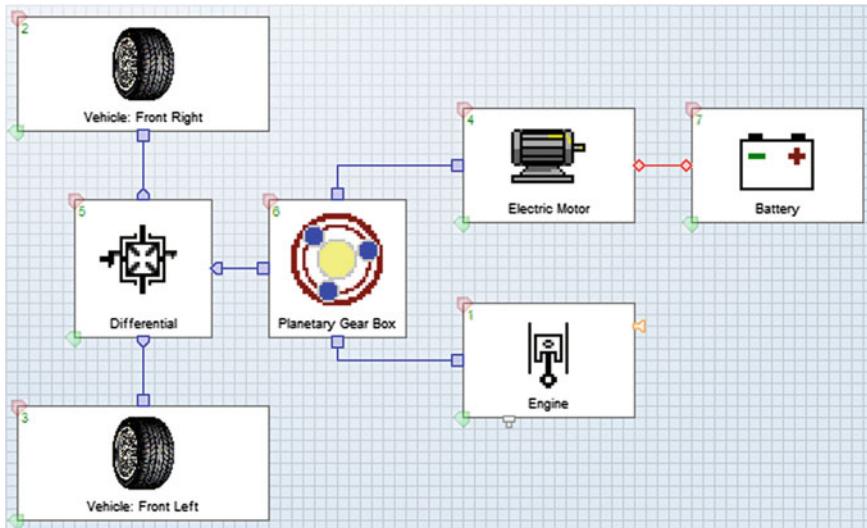
Fig. 2.4 Parallel hybrid architecture

In the parallel hybrid system both the internal combustion engine and the electric motor transmit power to the wheels, but this power can be provided by the two motors concomitantly, the system easily adapting to some predestined typical situations. The battery is recharged by the commutation of the electric motor to work as a generator, and the electric current from the batteries is used as an effective power flow to starts the wheels of the vehicle.

Although it has a more simple structure, the parallel hybrid system cannot use the power provided by the internal combustion engine to both start the wheels and to simultaneously charge the battery. To keep and put to maximum use the energy provided by the internal combustion engine, some systems like the power-assisted steering and the air conditioning are powered by the electric motor and are not attached to the internal combustion engine, fact which permits the functioning of these systems at constant velocities without being influenced by the speed of the internal combustion engine [8].

Parallel hybrid systems can be differentiated by the way in which the two energy generating motors are mechanically coupled. If they are coupled on a parallel axis the velocity should be identical. When only one of the motors is being used, the other one must function at idle speed or it must be connected through a clutch.

Hybrid vehicles with a mixed serial-parallel transmission of the energy flow or the Serial-Parallel Hybrid combines the advantages of the serial hybrid system with the advantages of the parallel hybrid system in order to maximize the advantages of both systems.

The two drive systems are used according to the driving conditions, so as to start the motor wheels only the electric motor can be used, or both the electric motor and the internal combustion engine to reach a level of maximum efficiency. The system
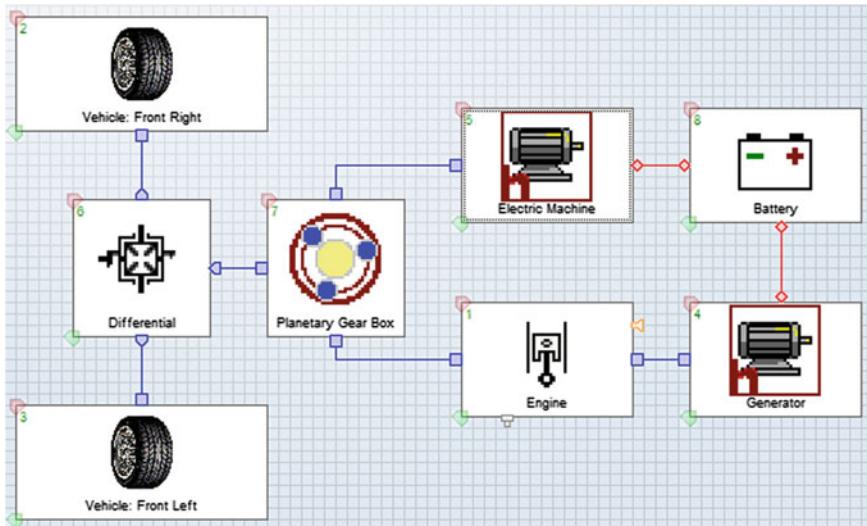
Fig. 2.5 Power split hybrid architecture

can start the motor wheels while also generating electric current through a generator powered by the internal combustion engine.

The hybrid system with a mixt transmission of the energy flow can be divided in the following categories: Power Split Hybrid, Serial-Parallel Hybrid, and Serial-Parallel with Transmission Hybrid [7].

Power Split Hybrid (Fig. 2.5) is the system where the energy generated by the internal combustion engine is transmitted through a differential mechanism towards the wheels, but concomitantly it will start a current generator which will create a brake torque for the motor.

The electric current obtained will be used to fuel the electric motor coupled to the wheel drive shaft, which will supplement the brake torque derived from the thermal engine thus causing the energy flow to be transmitted both via the mechanical system and the electric system, resulting separate power flows [9].

Serial-Parallel Hybrid (Fig. 2.6) is the system where the power generated by the internal combustion engine will start a current generator which will create a brake torque for the motor, and the obtained electric current will be used to fuel the electric motor coupled to the wheel drive shaft which will supplement the brake torque provided by the thermal engine [7].

Serial-Parallel with Transmission Hybrid (Fig. 2.7) is the system where the energy generated by the internal combustion engine will start a current generator which will create a brake torque for the motor and the electric current obtained will be used to fuel the electric motor coupled to the wheel drive shaft, which will supplement the brake torque provided by the thermal engine and, concomitantly, the internal combustion engine will also be coupled to the wheel drive shaft, with the possibility to select the drive mode [7].
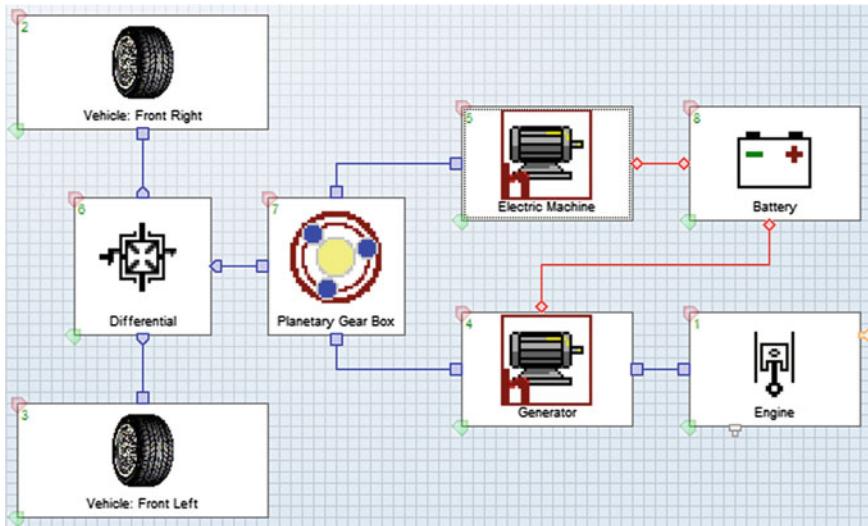
Fig. 2.6 Serial-parallel hybrid architecture
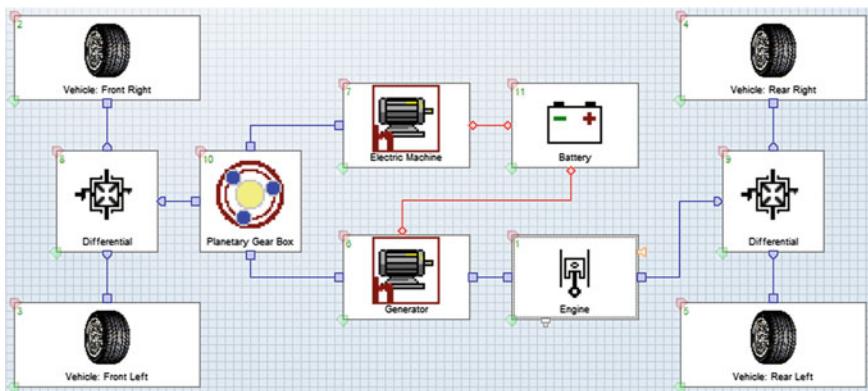
Fig. 2.7 Serial-parallel with transmission hybrid architecture

The great advantage of this system is the power divider, which is a connection element between the internal combustion engine, the electric motor and the current generator, and which has the role of adjusting the power flow which goes towards the shaft. Thus, the system functions as a serial model when the internal combustion engine starts the generator and fuels the electric motor, or as a parallel model when the internal combustion engine transmits the power directly towards the shaft, while being supplemented by the electric motor fueled by the batteries.

The management process of the control and functioning of the internal combustion engine and of the electric motor equipping a hybrid vehicle has the

constructive-functional characteristics of the fuel injection systems, electric systems, energy management systems, sensor systems, drive systems and also of the ECUs. Performance improvement of the hybrid vehicles, optimization of energy flow distribution, and reduction of fuel consumption and of pollutant emission are the desired goals of all major manufacturer of the automotive industry, but their main objective is reaching a low economic pole. This objective can be reached through an efficient management of the intelligent systems which control and coordinate the processes and phenomena taking place while a hybrid vehicle is running.

The management of the energy provided by the internal combustion engine, respectively by the electric motor, but also the control over the drive mode can be achieved with the help of the ECU, which—as opposed to classic vehicles—have the role of controlling and coordinating the distribution of the energy flow generated by the two drive systems.

The management of the drive system is based on the steps taking place in the functioning process of a hybrid vehicle, thus:

- When the vehicle starts off, hybrid vehicles use only the electric motors, powered by the battery, while the IC Engine remains shut off. An IC Engine cannot produce high torque in the low speed range, whereas electric motors can, delivering a very responsive and smooth start (Fig. 2.8a) [10].
- IC Engine is not energy efficient in running a vehicle in the low-speed range. On the other hand, electric motors are energy efficient in running a vehicle in the low-speed range. Therefore, hybrid vehicles use the electric energy stored in its battery to run the vehicle on the electric motors in low-speed range. If the battery charge level is low, the IC Engine is used to turn on the generator to supply power to the electric motors (Fig. 2.8b) [10].
- Hybrid vehicles use the IC Engine in the speed range in which it operates with good energy efficiency. The power produced by the IC Engine is used to drive the wheels directly, and depending on the driving conditions, part of the power is distributed to the generator. Power produced by the generator is used to feed the electric motors, to supplement the IC Engine. By making use of the engine/motor dual powertrain, the energy produced by the IC Engine is transferred to the road surface with minimal loss. If the battery charge level is low, the power output from the IC Engine is increased to increase the amount of electricity generated to recharge the battery (Fig. 2.8c) [10].
- Since hybrid vehicles operate the internal combustion engine in its high efficiency range, the internal combustion engine may produce more power than is necessary to drive the car. In this case, the surplus power is converted to electric energy by the generator to be stored in the battery (Fig. 2.8d) [10].
- When strong acceleration is called for the power from the battery is supplied to the electric motors to supplement driving power. By combining the power from the internal combustion engine and the electric motors, hybrid vehicles deliver power comparable to vehicles having one class larger engine displacement of one class higher (Fig. 2.8e) [10].

(a)
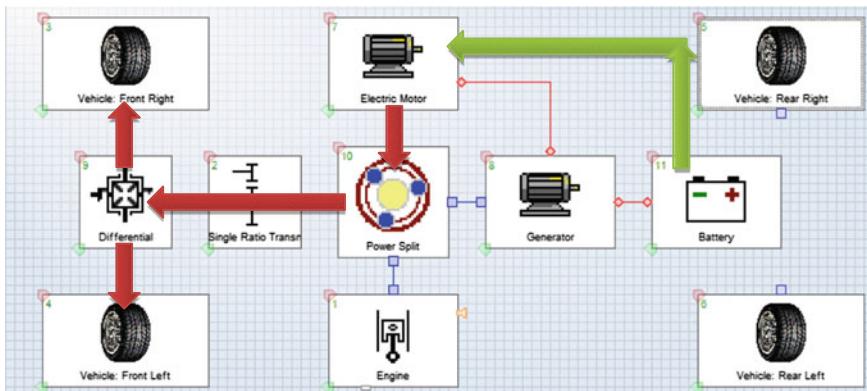
(b)
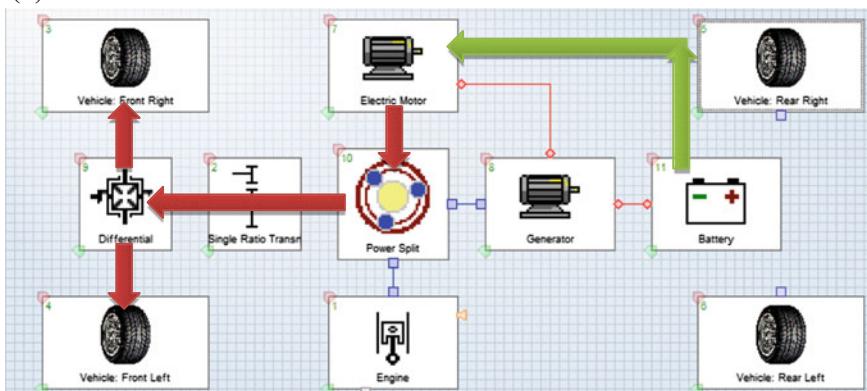
(c)
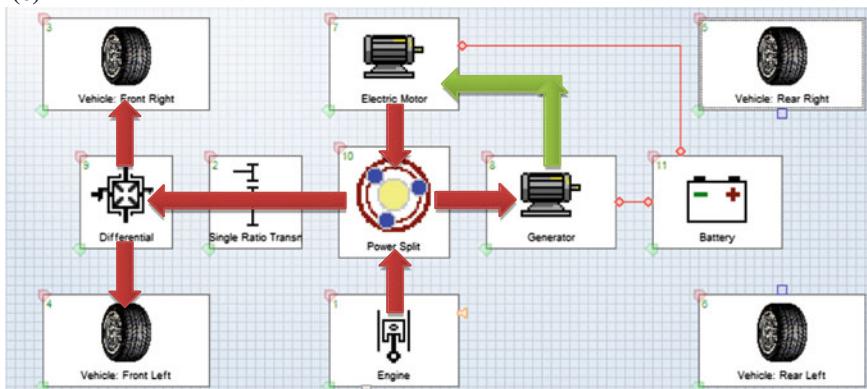
Fig. 2.8 The operation of the hybrid vehicle: **a** starting off, **b** low speed driving, **c** cruising, **d** cruising/recharging, **e** full acceleration, **f** deceleration/energy regeneration, **g** at rest

(d)
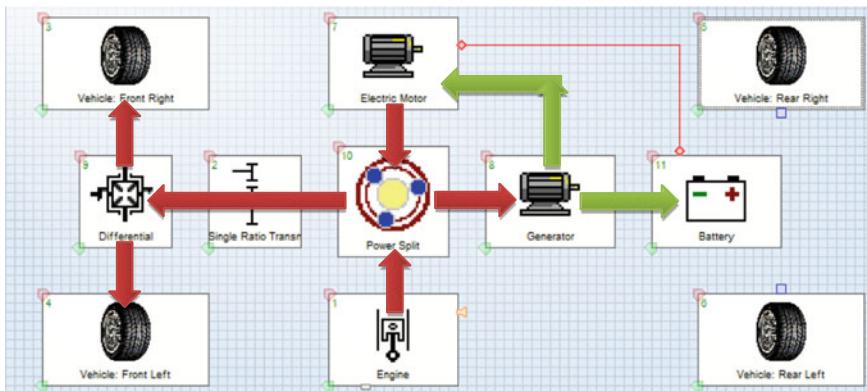
(e)

(f)

Fig. 2.8 (continued)

(g)
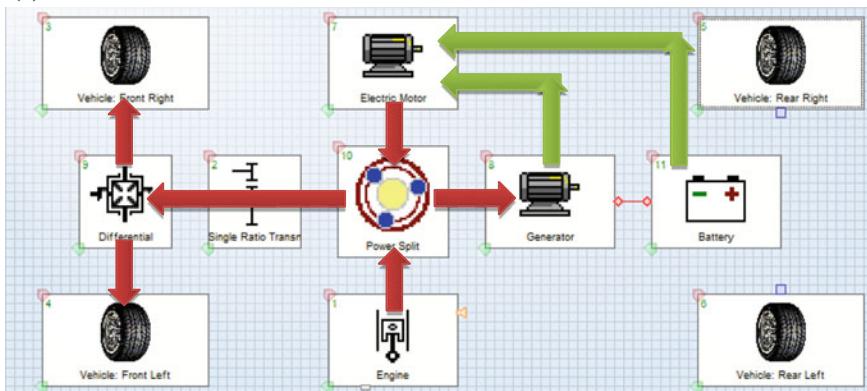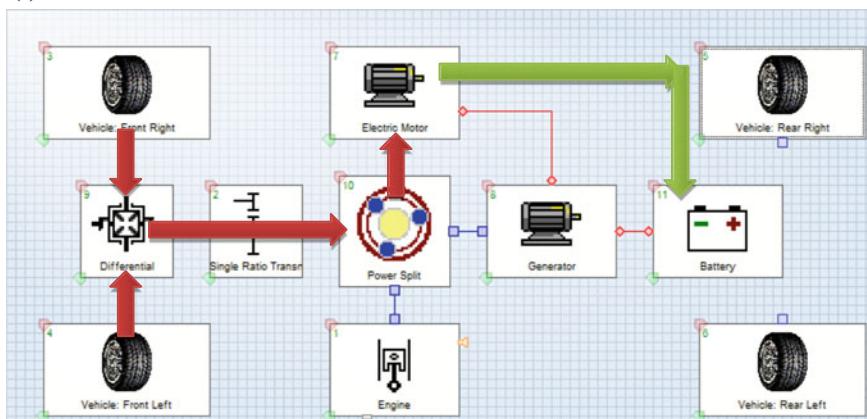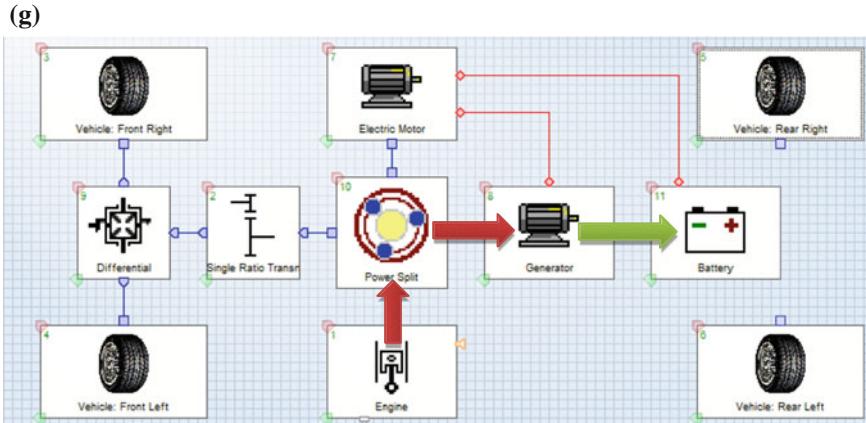
Fig. 2.8   (continued)

- Under braking or when the accelerator is lifted, hybrid vehicles use the kinetic energy of the car to let the wheels turn the electric motors, which function as regenerators. Energy that is normally lost as friction heat under deceleration is converted into electrical energy, which is recovered in the battery to be reused later (Fig. 2.8f) [10].
- The internal combustion engine, the electric motors and the generator are automatically shut down when the vehicle comes to rest. No energy is wasted by idling. If the battery charge level is low, the internal combustion engine is kept running to recharge it. In some cases, the internal combustion engine may be turned on in conjunction with the auxiliary systems switch operation (Fig. 2.8g) [10].

2.3   The Electric Drive System

The vehicles powered exclusively by a rechargeable battery are called battery electric vehicles (BEV) (Fig. 2.9).

The following are the parts composing an electric vehicle [1]:

- the rolling system composed of pneumatic wheels for steering (front) and motor wheels (back), mounted on two axels: steering axel (front) and rear axel (back);
- the steering mechanism with which the steering of the front wheels is achieved;
- the main transmission consisting of: reduction gear, mechanical differential and planetary axels;
- the chassis, on which the electric vehicle body is mounted and on which the electric traction motor is attached;
- the powertrain consisting of: electric drive motor, generator and electric battery.
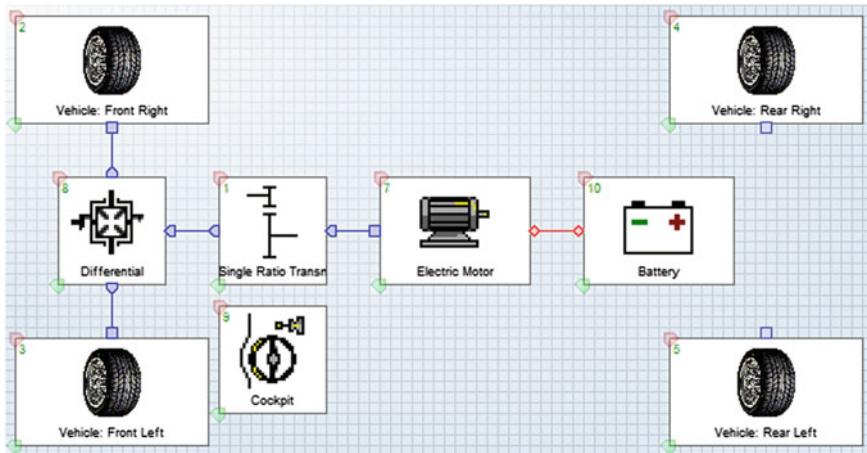
Fig. 2.9 Electric vehicle architecture

The buses using the electric drive system do not use an internal combustion engine, like the hybrid buses, because it is integrally based on the rechargeable electric batteries which set in motion the electric motor. Some buses, also known as opportunity charged electric buses, recharge on route—either in recharging points set on the circuit of the bus, or at the first or last stop. Other buses, known as night electric buses have their own batteries and they recharge during the night. Another recharging regime is that of combining the two methods of recharging during the night and of completing the charge level in the battery during the time the bus is in use [11].

The reduction of emissions generated by the electric vehicles depends on the mode in which the electric energy is produced, namely between 30 % in the case the electricity is generated from the national network with CO_2 emissions and up until 100 % in the case where the electricity is generated from renewable electricity sources.

Electric buses do not generate emissions through the exhaust pipe, which means zero local emissions. Although they require a greater initial investment, the electric buses offer the advantage of cost savings regarding the fuel and less maintenance costs due to a reduced number of components in motion.

By making a comparison between conventional buses and electric buses, the latter present a series of advantages, namely [2]:

- silent and vibration-free functioning, thus reducing the noise pollution;
- lack of local pollutant emissions;
- independence towards fossil fuels;
- high energetic efficiency;
- use of electric braking and energy regenerative braking;
- possibility of individual motor wheel drive.

The main disadvantages of electric vehicles are the following:

- the energy and power density of the batteries is significantly lower than that of the fuels (the energy density for a gasoline internal combustion engine is 10,000 Wh/kg and the energy density for an electric motor is 200 Wh/kg), fact which leads to a decreasing autonomy of electric vehicles (100–200 km) as opposed to the autonomy of classic vehicles (400–800 km), respectively a lower maximum velocity of electric vehicles (100–130 km/h) as opposed to the classic vehicles (180–200 km/h), also the accelerations achieved by electric vehicles are inferior to those of classic vehicles;
- the necessity of existent charging stations for batteries and the necessary recharging time: hours for a complete charge and tens of minutes for a partial recharge;
- the prices for electric vehicles are much higher than the prices for classic vehicles.

2.4 Classification of Electric Drive Systems

Electric drive systems can be classified according to the electric motor with which they are equipped. The technical characteristics of electric motors are presented in Table 2.2. Electric vehicles can also be classified according to the electric energy supply mode [6]:

- electric vehicles powered autonomously from own electric sources;
- non-autonomous electric vehicles, powered through a contact line from external electric sources.

Table 2.2 Technical-functional characteristics of electric motors [6]

Type of motor	Contacts	Coupling	Price	Maintenance	Efficiency	Complexity
DC with series excitation	Yes	Low	Medium	Yes	Low	Low
DC with separate excitation	Yes	Low	Medium	Yes	Low	Low
DC with permanent magnets	Yes	Medium	High	Yes	Medium	Low
AC asynchronous	No	Medium	Low	No	Low	High
DC brushless	No	High	High	No	High	Low
Variable reluctance	No	High	Low	No	Medium	Medium

Table 2.3 Technical-functional characteristics of the batteries [6]

Types of batteries	Energy density (Wh/kg) (Wh/l)		Specific power (W/kg)	Cycles of recharge/discharge	Industrial availability
Pb-Acid	31–40	75–90	90–125	600–1000	Yes
Ni-Cd	45–58	80–95	190	2000	Yes
NiMH	55–60	100–130	175	–	No
Ni-Fe	50–60	80–95	110	1000–1500	No
Na-S	80–100	110–135	100–120	500	No
Li	80–120	100–120	70	>200	No

According to the type of path, electric vehicles are classified as follows:

- electric vehicles with a guided path, conventional or nonconventional;
- electric vehicles with an air cushion or magnetic cushion;
- electric vehicles without a guided path (road).

Another type of classification of electric drive systems is according to the type of batteries they are equipped with. The technical characteristics of the types of batteries used are presented in Table 2.3.

References

1. Ehsani, M., Gao, Y., Gay, S. E. (2005). Modern electric, hybrid electric, and fuel cell vehicles, fundamentals, theory, and design. CRC Press Ed., ISBN: 0-8493-3154-4.
2. Surugiu, M.C., Maghiari, E. (2008). Emissions monitoring and trafic management system. In 8th international conference on technology and quality for sustained development, TQSD 2008.
3. http://en.wikipedia.org/wiki/Hybrid_electric_vehicle, web accessed 4 March 2016
4. Millo, F., Rolando, L., Andreata, M. (2011). Numerical simulation for vehicle powertrain development, computer and information science, Chapter 24, 2011, ISBN: 978-953-307-3897.
5. Ioța, C. (2012). Bosch—Tehnologie şi know-how pentru autovehiculele hibride, Ingineria Automobilului, (in Romanian) (Vol. 6, Nr. 1), ISSN: 1842-4074;
6. Racicovschi, V., Danciu, G., & Chefneux, M. (2007). *Automobile Electrice şi Hibride, (in Romanian)*. Bucureşti: Editura Electra. ISBN 978-973-7728-98-2.
7. Kubo, M. (2010). *Hybrid powertrain investigation using GT suite, The 2010 GT-Suite European conference*. Germany: Frankfurt.
8. Perez-Pinal, F.J. (2011). An integrated electric vehicle curriculum, computer and information science, Chap. 12, ISBN: 978-953-307-389-7.
9. Popovici, O., Popovici, D. (2009). Tracțiune electrică, (in Romanian), Editura Mediamira, Cluj-Napoca, 2009, ISBN: 978-973-713-230-7.
10. http://www.toyota-global.com/innovation/environmental_technology/hybrid/, web accessed 4 March 2016
11. http://news.thomasnet.com/fullstory/battery-features-thin-plate-pure-lead-design-800783, web accessed 4 March 2016

Chapter 3
Development and Implementation of the Hybrid and Electric Systems Architecture Through Methods of Numerical Analysis

The theory that is presented in Chapter 3 represents the mathematical models developed by AVL CRUISE team and points out the characteristic of each vehicle component used in the models created in the following chapters.

The theoretical models presented in this chapter represents a adaptation a the mathematical models presented in the Electric and Plug-In Hybrid Vehicles—Advanced Simulation Methodologies, Chap. 2, pp. 9–200, Chap. 3, pp. 223–287, Springer International Publishing Ed., ISBN: 978-3-319-18638-2—Varga, B.O., Mariaşiu, F., Moldovanu, D., Iclodean, C.

3.1 Mathematical Modeling of the Configuration Used in the Simulation Process

The vehicle models developed in the AVL CRUISE application consist of component elements which are identifiable to the real elements from both the point of view of the constructive characteristics and from the point of view of mathematical relations which govern their functioning. Thus, for each element taking part in the composition of the three type of bus models developed in this study, the following mathematical relations were define to help with the calculations of model processes and characteristics during the development of the simulation process within the AVL CRUISE application.

3.1.1 Equations of the Vehicle Element

The Vehicle is one of the main objects in a model. This component contains general data of the vehicle, such as nominal dimensions and weights. One and only one

vehicle component is needed in the model. Road resistances and dynamic wheel loads are calculated for road and dynamometer runs based on the dimensions and the load state. The wheel loads are calculated, taking motion into account (e.g., from acceleration, aerodynamic drag, rolling resistance). The aerodynamic, rolling, climbing, acceleration, and total resistance are calculated [1].

In the general case of travel for a vehicle having rear drive, with a variable velocity on a rectilinear road, with a α_p tilt angle in relation to the horizontal axis (Fig. 3.1), the equilibrium equations of forces in the direction of travel are the following [2]:

$$F_t - G_a \sin \alpha_p - R_t - R_a - R_{rul1} - R_{rul2} - R_{i1} - R_{i2} = 0 \tag{3.1}$$

where: R_{i1} and R_{i2} represent the resistant forces generated by the inertia of the wheels and of the parts connected to them, moving in cinematic rotation, F_t—total traction force (N), the R_{i1} and R_{i2} forces represent [2]:

$$R_{ij} = \frac{M_{ij}}{r_r} \, (\text{N}) \tag{3.2}$$

where M_{ij} is the moment given by the inertia of the respective parts (Nm). The inertial force of the mass in translational motion is given by the relation [2]:

$$R_{dt} = \frac{G_a}{g} \cdot \frac{dv}{dt} \, (\text{N}) \tag{3.3}$$

The total rolling resistance is:

$$R_{rul} = R_{rul1} + R_{rul2} \, (\text{N}) \tag{3.4}$$
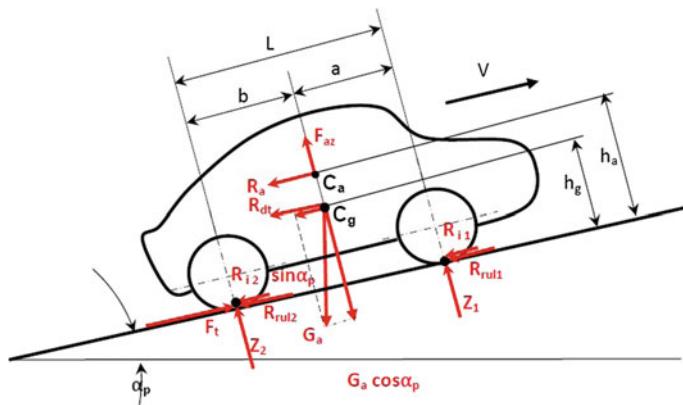
Fig. 3.1 Dynamic evaluation of the vehicle [2]

The total resistance due to parts in rotational motion is:

$$R_{dr} = R_{i1} + R_{i2} \, (\text{N}) \tag{3.5}$$

The slope climb resistance is:

$$R_p = G_a \cdot \sin \alpha_p \, (\text{N}) \tag{3.6}$$

Based on these relations (3.2–3.6) the equilibrium equation of forces in direction of travel expresses the traction balance of the vehicle [2]:

$$F_t = R_{rul} + R_p + R_a + R_d \, (\text{N}) \tag{3.7}$$

Taking into account the calculation formula for acceleration resistance, the general equation of rectilinear motion of vehicles results [2]:

$$\delta \cdot \frac{C_a}{g} \cdot \frac{dv}{dt} = F_t - \left(R_{rul} + R_p + R_a \right) \tag{3.8}$$

In traction regime, when the vehicle travels accelerated or at a constant velocity and we have one requirement of submissions:

$$\frac{dv}{dt} \geq 0 \tag{3.9}$$

The general equation for rectilinear motion of vehicles becomes [2]:

$$F_t \geq R_{rul} + R_p + R_a \tag{3.10}$$

The summation of all moments around the contact point between rear wheels and road has to be zero [1]. Out of this equation we can calculate the load of the front axis [1]:

$$\begin{aligned}
F_{w,x,f,ax} = m_{V,act} & \left[\left(1 - \frac{l_{V,cog,act}}{l_{V,fr}} \right) \cdot g \cdot \cos \alpha_U - \frac{h_{V,cog,act}}{l_{V,fr}} \cdot \left(a_V + g \cdot \sin \alpha_u \right) \right] \\
& - F_{V,lift,f}
\end{aligned} \tag{3.11}$$

The load of the rear axis is [1]:

$$F_{w,x,r,ax} = m_{V,act} \left[\frac{l_{V,cog,act} \cdot g \cdot \cos \alpha_U}{l_{V,fr}} + \frac{h_{C,cog,act}}{l_{V,fr}} \cdot \left(a_V + g \cdot \sin \alpha_U \right) \right] F_{V,lift,r} \tag{3.12}$$

where $F_{w,x,f,ax}$ is the rear axis load (N), $m_{V,act}$—vehicles mass (kg), $l_{V,cog,act}$—distance to weight center (m), $h_{V,cog,act}$—height of weight center (m), $F_{w,x,r,ax}$—front axis load (N), a_V—acceleration (m/s^2).

3.1.2 Equations of the Clutch Element

Stationary idle, transition to motion and interruption of the power flow are all made possible by the clutch. The clutch slips to compensate for the difference in the rotational speeds of engine and drivetrain when the vehicle is set in motion. When a change in operation conditions makes it necessary to change gears, the clutch disengages the engine from the drivetrain for the duration of the procedure.

The Clutch contains a model for a friction clutch as it is used in cars with manual gearboxes. In this case the clutch is controlled by the driver via the cockpit [1].

For the transmission of maximum torque from the clutch to be without slip during the entire duration of functioning, it is necessary for the clutch friction torque M_a to be greater than the maximum torque of the engine. For this purpose a safety coefficient β is introduced in the relation [3]:

$$M_c = \beta \cdot M_{max} \, (\text{Nm}) \tag{3.13}$$

For the total friction torque we have [3]:

$$M_a = \frac{2}{3} \pi \cdot \mu \cdot p \cdot \left(R_e^3 - R_i^3 \right) (\text{Nm}) \tag{3.14}$$

where R_e is the exterior radius of the friction surface, R_i—the interior radius of the friction surface, and p:

$$p = \frac{F}{\pi \cdot \left(R_e^2 - R_i^2 \right)} (-) \tag{3.15}$$

The clutch friction torque becomes [3]:

$$M_a = \frac{2}{3} \cdot \mu \cdot F \cdot i \cdot \frac{R_e^3 - R_i^3}{R_e^2 - R_i^2} (\text{Nm}) \tag{3.16}$$

The medium radius of the clutch ($r_{C,m}$) to which the force operates is given by the relation [3]:

$$r_{C,m} = \frac{M_a}{N_C \cdot \mu_{C,st} \cdot F_C} \, (\text{m}) \tag{3.17}$$

The friction coefficient for clutch actuation ($\mu_{C,act}$) is calculated as such [3]:

$$\mu_{C,act} = \mu_{C,sl} + \left(\mu_{C,st} - \mu_{C,sl}\right) \cdot e^{\left(-\frac{\left|\dot{\varphi}_{c,rel}\right| \cdot c_C}{\mu_{c,st} - \mu_{c,sl}}\right)} \ (-) \qquad (3.18)$$

The torque necessary for clutch coupling (M_a) is given by the relation [3]:

$$M_a = \left|M_{a,in} - M_{a,out}\right| (\mathrm{Nm}) \qquad (3.19)$$

3.1.3 Equations of the Gearbox Element

Gear transmissions featuring several fixed ratios can maintain a correspondence between the respective performance curves for engine and vehicle. The correspondence with the hyperbola for maximum engine output will be acceptable or indeed quite good, depending upon a multiplicity of factors including the number of available gears, the spacing of the individual ratios within the required conversion range and the engine's full load torque curve [1, 3, 4].

The component Gearbox contains a model for a gearbox with different gear steps. For every gear it is possible to define the transmission ratio, the mass moments of inertia, and the moment of loss [1].

In the component for manual gearboxes, the engine torque will be turned into a power take-off torque by considering the transmission, the mass moments of inertia, and the moment of loss [1].

The gearbox can be used for a manual or automatic gearbox. When used as an automatic gearbox, the gear shifting process will be controlled by the control module gearbox control or gearbox program. The driver will do this task when used as a manual gearbox [1].

The torque transmitted by the engine is determined according to the secondary shaft torque M_s for the first gear [1, 3, 4]:

$$M_s = M_m \cdot i_{cv1} \cdot h_{cv1}(\mathrm{Nm}) \qquad (3.20)$$

where M_m is the maximum torque transmitted by the engine (Nm), i_{cv1}—transmission ratio of the first gear (–), h_{cv}—gearbox efficiency (–).

The calculation for number of teeth on the primary shaft of the gearbox is given by:

$$z_k = \frac{2 \cdot A \cdot \cos \beta_k}{m \cdot (1 + i_{cvk})} \ (-) \qquad (3.21)$$

$$z_k' = \frac{2 \cdot A \cdot \cos \beta_k \cdot i_{cvk}}{m \cdot (1 + i_{cvk})} \ (-) \qquad (3.22)$$

where i_{cvk} is the transmission ratio of gear k.

The distance between axis can be calculated with the formula [5]:

$$a = \frac{m_n \cdot (z_i - z_i')}{2 \cdot \cos \beta} \; (m)$$

(3.23)

The frontal pressure angle for reference is calculated [5]:

$$\alpha_t = \arctan \left[\frac{\tan \alpha_n}{2 \cdot \cos \beta} \right] \; (°)$$

(3.24)

The frontal pitch angle is calculated using the relation [5]:

$$\alpha_{tw} = \arccos \left[\frac{a}{a_w} \cdot \cos \alpha_t \right] \; (°)$$

(3.25)

The normal coefficient of summed displacement profiles, in relation to the involution of the α_t and α_{tw} angle is calculated with the help of the relations [5]:

$$x_{ns} = \frac{z_1 + z_2}{2 \cdot \tan \alpha_n} \cdot (inv\alpha_{tw} - inv\alpha_t) = \frac{z_1 + z_2}{2 \cdot \tan \alpha_n} \cdot [(\tan \alpha_{tw} - \alpha_{tw}) - (\tan \alpha_t - \alpha_t)]$$

(3.26)

3.1.4   Equations for the Final Drive Element

The Single Ratio Transmission is a gear step with fixed ratio. It can be used, e.g., as transmission step of the differential (Final Drive Unit).

A drive torque will be transferred to a power take-off torque of the transmission step by considering the transmission, the mass moments of inertia and the moment of loss [1].

The torque transmitted by the engine to the Final Drive element can be calculated with the help of the following relation [3]:

$$M_{cm} = M_n \cdot i_{cv} \cdot \eta_{cv} \cdot i_{c2} \cdot \eta_{c2} \cdot \frac{\lambda_2}{1 + \lambda_2} \; (Nm)$$

(3.27)

where M_n is the nominal torque of the engine, i_{cv}—transmission ratio of the gearbox (–), i_{c2}—transmission ratio of the central transmission (–), η_{cv}—gearbox efficiency (–), η_{c2}—efficiency of the central transmission from the rear axel (–), λ_2—the efficiency of blocking the differential (–).

The torque to be calculated from the adherence condition is determined by using the relation [3]:

$$M_{c\varphi} = \frac{Q_2 \cdot \varphi r_2}{i_{f2} \cdot \eta_{f2}} \text{ (Nm)} \tag{3.28}$$

where i_{f2}—transmission ratio of the final transmission (–), η_{f2}—efficiency of rear final transmission (–), Q_2—weight distributed on a rear motor wheel (kg), r_2—dynamic radius of rear wheels (m), and φ—adherence coefficient (–).

On the final transmissions pitch act two forces, a tangential force (F_t) and a radial force (F_r) [3]:

$$F_t = \frac{2M}{mz_1} \text{ (N)} \tag{3.29}$$

$$F_r = F_t \cdot \tan \alpha \text{ (N)} \tag{3.30}$$

where z_1 is the number of teeth of the pinion (–), m—pitch module (–), α—pitch angle (°).

3.1.5 Equations of the Differential Element

The Differential unit compensates for discrepancies in the respective rotation rates of the drive wheels: between inside and outside wheels during cornering and between different drive axels on 4WD vehicles [1].

With rare exceptions for special applications, the differential is a bevel gear drive unit. When the output bevel gears on the left and right sides (most common arrangement) are of equal dimensions, the differential gears act as a balance arm to equalize the distribution of torque to the left and right wheels [1].

When unilateral variations in road surfaces result in different coefficients of friction at the respective wheels, this balance effect limits the effective drive torque to a level defined as twice the traction force available at the wheel (tire) with the lower coefficient of friction. This wheel then responds to the application of excessive force by spinning. To avoid such effects a positive lock is available at the component [1].

The differential (Fig. 3.2) is a mechanism with the purpose of dividing a motion towards two receptors, or of coupling two motions and transmitting them towards one receptor. The differential of the vehicle has as purpose the adaptation of the motor wheels movements to the road configuration.

The differential uses the following equation to determine the torque [1]:

$$\dot{\varphi}_{N,in} \cdot (i_n + 1) = \dot{\varphi}_{N,out,1} + \dot{\varphi}_{N,out,2} \cdot i_N \text{ (rad/s)} \tag{3.31}$$

where i_N is the slip factor, $\dot{\varphi}_{N,in}$—the angular velocity on drive side (rad/s), $\dot{\varphi}_{N,out,1(2)}$—angular velocity on drive power side (rad/s) [3].
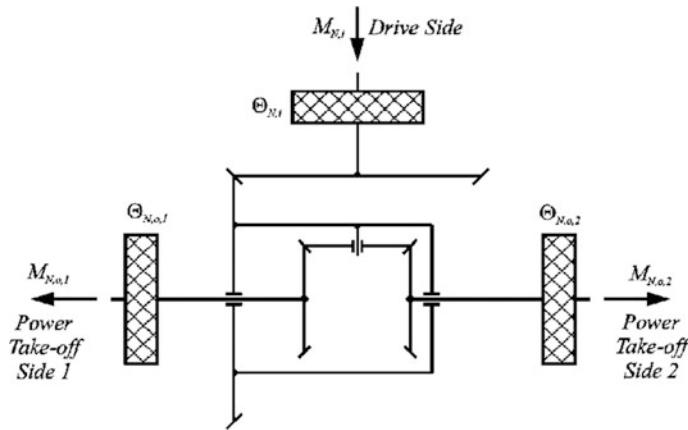
Fig. 3.2 Principle representation of a Differential [1]

3.1.6 Equations of the IC Engine Element

The component Engine contains a model for an internal combustion engine. As the characteristic curves for the full load, the fuel consumption and others can be freely defined by the user. In this component a temperature model is included to consider the influence of the temperature on the fuel consumption and emissions while the engine is cold. The engine will be modeled by a structure of characteristic curves and maps [1].

The external characteristic of the internal combustion engine is necessary to determine the traction and to study the performances of the vehicle. It presents two very important points, namely the maximum power P_m at maximum speed n_m, respectively the power corresponding to maximum coupling P_M at n_M speed.

The external characteristic can be determined using the following relations (3.32) for the power characteristic P_e, respectively (3.33) for the torque characteristic M_e [6]:

$$P_e = M_m \cdot \left[\alpha_1 \cdot \frac{n_e}{n_m} + \alpha_2 \cdot \left(\frac{n_e}{n_m} \right)^2 + \alpha_3 \cdot \left(\frac{n_e}{n_m} \right)^3 \right] \text{(kW)} \qquad (3.32)$$

$$M_e = M_m \cdot \left[\alpha_1 + \alpha_2 \cdot \frac{n_e}{n_m} + \alpha_3 \cdot \left(\frac{n_e}{n_m} \right)^2 \right] \text{(Nm)} \qquad (3.33)$$

where: $M_m = P_m/\omega_m$ is the torque corresponding to maximum power (Nm), $\omega_m = (2\pi n_m)/60$ is the angular velocity (rad/s), $\alpha_1 + \alpha_2 + \alpha_3 = 1$ are the coefficients which are determined using the relations [6]:

$$\alpha_1 = \frac{3 - 4 \cdot c}{2 \cdot (1 - c)} = 0.75 \qquad (3.34)$$

$$\alpha_2 = \frac{2 \cdot c}{2 \cdot (1 - c)} = 1.50 \qquad (3.35)$$

$$\alpha_3 = \frac{1}{2 \cdot (1 - c)} = -1.25 \qquad (3.36)$$

where: $c = n_M/n_m = 0.60$ is the elasticity coefficient.

Using the elasticity coefficient, the maximum torque speed can be determined:

$$n_M = c \cdot n_m \; (1/s) \qquad (3.37)$$

The maximum torque being given by the following relation [6]:

$$M_M = M_m \cdot \left[\alpha_1 + \alpha_2 \cdot \frac{n_M}{n_m} + \propto_3 \cdot \left(\frac{n_M}{n_m} \right)^2 \right] \; (Nm) \qquad (3.38)$$

The load characteristic expresses the measurements defining the engine performances, namely power, torque, and the average brake pressure BMEP (Brake Mean Effective Pressure) according to engine speed (φ) [1]:

$$\Delta p = p_{E,vk,help} - p_{E,sk,help} \qquad (3.39)$$

Interpolation of Full Load Characteristic and Motoring Curve for the actual engine speed for an engine speed lower than idle speed is [1]:

$$p_{eff,sk} = -\frac{\Delta p}{\dot{\varphi}_{E,idle}} \cdot f_{E,sk} \cdot \dot{\varphi}_{E,out} + p_{E,sk,help} + \Delta p \cdot f_{E,sk} \; (Pa) \qquad (3.40)$$

$$p_{eff,vk} = p_{eff,sk} + \frac{\Delta p}{\dot{\varphi}_{E,idle}^3} \cdot \left(f_{E,sk} - 1 \right) \cdot \dot{\varphi}_{E,out}^3 - \frac{\Delta p}{\dot{\varphi}_{E,idle}^2} \cdot \left(f_{E,sk} - 2 \right) \cdot \dot{\varphi}_{E,out}^2 \qquad (3.41)$$

and the factor $f_{E,sk} = 4$ for automatic gearboxes.

Considering the energy available in the air-fuel mixture as being 100 %, only 20 % from it gets to be used for vehicle drive. Approximately 80 % of the energy is lost through thermal transfer, mechanical friction and auxiliary equipment drive (Fig. 3.3).

The heat produced by the combustion will be computed from this formula [1]:

$$P_{E,heat} = b_{E,h,act} \cdot \rho_{E,fuel} \cdot H_{E,fuel} \; (kJ) \qquad (3.42)$$
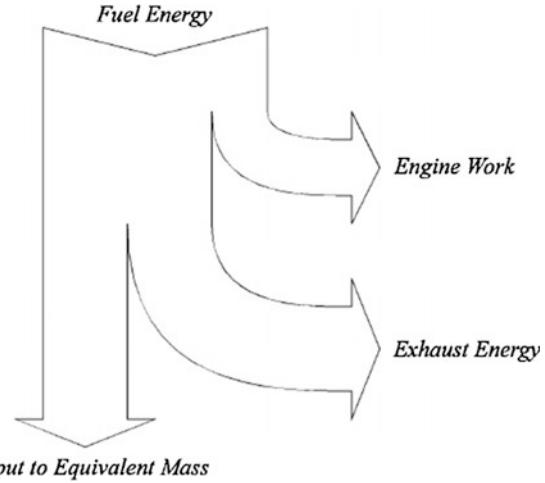
The mechanical power take-off [1]:

$$P_{E,act} = M_{E,act} \cdot \dot{\varphi}_{E,out} \ (kW) \tag{3.43}$$

The loss power in the exhaust emissions [1]:

$$P_{E,emis} = Z_{E,EE} \cdot \left(P_{E,heat} - P_{E,act} \right) \ (kW) \tag{3.44}$$

The rest energy has to go into the cooling system [1]:

$$P_{E,cool} = P_{E,heat} - P_{E,act} - P_{E,emis} \ (kW) \tag{3.45}$$

The characteristic for the friction mean pressure is given by the friction mean pressure at minimum ($p_{E,min}$) and maximum speed ($p_{E,max}$) and a curvature factor ($c_{E,fric,p}$) between them ($c_{E,fric,p} = 1$ means a linear characteristic).

At first, a reference value for the mean friction pressure BMEP ($p_{E,fric,ref}$) is calculated [1]:

$$f_B = \frac{p_{E,fric,max} - p_{E,fric,min}}{\left(\dot{\varphi}_{E,max} \right)^{c_{E,fric,p}} - \left(\dot{\varphi}_{E,idle} \right)^{c_{E,fric,p}}} \ (-) \tag{3.46}$$

where:

$$f_A = p_{E,fric,min} - f_B \cdot \left(\dot{\varphi}_{E,idle} \right)^{c_{E,fric,p}} \tag{3.47}$$

$$p_{E,fric,ref} = f_A + f_B \cdot \left| \dot{\varphi}_{E,out} \right|^{c_{E,fric,p}} \tag{3.48}$$

The crankshaft means effective pressure can be expressed as follows [1]:

$$\text{fmep} = c_{cb}\left(\frac{N\,D_b^3\,L_b\,n_b}{B^2\,S\,n_c}\right) + C_{cs}\left(\frac{D_b}{B^2\,S\,n_c}\right) + c_{td}\left(\frac{N^2\,D_b^2\,n_b}{n_c}\right)\ (\text{Pa}) \qquad (3.49)$$

where: B is the cylinder diameter (m), S—stroke (m), D_b—bearing diameter (m), L_b—bearing length (m), n_c—number of cylinders (–), n_b—number of bearings (–), N—engine speed (1/min), c_{cb}—coefficient of hydrodynamic losses in bearings (–), C_{cs}—coefficient of friction losses in bearings, C_{td}—coefficient of frictions losses due to viscosity (–).

The friction means effective pressure in the reciprocating group may be calculated using the following equation [1]:

$$\text{mep}_{pb} = c_{pb}\left(\frac{N\,D_b^3\,L_b\,n_b}{B^2\,S\,n_c}\right) + C_{ps}\left(\frac{V_p}{B}\right) + C_{pr}\left(1 + \frac{10^3}{N}\right)\left(\frac{1}{B^2}\right)C_o\frac{P_i}{P_a}\left(0.182\,r_c^{\left(1.33 - 2.38\,V_p\right)}\right)$$

$$(3.50)$$

where: c_{pb}—coefficient of hydrodynamic losses in connecting rod bearing (–), C_{ps}—coefficient of losses due to thermal transfer through cylinder wall (–), C_{pr}—coefficient of losses due to thermal transfer through piston rings (–), C_o—coefficient of losses for pressure of combustion gasses de (–), V_p—medium velocity of the piston (m/s).

The friction means effective pressure in the valve train is calculated using the following equation [1]:

$$\text{fmep}_{cv} = c_{vb}\left(\frac{N\,n_b}{B^2\,S\,n_c}\right) + c_{vo} + C_{vh}\left(\frac{L_v^{1.5}\,N^{0.5}\,n_v}{B\,S\,n_c}\right) + C_{vm}\left(1 + \frac{10^3}{N}\right)\frac{L_v n_v}{S\,n_c} + \text{fmep}_{cam\,follower}$$

$$(3.51)$$

$$\text{fmep}_{cam\,follower} = C_{vf}\left(1 + \frac{10^3}{N}\right)\frac{n_v}{S\,n_c}\ (\text{Pa}) \qquad (3.52)$$

$$\text{fmep}_{cam\,follower} = C_{vr}\left(\frac{N\,n_v}{S\,n_c}\right)\ (\text{Pa}) \qquad (3.53)$$

where: c_{vb}—coefficient of hydrodynamic losses in camshaft bearing (–), C_{vh}—coefficient of hydrodynamic lubrication due to oscillations (–), C_{vm}—coefficient of mixed lubrication due to oscillations (–), C_{vo}—coefficient of lubrication due to camshaft movement (–), L_v—maximum valve lift height (m), n_v—number of valves (–).

Means effective pressure due to the friction in the piston group is expressed as follows [1]:

$$\text{fmep}_{\text{crankshaft}} = c_{cb}\left(\frac{N^{0.6}\, D_b^3\, L_b\, n_b}{B^2\, S\, n_c}\right)\left(\frac{\mu}{\mu_{\text{ref}}}\right)^n + C_{cs}\left(\frac{D_b}{B^2\, S\, n_c}\right)\ (\text{Pa}) \qquad (3.54)$$

where: c_{cb}—coefficient of hydrodynamic losses in crankshaft bearing (–), C_{cs}—coefficient of losses through friction in shaft bearings (–), n—viscosity index (–), μ_{ref}—dynamic oil viscosity (m^2/s).

Means effective pressure due to the friction in the piston group is expressed as follows [1]:

$$\text{fmep}_{\text{piston}} = \left(c_{pb}\left(\frac{N^{0.6}\, D_b^3\, L_b\, n_b}{B^2\, S\, n_c}\right) + C_{ps}\left(\frac{V_p^{0.5}}{B}\right) + C_{pr}\left(\frac{V_p^{0.5}}{B^2}\right)\right)\left(\frac{\mu}{\mu_{\text{ref}}}\right)^n\ (\text{Pa})$$

$$(3.55)$$

where c_{pb}—coefficient of hydrodynamic losses in connecting rod bearing (–), C_{ps}—coefficient of losses due to thermal transfer through cylinder wall (–), C_{pr}—coefficient of losses due to thermal transfer through piston rings (–), n—viscosity index (0.4).

Total losses through friction for the distribution system is expressed through the relation [1]:

$$\text{fmep}_{vt} = c_{vb}\left(\frac{N^{0.6}\, n_b}{B^2\, S\, n_c}\right)\left(\frac{\mu}{\mu_{\text{ref}}}\right)^n + C_{vh}\left(\frac{L_v^{1.5}\, N^{0.5}\, n_v}{B\, S\, n_c}\right)\left(\frac{\mu}{\mu_{\text{ref}}}\right)^n + C_{vm}\left(2 + \frac{10}{5 + \mu N}\right)\frac{L_v n_v}{S\, n_c} + \text{fmep}_{cf}$$

$$(3.56)$$

$$\text{fmep}_{\text{cam follower}} = C_{vf}\left(2 + \frac{10}{5 + \mu N}\right)\frac{n_v}{S\, n_c} = C_{vr}\left(\frac{N\, n_v}{S\, n_c}\right) \qquad (3.57)$$

where c_{vb}—coefficient of hydrodynamic losses in camshaft (–), C_{vh}—coefficient of hydrodynamic lubrication due to oscillations (–), C_{vm}—coefficient of mixed lubrication due to oscillations (–), n—viscosity index (0.4).

3.1.7 Equations of the E-Machine (Generator) Element

The Generator (alternator) must provide the vehicle electrical system with a sufficient supply of current under all operating conditions in order to ensure that the State of Charge (SOC) in the engine storage device (battery) is consistently maintained at an adequate level. The object is to achieve balanced charging, i.e., the curves for performance and speed–frequency response must be selected to ensure that the amount of current generated by the alternator under actual operating

conditions is at least equal to the consumption of all electrical equipment within the same period [1].

Automotive alternators are designed to supply charge voltages of 28 V for heavy utility vehicles or buses, in order to maintain an adequate charge in 24 V batteries.

The alternator produces alternating current (AC). The vehicle's electrical system, on the other hand, requires direct current to recharge the battery and operate the electrical equipment; it is thus direct current that must ultimately be supplied to the electrical system. For this case a rectifier must be provided to convert the alternator's three-phase alternating current into direct current (DC).

This arrangement also provides the battery from discharging when the vehicle is stationary. In the input data for the component generator the already into direct current converted characteristics have to be given. The characteristics used here are measured behind the rectifier [1].

In the component generator a simple regulator is integrated. The regulator works in that way that a threshold voltage has to be defined. If the voltage of the onboard network is below this threshold the generator is activated.

The generator will be separated from the network if the voltage of the onboard network reaches the threshold [1].

The current delivered by the generator results from a map dependent on the speed and the mains voltage. By considering the internal resistance, the instantaneous current consumption helps to acquire the torque absorbed by the generator with the corresponding moments of loss [1].

The maximum values of the generator current and voltage $I_{L,max,act}$, $U_{L,max,act}$ for a given angular velocity is evaluated out of the maps. The minimum voltage is determined be the equation [1]:

$$U_{L,min,act} = U_{L,max,act} - \sqrt{\frac{I_{L,max,act}}{R_{G,equ}}} \, (V) \tag{3.58}$$

The controller current and voltage $I_{L,max,cont}$, $U_{L,max,cont}$ for a given angular velocity is evaluated out of the maps. The controller factor is defined as function of the controller current [1]:

$$C_{L,cont} = -R_{G,equ} \cdot \frac{1}{I_{L,max,cont}} \, (-) \tag{3.59}$$

The minimum voltage fixed by the controller [1]:

$$U_{L,min,cont} = U_{L,max,cont} + C_{L,cont} \cdot I_{c,max,act} \, (V) \tag{3.60}$$

The current flow depends on the net and the controller minimum and maximum voltages as well as the controller factor [1]:

$$I_L = -\frac{\left(U_{L,net} - U_{L,min,cont}\right) \cdot \lfloor 1 - \left(U_{L,net} - U_{L,max,cont}\right)\rfloor}{C_{L,cont} \cdot \left(U_{L,net} - U_{L,max,cont}\right)} \ (A) \tag{3.61}$$

In the Generator Characteristic, the current flow is fixed by the net and the controller minimum and maximum voltages as well as the maximum available generator current [1]:

$$
\begin{aligned}
I_L = &-I_{L,max,act} - R_{G,equ} \cdot \left(U_{L,net} - U_{L,max,act} + \sqrt{\frac{I_{L,max,act}}{R_{G,equ}}}\right)^2 \cdot \left(U_{L,net} - U_{L,min,act}\right) \\
&\cdot \left[1 - \left(U_{L,net} - U_{L,max,act}\right)\right] \ (A)
\end{aligned}
\tag{3.62}
$$

In the Mixed Characteristic, the conditions are changing between Generator Characteristic and Controller Characteristic. The switch voltage determines the actual used characteristic [1]:

$$U_{L,switch} = -\frac{b}{2 \cdot a} + \sqrt{\frac{b^2 - 4 \cdot a \cdot c}{2 \cdot a}}(V) \tag{3.63}$$

where the values of system parameter a, b and c are given using the following calculation relations:

$$a = -R_{G,equ} \ (-) \tag{3.64}$$

$$b = -2 \cdot \left(-U_{L,max,act} + \sqrt{\frac{I_{L,max,act}}{R_{G,equ}}}\right) \cdot R_{G,equ} - \frac{1}{C_{L,cont}} \ (-) \tag{3.65}$$

$$c = I_{C,max,act} \cdot R_{G,equ} \cdot \left(-U_{L,max,act} + \sqrt{\frac{I_{L,max,act}}{R_{G,equ}}}\right)^2 + \frac{U_{L,max,cont}}{C_{L,cont}} \ (-) \tag{3.66}$$

For the torque calculation, the loss moment and the working moment have to be added. The loss moment $M_{L,pd,act}$ is interpolated out of the loss function. Thus, we can write the equation for the whole generator torque [1]:

$$M_{L,in} = M_{L,pt,act} - \frac{I_L \cdot U_{L,net}}{Z_L \cdot \dot{\phi}_{L,in}} \ (Nm) \tag{3.67}$$

The overall efficiency value $\eta_{L,act}$ is evaluated out of the map for the actual current flow and the generator speed. Thus, we can write the equation for the whole generator torque [1]:

$$M_{L,in} = -\frac{1}{\eta_{L,act}} \cdot \frac{I_L \cdot U_{L,net}}{\eta_{L,el} \cdot \dot{\varphi}_{L,in}} \ (Nm) \tag{3.68}$$

3.1.8   Equations of the E-Machine (Motor) Element

The Electric Motor can be used for electrically driven vehicles, cars with hybrid drive or to operate auxiliaries such as a fan or an oil pump.

The electric motor is defined by means of characteristic curves. Therefore, different motor type models can be constructed [1].

The value of the voltage level should be entered at which the following Characteristic Maps of the machine have been measured. In addition to the U1 level, up to 4 further levels U2–U5 could be activated in the property window. For each activated level the corresponding voltage value must be defined and the corresponding Characteristic Maps.

Calculation of the actual current by the current–voltage map [1]:

$$I_{J,act} = \frac{P_{J,el,act}}{U_{J,act}} \ (A) \tag{3.69}$$

Calculation of the actual power and the actual current by the efficiency map and the starting current [1]:

$$P_{J,el,act} = \frac{P_{J,mech,act}}{J,act} \ (kW) \tag{3.70}$$

The actual moment of the drivetrain is given by [1]:

$$M_{EM,dt} = M_{EM} - \Theta_{EM,nom}\ddot{\varphi}_{EM,out} \ (Nm) \tag{3.71}$$

Functioning losses for the electric vehicle in motor-related mode are as follows [1]:

$$P_{EM,loss,act} = P_{EM,mech,act}\left(1/\eta_{EM}\left(M_{EM,out}, \dot{\varphi}_{EM,out}\right) - 1\right) \ (kW) \tag{3.72}$$

$$P_{EM,loss,act} = \dot{\varphi}_{EM,out,1}M_{EM,}\left(1/\eta_{EM}\left(M_{EM,out}, \dot{\varphi}_{EM,out}\right) - 1\right) \ (kW) \tag{3.73}$$

Functioning losses for electric vehicle in generator-related mode are as follows [1]:

$$P_{EM,loss} = \left| P_{EM,mech}(1 - \eta_{EM}(M_{EM}, \dot{\varphi}_{EM})) \right| (kW) \tag{3.74}$$

$$P_{EM,loss} = \left| \dot{\varphi}_{EM,1} M_{EM}(1 - \eta_{EM}(M_{EM}, \dot{\varphi}_{EM})) \right| (kW) \tag{3.75}$$

$$\begin{aligned} P_{EM,loss} = \dot{\varphi}_{EM} M_{EM,1} \big[a(M_{EM})\big(1/\eta_{EM}\big(M_{EM,1}, \dot{\varphi}_{EM}\big) - 1\big) \\ + (1 - a(M_{EM}))\big(1 - \eta_{EM}\big(M_{EM,1}, \dot{\varphi}_{EM}\big)\big) \big] (kW) \end{aligned} \tag{3.76}$$

$$\begin{aligned} P_{EM,loss} = \dot{\varphi}_{EM} M_{EM,1} \big[a(M_{EM})\big(1/\eta_{EM}\big(M_{EM,1}, \dot{\varphi}_{EM,1}\big) - 1\big) \\ + (1 - a(M_{EM}))\big(1 - \eta_{EM}\big(M_{EM,1}, \dot{\varphi}_{EM,1}\big)\big) \big] (kW) \end{aligned} \tag{3.77}$$

where:

$$a(M_{EM}) = \big(M_{EM} - M_{EM,drag}\dot{\varphi}_{EM}^2\big)/\big(M_{EM,1} - M_{EM,drag}\dot{\varphi}_{EM}^2\big) (kW) \tag{3.78}$$

The difference between the losses in motor-related mode and the losses in generator-related mode is given by the lowest torque in the Characteristic Map and the drag torque. In the domain above the smallest positive torque the motor-related mode is used and the efficiency is unique defined. In the domain below the negative torque and below the drag torque the generator-related mode is used. In the domain between the described domains again the motor-related mode is being used. There a smooth transition in the loss of power.

3.1.9 Equations of the Battery Element

Together with the components supercapacitor and electric machine, the component Battery H is used for modeling hybrid vehicles.

The basic model consists of a voltage source and a resistance. The resistance is constructed that way that complex processes within the battery can be considered. 2 RC elements can be added optionally. They describe the concentration overvoltage and the transition overvoltage.

Also, the resistance's dependence on the temperature can be activated optionally. There can be modeled single cells as well as a combination of them. Therefore, any modules can be constructed [1].

The thermal behavior of the battery is described by a thermal model. Here, the warming caused by the losses and the cooling caused by convection is taken under consideration [1].

The batteries of the vehicle convert the electric energy in potential chemical energy during charging, respectively the potential chemical energy in electric energy during discharging. A battery is made of elementary cells connected together. Each battery cell is composed of three primary elements: the positive electrode, the negative electrode and the electrolyte.

An important parameter of the battery is the SOC (State Of Charge), which is the ratio between the battery current capacity and total capacity. Modifying the SOC in the time interval dt with a constant charging current, respectively a discharging current i can be expressed as follows [6]:

$$dSOC = \frac{dQ}{Q(t)} = \frac{idt}{Q(i)} \tag{3.79}$$

where Q(i) is the battery capacity for the discharging current i.

Within state of charge the current has a negative value and within state of discharge the current has a positive value. Thus, the charge ratio of the battery can be expressed as [6]:

$$SOC = SOC_0 - \int \frac{idt}{Q(t)} \tag{3.80}$$

where SOC_0 is the initial value of the charge rate. The power taken by load resistance is expressed as follows [6]:

$$P_{load} = R_{load} \cdot I_b^2 = R_{load} \left(\frac{v_0}{R_{int} + R_{load} + R_{ohm}} \right) (\text{kW}) \tag{3.81}$$

The model of a battery with elements used for an electric motor is the one from Fig. 3.4 [1].

The electrical equations of a battery cell are described as follows [1]:

$$U_{QH,term} = U_{QH,idle} \left(I_{QH,term}, SOC \right) - I_{QH,ohmic} \cdot R_{QH} \left(I_{QH,term} \right) \\ - Q_{QH,conc}/C_{QH,conc} - Q_{QH,trans}/C_{QH,trans} \ (\text{V}) \tag{3.82}$$

$$I_{QH,ohmic,trans} = Q_{QH,trans}/\left(C_{QH,trans} \cdot R_{QH,trans} \right) (\text{A}) \tag{3.83}$$

$$I_{QH,ohmic,conc} = Q_{QH,conc}/\left(C_{QH,conc} \cdot R_{QH,conc} \right) (\text{A}) \tag{3.84}$$
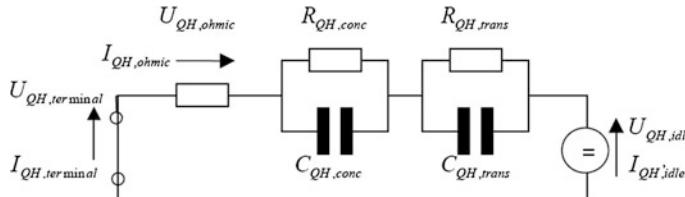
Fig. 3.4   Model for battery with elements [1]

Here the current influences the idle voltage and the resistance only by its sign. The maximal currents of the battery cell are calculated by [1]:

$$I_{QH,max,charge} = \frac{\left[U_{QH,idle,charge}\left(I_{QH,term}, SOC\right) - U_{QH,max} - \frac{Q_{QH,conc}}{C_{QH,conc}} - \frac{Q_{QH,trans}}{C_{QH,trans}}\right]}{R_{QH}\left(I_{QH,terminal}\right)} \ (A)$$

(3.85)

$$I_{QH,max,discharge} = \frac{\left[U_{QH,idle,discharge}\left(I_{QH,term}, SOC\right) - U_{QH,min} - \frac{Q_{QH,conc}}{C_{QH,conc}} - \frac{Q_{QH,trans}}{C_{QH,trans}}\right]}{R_{QH}\left(I_{QH,terminal}\right)}$$

(3.86)

The initial values are calculated by [1]:

$$Q_{QH,init} = SOC_{QH,init} \cdot Q_{QH,max} = \frac{Q_{QH}}{Q_{QH,max}} \cdot Q_{QH,max}$$

(3.87)

The basic equation for the heating within a material is [1]:

$$dQ = m_{QH,cell} \cdot C_{QH,heat} dT_{QH,bat} = P_{QH,th} dt$$

(3.88)

Here, $P_{QH,th}$ is the total power that is converted into heat. It consists of the heat power inside the cell caused by electrical losses, and of the heat transfer to the environment [1]:

$$P_{QH,th} = P_{QH,th,el} + P_{QH,th,ambient} \ (kW)$$

(3.89)

$$P_{QH,th,ambient} = \alpha_{QH,th,trans}\left(T_{QH,bat} - T_{QH,ambient}\right) \ (kW)$$

(3.90)

$$\begin{aligned} P_{QH,th,el} = {} & I_{QH,ohmic}^2 \cdot R_{QH} + I_{QH,ohmic,trans}^2 \cdot R_{QH,trans} + I_{QH,conc}^2\left(T_{QH,act}\right) \cdot R_{QH,conc} \\ & + \left|0.5 I_{QH,terminal} \cdot \left(U_{QH,idle}\left(I_{QH,terminal} \cdot SOC_{QH}\right) - U_{QH,idle}\left(-I_{QH,terminal}, SOC_{QH}\right)\right)\right| \end{aligned}$$

(3.91)

With the last term describing the losses caused by the polarization voltage [1].

3.1.10 Equations of the GB Control Element

The GB Control is needed to define an automatic gearbox. In the GB Control, the gear shifting process can be defined automatically without any influence of the driver [1].

The GB Control shifts the gears dependent on a speed or a velocity. The decision which one of the two shifting strategies is used is done in the calculation tasks.

Which speed, respectively which velocity is used can be defined via the Data Bus. It is possible to define the engine speed but it is also possible to define the wheel speed as reference [1].

The GB Control is also the connection between the gearbox program and the gearbox [1].

The gear shifting strategy up ($Z_{cont,up}$) and down ($Z_{cont,dn}$) has the information from where the GB Control should take the target gear: profile shifting, velocity shifting, speed shifting, program shifting. The target gear position comes from the driving profile [1].

The target gear position comes from the driving profile [1]:

$$\left(j_{G,target} \geq j_{G,act}\right) \rightarrow j_{G,new,up} = j_{G,target} \tag{3.92}$$

$$\left(j_{G,target} \leq j_{G,act}\right) \rightarrow j_{G,new,dn} = j_{G,target} \tag{3.93}$$

The reference is the vehicle velocity [1]:

$$\left(j_{G,act} < N_G\right) \wedge \left(V_{v,act} \geq V_{o,incr}\lfloor j_{G,act}\rfloor\right) \rightarrow j_{G,new,up} = j_{G,act} + 1 \tag{3.94}$$

$$\left(j_{G,act} > 1\right) \wedge \left(V_{v,act} \leq V_{o,decv}\lfloor j_{G,act}\rfloor\right) \rightarrow j_{G,new,dn} = j_{G,act} - 1 \tag{3.95}$$

Each angular velocity could be selected via Data Bus for the reference speed [1]:

$$\left(j_{G,act} < N_G\right) \wedge \left(\dot{\varphi}_{ref,act} \geq \dot{\varphi}_{o,incr}\lfloor j_{G,act}\rfloor\right) \rightarrow j_{G,new,up} = j_{G,act} + 1 \tag{3.96}$$

$$\left(j_{G,act} > 1\right) \wedge \left(\dot{\varphi}_{ref,act} \leq \dot{\varphi}_{o,deu}\lfloor j_{G,act}\rfloor\right) \rightarrow j_{G,new,dn} = j_{G,act} - 1 \tag{3.97}$$

The shifting information is taken from the shifting program. For up- and downshifting [1]:

$$\left(j_{G,prog} \geq j_{G,act}\right) \rightarrow j_{G,new,up} = j_{G,prog} \tag{3.98}$$

$$\left(j_{G,prog} \leq j_{G,act}\right) \rightarrow j_{G,new,dn} = j_{G,prog} \tag{3.99}$$

The new gear position is chosen as follows [1]:

$$\left(j_{G,new,up} \geq j_{G,act} + 1\right) \rightarrow j_{G,new} = j_{G,act} + 1 \tag{3.100}$$

$$\left(j_{G,new,dn} \leq j_{G,act} - 1\right) \rightarrow j_{G,new} = j_{G,act} - 1 \tag{3.101}$$

$$else \rightarrow j_{G,new} = j_{G,act} \tag{3.102}$$

3.1.11   Equations of the GB Program Element

GB Program is used for automatic gearboxes in combination with the gearbox control. The gearbox program allows for a more complicated gear shifting process than the gearbox control, because here in addition the load signal of the engine is considered [1].

The gearbox program shifts the gears according to given curves. The curves are given as a function of the load signal and the engine speed. The target gear determined by the program is transmitted to the gearbox control that transmits it to the gearbox. Furthermore the curves could be optimized using iSIGHT. These optimized curves (optimized shifting program) could also be used as input curves for the gearbox program [1].

The basics of SQP algorithms is described in more detail below. The idea of this algorithm is to formulate and solve a quadratic programming sub problem in each iteration which is obtained by linearizing the constraints and approximating the Lagrangian function [1]:

$$L(x, u) := f(x) - \sum_{j=1}^{m} u_j g_j(x) \tag{3.103}$$

$$\min \frac{1}{2} d^T B_k d + \nabla f(x_k)^T d,$$
$$d \in IR^n : \nabla g_j(x_k)^T d + g_j(x_k) = 0, \, j = 1, \ldots, m_e \tag{3.104}$$

$$\nabla g_j(x_k)^T d + g_j(x_k) \geq 0, \, j = m_e, \ldots, m,$$
$$\begin{pmatrix} x_{k+1} \\ v_{k+1} \end{pmatrix} := \begin{pmatrix} x_k \\ v_k \end{pmatrix} + \alpha_k \begin{pmatrix} d_k \\ u_k - v_k \end{pmatrix} \tag{3.105}$$

$$q_k := \nabla_x L(x_{k+1}, u_k) - \nabla_x L(x_k, u_k),$$
$$w_k := x_{k+1} - x_k, \, B_{k+1} := \prod (B_k, q_k, w_k) \tag{3.106}$$

3.1.12   Equations of the Wheel Element

The wheels and tires link the vehicle to the road. The component Wheel allows to consider many influencing variables and their effect on the rolling state.

The moment of rolling drag can be computed on the basis of the wheel load, the corrected dynamic rolling radius, and the coefficient of rolling drag [1].

The longitudinal tire force (circumferential force) results from the friction coefficient, the wheel load as well as from the wheel load factor and the slip factor.

It is possible to define variable friction coefficients along the driving profile when different road conditions are considered [1].

The wheel component also includes a detailed rolling resistance. This model describes the rolling resistance of the tire depending on the tire inflation pressure, load, translation speed, the ambient temperature and the time [1].

Rolling Drag Moment is [1]:

$$M_{W,roll} = F_{W,in} \cdot c_{W,r}(v_{V,act}) \cdot r_{W,dyn} \ (Nm) \qquad (3.107)$$

The rolling resistance coefficient is evaluated out of the map $C_{w,f}(V_v)$ for the actual vehicle velocity. The rolling resistance is defined as followed [1]:

$$c = c_v + c_\rho + c_{RL} + c_T + c_p \ (-) \qquad (3.108)$$

where c is the rolling resistance coefficient (–), c_v—real vehicle velocity (m/s), c_ρ— rolling resistance influenced by the lateral slip angle, namely [1]:

$$c_\rho = \frac{m_{vehicle} \cdot v_{vehicle}^2}{\rho \cdot g} \cdot abs\left(sin\left(\alpha_{f(r)}\right)\right) \ (Nm) \qquad (3.109)$$

where $\alpha_{f(r)}$ is the slip angle (°), c_{RL}—load on each motor wheel (Nm), c_T—wheel temperature (°C), c_p—wheel pressure (Pa).

With this, we calculate the slip coefficients [1]:

$$C_{w,coeff1} = 2 - \frac{2 \cdot arcsin\left(\mu_{w,asxm,act}\right)}{\pi} \ (-) \qquad (3.110)$$

$$C_{w,coeff2} = \frac{1}{S_{W,peak,act}} \cdot tan\frac{\pi^2}{4 \cdot \left(\pi - arcsin\left(\mu_{w,asym,act}\right)\right)} (-) \qquad (3.111)$$

where:

$$s_W = \frac{\dot{\phi}_{W,in} \cdot r_{W,dyn} - v_{V,act}}{v_{W,ref}} \quad for \ \left|v_{W,ref}\right| < 10^{-4} s_W = 0 \qquad (3.112)$$

The Transmittable Longitudinal Wheel Force is the force value which can be transmitted by the wheel—road friction. The maximum slip correction factor is [1]:

$$C_{W,lim} = sin C_{W,coeff1} \cdot arctan\left(C_{W,coeff2} \cdot S_W\right)$$
$$\cdot tan\left[3.6 \cdot \left(v_{V,act}^2 + 0.0278 + \left(\dot{\phi} \cdot r_{W,dyn}\right)^2 \cdot 0.02\right)\right] (-) \qquad (3.113)$$

The steady state rolling resistance value $F_{W,roll,stab}$ at current conditions as a function of tire load $F_{W,act}$, tire inflation pressure $z_{V,load}$, tire translation speed $v_{W,act}$ and ambient temperature T_u [1]:

$$F_{W,roll,stab} = c_{W,roll,ISO}$$
$$\cdot F_{W,act} \left(\frac{p_{act}}{p_{W,ISO}}\right)^{\alpha_w} \left(\frac{F_{W,act}}{F_{W,ISO}}\right)^{\beta_w} \cdot \left[1 + b\left(\frac{v_{W,act} - v_{W,ISO}}{v_{W,ISO}}\right) + c\left(\frac{v_{W,act} - v_{W,ISO}}{v_{W,ISO}}\right)^2\right]$$
$$\cdot \left[1 + c_{W,ambient}\left(T_{W,ISO} - T_U\right)\right] (N) \tag{3.114}$$

The instantaneous average tire temperature at each time increment is then obtained by integrating [1]:

$$T_{W,act}(t) - T_{W,act,last} = \frac{1}{m_W \cdot C_{W,heq}} \int_0^t \left[F_{W,roll} \cdot v_{W,act} - c_{W,heat}\right.$$
$$\left. \cdot A_W\left(T_{W,act,last} - T_U\right)\right] d\tilde{t} \tag{3.115}$$

where:

$$F_{W,roll} = F_{W,roll,stab}\left[1 + k_{W,emp}\left(T_{W,act} - T_{W,stab}\right)\right] \tag{3.116}$$

$$F_{W,roll} = F_{W,roll} + c_{W,aero}\left(\frac{v_{W,act}}{v_{W,ISO}}\right)^2 \tag{3.117}$$

3.2   Algorithm of the Simulation Process

The AVL CRUISE application is a suite software instruments used for simulation for a variety of vehicle models, with which one can generate, develop and study diverse constructive categories from vehicles to buses. The preprocessing program is used to enter the initial data, the input data and the technical characteristics of the vehicle to be constructed as a model for the simulation process. After the effective assembly of the elements composing the vehicle, together with the annexed systems, mathematical equations and the calculation algorithms of the model lying behind the GUI (Graphical User Interface), the processes requested during the simulations are analyzed and calculated [3].

The steps made in order to define the algorithm of the computer simulation process (Fig. 3.5) are as follows [1]:

- creation of the project, respectively the model version of the simulated vehicle;
- insertion of defined elements in the graphical interface of the program;
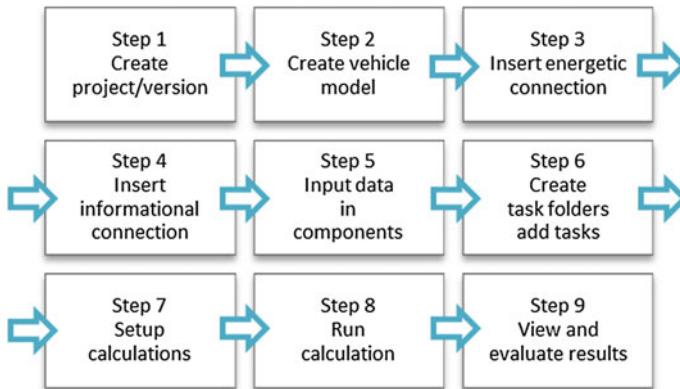
Fig. 3.5 Algorithm of the simulation process

- connection of defined elements through energetic connections and data connections;
- defining the functional parameters for defined component elements in the model;
- defining the control parameters of the simulation process (task folders and tasks);
- defining the simulation series;
- running the computer simulations to determine energetic flows of the model of vehicle built, analysis and interpretation of the results obtained from the simulations.

For the analysis of hybrid and electric vehicles from the point of view of consumption, many analysis methods are used amongst which the average operating point approach, the quasi-static method and the dynamic modelling. In this step firstly are determined the requirements and restrictions of the model, and then the system components are designed.

The numerical simulation is a methodology used for optimizing the performances of hybrid and electric vehicles. This type of analysis is also used by vehicle manufacturers to reduce the development costs for prototypes and the time necessary for their execution. The architecture of vehicles contains different subsystems, interconnected through mechanical, electric and control connections. That is why a computer simulation is based on mixed signals.

One essential requirement imposed for Embedded Systems and DSP-Based Systems is to operate in real time, with the guarantee of respecting the time intervals imposed by design and environmental specifications. An easy and quick transition can be made from project concepts to experimental verifications with the help of some adequate instruments: CACSD (Computer Aided Control Systems Design). The CACSD instruments are more and more intensely used by vehicle manufacturers [7].

The simulation processes offer a series of advantages, such as reduces costs for the construction of a model, the possibility of changing its structure during any step of the simulation process and of adapting the model characteristics to the requests of the user in a very short time interval. By using computer simulations validated through experimental measurements we have the certainty of obtaining exact results during our research work.

The data obtained from computer simulations were then subjects to validation tests through statistical methods of eliminating errors for measurement values recorded by using the Fisher statistical test [7].

After validating the results obtained from experimental determinations, they were analyzed in comparison with the results obtained from computer simulations.

3.3   Simulation for the Classic Bus Model in AVL CRUISE

To simulate how a classic bus powered by diesel engine works, a model was created and developed for computer simulation in the AVL CRUISE application for a bus equipped with an internal combustion engine (Fig. 3.6).

The elements composing the model are as follows:

• Vehicle (1)	• Front Disk Brake (13)
• IC Engine (2)	• Rear Disk Brake (14)
• Clutch (3)	• Front Disk Brake (15)
• Gearbox (4)	• Rear Differential (16)
• Final Drive Rear (5)	• Cockpit (17)
• Vehicle Rear Right (6)	• GB Control (18)
• Vehicle Front Right (7)	• GB Program (19)
• Vehicle Rear Left (8)	• Catalyst (20)
• Vehicle Front Left (9)	• Multiplex Function (21)
• Vehicle Rear Right (10)	• Monitor (22)
• Vehicle Rear Left (11)	• AMT Control (23)
• Rear Disk Brake (12)	

All the connections in the Data Bus for this model are described in Table 3.1 [4]. Validation of the connections are marked using bold and are required for the functioning of the model.

Vehicle (1) is one of the main objects in a model. This component contains general data of the vehicle, such as nominal dimensions and weights. Only one vehicle component is required in a model. Road resistances and dynamic wheel loads are calculated for road and dynamometer runs based on the dimensions and the load state. The wheel loads are calculated considering motion. The aerodynamic, rolling, climbing, acceleration, and total resistance are calculated [1].
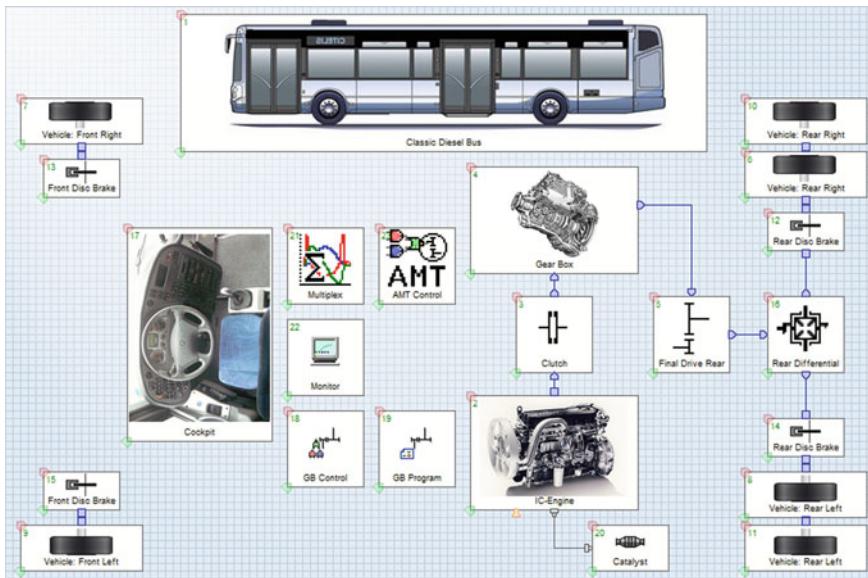
Fig. 3.6 Classic bus model

To define component input data (Table 3.2) double click on the icon or click on it the right mouse button and select edit to open the following window.

IC Engine (2) component contains a model for an internal combustion engine. The characteristic curves for the full load, fuel consumption, and others can be freely defined by the user. It is possible to define a gasoline engine as well as a diesel engine. In this component a temperature model is included to consider the influence of the temperature on the fuel consumption and emissions while the engine is cold. The engine will be modeled by a structure of characteristic curves and maps [1].

Characteristic curves for maximum load, fuel consumption etc. can be defined by the user by entering the initial data (Table 3.3). The graphic for internal combustion engine torque variation is presented in Fig. 3.7.

The calculation for injection parameters can be made based on the Fuel Consumption Map (Fig. 3.8).

The Clutch (3) makes stationary idle possible, transition to motion, and interruption of the power flow. The clutch slips to compensate for the difference in the rotational speeds of engine and drive train when the vehicle is set in motion. When a change in operation conditions makes it necessary to change gears, the clutch disengages the engine from the drivetrain for the duration of the procedure [1].

To define component input data (Table 3.4) double click on the icon and select edit to open the following window.

Table 3.1 Data Bus Connection

Component requires	Input information	Component delivering	Output information
AMT Control	**Current Gear**	Gearbox	Current Gear
	Desired Gear	GB Control	Desired Gear
	Input Speed	Clutch	Input Speed
	Load Signal	Cockpit	Load Signal
	Output Speed	Clutch	Output Speed
	Velocity	Vehicle	Velocity
Rear Brake	**Brake Pressure**	Multiplex	Cockpit_brake_pressure
Front Brake	**Brake Pressure**	Multiplex	Cockpit_brake_pressure
Rear Brake	**Brake Pressure**	Multiplex	Cockpit_brake_pressure
Front Brake	**Brake Pressure**	Multiplex	Cockpit_brake_pressure
Clutch	**Desired Clutch Release**	AMT Control	Desired Clutch Release
Cockpit	**Gear Indicator**	Gearbox	Current Gear
	Operation Control	IC Engine	Operation Control
	Speed	IC Engine	Engine Speed
IC Engine	**Load Signal**	AMT Control	Load Signal
	Start Switch	Cockpit	Start Switch
Multiplex	Vehicle_brake_pressure	Cockpit	Brake Pressure
Gearbox	**Desired Gear**	GB Control	Desired Gear
GB Control	**Current Gear**	Gearbox	Current Gear
	Desired Gear (Cockpit)	Cockpit	Desired Gear
	Desired GB Program	GB Program	Desired Gear
	Gear Select Down	Cockpit	Gear Select Down
	Gear Select Up	Cockpit	Gear Select Up
	Operation Control	Cockpit	Operation Control
	Reference Speed	IC Engine	Engine Speed
	Velocity	Cockpit	Velocity
GB Program	**Current Gear**	Gearbox	Current Gear
	Load Signal	Cockpit	Load Signal
	Speed	IC Engine	Engine Speed
Monitor	Vehicle Acceleration	Vehicle	Acceleration
	Vehicle Velocity	Vehicle	Velocity
	Vehicle Distance	Vehicle	Distance
	Engine Load Signal	IC Engine	Actual Load Signal
	Engine Speed	IC Engine	Engine Speed

Gearbox (4) transmissions featuring several fixed ratios can maintain a correspondence between the respective performance curves for engine and vehicle. The correspondence with the hyperbola for maximum engine output will be acceptable

Table 3.2 Vehicle component input data

Name	Value	Unit
Gas Tank Volume	0.30	m^3
Distance from Hitch to Front Axle	9280.0	mm
Height of Support Point at Bench Test	100.0	mm
Wheel Base	6120.0	mm
Distance of Gravity Center empty/half/full	3000.0/3100.0/3200.0	mm
Height of Gravity Center empty/half/full	552.0/545.0/530.0	mm
Height of Hitch empty/half/full	400.0/390.0/368.0	mm
Tire Inflation Pressure Front Axle	7.5/7.5/7.5	bar
Tire Inflation Pressure Rear Axle	7.5/7.5/7.5	bar
Curb Weight/Gross Weight	12080.0/14300.0	kg
Frontal Area	7.50	m^2
Lift Coefficient Front Axle	0.032	–
Drag Coefficient	0.520	–
Lift Coefficient Rear Axle	0.010	–
Chassis Data Track Width Front/Rear	2000.0/2020.0	mm
Chassis Data Axle Stiffness Front/Rear	1500.0/1200.0	N/°

Table 3.3 IC Engine component input data

Name	Value	Unit
Engine Displacement	7800	cm^3
Engine Type	Diesel	–
Charger Type	TC with Intercooler	–
Engine Working Temperature	80.0	°C
Number of Cylinders	6	–
Number of Strokes	4	–
Idle Speed	800.0	min^{-1}
Maximum Speed	2000.0	min^{-1}
Inertia Moment	1.534	kg m²
Response Time	0.1	s
Heating Value for Diesel	44000.0	kJ/kg
Fuel Density	0.84	kg/l
Specific Carbon Content	0.86	–
Idle Consumption	3.03609	l/h
Exhaust Proportion of Waste Energy	0.48	–
FMEP at Minimum Speed	3.45	bar
Exponent of FMEP Characteristic	0.16	–
Dynamic Oil Viscosity	0.09	Pas
FMEP at Maximum Speed	5.5	bar
Curvature Factor	1.42	–

Fig. 3.7 Torque variation for
internal combustion engine
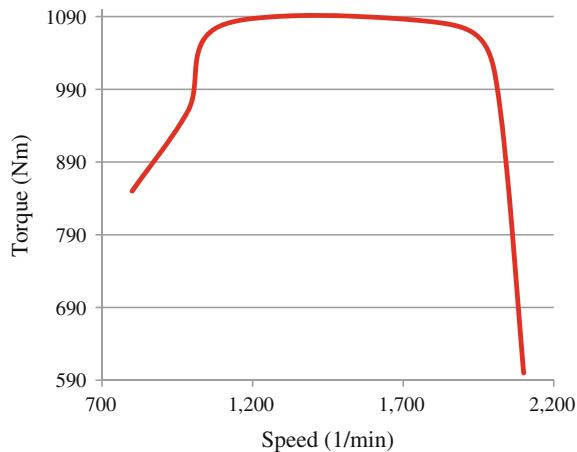
Fig. 3.8 Fuel consumption
map
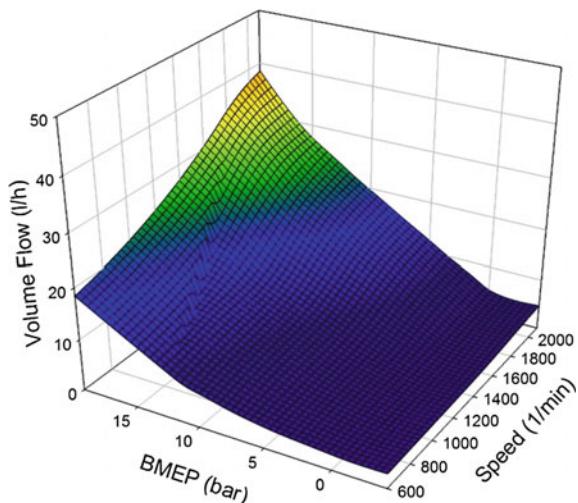
Table 3.4 Clutch component
input data

Name	Value	Unit
Inertia Moment In	0.001	kg m^2
Inertia Moment Out	0.001	kg m^2
Maximum Transferable Torque	1300	Nm

or indeed quite good, depending on a multiplicity of factors including the number of
available gears, the spacing of the individual ratios within the required conversion
range, and the engines' full-load torque curve [1].

The component Gearbox contains a model for a gearbox with different gear steps. The user can define as many gears as needed. When it is used as an automatic gearbox, the gear shifting process will be controlled by the control module gearbox control and program. To define component input data for Gear Ratio Table double click on the icon and select edit to open the following window (Table 3.5) [1].

Final Drive (5) is a gear step with fixed ratio. It can be used as a transmission step of the differential (final drive unit). A drive torque will be transferred to a power take-off torque of the transmission step by considering the transmission, the mass moments of inertia, and the moment of loss [1]. To define component input data double click on the Single Ratio Transmission icon and enter the following data (Table 3.6).

The Wheels and Tires link the vehicle to the road. The wheel components take into consideration many influencing variables and their effect on the rolling state.

The moment of rolling drag can be computed on the basis of the wheel load, he corrected dynamic rolling radius, and the coefficient of rolling drag.

The longitudinal tire force results from the friction coefficient, the wheel load as well as from the wheel load factor and the slip factor. It is possible to define variable friction coefficients along the driving profile when different road conditions are considered [1].

Information data for the four wheels are the same (Vehicle Front Right (7), Vehicle Rear Right (6, 10), Vehicle Front Left (9), and Vehicle Rear Left (8, 11)).

Double click on the wheel and enter the following data (Table 3.7). Select Properties menu and define the appropriate wheel location for each wheel (Vehicle: Front Right, Rear Right, Front Left, and Rear Left) [1].

Table 3.5 Gearbox component input data

Gear (–)	Ratio (–)	Inertia In (kg m^2)	Inertia Out (kg m^2)	Teeth In (–)	Teeth Out (–)	Efficiency (–)
0	1.00	0.0015	0.005	10	10	0.95
1	3.43	0.0015	0.005	100	343	0.95
2	2.01	0.0015	0.005	100	201	0.95
3	1.42	0.0015	0.005	50	71	0.95
4	1.00	0.0015	0.005	10	10	0.95
5	0.83	0.0015	0.005	100	83	0.95

Table 3.6 Final Drive component input data

Name	Value	Unit
Transmission Ratio	5.900	–
Inertia Moment In	0.008	kg m^2
Inertia Moment Out	0.015	kg m^2
Efficiency	0.970	–

Table 3.7 Wheel component input data

Name	Value	Unit
Wheel Inertia Moment	0.51	kg m^2
Friction Coefficient of Tire	0.95	–
Reference Wheel Load	2500.0	N
Wheel Load Correction Coefficient	0.02	–
Static Rolling Radius	436.0	mm
Circumference	2739.47	mm
Dynamic Rolling Radius	464.0	mm
Circumference	2915.40	mm
Tire Section Width	275.0	mm
Tire Aspect Ratio	70.0	%
Tire Seat Diameter	22.5	inch
Rolling Resistance Coefficient	0.00614	–
Tire Inflation Pressure	7.5	bar
Tire Load	2200.00	kg
Tire Velocity	90.0	m/s
Reference Temperature	25.0	°C
Convection Coefficient	25.0	W/m^2 K
Pressure Sensitivity Coefficient	−0.2	–
Linear Speed Coefficient	0.05	–
Temperature Sensitivity Coefficient	0.007	–
Tire Mass	57.0	kg
Empirical Rolling Resistance Coefficient	−0.01	1/K
Load Sensitivity Exponent	0.00	–
Square Speed Coefficient	0.1137	–
Convection Coefficient Exponent	0.25	–
Specific Heat Capacity of Tire	1350.0	J/kg K

The Brake component is described by brake data and dimensions. It is possible to define drum brakes as well as disk brakes. The retarder is used for heavy vehicles and is described below.

The braking torque is computed considering the braking dimensions and the input brake pressure. This brake pressure can come from the cockpit component or brake control. If the vehicle is standing still, the degrees of freedom will be reduced as this also reduces the calculation time. This reduction is done in a way that the equation system is switched if a small velocity threshold is reached. In this case movement is suppressed [1].

At the same time, the instantaneous compulsive force is checked (if it is smaller than the braking torque). If this condition is no longer true the brake is released. Input data for the two front brakes are the same and also the data for the two rear brakes are the same (Front Disk Brake Right (13), Rear Drum Brake Right (12),

Front Disk Brake Left (15) and Rear Drum Brake Left (14)). Double click on the brake icon and enter the following data (Table 3.8).

Differential (16) unit compensates for discrepancies in the respective rotation rates of the drive wheels: between inside and outside wheels during cornering and between different drive axels on 4WD vehicles.

When there is a unilateral variation in road surfaces it results in different coefficients of friction at the respective wheels, this balance effect limits the effective drive torque to a level defined as twice the traction force available at the wheel (tire) with the lower friction coefficient [1].

This wheel then responds to the excessive force by spinning. To avoid such effects a positive lock is available at the component. In the differential it is possible to define the torque split factor. This is needed if it is used as a central differential for a four wheel drive. To define component input data double click on the differential icon and enter the following data (Table 3.9).

The Kinematic Chain Browser can be launched in the pop-up menu of a selected component. All mechanical connections starting from the selected component are shown in a tree structure on the left side of the window. When a second component is selected in the tree structure, all speeds between the selected components are shown in the table on the right side of the window, each row representing one gear of the gearbox [1].

Cockpit (17) links the driver and the vehicle. In this component connections are only made via Data Bus. The driver gets information such as vehicle velocity and vehicle acceleration, but also generates information such as the pedal positions for other components. The pedal positions are transferred to corresponding indicators via the pedal characteristics (Table 3.10) [1].

Table 3.8 Brake component input data

Name	Value	Value	Value	Value	Unit
Brake	Front Right	Rear Right	Front Left	Rear Left	–
Piston Surface	5000.0	5000.0	5000.0	5000.0	mm^2
Specific Factor	3.0	3.0	3.0	3.0	–
Efficiency	0.99	0.99	0.99	0.99	–
Inertia Moment	0.05	0.05	0.05	0.05	kg m^2
Friction Coefficient	0.25	0.25	0.25	0.25	–
Friction Radius	300	300	300	300	mm

Table 3.9 Differential component input data

Name	Value	Unit
Differential Lock	Unlocked	–
Torque Split Factor	1.0	–
Inertia Moment In	0.015	kg m^2
Inertia Moment Out1/Out2	0.015/0.015	kg m^2

Table 3.10 Cockpit component input data

Name	Value	Unit
Shift Mode	Automatic	–
Number of Gears Forward/Back	5/1	–
Maximum Brake Force	250.0	N
Brake Light Switch Threshold	1.0	%

The GB Control (18) is required to define an automatic gearbox. In the GB Control, the gear shifting process can be defined automatically without any influence of the driver.

The GB Control shifts the gears dependent on a speed or velocity. In the calculation tasks it is decided which of the two shifting strategies is used. The speed or velocity can be defined via the Data Bus. It is possible to define the engine speed and the wheel speed as Ref. [1].

Therefore, it is necessary to define the upshifting and downshifting velocities always only for one gear less than are available in the gearbox.

To define component input data double click on the GB Control icon and enter the following data (Table 3.11) [1].

The GB Control is also the connection between the GB Program and the gearbox. The velocities for upshifting and downshifting can be checked in the following way: the upshifting velocity of the 2nd gear means that at this velocity the GB Control is upshifting from the 2nd into the 3rd gear. The downshifting velocity for the 2nd gear means that at this velocity the GB Control is downshifting from the 3rd into the 2nd gear [1].

The GB Program (19) is used for automatic gearboxes in combination with the GB Control. The GB Program allows for a more complicated gear shifting process than the GB Control, as the load signal of the engine is considered. The GB Program shifts the gears according to given curves. The curves are given as a function of the load signal and the engine speed.

The target gear determined by the program is transmitted to the GB Control that transmits it to the gearbox.

Furthermore, the curves could be optimized using iSIGHT interface module.

Table 3.11 GB Control component input data

Name	Unit	Value				
Gear	–	1	2	3	4	5
Upshifting Velocity	km/h	15	20	28	36	44
Downshifting Velocity	km/h	13	17	25	32	40
Upshifting Speed	min^{-1}	1200	1400	1600	1800	–
Downshifting Speed	min^{-1}	1000	1200	1400	1600	–

These optimized curves (optimized shifting program) could also be used as input curves for the GB Program [1].

The gear shifting process is done similar to the GB Control. The only difference is the dependence on the load signal of the engine. If the shifting program should be defined not by speed but by velocity, the Data Bus input velocity must be connected.

The units of the shifting program and the optimized shifting program influence each other. This means that if one of these programs is loaded with a different unit, the other program also gets this new unit.

With the Data Bus input shifting program selector (which provides a double value), interpolations between the defined shifting programs can be done (Fig. 3.9) [1].

The speeds for upshifting and downshifting can be checked in the following way: the upshifting speed of the 2nd gear with the special load signal means that at this speed with this load signal the gearbox control is upshifting from the 2nd into the 3rd gear. The downshifting speed for the 2nd gear with the special load signal means that at this speed with this load signal the gearbox control is downshifting from the 3rd into the 2nd gear [1].

Fig. 3.9 Shifting programs standard: **a** upshifting, **b** downshifting
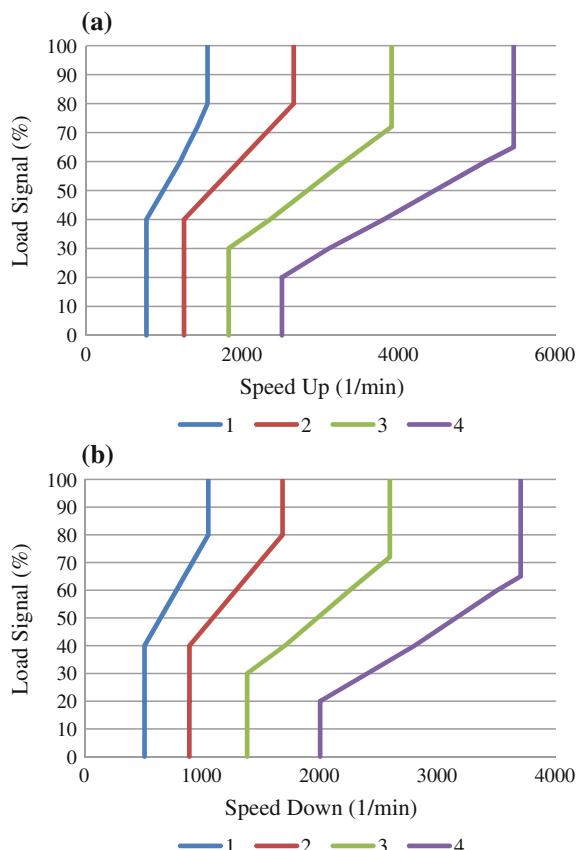
Table 3.12 Catalyst component input data

Name	Value	Unit
Heat Loss Coefficient	0.93	–
Weight of Catalyst	11.0	kg
Specific Heat Capacity of Catalyst	210.0	J/kg K
Reference Area Catalyst/Air	0.27	m^2
Heat Transfer Coefficient Catalyst/Air	25.0	W/m^2 K
Operating Temperature Catalyst	450.0	°C

Catalyst (20) or exhaust systems consider the effects of the catalytic converter and soot filler on the raw emissions of the engine. To define component input data double click on the catalyst icon and enter the following data (Table 3.12).

Conversion efficiencies of the different emissions (NO$_x$, CO, HC, and Soot) can be defined dependent on the actual temperature of the catalytic converter (Fig. 3.10).

The Multiplex (21) element is a function defined by the user, which is used for controlling bus braking [1]. The function is defined in C-Code according to data from Fig. 3.11 and the Data Bus connections in Table 3.13.

Fig. 3.10 Efficiencies of the different emissions
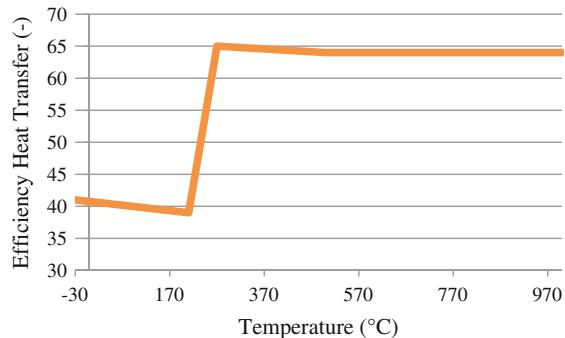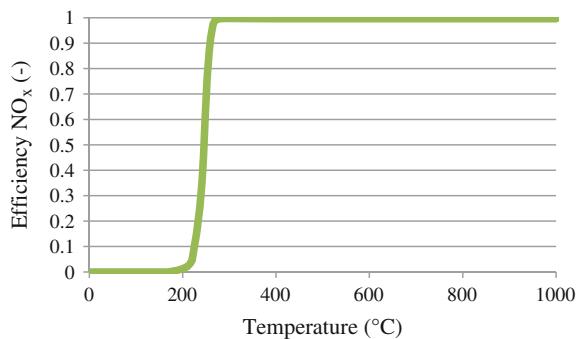
/*double realTime;*/
y[0]=a[0];

Fig. 3.11   Function Multiplex in C-Code

Table 3.13   Function Multiplex input data

Data Bus	Description	Unit	Connection	Decouple
a[0]	Vehicle_brake_pressure	bar	Optional	Coupled
y[0]	Cockpit_brake_pressure	bar	Optional	Coupled

The Monitor component (22) can be introduced, if the calculation run must be detected. It is possible to show some results of the calculation while the calculation is running.

Click on the description of Data Bus tab and open the following dialog. To select a Data Bus channel, click to access at the available list. Enter the text for the description and then click on to select the unit (Table 3.14).

The AMT Control (23) element commands the automatic operation of the clutch while shifting gears (Automated Manual Transmission Control). The AMT Control element also has the supplementary task of adapting the load (respectively the torque) while shifting gears and of controlling the clutch operation while the vehicle is stationary. The entry data for the AMT Control element are presented in Table 3.15.

Table 3.14   Monitor component input data

Name	Value	Unit
Input 0	Vehicle Acceleration	m/s^2
Input 1	Vehicle Velocity	km/h
Input 2	Vehicle Distance	m
Input 3	Engine Load Signal	–
Input 4	Engine Speed	1/min

Table 3.15   AMT Control component input data

Name	Value	Unit
Shifting Time	0.5	s
Clutch Disengagement Full	45	%
Gear Change	50	%
Zero Load-Start	28	%
Clutch Engagement Start	60	%
Zero-Load End	72	%

3.4   Simulation for the Hybrid Bus Model in AVL CRUISE

To simulate how a hybrid bus works, a model was created and developed for computer simulation in the AVL CRUISE application (Fig. 3.12).

The elements composing the model are as follows:

|	
• Vehicle (1)	• Rear Disk Brake (14)
• IC Engine (2)	• Front Disk Brake (15)
• Clutch (3)	• E-Machine (16)
• Gearbox (4)	• Rear Differential (17)
• Final Drive Rear (5)	• Cockpit (18)
• Vehicle Rear Right (6)	• GB Control (19)
• Vehicle Front Right (7)	• GB Program (20)
• Vehicle Rear Left (8)	• Battery H (21)
• Vehicle Front Left (9)	• Catalyst (22)
• Vehicle Rear Right (10)	• Multiplex Function (23)
• Vehicle Rear Left (11)	• Monitor (24)
• Rear Disk Brake (12)	• AMT Control (25)
• Front Disk Brake (13)	

Fig. 3.12 Hybrid bus model

All the connections in the Data Bus for this model are described in Table 3.16 [1]. Validation of the connections are marked using bold and are required for the functioning of the model.

Table 3.16 Data Bus Connections

Component requires	Input information	Component delivering	Output information
AMT Control	**Current Gear**	Gearbox	Current Gear
	Desired Gear	GB Control	Desired Gear
	Input Speed	Clutch	Input Speed
	Load Signal	Cockpit	Load Signal
	Output Speed	Clutch	Output Speed
	Velocity	Vehicle	Velocity
Rear Brake	**Brake Pressure**	Multiplex	Cockpit_brake_press
Front Brake	**Brake Pressure**	Multiplex	Cockpit_brake_press
Rear Brake	**Brake Pressure**	Multiplex	Cockpit_brake_press
Front Brake	**Brake Pressure**	Multiplex	Cockpit_brake_press
Clutch	**Desired Clutch**	AMT Control	Desired Clutch
Cockpit	**Gear Indicator**	Gearbox	Current Gear
	Operation Control 0	IC Engine	Operation Control
	Speed	IC Engine	Engine Speed
E-Machine	Temperature	Cockpit	Course Ambient
	Load Signal	IC Engine	Actual Load Signal
	Temperature	Cockpit	Course Ambient
IC Engine	**Load Signal**	AMT Control	Load Signal
	Start Switch	Cockpit	Start Switch
Multiplex	Vehicle_brake_press	Cockpit	Brake Pressure
Gearbox	**Desired Gear**	GB Control	Desired Gear
GB Control	**Current Gear**	Gearbox	Current Gear
	Desired Gear	Cockpit	Desired Gear
	Desired Gear GB	GB Program	Desired Gear
	Gear Selection Down	Cockpit	Gear Selection Down
	Gear Selection Up	Cockpit	Gear Selection Up
	Operation Control	Cockpit	Operation Control
	Reference Speed	IC Engine	Engine Speed
	Velocity	Cockpit	Velocity
GB Program	**Current Gear**	Gearbox	Current Gear
	Load Signal	Cockpit	Load Signal
	Speed	IC Engine	Engine Speed
Monitor	Vehicle Acceleration	Vehicle	Acceleration
	Vehicle Velocity	Vehicle	Velocity
	Vehicle Distance	Vehicle	Distance
	Engine Load Signal	IC Engine	Actual Load Signal
	Engine Speed	IC Engine	Engine Speed

Vehicle (1) is one of the main objects in a model. This component contains general data of the vehicle, such as nominal dimensions and weights. Only one vehicle component is required in a model. Road resistances and dynamic wheel loads are calculated for road and dynamometer runs based on the dimensions and the load state. The wheel loads are calculated considering motion. The aerodynamic, rolling, climbing, acceleration and total resistance are calculated [1].

To define component input data (Table 3.17) double click on the icon or click on it the right mouse button and select edit to open the following window.

IC Engine (2) component contains a model for an internal combustion engine. The characteristic curves for the full load, fuel consumption, and others can be freely defined by the user. It is possible to define a gasoline engine as well as a diesel engine. In this component a temperature model is included to consider the influence of the temperature on the fuel consumption and emissions while the engine is cold. The engine will be modeled by a structure of characteristic curves and maps [1].

The characteristic curves for maximum load, fuel consumption etc. can be defined by the user by loading the initial data (Table 3.18).

The graphic for torque variation of the internal combustion engine is presented in Fig. 3.13.

Injection parameters are calculated based on the Fuel Consumption Map (Fig. 3.14).

The Clutch (3) makes stationary idle possible, transition to motion, and interruption of the power flow. The clutch slips to compensate for the difference in the rotational speeds of engine and drive train when the vehicle is set in motion. When

Table 3.17 Vehicle component input data

| Name	Value	Unit
Distance from Hitch to Front Axle	9380.0	mm
Height of Support Point at Bench Test	100.0	mm
Wheel Base	5945.0	mm
Distance of Gravity Center empty/half/full	3000.0/3100.0/3200.0	mm
Height of Gravity Center empty/half/full	560.0/540.0/530.0	mm
Height of Hitch empty/half/full	400.0/390.0/370.0	mm
Tire Inflation Pressure Front Axle	7.5/7.5/7.5	bar
Tire Inflation Pressure Rear Axle	7.5/7.5/7.5	bar
Curb Weight	12000.0	kg
Gross Weight	18900.0	kg
Frontal Area	7.50	m^2
Lift Coefficient Front Axle	0.03	–
Drag Coefficient	0.5	–
Lift Coefficient Rear Axle	0.01	–
Chassis Data Track Width Front/Rear	2000.0/2000.0	mm
Chassis Data Axle Stiffness Front/Rear	1500.0/1200.0	N/°

Table 3.18 IC Engine component input data

| Name	Value	Unit
Engine Displacement	4760	cm^3
Engine Type	Diesel	–
Charger Type	TC with Intercooler	–
Engine Working Temperature	80.0	°C
Number of Cylinders	4	–
Number of Strokes	4	–
Idle Speed	800.0	min^{-1}
Maximum Speed	2000.0	min^{-1}
Inertia Moment	1.5	$kg\ m^2$
Response Time	0.1	s
Heating Value for Diesel	44000.0	kJ/kg
Fuel Density	0.84	kg/l
Specific Carbon Content	0.86	–
Idle Consumption	5.2	l/h
Exhaust Proportion of Waste Energy	0.5	–
FMEP at Minimum Speed	3.5	bar
Exponent of FMEP Characteristic	0.2	–
Dynamic Oil Viscosity	0.09	Pas
FMEP at Maximum Speed	5.5	bar
Curvature Factor	1.5	–

a change in operation conditions makes it necessary to change gears, the clutch disengages the engine from the drivetrain for the duration of the procedure [1].

The characteristics of the clutch element are presented in Table 3.19 and the graphic for clutch decoupling force variation in Fig. 3.15.

**Fig. 3.13** Torque variation for internal combustion engine
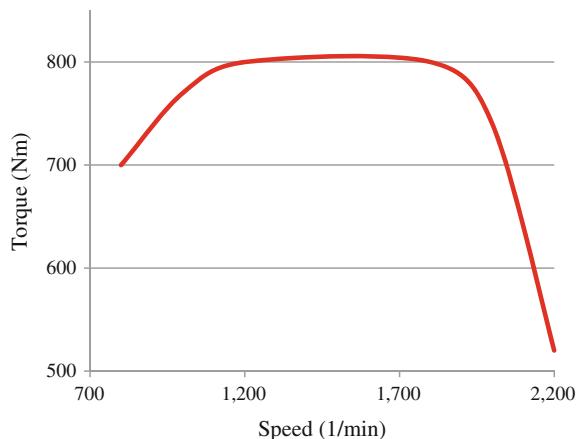
Fig. 3.14 Fuel Consumption
Map
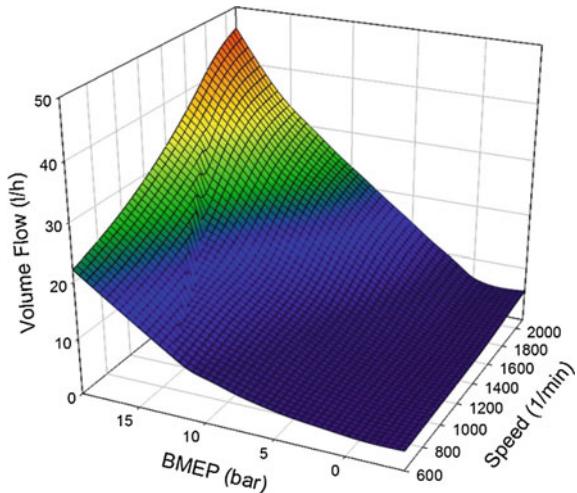
Table 3.19 Clutch
component input data

Name	Value	Unit
Inertia Moment In	0.001	kg m^2
Inertia Moment Out	0.001	kg m^2
Maximum Transferable Torque	1300	Nm

Fig. 3.15 Clutch decoupling
force variation
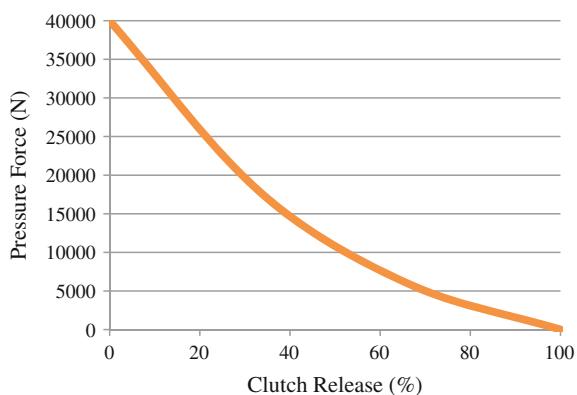
The Gearbox (4) contains a model for a gearbox with different gear steps. The user can define as many gears as needed. When it is used as an automatic gearbox, the gear shifting process will be controlled by the control module gearbox control and program. To define component input data for Gear Ratio Table double click on the icon and select edit to open the following window (Table 3.20) [1].

Table 3.20 Gearbox component input data

Gear (–)	Ratio (–)	Inertia In (kg m^2)	Inertia Out (kg m^2)	Efficiency (–)	Gear (–)
0	1.00	0.0015	0.005	0.95	0
1	14.94	0.0015	0.005	0.95	1
2	11.73	0.0015	0.005	0.95	2
3	9.04	0.0015	0.005	0.95	3
4	7.09	0.0015	0.005	0.95	4
5	5.54	0.0015	0.005	0.95	5
6	4.35	0.0015	0.005	0.95	6
7	3.44	0.0015	0.005	0.95	7
8	2.70	0.0015	0.005	0.95	8
9	2.08	0.0015	0.005	0.95	9
10	1.63	0.0015	0.005	0.95	10
11	1.27	0.0015	0.005	0.95	11
12	1.00	0.0015	0.005	0.95	12
R1	17.48	0.0015	0.005	0.95	R1
R2	3.73	0.0015	0.005	0.95	R2
R3	4.02	0.0015	0.005	0.95	R3
R4	3.16	0.0015	0.005	0.95	R4

Final Drive (5) is a gear step with fixed ratio. It can be used as a transmission step of the differential (final drive unit). To define component input data double click on the final drive icon and enter the following data (Table 3.21).

The Wheels and Tires (6–11) link the vehicle to the road. The wheel component considers many influencing variables and their effect on the rolling state. Double click on the wheel and enter the following data (Table 3.22).

Information data for the four wheels are the same (Vehicle Rear Right (6, 10), Vehicle Front Right (7), Vehicle Rear Left (8, 11), and Vehicle Front Left (9)).

Select Properties menu and define the appropriate wheel location for each wheel (Vehicle: Front Right, Rear Right, Front Left, and Rear Left). The static rolling radius is the distance between the center of the wheel and the road surface for the loaded, not moving vehicle.

The Brake component is described by brake data and dimensions. It is possible to define drum brakes as well as disk brakes. Input data for the two front brakes is the same and also the data for the two rear brakes is the same (Rear Brake Right

Table 3.21 Final Drive component input data

Name	Value	Unit
Transmission Ratio	4.72	–
Inertia Moment In	0.008	kg m^2
Inertia Moment Out	0.015	kg m^2
Efficiency	0.97	–

Table 3.22 Wheel component input data

Name	Value	Unit
Wheel Inertia Moment	0.51	kg m^2
Friction Coefficient of Tire	0.95	–
Reference Wheel Load	2500.0	N
Wheel Load Correction Coefficient	0.02	–
Static Rolling Radius	436.0	mm
Circumference	2739.47	mm
Dynamic Rolling Radius	464.0	mm
Circumference	2915.40	mm
Tire Section Width	275.0	mm
Tire Aspect Ratio	70.0	%
Tire Seat Diameter	22.5	inch
Rolling Resistance Coefficient	0.00614	–
Tire Inflation Pressure	7.5	bar
Tire Load	2200.00	kg
Tire Velocity	90.0	m/s
Reference Temperature	25.0	°C
Convection Coefficient	25.0	W/m^2 K
Pressure Sensitivity Coefficient	−0.2	–
Linear Speed Coefficient	0.05	–
Temperature Sensitivity Coefficient	0.007	–
Tire Mass	57.0	kg
Empirical Rolling Resistance Coefficient	−0.01	1/K
Load Sensitivity Exponent	0.00	–
Square Speed Coefficient	0.1137	–
Convection Coefficient Exponent	0.25	–
Specific Heat Capacity of Tire	1350.0	J/kg K

(12), Front Brake Right (13), Rear Brake Left (14) and Front Brake Left (15)). Double click on the brake icon and enter the following data (Table 3.23).

Using E-Machine component (15) together with the battery H, the user can simulate hybrid systems. The model of the electric machine contains two components, the inverter and the electric motor.

For this type of model a characteristic map for the efficiency is used to calculate the loss of power. The thermic model takes the warm up of the electric machine into account regarding the occurring losses. The warm up of the environment with respect to the cooling system due to the electric machine is not considered in the electric machine component.

The maximal power should be restricted to avoid exceeding the given limit for the temperature due to the occurring losses. Therefore, the permissible losses are

Table 3.23 Brake component input data

Name	Value	Value	Value	Value	Unit
Brake	Front Right	Rear Right	Front Left	Rear Left	–
Piston Surface	4000.0	4000.0	4000.0	4000.0	mm^2
Specific Factor	3.0	3.0	3.0	3.0	–
Efficiency	0.99	0.99	0.99	0.99	–
Inertia Moment	0.085	0.085	0.085	0.085	kg m^2
Friction Coefficient	0.25	0.25	0.25	0.25	–
Friction Radius	300	300	300	300	mm

dependent on the actual temperature of the motor and the maximal moment of inertia is determined according to these values [1].

Double click on the E-Machine icon and enter the following data (Table 3.24).

The calculation for power loss is made based on power characteristic maps: Maximum Power (Torque) Mechanical Map (Fig. 3.16) and Efficiency Map (Fig. 3.17).

Differential (17) unit compensates for discrepancies in the respective rotation rates of the drive wheels: between inside and outside wheels during cornering and between different drive axels on 4WD vehicles.

When there is a unilateral variation in road surfaces it results in different coefficients of friction at the respective wheels, this balance effect limits the effective drive torque to a level defined as twice the traction force available at the wheel (tire) with the lower friction coefficient [1].

Table 3.24 E-Machine component input data

Name	Value	Unit
Type of Machine	PSM (*Permanent Magnet Motor*)	–
Characteristic Maps and Curves	*Overall*	–
Nominal Voltage	600	V
Inertia Moment	0.025	kg m^2
Maximum Current—Motor	120	A
Maximum Current—Generator	300	A
Maximum Speed	8000	min^{-1}
Drag Torque at Maximum Speed	0	Nm
Mass of Machine	30	kg
Initial Temperature	70	°C
Maximum Temperature	70	°C
Specific Heat Transition	2200	W/K
Specific Heat Capacity	430	J/kg K
Thermal Time Constant	1.0	s

Fig. 3.16 Torque
characteristic
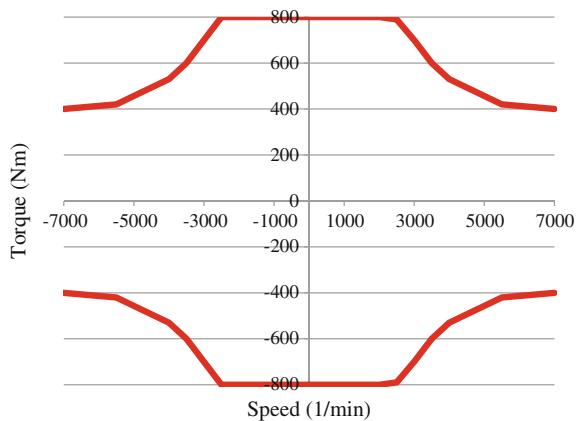
Fig. 3.17 Electric motor
efficiency
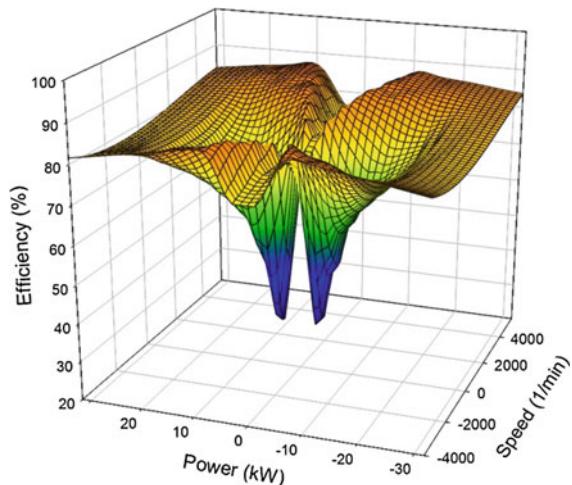
To define component input data double click on the differential icon and enter
the following data (Table 3.25).

Cockpit (18) links the driver and the vehicle. In this component connections are
only made via Data Bus. The driver gets information such as vehicle velocity and
vehicle acceleration, but also generates information such as the pedal positions for

Table 3.25 Differential
component input data

Name	Value	Unit
Differential Lock	Unlocked	–
Torque Split Factor	1.0	–
Inertia Moment In	0.015	kg m^2
Inertia Moment Out1	0.015	kg m^2
Inertia Moment Out2	0.015	kg m^2

other components. The pedal positions are transferred to corresponding indicators via the pedal characteristics (Table 3.26) [1].

The GB Control (19) is required to define an automatic gearbox. In the GB Control, the gear shifting process can be defined automatically without any influence of the driver.

The GB Control shifts the gears dependent on a speed or velocity. In the calculation tasks it is decided which of the two shifting strategies is used. The speed or velocity can be defined via the Data Bus. It is possible to define the engine speed and the wheel speed as Ref. [1].

Therefore, it is necessary to define the upshifting and downshifting velocities always only for one gear less than are available in the gearbox. To define component input data double click on the GB Control icon and enter the following data (Table 3.27) [1].

The GB Control is also the connection between the GB Program and the gearbox. The velocities for upshifting and downshifting can be checked in the following way: the upshifting velocity of the 2nd gear means that at this velocity the GB Control is upshifting from the 2nd into the 3rd gear. The downshifting velocity for the 2nd gear means that at this velocity the GB Control is downshifting from the 3rd into the 2nd gear [1].

Table 3.26 Cockpit component input data

Name	Value	Unit
Shift Mode	Automatic	–
Number of Gears Forward	12	–
Number of Gears Back	4	–
Maximum Brake Force	250.0	N
Brake Light Switch Threshold	1.0	%
Number of Retarder Steps	0	–

Table 3.27 GB Control component input data

Name	Gear Step											
Gear (–)	1	2	3	4	5	6	7	8	9	10	11	12
Up Velocity (km/h)	12	16	20	24	27	30	32	35	40	45	55	65
Down Velocity (km/h)	8	12	16	20	24	27	30	32	35	40	50	60
Up Speed (1/min)	1000	1100	1200	1300	1400	1500	1600	1700	1800	1900	2000	xxxx
Down Speed (1 min)	900	1000	1100	1200	1300	1400	1500	1600	1700	1800	1900	xxxx

The GB Program (20) is used for automatic gearboxes in combination with the GB Control. The GB Program allows for a more complicated gear shifting process than the GB Control, as the load signal of the engine is considered. The GB Program shifts the gears according to given curves. The curves are given as a function of the load signal and the engine speed. The target gear determined by the program is transmitted to the GB Control that transmits it to the gearbox.

Furthermore, the curves could be optimized using iSIGHT interface module. These optimized curves (optimized shifting program) could also be used as input curves for the GB Program [1].

The gear shifting process is done similar to the GB Control. The only difference is the dependence on the load signal of the engine. If the shifting program should be defined not by speed but by velocity, the Data Bus input velocity must be connected.

The units of the shifting program and the optimized shifting program influence each other. This means that if one of these programs is loaded with a different unit, the other program also gets this new unit. With the Data Bus input shifting program selector (which provides a double value), interpolations between the defined shifting programs can be done (Fig. 3.18a, b) [1].

Fig. 3.18 Shifting programs standard: **a** upshifting, **b** downshifting

The speeds for upshifting and downshifting can be checked in the following way: the upshifting speed of the 2nd gear with the special load signal means that at this speed with this load signal the gearbox control is upshifting from the 2nd into the 3rd gear. The downshifting speed for the 2nd gear with the special load signal means that at this speed with this load signal the gearbox control is downshifting from the 3rd into the 2nd gear [1].

The Battery H (21) component is used for simulating hybrid and electric vehicles. The basic model consists of a voltage source and an ohmic resistance [1].

Double click on the battery H icon and enter the following data (Table 3.28). The resistance is constructed in a way that a big part of the complex processes within the battery are taken into consideration. 2 RC elements which describe the concentration overvoltage and the transfer overvoltage can be added optionally.

The thermal behavior of the battery H is described by a thermal substitution model. The warming caused by the losses inside the battery H and the cooling caused by convection is taken into consideration. Single cells can be modelled as well as any combination of cells. There is no electrical consumer; it is a function of the State of Charge SOC (Fig. 3.19).

Table 3.28 Battery H component input data

Name	Value	Unit
Maximum Charge	11.25	Ah
Nominal Voltage	20.00	V
Maximum Voltage	30.00	V
Initial Charge	60.00	%
Minimum Voltage	12.00	V
Number of Cells per Cell-Row	1	–
Number of Cell-Row	20	–
Resistance charge/discharge	0.02/0.03	Ω

Fig. 3.19 Battery SOC (State Of Charge)
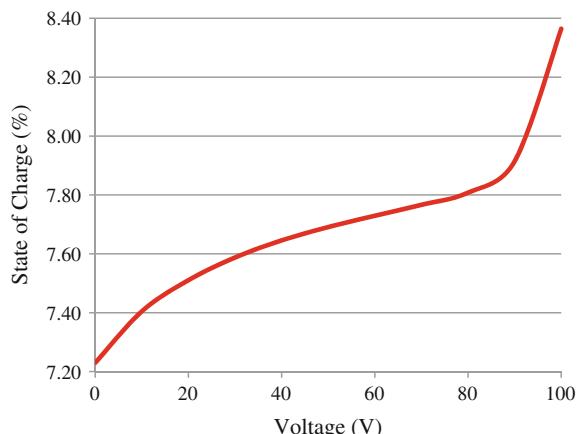
Catalyst (22) or exhaust systems consider the effects of the catalytic converter and soot filler on the raw emissions of the engine.

Starting with the temperature of the catalytic converter, factors for the conversion will be computed for the single emission components using temperature dependent maps. The heat loss coefficient is the percentage of the exhaust energy delivered by the engine which reaches the exhaust system [1].

To define component input data double click on the catalyst icon and enter the following data (Table 3.29). Conversion efficiencies of the different emissions (NO_x, CO, HC and Soot) can be defined dependent on the actual temperature of the catalytic converter (Fig. 3.20).

In the AVL CRUISE application the catalyst element Catalyst is defined solely as a component of the exhaust system for gases resulted from fuel combustion, which generates gas debits and pressure drops between the elements without treating exhaust gases chemically.

The Multiplex (23) element is a function defined by the user which is used for controlling bus braking. The function is define in C-Code according to data from Fig. 3.21 and the Data Bus Connection in Table 3.30.

The Monitor component (24) can be introduced, if the calculation run must be detected. It is possible to show some results of the calculation while the calculation is running.

Click on the description of Data Bus tab and open the following dialog. To select a Data Bus channel, click to access at the available list. Enter the text for the description and then click on to select the unit (Table 3.31).

The AMT Control (25) element commands the automatic operation of the clutch while shifting gears (Automated Manual Transmission Control). The AMT Control element also has the supplementary task of adapting the load (respectively the torque) while shifting gears and of controlling the clutch operation while the vehicle is stationary. The entry data for the AMT Control element are presented in Table 3.32.

Table 3.29 Catalyst component input data

Name	Value	Unit
Heat Loss Coefficient	0.95	–
Weight of Catalyst	10.0	kg
Specific Heat Capacity of Catalyst	250.0	J/kg K
Reference Area Catalyst/Air	0.25	m^2
Heat Transfer Coefficient Catalyst/Air	30.0	W/m^2 K
Operating Temperature Catalyst	550.0	°C
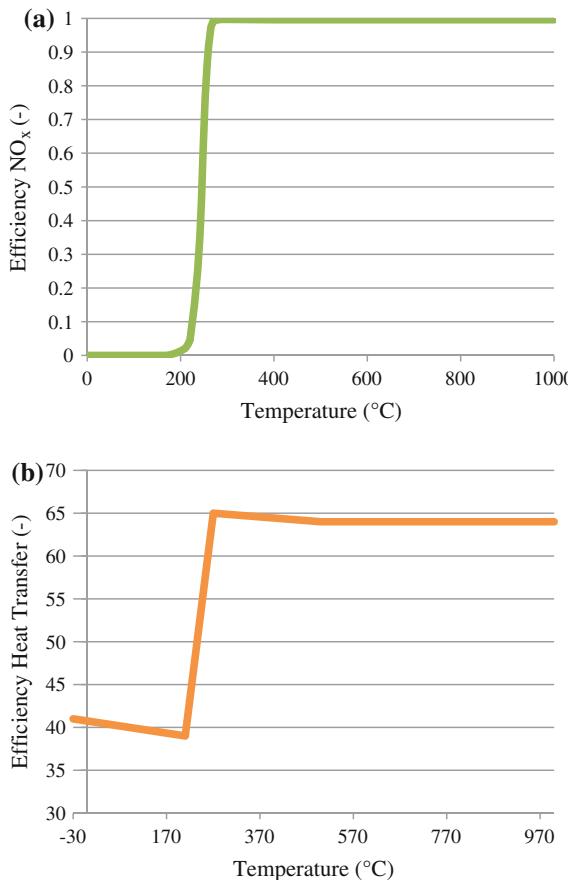
Fig. 3.20 Pollutant emissions variation: **a** NO_x Efficiency, **b** Heat Transfer Efficiency

/*double realTime;*/
y[0]=a[0];

Fig. 3.21 The Multiplex function

Table 3.30 Data Bus connections for the Multiplex function

Data Bus	Description	Unit	Connection	Decouple
a[0]	Vehicle_brake_pressure	bar	Optional	Coupled
y[0]	Cockpit_brake_pressure	bar	Optional	Coupled

Table 3.31 Monitor component input data

Name	Value	Unit
Input 0	Vehicle Acceleration	m/s^2
Input 1	Vehicle Velocity	km/h
Input 2	Vehicle Distance	m
Input 3	Engine Load Signal	–
Input 4	Engine Speed	min^{-1}

Table 3.32 AMT Control component input data

Name	Value	Unit
Shifting Time	0.5	s
Clutch Disengagement Full	45	%
Gear Change	50	%
Zero Load-Start	28	%
Clutch Engagement Start	60	%
Zero-Load End	72	%

3.5   Simulation for the Electric Bus Model in AVL CRUISE

To simulate how an bus equipped with an electric motor functions, a model was created and developed for computer simulation in the AVL CRUISE application. The elements composing the model (Fig. 3.22) are as follows:

• Vehicle (1)	• Front Disk Brake (13)
• Final Drive Left (2)	• E-Machine Rear Left(14)
• Final Drive Right (3)	• E-Machine Rear Right(15)
• Vehicle Rear Left (4)	• Cockpit (16)
• Vehicle Rear Right (5)	• ASC (17)
• Vehicle Rear Left (6)	• Electrical Consumer (18)
• Vehicle Rear Right (7)	• Battery H (19)
• Vehicle Front Left (8)	• eDrive Control System (20)
• Vehicle Front Right (9)	• eBrake & mBrake (21)
• Rear Disk Brake (10)	• Monitor (22)
• Front Disk Brake (11)	• Constants (23)
• Rear Disk Brake (12)	

All the connections in the Data Bus for this model are described in Table 3.33 [1]. Validation of the connections are marked using bold and are required for the functioning of the model.

Vehicle (1) is one of the main objects in a model. This component contains general data of the vehicle, such as nominal dimensions and weights. Only one vehicle component is required in a model. Road resistances and dynamic wheel loads are calculated for road and dynamometer runs based on the dimensions and
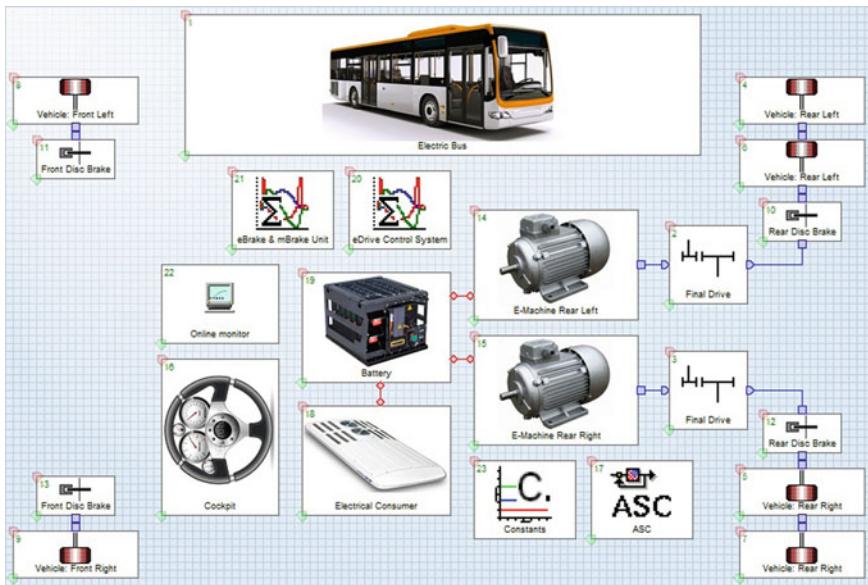
Fig. 3.22 Electric bus model

the load state. The wheel loads are calculated considering motion. The aerodynamic, rolling, climbing, acceleration and total resistance are calculated [1].

To define component input data (Table 3.34) double click on the icon or click on it the right mouse button and select edit to open the following window.

Final Drive Left (2) and Final Drive Left (3) is a gear step with fixed ratio. It can be used as a transmission step of the differential (final drive unit). A drive torque will be transferred to a power take-off torque of the transmission step by considering the transmission, the mass moments of inertia, and the moment of loss [1]. To define component input data double click on the Single Ratio Transmission icon and enter the following data (Table 3.35).

The Wheels and Tires (4–9) link the vehicle to the road. The wheel component considers many influencing variables and their effect on the rolling state. Double click on the wheel and enter the following data (Table 3.36).

The longitudinal tire force results from the friction coefficient, the wheel load as well as from the wheel load factor and the slip factor. It is possible to define variable friction coefficients along the driving profile when different road conditions are considered [1].

The Brake component (10–13) is described by brake data and dimensions. It is possible to define drum brakes as well as disk brakes.

Input data for the two front brakes is the same and also the data for the two rear brakes is the same. Double click on the brake icon and enter the following data (Table 3.37).

Table 3.33 Data Bus Connections

Component requires	Input information	Component delivering	Output information
ASC	Clutch Release	Cockpit	Course Ambient
	Load Signal	Cockpit	Load Signal
	Slip Signal Rear Left	Wheel Rear Right	Slip Signal
	Slip Signal Rear Right	Wheel Rear Left	Slip Signal
Battery H	Ambient Temperature	Cockpit	Course Ambient
	Temperature External	Cockpit	Course Ambient
Brake Rear	**Brake Pressure**	E-Brake & M-Brake	BRK_dp_Recup
Brake Front	**Brake Pressure**	E-Brake & M-Brake	BRK_dp_Recup
Brake Rear	**Brake Pressure**	E-Brake & M-Brake	BRK_dp_Recup
Brake Front	**Brake Pressure**	E-Brake & M-Brake	BRK_dp_Recup
Cockpit	**Gear Indicator**	E-Machine Left	Operating Mode
	Operation Control 0	E-Machine Left	Operation Ctrl
	Speed	E-Machine Left	Speed
E-Machine Rear Left	Ambient Temperature	Cockpit	Course Ambient
	Load Signal	E-Drive	Mod Load Signal
	Temperature External	Cockpit	Course Ambient
E-Machine Rear Right	Ambient Temperature	Cockpit	Course Ambient
	Load Signal	E-Drive	Mod Load Signal
	Temperature External	Cockpit	Course Ambient
Consumer	Set Value X	Battery H	Net Voltage
E-Drive	Vehicle Velocity	Cockpit	Velocity
	Vehicle Acceleration	Cockpit	Acceleration
	Load Signal	Cockpit	Load Signal
	Brake Pressure	Cockpit	Brake Pressure
	Maxim Brake Pressure	Constants	Maxim Brake
	Bremsfactor	Constants	Brake Factor
E&M-Brake	eDrive_Torque	E-Machine	Torque
	iFD	Constants	iFD
	iTR	Constants	iTR
	Brake_Factor_Front	Constants	Brake_Front
	Brake_Factor_Rear	Constants	Brake_Rear
	Brake_Press_Driver	Cockpit	Brake Pressure
Monitor	LoadSignal_Cockpit	Cockpit	Load Signal
	Velocity	Cockpit	Velocity
	Torque eDrive	E-Machine	Torque

Table 3.34 Vehicle component input data

Name	Value	Unit
Distance from Hitch to Front Axle	9300.0	mm
Height of Support Point at Bench Test	100.0	mm
Wheel Base	6200.0	mm
Distance of Gravity Center empty/half/full	3000.0/3100.0/3200.0	mm
Height of Gravity Center empty/half/full	550.0/540.0/530.0	mm
Height of Hitch empty/half/full	400.0/380.0/360.0	mm
Tire Inflation Pressure Front Axle	7.5/7.5/7.5	bar
Tire Inflation Pressure Rear Axle	7.5/7.5/7.5	bar
Curb Weight	14000.0	kg
Gross Weight	18500.0	kg
Frontal Area	7.50	m^2
Lift Coefficient Front/Rear Axle	0.03/0.01	–
Drag Coefficient	0.5	–
Chassis Data Track Width Front/Rear	2000.0/2000.0	mm
Chassis Data Axle Stiffness Front/Rear	1500.0/1200.0	N/°

Table 3.35 Final Drive component input data

Name	Value	Unit
Transmission Ratio	6.00	–
Inertia Moment In	0.015	$kg\ m^2$
Inertia Moment Out	0.015	$kg\ m^2$
Efficiency	0.97	–

Table 3.36 Wheel component input data

Name	Value	Unit
Wheel Inertia Moment	0.50	$kg\ m^2$
Friction Coefficient of Tire	0.95	–
Reference Wheel Load	2500.0	N
Wheel Load Correction Coefficient	0.02	–
Static Rolling Radius/Circumference	436.0/2739.47	mm
Dynamic Rolling Radius/Circumference	464.0/2915.40	mm

E-Machine Rear Left (14) and E-Machine Rear Right (15) component together with the battery H, the user can simulate hybrid systems. The model of the electric machine contains two components, the inverter and the electric motor.

For this type of model a characteristic map for the efficiency is used to calculate the loss of power. The thermic model takes the warm up of the electric machine into

Table 3.37 Brake component input data

Name	Value	Value	Value	Value	Unit
Brake	Front Right	Rear Right	Front Left	Rear Left	–
Piston Surface	5000.0	5000.0	5000.0	5000.0	mm^2
Specific Factor	3.0	3.0	3.0	3.0	–
Efficiency	0.99	0.99	0.99	0.99	–
Inertia Moment	0.05	0.05	0.05	0.05	kg m^2
Friction Coefficient	0.25	0.25	0.25	0.25	–
Friction Radius	300	300	300	300	mm

account regarding the occurring losses. The warm up of the environment with respect to the cooling system due to the electric machine is not considered in the electric machine component.

The maximal power should be restricted to avoid exceeding the given limit for the temperature due to the occurring losses. Therefore, the permissible losses are dependent on the actual temperature of the motor and the maximal moment of inertia is determined according to these values [1].

Double click on the E-Machine icon and enter the following data (Table 3.38).

For the calculation of power losses the power characteristic and efficiency characteristic maps are defined: Maximum Power (Torque) Mechanical Map (Fig. 3.23) and Efficiency Map (Fig. 3.24).

Cockpit (16) links the driver and the vehicle. In this component connections are only made via Data Bus. The driver gets information such as vehicle velocity and vehicle acceleration, but also generates information such as the pedal positions for other components. The pedal positions are transferred to corresponding indicators via the pedal characteristics (Table 3.39) [1].

The ASC Anti-Slip Control (17) element represents the transmission factor of the tractor force towards the wheels connected to powertrain. The ASC element is active only in the situation in which the model is calculated quasi-stationary and the entry of initial data is not necessary.

Table 3.38 E-Machine component input data

Name	Value	Unit
Type of Machine	ASM (Asynchronous Motors)	–
Nominal Voltage	320.0	V
Inertia Moment	1.0e-4	kg m^2
Maximum Speed	10000.0	min^{-1}
Voltage U1/U2	100.0/1000.0	V
Characteristic Maps and Curves	overall	–

Fig. 3.23 Torque characteristic
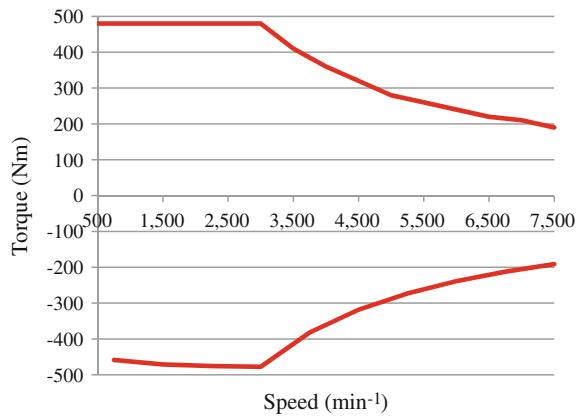
Fig. 3.24 Electric motor efficiency
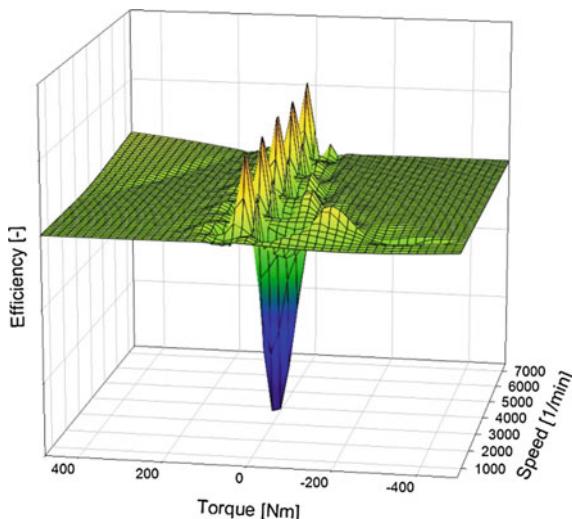
The Electrical Consumer (18) are represented as ohmic resistors in the onboard network. They represent an electric current loss. The number of the resistors that can be defined is user-dependent.

The resistors can be fixed by a constant value or by means of characteristic curves. It is possible to define resistors as a function of any external input value. It is also possible to define an external switch that switches on and off the resistor depending on the exceeding of an external value [1].

The resistors parameter can be fixed by a constant value or by means of characteristic curves. It is possible to define resistors as a function of any external input value. Double click on the electrical consumer icon and enter the data (Table 3.40, Fig. 3.25).

Table 3.39 Cockpit component input data

Name	Value	Unit
Shift Mode	Automatic	–
Number of Gears Forward	1	–
Number of Gears Back	1	–
Maximum Brake Force	250.0	N
Brake Light Switch Threshold	1.0	%
Number of Retarder Steps	0	–

Table 3.40 Electrical Consumer component input data

Name	Value	Unit
Nominal Voltage	320	V
Direction	Positive	–
Exceeding Value Range	Admissible	–
Threshold Value	0.5	–
Reference	Absolute	–

Fig. 3.25 Resistance variation in the electric network
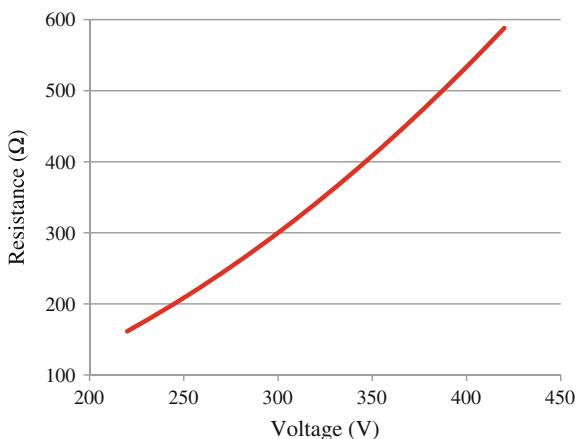
The Battery H (19) component is used for simulating hybrid and electric vehicles. The basic model consists of a voltage source and an ohmic resistance [1].

Double click on the battery H icon and enter the following data (Table 3.41). The resistance is constructed in a way that a big part of the complex processes within the battery are taken into consideration. 2 RC elements which describe the concentration overvoltage and the transfer overvoltage can be added optionally.

The thermal behavior of the battery H is described by a thermal substitution model. The warming caused by the losses inside the battery H and the cooling caused by convection is taken into consideration. Single cells can be modelled as well as any combination of cells. There is no electrical consumer; it is a function of the State of Charge SOC (Fig. 3.26).

Table 3.41 Battery H component input data

Name	Value	Unit
Maximum Charge	10	Ah
Nominal Voltage	320	V
Maximum Voltage	420	V
Initial Charge	95	%
Minimum Voltage	220	V
Number of Cells per Cell-Row	1	–
Number of Cell-Row	5	–
Internal Resistance charge/discharge	0.8/0.6	Ω

Fig. 3.26 Battery SOC (State Of Charge)
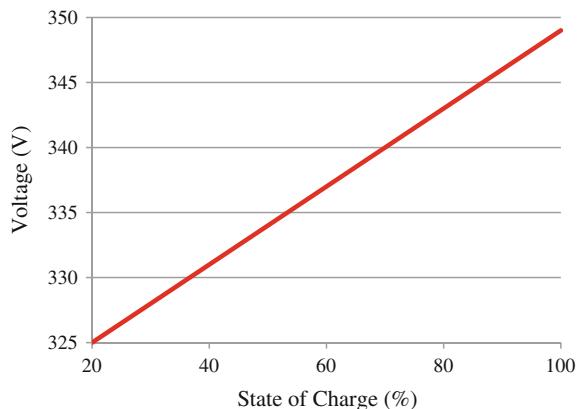
E-Drive (20) component is a function that can be used for calculations (with User-defined functions) (Fig. 3.27). To define component input data, double click on the C code icon and enter the following data for function, and for description of Data Bus (Table 3.42) [1].

E-Brake & M-Brake (21) component is a function can be used for calculating with User-defined functions used to conversion of E-Drive torque to brake pressure (Fig. 3.28). To define component input data, double click on the C code icon and enter the data for function and for Data Bus (Table 3.43) [1].

Fig. 3.27 The E-Drive function

```
/* Translation from edriving to ebraking*/
        if(a[3] > 0 && a[0] >0.1)
                {
        y[0] = a[3]/a[4]*(-1)*a[5];
                }
              else
                {
            y[0] = a[2];
                }
```

Table 3.42 Data Bus Connections for E-Drive

Data Bus	Description	Unit	Connection	Decouple
a[0]	Vehicle Velocity	km/h	Optional	Coupled
a[1]	Vehicle Acceleration	m/s^2	Optional	Coupled
a[2]	Load Signal	–	Optional	Coupled
a[3]	Brake Pressure	bar	Optional	Coupled
a[4]	Maximum Brake Pressure	bar	Optional	Coupled
a[5]	Bremsfactor	–	Optional	Coupled
a[6]	a[6]	–	Optional	Coupled
y[0]	Mod Load Signal	–	Optional	Coupled

```
/*Conversion routine Converting brake Torque into Pressure for all Brakes*/
                           double eBrake;
                           if (a[0] < 0 )
              {  eBrake = a[0]*2*a[1]*a[2]/(2*(a[3]+a[4]));  }
                              else
                      {  eBrake = 0.;  }
/*Calculation of reduced mechanical Brake & Function to a maximum value*/
                      if ((eBrake+a[5])>0.0)
                              {
                      y[0]= (eBrake+a[5]);
                              }
                            else
                              {
                        y[0]= 0.0;
                              }
```

Fig. 3.28 E-Brake & M-Brake function

Table 3.43 Data Bus Connections for E-Brake & M-Brake

Data Bus	Description	Unit	Connection	Decouple
a[0]	Vehicle Velocity	km/h	Optional	Coupled
a[1]	Vehicle Acceleration	m/s^2	Optional	Coupled
a[2]	Load Signal	–	Optional	Coupled
a[3]	Brake Pressure	bar	Optional	Coupled
a[4]	Maximum Brake Pressure	bar	Optional	Coupled
a[5]	Bremsfactor	–	Optional	Coupled
a[6]	a[6]	–	Optional	Coupled
y[0]	Mod Load Signal	–	Optional	Coupled

Table 3.44 Monitor component input data

Name	Value	Unit
Input 0	LoadSignal_Cockpit	–
Input 1	Velocity	km/h
Input 2	Torque_eDrive	Nm

Table 3.45 Constants component input data

Channel	Name	Value	Unit	Data Type
Constant 0	Brake_Factor_front	0.00012	–	Double
Constant 1	Brake_Factor_rear	0.00008	–	Double
Constant 2	iFD	3.65000	–	Double
Constant 3	iTr	1.00000	–	Double
Constant 4	Maximum Brake Pressure	50.0000	bar	Double
Constant 5	Brake Factor	1.00000	–	Double

The Monitor component (22) can be introduced, if the calculation run must be detected. It is possible to show some results of the calculation while the calculation is running. Click on the description of Data Bus tab and open the following dialog. To select a Data Bus channel, click to access at the available list. Enter the text for the description and then click on to select the unit (Table 3.44).

Constants (23) component enables the user to define up to 99 constant values which can be used by other components through the Data Bus. The values can be of type integer, double or string (Table 3.45) [1].

References

1. Varga, B. O., Mariașiu, F., Moldovanu, D., & Iclodean, C. (2015). Electric and plug-in hybrid vehicles—advanced simulation methodologies, chapter 2, pp. 9–200, chapter 3, pp. 223–287. Springer International Publishing Ed., ISBN: 978-3-319-18638-2.
2. Retrieved December 9, 2015, from http://www.autovehicule-rutiere.ro/wp-content/uploads/cursuri/dinamica_autovehiculelor/Dinamica-autovehiculelor-Cap-5.pdf, (in Romanian).
3. AVL CRUISE (2011) Users guide, AVL list GmbH, Graz, Austria, Document no. 04.0104.2011, Edition 06.2011.
4. AVL CRUISE (2009) Theory manual, AVL list GmbH, Graz, Austria, Document no. 04.0108.2009, Edition 06.2009.
5. AVL CRUISE version 2011. (2011) Gear Shifting Program (GSP), AVL List GmbH, Graz, Austria, Document no. 04.0114.2011, Edition 06.2011.
6. Stone, R., & Ball, J. K. (2004). *Automotive engineering fundamentals, SAE* (International ed.). US: Warrendale. ISBN 0-7680-0987-1.
7. Millo, F., Rolando, L., & Andreata, M., (2011) Numerical simulation for vehicle powertrain development, computer and information science, chapter 24, 2011. ISBN: 978-953-307-3897.

Chapter 4
Study Case: Comparative Analysis Regarding the Buses Used for Urban Public Transportation for People Within Cluj-Napoca Municipality

4.1 Present Situation of the Urban Public Transportation System in Cluj-Napoca

The present situation within the Public Transportation Company (CTP—Compania de Transport Public) is as follows: the auto park is made of 252 buses which fit in the EURO 0—EURO 5 European norms, with a high fuel consumption, equipped with 4–6 L diesel engines and semi-automated gearboxes with pneumatic actuators [1].

Presently within CTP Cluj-Napoca there are only classic buses equipped with internal combustion diesel engines, buses which have a standard length of 12 m and a transport capacity of up to 100 passengers, respectively a standard length of 18 m (articulated buses) and a transport capacity of up to 130 passengers [2].

Although they are more independent from the point of view of the mobility, the existing buses have a harmful effect on both the transported passengers and the other residents of the municipality, because most buses are equipped with engines which correspond to EURO 3 pollution norms, thus resulting in a great volume of pollutants emitted into the atmosphere. Furthermore, there are 10 buses manufactured in the 1986–1987 which are about to be changed with more modern and more ecofriendly means of transportation, because they are about to reach their maximum usage period.

The greenhouse effect (GHG) is a process through which the atmosphere captures a part of the solar energy, thus warming the earth and moderating the climate. Experts in the climatic domain believe that an increase of greenhouse gases level represents an increase caused by human activities which artificially accentuate the greenhouse effect, resulting in an increase of global temperatures and a climate disorder.

One third of the gas emissions responsible for the greenhouse effect, respectively for the effect of global warming of the planet is due to the vehicles equipped with IC Engines, powered by fossil fuels. Consequently, replacing the classic drive

systems with hybrid and electric drive systems is a way of reducing or limiting the effects of global warming [3, 4].

Global warming implies two major problems: the necessity to reduce greenhouse gas emissions in order to stabilize the concentration level of these gases into the atmosphere, to prevent the anthropic influence over the climatic system, and the necessity to adapt to the effect of climatic changes, taking into consideration the fact that these effects are already visible in the environment because the inertia of the climatic system, no matter the present results of actions made to reduce the emissions [5].

Greenhouse gases include carbon dioxide (CO_2), resulted from burning fossil fuel, methane, released from plantations and waste deposits, or from products resulting from burns and different industrial chemical compounds [3].

Over 70 % of the air pollution in megalopolises is resulted from the transportation sector, having vehicles with IC Engines fueled with fossil fuels.

Annually a vehicle emits into the atmosphere a quantity of CO_2 with a mass four times bigger that its own mass. The dependence of the transportation sector to fossil fuels is most acute as compared to other domains, from where results the increased pollution grade that this sector possesses.

From the perspective of diverse economic sectors of the European Union, the generation of electric energy is responsible for 37 % of the total CO_2 emissions, transportation activities for 28 %, household activities for 16 %, and services for 5 % [3].

The major problem is regarding the forecasted increase of CO_2 emissions up until the year 2040 which, according to recent estimations, will result 90 % from the transportation sector, from which road transport is responsible for a percentage of over 80 % [3].

Due to the existence of a strict legislation in the domain of pollution reduction, the European Union has reduced the contribution to global warming to a value of 14 %, as opposed to the United States of America 29 % and Asia 25 % [3].

One of the main sources generating greenhouse gases is transport, and one of the solutions to the climatic changes problem, respectively to reduce the emissions of greenhouse gases, consists of reducing the use of fossil fuels (petrol, gas, coal etc.).

In the case of urban transport for passengers, the solutions adopted for reducing greenhouse gas emission consists of replacing the vehicles using conventional fuel with vehicles with hybrid and electric drive.

The reduction of pollution generated by urban transport for passengers can be made through the following:

- reducing the urban passenger traffic;
- changing the travelling mode in the traffic;
- improving the effects generated by passenger traffic.

The structure of these methods for improving passenger traffic in Cluj-Napoca municipality can be distributed as follows:

- planning the optimal use of urban routes for passenger transport;
- improving the existing infrastructure;
- legislation, regulations, restrictions, decisions of the Local Council;
- economic instruments which advantage the passengers and stimulate the use of public transportation;
- informing the citizens of the municipality;
- interdiction of circulation for heavy traffic during free days;
- moving the circulation of heavy vehicles towards the peripheries, while forbidding them to use the central zones.

The experience of CTP Cluj-Napoca SA regarding the reduction of energetic consumption of public transportation and the promotion of an environmentally friendly transport has materialized until now through the following measures:

- in the year 2005 CTP developed a research project regarding the use of biofuels for public transportation;
- in the year 2009 the Recodrive program was implemented in order to reduce energy consumption through economical driving. By applying this program diesel fuel consumption was reduces by 8 % and electric energy consumption by 6 %.

As a member of the European Union, Romania assumed its responsibilities and commitments regarding the environmental protection and limitation of the effects of climatic changes, thus joining the common demarches of the states preoccupied with pollution control. Romania is also one of the signatory states of the Kyoto Protocol, which has as objective the reduction of the level of carbon dioxide emissions by 20 % until the year 2020 [4].

European politics from the energy and environmental protection domain emphasize the negative impact that the large urban areas and the increasing number of classic drive vehicles have over the environment.

Generally it's considered that urban traffic generates up to 40 % of carbon dioxide emissions and up to 70 % of other pollutant emissions [1].

The vehicles equipped with internal combustion engines are the pollutant factor taken into consideration more and more often.

The pollutant emissions of the vehicles have the following particularities:

- the elimination of pollutant emissions is made very close to the ground, fact which lead to the creation of high concentrations at very low heights, even for gases with low density and great capacity of diffusion into the atmosphere;
- pollutant emissions take place on the entire surface of the locality, the concentration differences depending on the intensity of the traffic and the ventilation possibilities of the routes.

Of all pollutant emissions, carbon dioxide CO_2 and methane CH_4 are considered greenhouse gases which contribute to reducing the permeability of the atmosphere for the caloric radiations reflected by the Earth through the cosmic space, thus generating the global warming phenomena.

At EU level almost 28 % of greenhouse gas emissions are due to transportations and 84 % of these are due to road transport, with the mention that 10 % come from urban road traffic. Globally, the tendency is to reduce CO_2 and CH_4 emissions through innovative drive technologies and equipment for public road transportation means, like for example hybrid and electric vehicles [5].

Presently on the market there are three vehicle concepts, which can be connected to the electric energy network for recharging the accumulator batteries used by vehicles for propulsion. These concepts are: the Plug-in hybrid electric vehicle PHEV, Range Extender electric vehicle REV and the Battery electric vehicle BEV. PHEV and REV use two energy sources (classic fuel and electric battery from the national network), while BEV uses only electric energy.

All electric vehicles are considered conformable to EURO 6 emission norms. However, they are different when it comes to CO_2 emissions, which can be considered zero only when using electric energy which comes exclusively from clean hydroelectric energy, wind energy, photovoltaic energy etc.

The national strategy objectives in the transport domain are described as follows [6]:

- the diminution of emission generated by the urban and interurban transport network in order to reduce the impact on the environment;
- the achievement of durable levels of energy consumption for transport by diminishing greenhouse gas emissions;
- the reduction of noise generated by the means of transport to minimize the impact on the health of the population;
- achieving and maintaining CO_2 emissions of vehicles under 120 g/km;
- reaching the desideratum of 6 % biofuel use from the quantity of conventional fuels.

The local strategy objectives of Cluj-Napoca municipality aim through strategic decisions, previous planning and reports regarding a durable urban transport to achieve the conditions necessary for the title of next European capital. The main strategic objectives are developing a durable urban structure by reducing the use of private vehicles, encouraging the use of public transportation and the development of public transport infrastructure in order to reduce greenhouse gas emissions.

Implementing a new public transport system based on hybrid and electric buses assures a tendency of increasing the dynamic of public transportation, as opposed to individual transport with personal vehicles which in an urban agglomeration contributes to maintaining and improving the qualitative parameters of the state of the environment by reducing air pollution and by minimizing CO_2 emissions.

Another reason which justifies the efficiency of using hybrid and electric drive vehicles is the reduction of the noise level in the urban environment. According to H.G. 321/2005 regulations regarding the evaluation and management of ambient noise, in Romania the target value to be reached for noise efferent to road traffic is 50 dB(A). Presently conducted studies show that the level of noise efferent to existing passenger transport vehicles is somewhere between 60 … 95 dB(A).

Likewise, according to the "Action plan for preventing and reducing the ambient noise in Cluj-Napoca municipality" a reduction of 1 dB or road noise will determine an increase of the value of affected buildings by up to 0.6 % [7].

In the current context of reaching and applying the local strategy objectives of Cluj-Napoca municipality to promote a sustainable public transport from the point of view of minimizing the pollutant emissions in the atmosphere, it is required to identify some optimal solutions of partially replacing the existing bus park.

The new regulations regarding the EURO 6 pollution norms bring significant modifications to reducing by 50 % the level of pollutant emissions measured for the following indicators: carbon dioxide (CO_2), hydrocarbons (HC), methane (CH_4), azote oxides (NO_x) and particulate matter (PM). For hybrid drive systems these indicators come within the limits required by the EURO 6 pollution norms, whereas for electric drive systems all these emission indicators have the value zero (locally).

The carbon footprint given by the road transport represents the quantity of carbon dioxide (CO_2) emitted during a year from transport activity and it is calculated according to the fuel quantity consumed within a year.

Just as it results from the comparative studies between the elaborated drive systems, CO_2 emissions are considerably reducing, reaching even zero in the case of electric drive, only in the situation in which recharging the batteries only uses electric energy provided exclusively from renewable energy [1].

The comparative studies created for the noise factors and vibrations show in the case of using classic and electric drive buses that the level of noise generated while the bus functions with electric propulsion is of approximately 55 dB(A), as opposed to when the bus only uses classic propulsion when the level is of approximately 90 dB(A).

In conclusion, following the detailed comparative analyses, the buses with electric drive are within the parameters of total reduction of local CO_2 emissions and also of other emission indicators, as opposed to the buses powered by internal combustion engines.

Likewise, just as it was shown above, from the analysis of the noise level generated by a bus with electric drive it results that its level is 35 dB(A) lower that the level of noise created by a bus equipped with internal combustion engine, which leads to a higher comfort level for the passengers.

As far as supply systems go, the batteries used in the case of an electric bus have a life span of up to 5 years and they are 100 % recyclable.

Replacing the classic buses equipped with internal combustion engines with buses equipped with electric motors and Plug-in recharging systems has the following advantages from an economical-social point of view:

- the possibility of creating central zones with lower pollution;
- the assurance of a higher comfort for the passengers and traffic participants through lack of vibrations generated by high capacity internal combustion engines;

- the lack of vibrations will not harm the infrastructure and historical buildings from the central area;
- the inexistence of pollutant emissions with negative impact from depositing themselves of the surface of the buildings;
- reduced pollutant emissions (CO, NO_x, HC, PM, CO_2 etc.) and the elimination of exposing the passengers and pedestrians to these emissions;
- lower maintenance costs due to lack of systems specific to IC Engines;
- lower exploitation costs due to the lower price of electric energy as compared to the price for classic fuel, according to traveled distances;
- no need to instruct the maintenance personnel for the diesel hybrid system.

In the specific case of Cluj-Napoca municipality because of the existing infrastructure for the network of trolleybus and tramway, the optimal solution to fast recharging of the batteries is connecting through a pantograph to the trolleybus lines (750 V), and the slow recharging station through an outlet to the 380 V network to which the Plug-in buses will connect to recharge during the night.

Thus the autonomy of Plug-in hybrid buses can be extended, the buses can be exploited during the entire day and the batteries will be brought to optimum level of charge during the night through a conventional recharge, directly from the three-phase network.

The advantages of electric buses with fixed recharging station are the following [1]:

- zero pollution (emissions produced locally);
- superior efficiency of electric vehicles (>90 %) compared to the efficiency of internal combustion engine ($\sim$30 %);
- they reach a maximum velocity similar to the one of classic vehicles, but with a more superior value for acceleration because of the electric motors with which they are equipped;
- the electric vehicle capacity of working in a generator regime when braking and the energy produced is stocked in the batteries;
- electric vehicles respond easier to commands compared to classic vehicles, thus having a higher maneuverability, fact which makes them easier to use especially for urban passenger transport;
- a minimum investment is necessary for creating fast recharging stations, because the existent infrastructure can be used and because their autonomy can be extended limitlessly through partial recharges between courses;
- they respond to the needs of citizens from the urban environment for daily transportation, needs which do not exceed distances greater than 100 km daily;
- reduced maintenance and operating costs due to the reliability of the electric motors with which they are equipped, as compared to classic buses.

4.2   Comparative Analysis of the Types of Buses in Operation

Presently CTP Cluj-Napoca services a number of 42 bus routes within Cluj-Napoca municipality, having a length of over 100 km, on which operate a total number of 252 bus type vehicles for public transportation [2].

The municipality is crossed by 662 km of streets, from which 443 km are equipped with modern facilities (steady street structure, public service equipment etc.). Public transportation is made on 342 km from the network of internal roads, via many routes for buses, minibuses, trolleybuses and tramways.

The CTP Cluj-Napoca auto park was extended by acquiring a number of 40 new buses, delivered by the companies Solaris Bus & Coach and Iveco, buses which are equipped with EURO 6 engines and which have the following technical characteristics [2]:

- they correspond to all European norms regarding passenger transport;
- they have a transport capacity of up to 143 passengers, with easy access for persons with motor disabilities and for the elderly;
- they have a service live of up to 15 years;
- they are equipped with cameras in order to identify possible acts of vandalism and to assure traffic safety;
- they are equipped with a completely lowered floor and a ramp for boarding carriages for persons with disabilities;
- they are equipped with automated doors with anti-crushing protection, with the possibility of opening them from the inside and outside in case of emergency and with the possibility of counting the passengers while boarding or deboarding;
- they use a climatization system (heating, cooling, air-conditioning, ventilation) both for the driver and for the passengers;
- they have electronic systems installed with LED display to inform the passengers on the inside and outside, respectively sound systems for inside;
- the body frame is made of stainless steel, the body parts are mare of composite materials resistant to corrosion and the lateral panels of the body are made of aluminum;
- they are equipped with diesel engines which respect the EURO 6 pollution norm;
- they have automated taxation systems compatible with the ones implemented in Cluj-Napoca;
- they have an onboard computer for the administration, diagnostic and management for the vehicle which collects, stockpiles and transmits the data regarding the bus activity;
- they can be tracked through GPS, by using equipment compatible with the ones already existing in endowment of CTP Cluj-Napoca.

Some of the most important and modern models of classic buses which are part of CTP Cluj-Napoca are the following:

Renault Agora S (Fig. 4.1) is a standard bus having 12 m in length, designed and manufactured by the Renault Company up until the year 2005. The constructive characteristics are presented in Table 4.1 [8].

Fig. 4.1 The Renault Agora S bus [9]

Table 4.1 Constructive characteristics of Renault Agora S [8]

No.	Parameter	Description	U.M.	Value
1	Constructive dimensions	Length	mm	11990
		Width	mm	2500
		Height	mm	2850
		Passenger transport capacity	–	100
		Tire sizes	–	265/70R19.5
		Weight without passengers	kg	11500
		Diesel tank capacity	l	240
2	Dynamic performances	Maximum velocity	km/h	74
		Fuel consumption per 100 km	l	35
		Climb	%	10
		Gyration radius	m	12
		Angle of approach	°	7
3	Thermal engine characteristics	Model Renault	–	V3 EURO 3
		Maximum power	kW/CP	187/253
		Maximum coupling	Nm	890
4	Emission according to the EURO norms	CO emissions	g/kWh	2.10
		HC emissions	g/kWh	0.66
		NO_x emissions	g/kWh	5.00
		PM emissions	g/kWh	0.10
		Smoke emissions	g/kWh	0.80

Renault Agora L (Fig. 4.2) is an articulated bus having 18 m in length, with 2 doors in the first module and 1 or 2 doors in the second module, designed and manufactured by the Renault Company up until the year 2005. The constructive characteristics are presented in Table 4.2 [8].

Fig. 4.2 The Renault Agora L bus [9]

Table 4.2 Constructive characteristics of Renault Agora L [8]

No.	Parameter	Description	U.M.	Value
1	Constructive dimensions	Length	mm	17800
		Width	mm	2500
		Height	mm	3100
		Passenger transport capacity	–	130
		Tire sizes	–	265/70R19.5
		Weight without passengers	kg	16400
		Diesel tank capacity	l	260
2	Dynamic performances	Maximum velocity	km/h	75
		Fuel consumption per 100 km	l	42
		Climb	%	10
		Gyration radius	m	12
		Angle of approach	°	7
3	Thermal engine characteristics	Model Renault	–	V3 EURO 3
		Maximum power	kW/CP	187/253
		Maximum coupling	Nm	925
4	Emission according to the EURO norms	CO emissions	g/kWh	2.10
		HC emissions	g/kWh	0.66
		NO_x emissions	g/kWh	5.00
		PM emissions	g/kWh	0.10
		Smoke emissions	g/kWh	0.80

Renault R312 (Fig. 4.3) is a standard bus having 12 m in length, designed and manufactured by the Renault Company up until the year 2000. The constructive characteristics are presented in Table 4.3 [10].

Fig. 4.3 The Renault R312 bus [9]

Table 4.3 Constructive characteristics of Renault R312 [10]

No.	Parameter	Description	U.M.	Value
1	Constructive dimensions	Length	mm	11900
		Width	mm	2500
		Height	mm	3100
		Passenger transport capacity	–	90
		Tire sizes	–	265/70R19.5
		Weight without passengers	kg	11450
		Diesel tank capacity	l	180
2	Dynamic performances	Maximum velocity	km/h	75
		Fuel consumption per 100 km	l	42
		Climb	%	10
		Gyration radius	m	12
		Angle of approach	°	7
3	Thermal engine characteristics	Model Renault	–	Mid EURO 2
		Maximum power	kW/CP	187/253
		Maximum coupling	Nm	925
4	Emission according to the EURO norms	CO emissions	g/kWh	4.00
		HC emissions	g/kWh	1.10
		NO_x emissions	g/kWh	7.00
		PM emissions	g/kWh	0.25
		Smoke emissions	g/kWh	–

Irisbus Citelis 12 (Fig. 4.4) is a standard bus having 12 m in length, designed and manufactured by the Irisbus S.A. Company; this model is still being manu- factured nowadays. The constructive characteristics are presented in Table 4.4 [11].

Fig. 4.4 The Irisbus Citelis 12 [9]

Table 4.4 Constructive characteristics of Irisbus Citelis 12 [11]

No.	Parameter	Description	U.M.	Value
1	Constructive dimensions	Length	mm	11900
		Width	mm	2500
		Height	mm	3300
		Passenger transport capacity	–	110
		Tire sizes	–	275/70 R 22.5
		Weight without passengers	kg	12820
		Diesel tank capacity	l	180
2	Dynamic performances	Maximum velocity	km/h	75
		Fuel consumption per 100 km	l	42
		Climb	%	10
		Gyration radius	m	12
		Angle of approach	°	7
3	Thermal engine characteristics	Model Renault	–	F2B EURO 5
		Maximum power	kW/CP	213/290
		Maximum coupling	Nm	1100
4	Emission according to the EURO norms	CO emissions	g/kWh	1.50
		HC emissions	g/kWh	0.46
		NO_x emissions	g/kWh	2.00
		PM emissions	g/kWh	0.02
		Smoke emissions	g/kWh	0.50

Solaris Urbino 18 (Fig. 4.5) is a standard bus having 18 m in length, designed and manufactured by Solaris Bus & Coach S.A.; this model is still being manufactured nowadays. The constructive characteristics are presented in Table 4.5 [12].

Fig. 4.5 The Solaris Urbino 18 [9]

Table 4.5 Constructive characteristics of Solaris Urbino 18 [12]

No.	Parameter	Description	U.M.	Value
1	Constructive dimensions	Length	mm	17900
		Width	mm	2550
		Height	mm	2850
		Passenger transport capacity	–	147
		Tire sizes	–	275/70 R 22.5
		Weight without passengers	kg	17500
		Diesel tank capacity	l	350
2	Dynamic performances	Maximum velocity	km/h	72
		Fuel consumption per 100 km	l	–
		Climb	%	10
		Gyration radius	m	10
		Angle of approach	°	7
3	Thermal engine characteristics	Model DAF	–	MX EURO 6
		Maximum power	kW/CP	228/310
		Maximum coupling	Nm	1500
4	Emission according to the EURO norms	CO emissions	g/kWh	1.50
		HC emissions	g/kWh	0.13
		NO_x emissions	g/kWh	0.40
		PM emissions	g/kWh	0.01
		Smoke emissions	g/kWh	–

Iveco Urbanway 12 (Fig. 4.6) is a standard bus having 12 m in length, designed and manufactured by Iveco S.A.; this model is still being manufactured nowadays. The constructive characteristics are presented in Table 4.6 [13].

Fig. 4.6 The Iveco Urbanway 12 [9]

Table 4.6 Constructive characteristics of Iveco Urbanway 12 [13]

No.	Parameter	Description	U.M.	Value
1	Constructive dimensions	Length	mm	12000
		Width	mm	2500
		Height	mm	3066
		Passenger transport capacity	–	90
		Tire sizes	–	275/70 R 22.5
		Weight without passengers	kg	11500
		Diesel tank capacity	l	250
2	Dynamic performances	Maximum velocity	km/h	85
		Fuel consumption per 100 km	l	–
		Climb	%	10
		Gyration radius	m	12
		Angle of approach	°	7
3	Thermal engine characteristics	Model Iveco	–	EURO 6
		Maximum power	kW/CP	265/360
		Maximum coupling	Nm	1550
4	Emission according to the EURO norms	CO emissions	g/kWh	1.50
		HC emissions	g/kWh	0.13
		NO_x emissions	g/kWh	0.40
		PM emissions	g/kWh	0.01
		Smoke emissions	g/kWh	–

Iveco Urbanway 18 (Fig. 4.7) is a standard bus having 18 m in length, designed and manufactured by Iveco S.A.; this model is still being manufactured nowadays. The constructive characteristics are presented in Table 4.7 [14].

Fig. 4.7 The Iveco Urbanway 18 [9]

Table 4.7 Constructive characteristics of Iveco Urbanway 18 [14]

No.	Parameter	Description	U.M.	Value
1	Constructive dimensions	Length	mm	17910
		Width	mm	2500
		Height	mm	3066
		Passenger transport capacity	–	96
		Tire sizes	–	275/70 R 22.5
		Weight without passengers	kg	16500
		Diesel tank capacity	l	340
2	Dynamic performances	Maximum velocity	km/h	92
		Fuel consumption per 100 km	l	–
		Climb	%	10
		Gyration radius	m	10
		Angle of approach	°	7
3	Thermal engine characteristics	Model Iveco	–	L6 EURO 6
		Maximum power	kW/CP	294/400
		Maximum coupling	Nm	1700
4	Emission according to the EURO norms	CO emissions	g/kWh	1.50
		HC emissions	g/kWh	0.13
		NO_x emissions	g/kWh	0.40
		PM emissions	g/kWh	0.01
		Smoke emissions	g/kWh	–

4.3   Selection of Bus Operating Routes for Public Transport

The bus routes selected for the elaboration of the research study—which is the subject of this book—are the following: 27, 28, 30 and 32. According to the data provided by CTP Cluj-Napoca, the characteristics of these routes are:

Route 27 Grigorescu neighborhood—Piața Gării (Fig. 4.8) has a length of 9.7 km, it can be traveled in a medium time of 38 min and is served by three buses. The number of stations on the round-trip route is 19, the succession interval between two buses is of 35 min and the medium distance between the stations is of 0.5 km [2].

The stations for the passengers are as follows (Fig. 4.9): Grigorescu—tour, 1 Dec. 1918 I—tour, Petuniei—tour, Vlahuță—tour, P-ța 14 Iulie I—tour, Napoca I—tour, Dragalina I—tour, Horea—tour, Piața Gării—tour, Traian—retour, Dacia—retour,
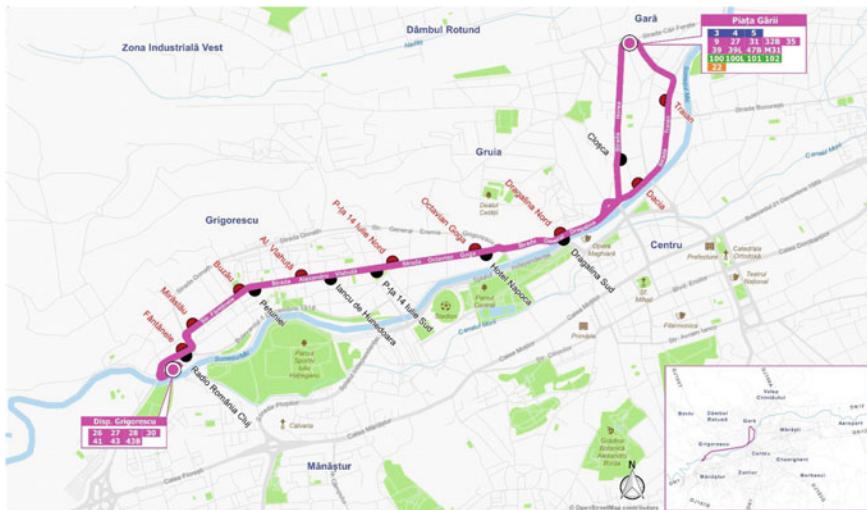
Fig. 4.8 Bus route 27 [2]
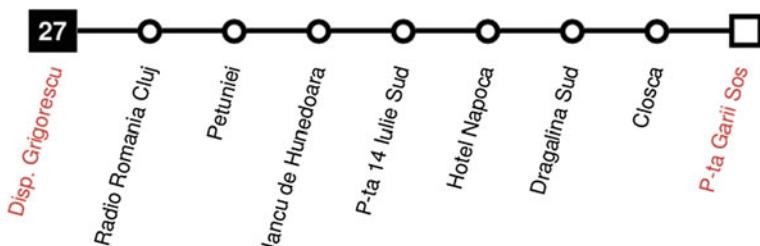
Fig. 4.9 Stations for passengers—route 27 [2]
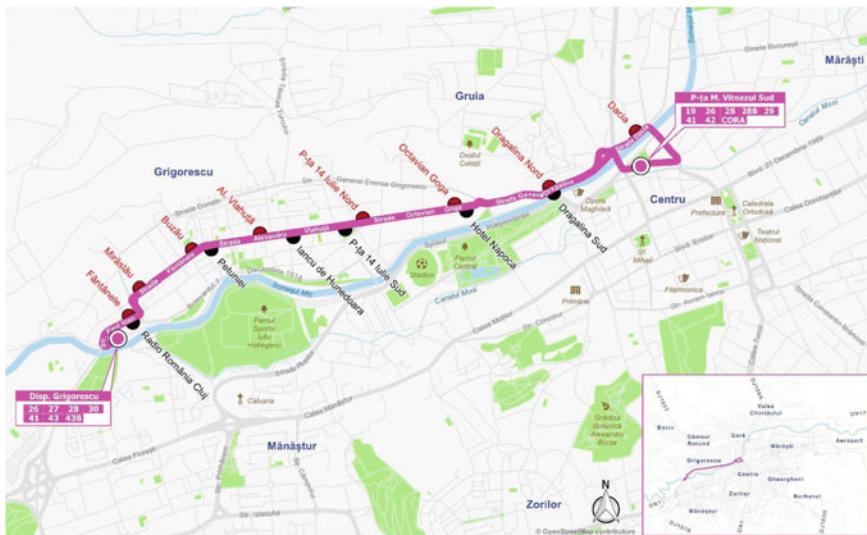
Fig. 4.10 Bus route 28 [2]
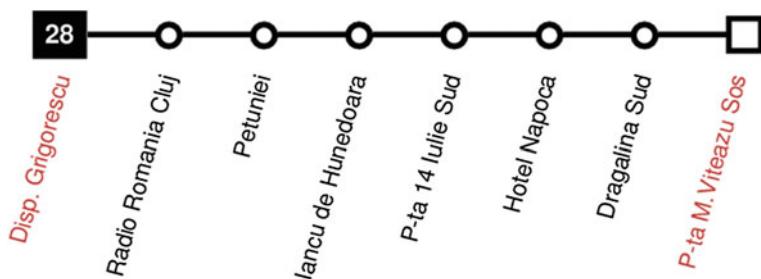
Fig. 4.11 Stations for passengers—route 28 [2]

Dragalina II—retour, Napoca II—retour, P-ța 14 Iulie II—retour, Al. Vlahuță II—retour, Buzău—retour, Mirăslău—retour, Grigorescu—retour [2].

Route 28 Grigorescu neighborhood—Piața Mihai Viteazul (Fig. 4.10) has a length of 8.5 km, can be traveled in 36 min and it is served by two buses. The number of stations for a round-trip route is 16, the succession interval between two buses is 36 min, and the medium distance between stations is 0.51 km [2].

The stations for the passengers are as follows (Fig. 4.11): Grigorescu—tour, 1 Dec. 1918 I—tour, Petuniei—tour, Vlahuță—tour, P-ța 14 Iulie I—tour, Napoca I—tour, Dragalina I—tour, P-ța Mihai Viteazul—retour, Dacia—retour, Dragalina II—retour, Napoca II—retour, P-ța 14 Iulie II—retour, Al. Vlahuță II—retour, Buzău—retour, Mirăslău—retour, Grigorescu—retour [2].

Fig. 4.12 Bus route 30 [2]

Route 30 Grigorescu neighborhood—Aurel Vlaicu Street (Fig. 4.12) has a length of 17.2 km, it can be traveled in 72 min and is served by 16 buses. The number of stations for a round-trip route is 32, the succession interval between buses is 5 min and the medium distance between the stations is 0.54 km [2].

The stations for the passengers are as follows (Fig. 4.13): Grigorescu—tour, 1 Dec. 1918 I—tour, Petuniei—tour, Vlahuță—tour, 14 Iulie I—tour, Uzinei Electrice I—tour, Parcul Central I—tour, Spitalul de Copii I—tour, Memorandumului I—tour, Regionala CFR I—tour, Someşul I—tour, Piaţa Mărăşti I—tour, Mareşal C-tin Prezan—tour, Siretului—tour, Atlas I—tour, IRA II—retour,
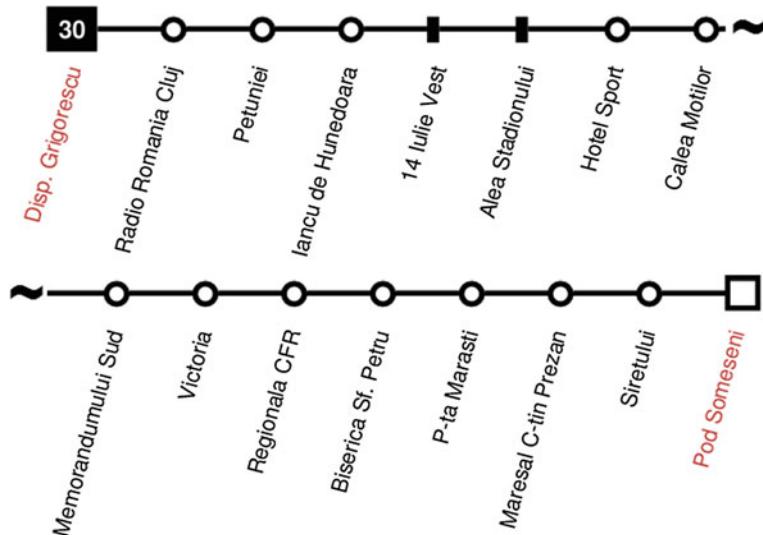
Fig. 4.13 Stations for passengers—route 30 [2]
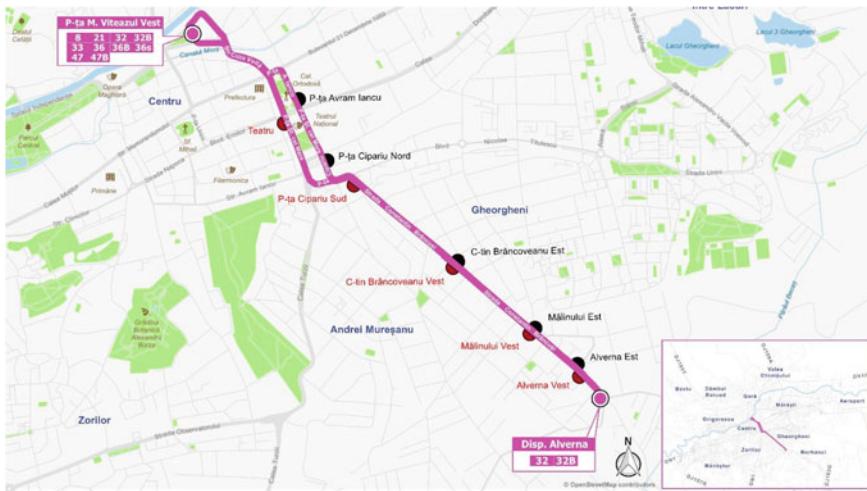
Fig. 4.14 Bus route 32 [2]

Atlas II—retour, A. Vlaicu—retour, Arte Plastice II—retour, P-ţa Mărăşti II—retour, Someşul II—retour, Regionala CFR II—retour, Memorandumului II—retour, Spitalul de Copii II—retour, Parcul Central II—retour, Uzinei Electrice II—retour, 14 Iulie II—retour, Al. Vlahuţă II—retour, Buzău—retour, Mirăslău—retour, Grigorescu—retour [2].

Route 32 Gheorgheni neighborhood Constantin Brâncuşi Street—Piaţa Mihai Viteazul (Fig. 4.14) has a length of 6.6 km, it can be traveled in 35 min and is served by 4 buses. The number of stations for a round-trip route is 13, the succession interval between two buses is 5 min and the medium distance between two stations is 0.51 km [2].

The stations for the passengers are as follows (Fig. 4.15): Alverna—tour, Alverna 1—tour, Mălinului 1—tour, Constantin Brâncoveanu 1—tour, P-ţa Cipariu I—tour, P-ţa Avram Iancu—tour, PMV 2—retour, Opera I—retour, P-ţa Cipariu 3
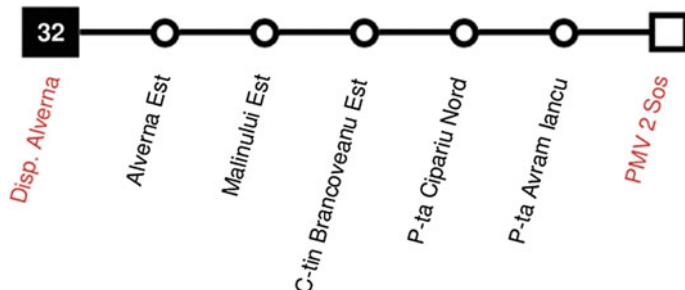
Fig. 4.15 Stations for passengers—route 32 [2]

—retour, Constantin Brâncoveanu 2—retour, Mălinului—retour, Alverna 2—re-tour, Alverna—retour [2].

The terminals for bus maintenance are situated in Grigorescu neighborhood for route 27 and route 28, respectively on Aurel Vlaicu Street for route 30 and on Constantin Brâncoveanu Street for route 32.

References

1. Varga, B.O., (2015). Energy efficiency of vehicles equipped with hybrid or electrical powertrain for urban public transport (in Romanian), Habilitation thesis, Technical University of Cluj-Napoca, Romania, 18 September 2015.
2. Retrieved Dec 9 2015 from http://ctpcj.ro/index.php/ro/, (in Romanian).
3. Racicovschi, V., Danciu, G., & Chefneux, M. (2007). *Automobile Electrice şi Hibride (in Romanian)*. Bucureşti: Editura Electra. ISBN 978-973-7728-98-2.
4. Retrieved Mar 11 2016 from http://www.legex.ro/Legea-3–2001-23945.aspx, Legea nr. 3/2001 pentru ratificarea Protocolului de la Kyoto la Convenţia-cadru a Naţiunilor Unite asupra schimbărilor climatice, adoptat la 11 decembrie 1997, (in Romanian).
5. Retrieved Mar 2016 from http://www.primariasv.ro/portal/Suceava/portal.nsf/AC9D390CFE0A98C7C2257BEC00252C03/$FILE/brosura%20masini%20electrice%203.pdf, Proiect EVUE (2010)—Mijloace de transport electrice în zonele urbane din Europa, Primăria Municipiului Suceava, România, Proiect Nr. 38659/2010 (in Romanian).
6. Retrieved Dec 12 2015 from http://www.mt.ro/web14/documente/strategie/strategii_sectoriale/strategie_dezvoltare_durabila_noua_ultima_forma.pdf, (in Romanian).
7. Retrieved Dec 12 2015 from http://www.primariaclujnapoca.ro/informatii-publice/harta-de-zgomot.html, (in Romanian).
8. Retrieved Dec 20 2015 from https://en.wikipedia.org/wiki/Irisbus_Agora
9. Retrieved Dec 20 2015 from http://tramclub.org/viewtopic.php?t=4093&sid=73834042f9ceb48590252676a64068bc
10. Retrieved Dec 20 2015 from https://en.wikipedia.org/wiki/Renault_R312
11. Retrieved Dec 20 2015 from https://en.wikipedia.org/wiki/Irisbus_Citelis
12. Retrieved Dec 20 2015 from https://www.solarisbus.com/vehicle/urbino-18
13. Retrieved Dec 20 2015 from http://www.iveco.com/France/collections/technical_sheets/Documents/Iveco_Bus_Update/Urbanway/Urbanway-Cursor8/Urbanway-12m-Cursor-8.pdf
14. Retrieved Dec 20 2015 from http://www.iveco.com/France/collections/technical_sheets/Documents/Iveco_Bus_Update/Urbanway/Urbanway-Cursor8/Urbanway-18m-Cursor-8.pdf

Chapter 5
Virtual Infrastructure Design of the Routes Used in Computer Simulations

5.1 The AVL Road Importer

AVL Road Importer is an AVL CONCERTO™ option. The purpose of this option is to convert any GPS data or x, y data of a real road into a format readable by AVL CONCERTO™ [1].

This tool is not a GIS tool in the sense that it does not permit to log GPS data nor does it have any link to any mapping tool. All the data are provided by the user.

Therefore, the generated road is representative of that data. The only given information about the road are the points, which the user can limit in case they cannot be done with the given set of parameters [1].

AVL CONCERTO™ is a graphical evaluation software application for the post-processing analysis of measurements results on the laboratory test stand, or in real time on vehicles which allow recording within a database of all information regarding the functional parameters of a vehicle so that it could be used later as initial data within computer simulations [2].

The route selected by the user in Google Earth is composed of data regarding geographical coordinates of the route, namely: latitude, longitude and altitude. To define the virtual route it is necessary to digitize these data with the help of AVL Road Importer application.

This subchapter describes the possibilities of AVL Road Importer (Fig. 5.1) as well as its intended use. To navigate, use the command bar available on the left part of the screen. It is composed of four sections [1]:

- Data—in this section, the user is able to either import GPX (GPS Exchange Format) or KML (Keyhole Markup Language) files to AVL CONCERTO™ or simply choose a file in AVL CONCERTO™ Data Explorer;
- Road—in this section, the user is able to choose what data to work with, but also prepare it before the main algorithm;
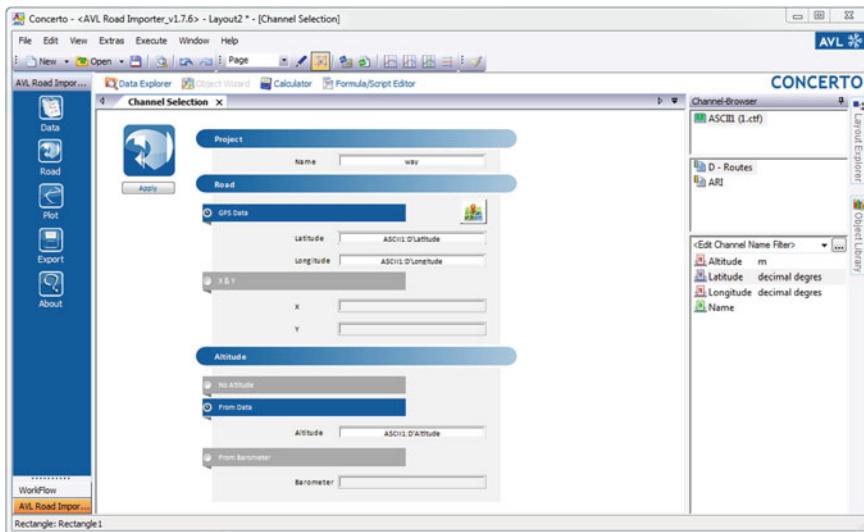
Fig. 5.1 The AVL Road Importer application—main menu

- Plot—in this section, the user can find supplementary tools to verify the quality of the road just generated but also you will be able to specify additional elements such as speed limits;
- Export—in this section, the user will find the necessary tools to export to IPG TruckMaker or AVL CRUISE format.

The **Data** submenu is accessible by clicking on the button Data in the command bar. In the submenu there are the following possibilities [1]:

- Open Data Explorer—this opens the AVL CONCERTO™ Data Explorer and the user is able to access any AVL CONCERTO™ file (read). This is also where previously imported KML and GPX files can be accessed.
- Import KML File—the user is able to import KML through this (by choosing the KML files wish to import and click ok). KML (Keyhole Markup Language) is an XML language focused on geographic visualization, including annotation of maps and images. Geographic visualization includes not only the presentation of graphical data on the globe, but also control of the user's navigation in the sense of where to go and where to look. After importing a KML file, it will appear in the Channel-Browser. The imported files are saved to the directory/Roads/KML/as a CONCERTO™ Transport File (CTF).
- Import GPX File—the user will be able to import GPX through this (by choosing the GPX files you wish to import and click ok). GPX (GPS eXchange Format) is a lightweight XML data format for interchange of GPS data (waypoints, routes, and tracks) between applications and web services on the Internet. After importing a GPX file, it will appear in the Channel-Browser. The

imported files are saved to the directory/Roads/GPX/as a CONCERTO™ Transport File (CTF).

The **Road** submenu is accessible by clicking on the button Road in the command bar. In the submenu the user will find the following possibilities [1]:

- Channel Selection—by clicking on this button, the user can access the channel selection page. Each modification of the parameters needs to be saved by clicking on the Apply button.

  – Project defines the project name here. The project name in itself is not used by the algorithm but it helps predefine the name of the output files.
  – Road defines which channel to use for either latitude or longitude or x and y. Each zone can be activated by checking the corresponding checkbox. If GPS data is specified, the algorithm will convert it into UTM coordinates.
  – Altitude defines which channel to use for the altitude. A channel can be chosen directly into (from data) or the channel containing the barometric pressure (from barometer). If the barometric pressure is chosen, the algorithm will convert the pressure into an altitude in meters. The altitude of the road was generated using the online application KML Altitude Filler, which based on the .KML file which contains the virtual road punctually adds the altitude values over the sea level for each set of GPS coordinates for latitude and longitude [3].
  Other application to define the altitude is GPSPRUNE, an application for viewing, editing and converting coordinate data from GPS systems. Basically it's a tool to let you play with your GPS data after you get home from your trip. It can load data from arbitrary text-based formats (for example, any tab-separated or comma-separated file) or Xml, or directly from a GPS receiver. It can display the data (as map view using Open Street Map OSM images and as altitude profile), edit this data (for example delete points and ranges, sort waypoints, compress tracks), and save the data (in various text-based formats). It can also export data as a GPX file, or as KML file for import into Google Earth, or send it to a GPS receiver [4].

- Preprocessing—by clicking on this button, the preprocessing page is accessed (Fig. 5.2) [1]. This page serves two purposes:

  – The first purpose is to be able to view quickly the selected data in the Channel Selection page;
  – The second purpose is to declare invalid points in the data easily by selecting the part which is invalid with the available cursors.
  – Invalidating data will make the algorithm ignore those points for road creation.

- Parameters—by clicking on this button, the parameters page is accessed (Fig. 5.3) [1]. Each modification of the parameters needs to be saved by clicking
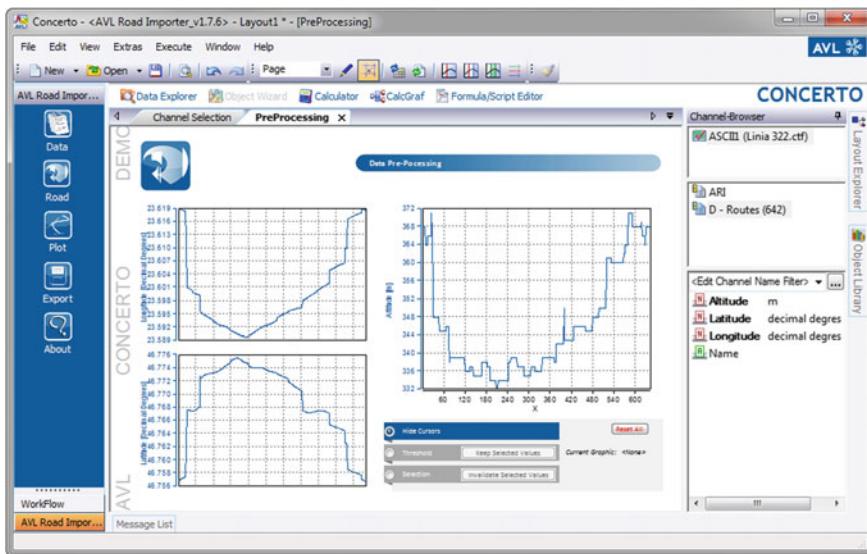
Fig. 5.2 AVL Road Importer—pre-processing menu
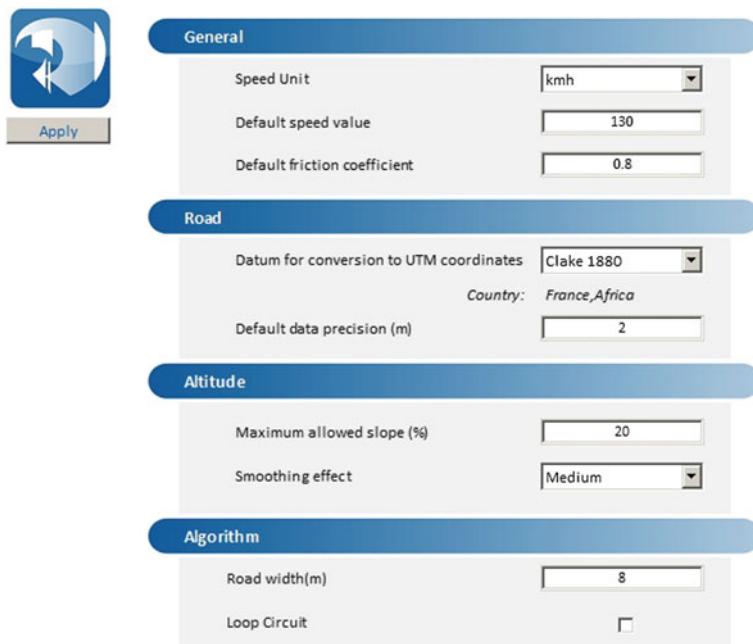
Fig. 5.3 AVL Road Importer—parameters menu

on the Apply button. This page regroups all parameters for the main algorithm. It is cut down in several parts each regarding a certain aspect of the road.

- General—this section regroups all the general parameters for the road:

    i. Speed limits—define a default speed limit as well as the unit used for speeds;
    ii. Friction—defines a default friction between 0 and 1 for the entire road.

- Road—this section regroups two options:

    i. Datum for conversion to UTM coordinates—you may choose the datum used to convert the GPS data. The datum has a different precision depending on the country;
    ii. Default data precision—this value allows the user to filter the data depending on the distance between two points. If this value is set to 5, it will only keep points that are lower than 5 m apart and the minimum value is set to 0.1 m.

- Altitude—this section contains all options relative to the altitude:

    i. Maximum allowed slope—choose the datum used to convert the GPS data. The datum has a different precision depending on the country;
    ii. Smoothing effect—this defines the applied smoothing to altitude. The used algorithm is a moving average. If none is set, no smoothing is applied. If low, medium, or strong is set the moving average applied once, twice, or three times respectively.

- Algorithm—this section contains all options that only concern the algorithm:

    i. Road Width—this is the only parameter defining the road. This value is used to determine if the points will be removed or not depending on if the turn is doable. The larger the value the harder it is to make the turn, hence more values will be removed from the data;
    ii. Loop Circuit—this parameter is still experimental. It enables the creation of a closed track. Activating this option will not only reconnect the endpoint to the first point but it will also try to cor-rect the altitude to fully connect the three dimensions of the road.

- Execute—this is how to start the algorithm. Depending on the file size this step may take some time. Once the algorithm finishes a file appears in the data explorer [1].

The Plot submenu is accessible by clicking on the button Plot in the command bar. In the submenu there are the following possibilities [1]:

- Elevation Profile—clicking on this button, will access the elevation profile page. The purpose of this page is to verify the quality of the altitude (Fig. 5.4).
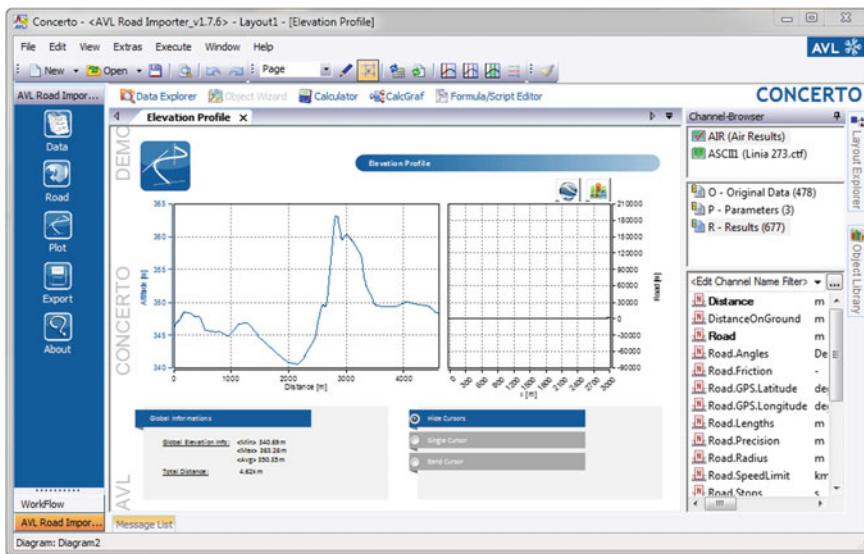
Fig. 5.4 AVL Road Importer—elevation profile menu

- Speed Limits—by clicking this button, the speed limits page is accessed. On this page, the specific speed limits for all parts of the road are defined (Fig. 5.5).

The user can define the speed limits using the band cursor to select a portion of the road, and then click on a speed to be applied on this portion. By default the user may choose between 50, 70, 90, or 110 km/h. The used unit is the one that the user specified in parameters submenu [1].

If the default values are not enough, the user can define own values in the textbox on the right and click on Apply. The graphs on the bottom left of the page allow the user to see the set speed limits and it is updated every time a change is made [1].

The speed limits can be set up by automatic definition. In this section several methods are available to try and automatically define the speed limit based on the input vehicle speed coming from the data [1]. These methods are:

i. Method Percentage—this algorithm will create speed limit zones based on the maximum vehicle speed witnessed in the data. Four zones will be identified as: 25, 50, 75, and 100 % of the maximum vehicle speed. The definition of maximum velocity limits using the percentage method can be applied in the case of road where one keeps track of vehicle movement having a constant velocity (long roads, outside localities);

ii. Method Specific Country—this algorithm will determine the speed limits to apply based on the vehicle speed and thresholds defined by the user. To define the thresholds type them in the popup window. This algorithm will determine the velocity limits which will be applied in vehicle movements based on the
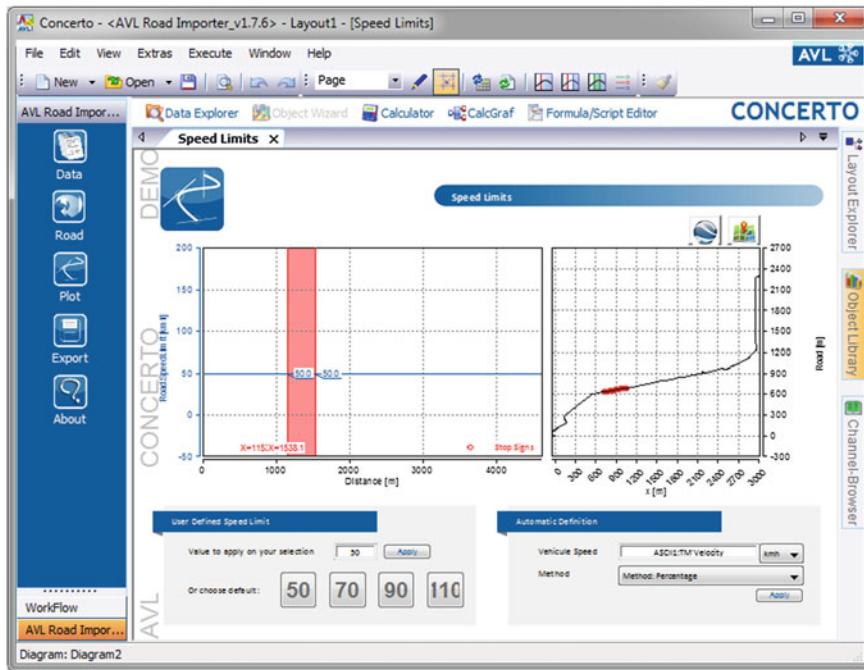
Fig. 5.5 AVL Road Importer—speed limits menu

limits defined by the user, which reflect the legal velocity limits for certain road sectors and can be adapted specifically for European countries, or can be used just to simulate vehicle movement for a certain maximum velocity value for a road sector;

iii. Method Max Speed Break Down Every X—this algorithm will determine the cut-off vehicle speed into zones depending on the distance traveled X, where X can be either 5, 10, or 50 m. The algorithm will then apply the maximum of the vehicle speed in the defined zones as the speed limits for the road.

For each algorithm above, there will be a detection of zero values for the vehicle speed. Every time a vehicle stop is detected there will be a stop panel added to the road automatically that will be the duration of the stop event.

The Export submenu is accessible by clicking on the button Export in the command bar. In the submenu there are the following options [1]:

- IPG TruckMaker test run—when clicking on IPG TruckMaker test run, the user will be prompted for a directory to save the test run. The extension is ROAD, and this test run only contains information linked to the road. It cannot be used as a standalone in IPG TruckMaker (Fig. 5.6). It can, however, be imported directly in the Road menu of IPG CarMaker (this test run is not a digitalized road, the user has to import the road segments it contains);
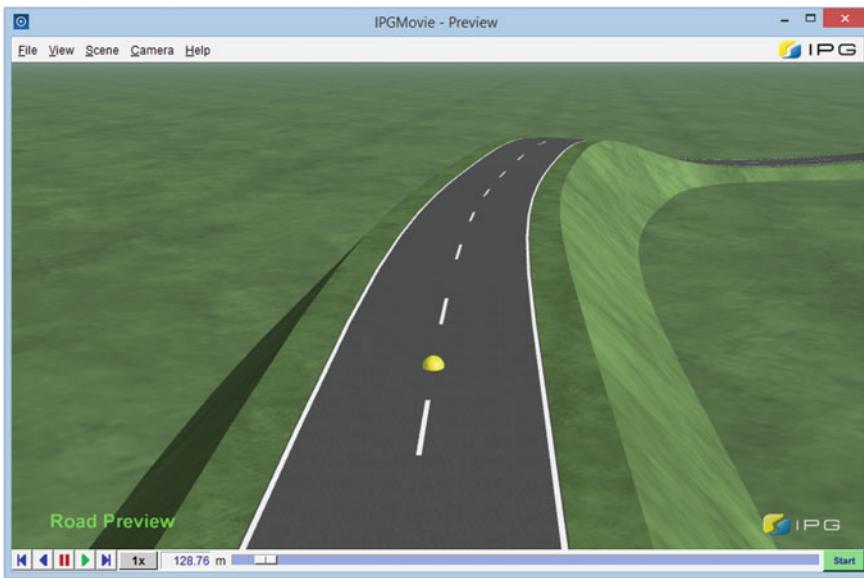
Fig. 5.6 AVL Road Importer—IPG TruckMaker test run menu

- AVL CRUISE way file—when clicking on AVL CRUISE way file, the user will be prompted for a directory to save the way file. The extension is WAY, and this file contains only the altitude profile versus the distance for now;
- HTML Google Map preview—when the original data is in GPS coordinates (latitude, longitude) there is an HTML file generated automatically along with the AVL CRUISE way file or the IPG TruckMaker test run. To view their content, must be opened by using an Internet browser (Fig. 5.7).
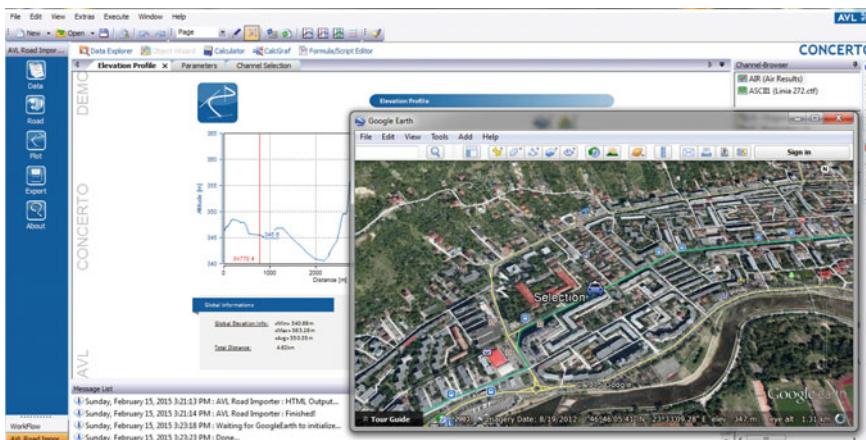
Fig. 5.7 AVL Road Importer—HTML preview menu

5.2   Generating the Routes Selected for Urban Public Transportation for People

After defining the virtual tracks for the urban bus routes selected, there is the possibility of visualizing these tracks together with the parameters set online by connecting either to Google Earth or Google Maps application. Within Goggle Earth of Google Maps application once the digitized data are entered, the defined tracks will be displayed automatically.

The data provided by Compania de Transport Public Cluj-Napoca S.A. (CTP—Public Transportation Company) specifies the existence of 252 buses in the company auto park, from which 150 buses are used at maximum capacity during a working day (respectively 70 buses during weekends). The buses serve a number of 42 routes with a total length of approximately 100 km (Fig. 5.8), assuring the transport for a percentage of 65 % from the total number of transported passengers (the difference are transported with trolleybuses and tramways) [5].

The bus routes selected for the elaboration of the research project are as follows: 27, 28, 30 and 32. According to the data provided by CTP Cluj-Napoca, the characteristics of these routes are presented further, being used as initial data for the generation of the digitized virtual routes.
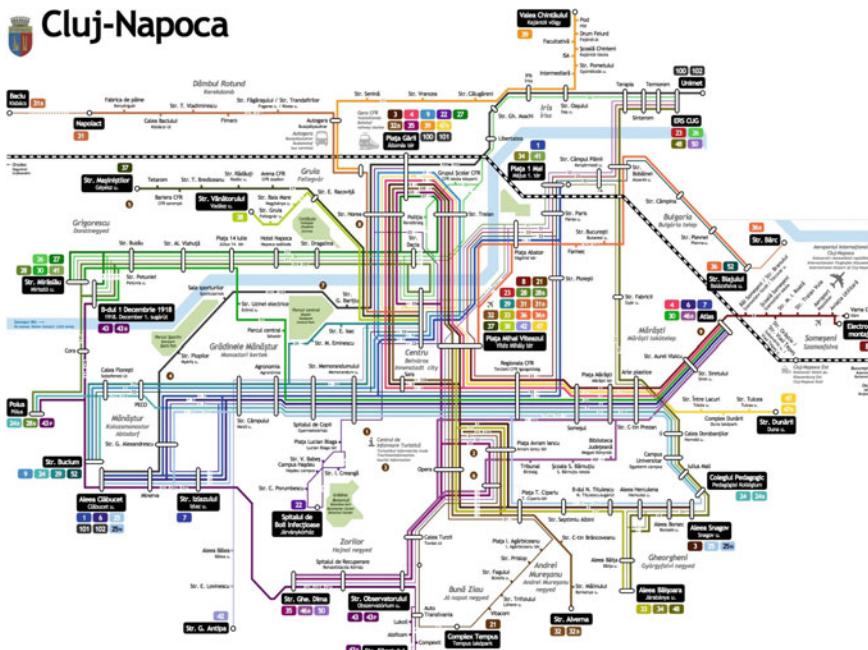
Fig. 5.8 Public transportation network of Cluj-Napoca municipality [6]
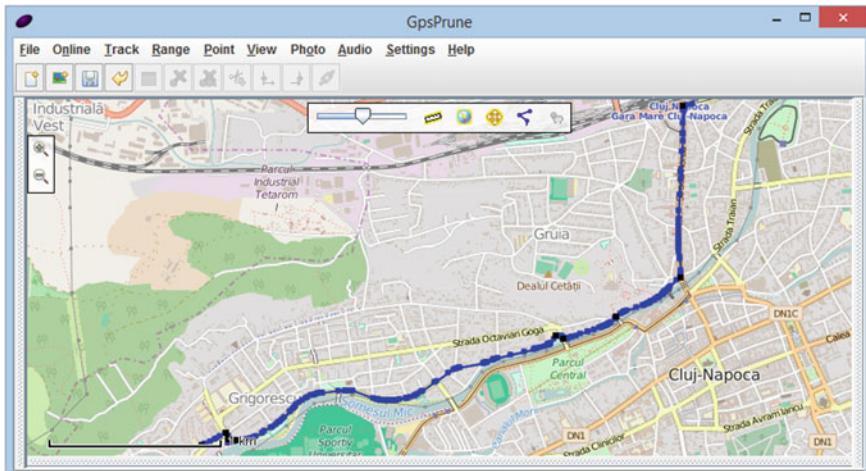
Fig. 5.9 Virtual track for bus route 27

Route 27 Grigorescu neighborhood—Piața Gării (Fig. 5.9) has a length of 9.7 km, it can be traveled in a medium interval of 38 min and is served by three buses. The number of stations on a round-trip route is 19 and the medium distance between the stations is of 0.5 km (Table 5.1).

Table 5.1 Route 27 Grigorescu neighborhood—Piața Gării

No.	Station	Course	Distance (m)	Time (s)	Latitude (°)	Longitude (°)	Altitude (m)
1	Grigorescu	tour	0	0	46° 45′ 53″	23° 32′ 55″	349
2	1 Dec 1918	tour	195	70	46° 45′ 55″	23° 32′ 54″	350
3	Petuniei	tour	784	283	46° 46′ 10″	23° 33′ 19″	348
4	Vlahuță	tour	246	89	46° 46′ 12″	23° 33′ 30″	349
5	Vlahuță	tour	339	122	46° 46′ 13″	23° 33′ 45″	346
6	Pța 14 Iulie	tour	352	127	46° 46′ 15″	23° 34′ 00″	344
7	Napoca	tour	783	283	46° 46′ 18″	23° 34′ 53″	345
8	Dragalina	tour	561	203	46° 46′ 21″	23° 34′ 57″	347
9	Horea	tour	812	293	46° 46′ 40″	23° 35′ 14″	339
10	Piața Gării	tour	776	280	46° 47′ 03″	23° 35′ 18″	337
11	Traian	retour	426	154	46° 46′ 48″	23° 35′ 25″	336
12	Dacia	retour	749	270	46° 46′ 33″	23° 35′ 21″	335
13	Dragalina	retour	652	235	46° 46′ 22″	23° 34′ 56″	351
14	Napoca	retour	573	207	46° 46′ 18″	23° 34′ 31″	345
15	Pța 14 Iulie	retour	594	214	46° 46′ 16″	23° 34′ 04″	343
16	Vlahuță	retour	697	252	46° 46′ 13″	23° 33′ 35″	348
17	Buzău	retour	463	167	46° 46′ 10″	23° 33′ 17″	348
18	Mirăslău	retour	449	162	46° 46′ 02″	23° 33′ 00″	350
19	Grigorescu	retour	246	89	46° 45′ 53″	23° 32′ 55″	349

The entry data were processed with the help of AVL Road Importer application based on the parameters of the main algorithm for digitization according to the GPS coordinates for track latitude, longitude and altitude (Fig. 5.10a–c).
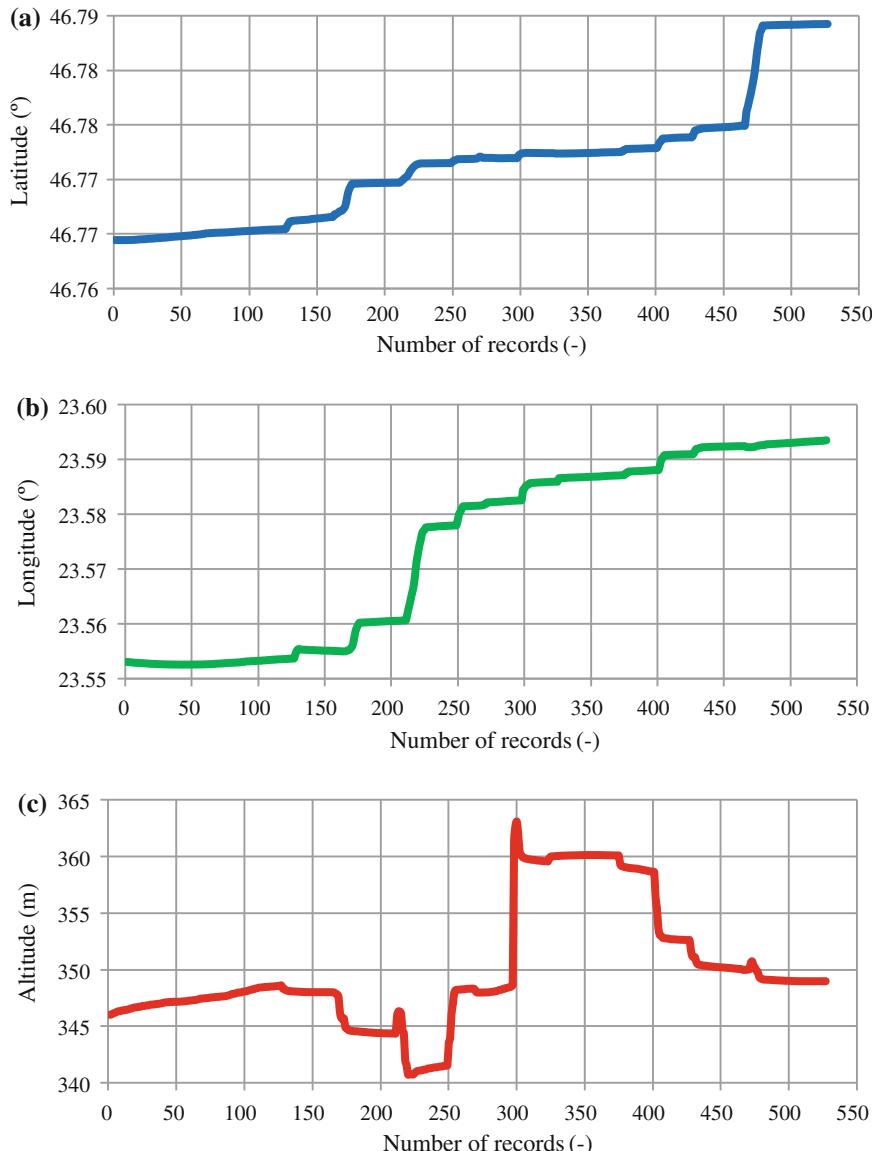
Fig. 5.10 GPS Coordinates for bus route 27: **a** latitude, **b** longitude, **c** altitude
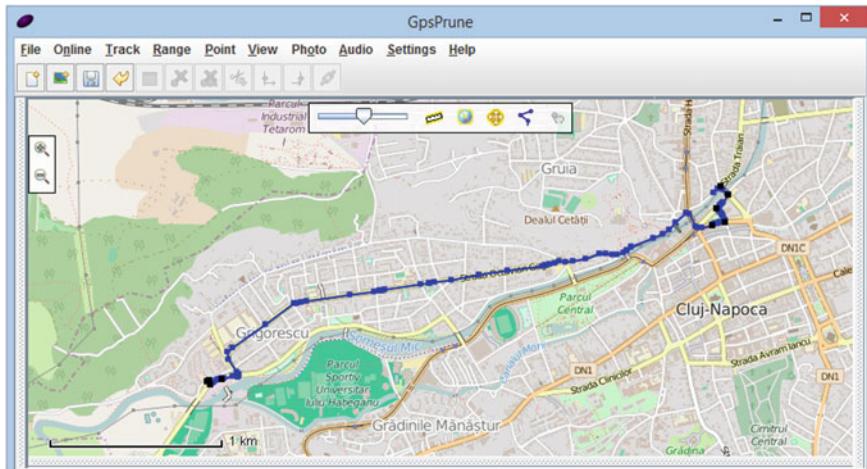
Fig. 5.11 Virtual track for bus route 28

Route 28 Grigorescu neighborhood—Piața Mihai Viteazul (Fig. 5.11) has a
length of 8.5 km, it can be traveled in 36 min and it is served by two buses. The
number of stations for a round-trip route is 16 and the medium distance between
stations is 0.51 km (Table 5.2).

The entry data were processed with the help of AVL Road Importer application
based on the parameters of the main algorithm for digitization according to the GPS
coordinates for track latitude, longitude and altitude (Fig. 5.12a–c), thus obtaining

Table 5.2 Route 28 Grigorescu neighborhood—Piața Mihai Viteazul

No.	Station	Course	Distance (m)	Time (s)	Latitude (°)	Longitude (°)	Altitude (m)
1	Grigorescu	tour	0	0	46° 45′ 53″	23° 32′ 55″	349
2	1 Dec 1918	tour	195	70	46° 45′ 55″	23° 32′ 54″	350
3	Petuniei	tour	784	283	46° 46′ 10″	23° 33′ 19″	348
4	Vlahuță	tour	246	89	46° 46′ 12″	23° 33′ 30″	349
5	Pța 14 Iulie	tour	352	127	46° 46′ 15″	23° 34′ 00″	344
6	Napoca	tour	812	293	46° 46′ 18″	23° 34′ 53″	345
7	Dragalina	tour	561	203	46° 46′ 21″	23° 34′ 57″	347
8	M Viteazul	retour	856	309	46° 46′ 28″	23° 35′ 24″	339
9	Dacia	retour	823	297	46° 46′ 33″	23° 35′ 21″	335
10	Dragalina	retour	712	257	46° 46′ 22″	23° 34′ 56″	351
11	Napoca	retour	613	221	46° 46′ 18″	23° 34′ 31″	345
12	Pța 14 Iulie	retour	594	214	46° 46′ 16″	23° 34′ 04″	343
13	Vlahuță	retour	697	252	46° 46′ 13″	23° 33′ 35″	348
14	Buzău	retour	463	167	46° 46′ 10″	23° 33′ 17″	348
15	Mirăslău	retour	449	162	46° 46′ 02″	23° 33′ 00″	350
16	Grigorescu	retour	246	89	46° 45′ 53″	23° 32′ 55″	349
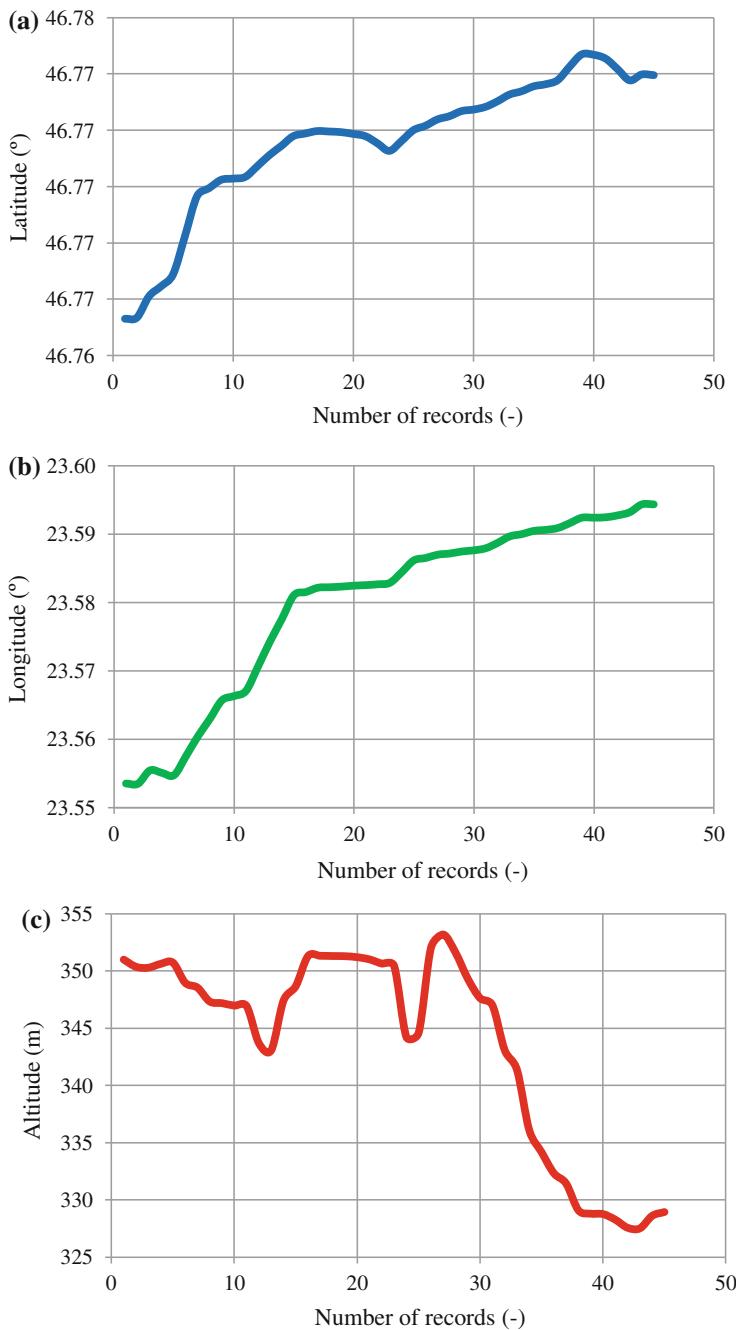
Fig. 5.12 GPS coordinates for bus route 28: **a** latitude, **b** longitude, **c** altitude
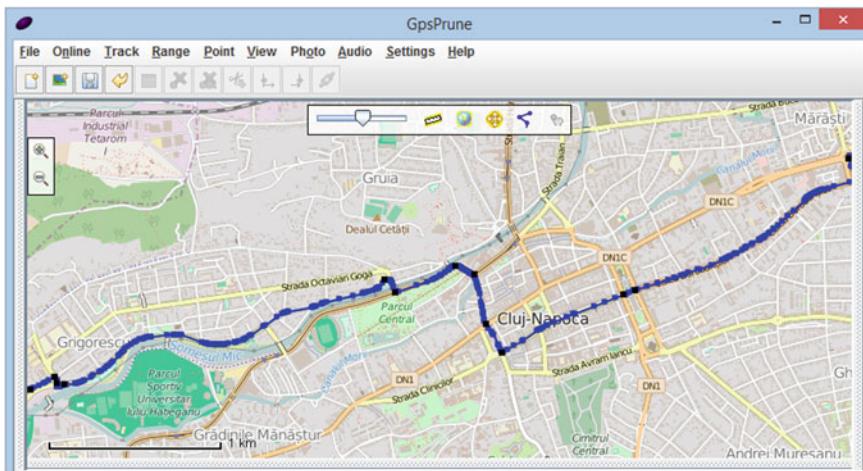
Fig. 5.13 Virtual track for bus route 30

the virtual track used for creating computer simulations with the help of the built bus models.

Route 30 Grigorescu neighborhood—Aurel Vlaicu Street (Fig. 5.13) has a length of 17.2 km, it can be traveled in 72 min and is served by 14 buses. The number of stations for a round-trip route is 32 and the medium distance between the stations is 0.54 km (Table 5.3).

The entry data were processed with the help of AVL Road Importer application based on the parameters of the main algorithm for digitization according to the GPS coordinates for track latitude, longitude and altitude (Fig. 5.14a–c), thus obtaining the virtual track used for creating computer simulations with the help of the built bus models.

Route 32 Gheorgheni neighborhood Constantin Brâncuși Street—Piața Mihai Viteazul (Fig. 5.15) has a length of 6.6 km, it can be traveled in 35 min and is served by four buses. The number of stations for a round-trip route is 13 and the medium distance between two stations is 0.51 km (Table 5.4).

The entry data were processed with the help of AVL Road Importer application based on the parameters of the main algorithm for digitization according to the GPS coordinates for track latitude, longitude and altitude (Fig. 5.16a–c), thus obtaining the virtual track used for creating computer simulations with the help of the built bus models.

The terminals for bus maintenance and parking are situated in Grigorescu neighborhood for route 27 and route 28, respectively on Aurel Vlaicu Street for route 30 and on Constantin Brâncoveanu Street for route 32.

Table 5.3 Route 30 Grigorescu neighborhood—Aurel Vlaicu Street

No.	Station	Course	Distance (m)	Time (s)	Latitude (°)	Longitude (°)	Altitude (m)
1	Grigorescu	tour	0	0	46° 45′ 53″	23° 32′ 55″	349
2	1 Dec 1918	tour	195	70	46° 45′ 55″	23° 32′ 54″	350
3	Petuniei	tour	784	283	46° 46′ 10″	23° 33′ 19″	348
4	Alexandru Vlahuță	tour	246	89	46° 46′ 12″	23° 33′ 30″	349
5	Piața 14 Iulie	tour	352	127	46° 46′ 15″	23° 34′ 00″	344
6	Uzinei Electrice	tour	760	274	46° 46′ 01″	23° 34′ 09″	342
7	Parcul Central	tour	556	201	46° 46′ 05″	23° 34′ 30″	344
8	Spitalul Copii	tour	675	244	46° 45′ 58″	23° 34′ 47″	344
9	Memorandumului	tour	690	249	46° 46′ 10″	23° 35′ 13″	349
10	Regionala	tour	1016	367	46° 46′ 23″	23° 35′ 49″	340
11	Someșul	tour	749	270	46° 46′ 34″	23° 36′ 20″	337
12	Piața Mărăști	tour	512	185	46° 46′ 39″	23° 36′ 41″	335
13	Constantin Prezan	tour	384	139	46° 46′ 42″	23° 36′ 57″	336
14	Siretului	tour	924	334	46° 46′ 50″	23° 37′ 37″	334
15	Atlas	tour	673	243	46° 46′ 53″	23° 38′ 07″	328
16	IRA	retour	198	71	46° 46′ 57″	23° 38′ 15″	326
17	Atlas	retour	203	73	46° 46′ 55″	23° 38′ 07″	327
18	Aurel Vlaicu	retour	618	223	46° 46′ 51″	23° 37′ 40″	331
19	Arte Plastice	retour	859	310	46° 46′ 44″	23° 37′ 00″	334
20	Piața Mărăști	retour	447	161	46° 46′ 40″	23° 36′ 41″	335
21	Someșul	retour	562	203	46° 46′ 34″	23° 36′ 17″	338
22	Regionala	retour	634	229	46° 46′ 25″	23° 35′ 51″	339
23	Memorandumului	retour	1007	364	46° 46′ 11″	23° 35′ 12″	349
24	Spitalul Copii	retour	649	234	46° 45′ 59″	23° 34′ 49″	344
25	Parcul Central	retour	583	210	46° 46′ 05″	23° 34′ 29″	344
26	Uzinei Electrice	retour	527	190	46° 46′ 02″	23° 34′ 09″	341
27	Piața 14 Iulie	retour	594	214	46° 46′ 16″	23° 34′ 04″	343
28	Alexandru Vlahuță	retour	697	252	46° 46′ 13″	23° 33′ 35″	348
29	Buzău	retour	463	167	46° 46′ 10″	23° 33′ 17″	348
30	Mirăslău	retour	449	162	46° 46′ 02″	23° 33′ 00″	350
31	Grigorescu	retour	246	89	46° 45′ 53″	23° 32′ 55″	349

5.3 The IPGRoad

A Virtual Road is a representation obtained from computer digitizing a real road sector generated with the help of IPGRoad, part of the standard installation package of IPG CarMaker/TruckMaker based on the coordinated provided by a software platform displaying in detail the terrain surface (Google Earth, Google Map, Bing Map, Navteq ADAS, Navstar GPS etc.), or on a track generated by the user (AVL
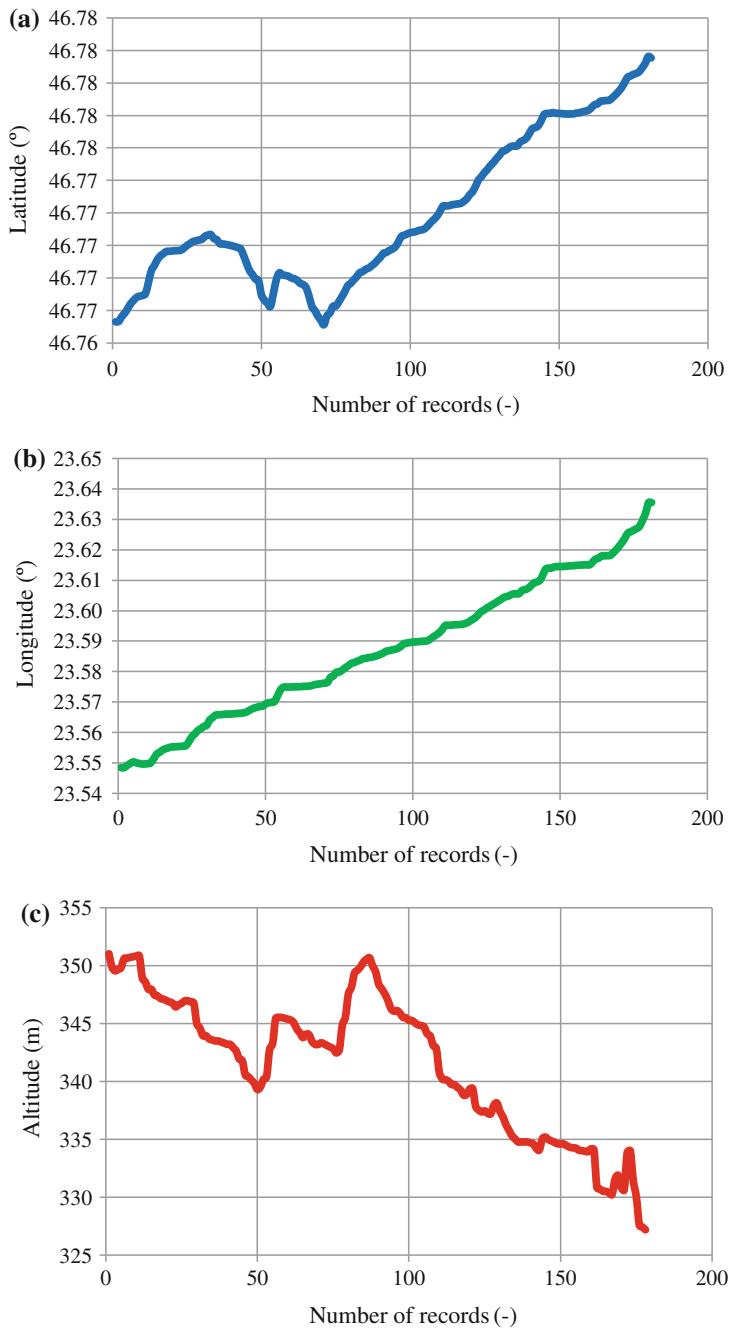
Fig. 5.14 GPS coordinates for bus route 30: **a** latitude, **b** longitude, **c** altitude
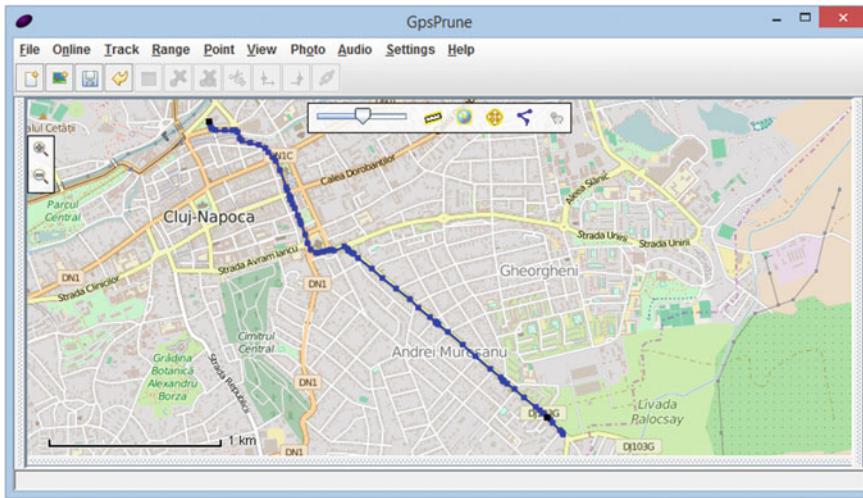
Fig. 5.15   Virtual track for bus route 32

Road Importer). Tracks can also be generated directly in IPG CarMaker/TruckMaker or using the AVL Road Importer.

In addition to the AVL Road Importer application, IPGRoad (Fig. 5.17) can also simulate real traffic conditions, namely: atmospheric conditions (wind, rain, snow etc.), road geometry (turns, slopes, straight road, rough road etc.), road particularities

Table 5.4   Route 32 Constantin Brâncuși Street—Piața Mihai Viteazul

No.	Station	Course	Distance (m)	Time (s)	Latitude (°)	Longitude (°)	Altitude (m)
1	Alverna	tour	0	0	46° 45′ 25″	23° 37′ 06″	373
2	Alverna	tour	303	109	46° 45′ 29″	23° 37′ 03″	372
3	Mălinului	tour	282	102	46° 45′ 37″	23° 36′ 51″	371
4	C-tin Brâncoveanu	tour	513	185	46° 45′ 49″	23° 35′ 31″	363
5	Piața Cipariu	tour	817	295	46° 46′ 07″	23° 35′ 37″	346
6	Avram Iancu	tour	384	139	46° 46′ 18″	23° 35′ 49″	346
7	Mihai Viteazul	retour	823	297	46° 46′ 29″	23° 35′ 24″	339
8	Opera	retour	826	298	46° 46′ 14″	23° 35′ 48″	345
9	Piața Cipariu	retour	826	298	46° 46′ 02″	23° 36′ 05″	351
10	C-tin Brâncoveanu	retour	619	223	46° 45′ 50″	23° 36′ 28″	363
11	Mălinului	retour	649	234	46° 45′ 37″	23° 36′ 50″	371
12	Alverna	retour	414	149	46° 45′ 29″	23° 37′ 03″	373
13	Alverna	retour	236	85	46° 45′ 25″	23° 37′ 06″	373
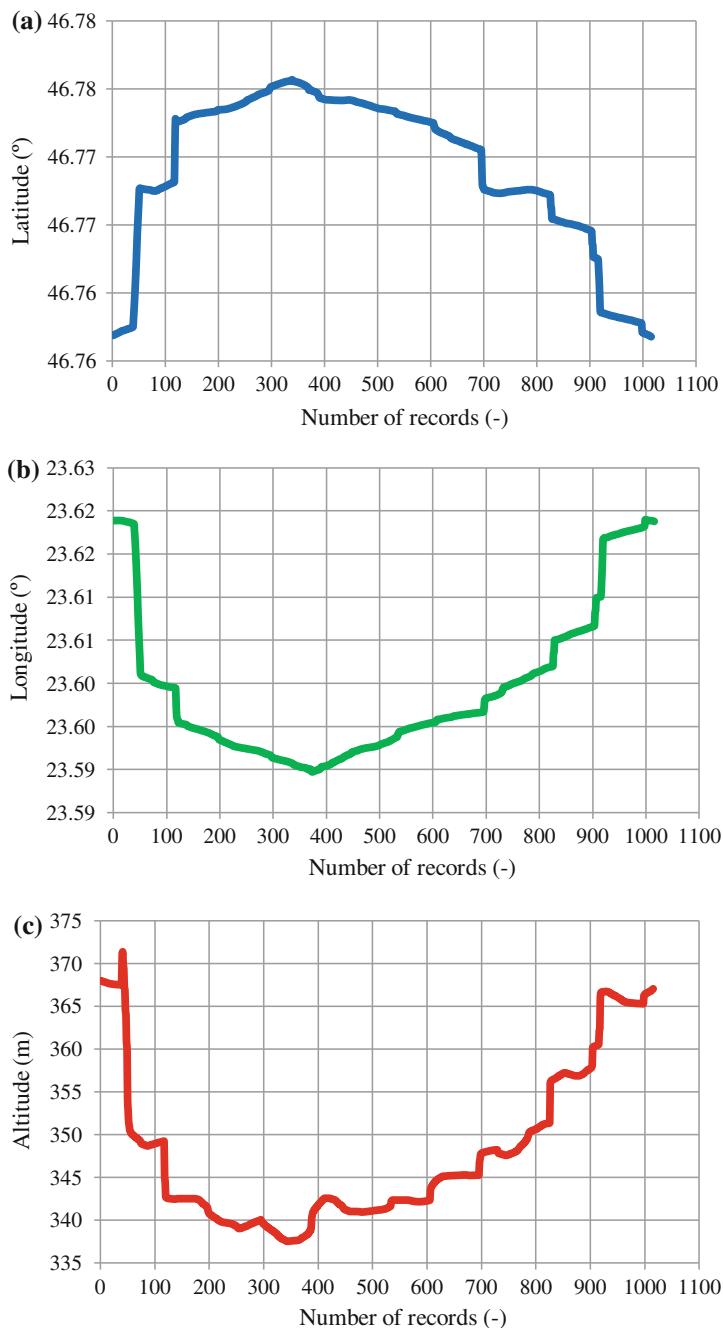
Fig. 5.16 GPS coordinates for bus route 32: **a** latitude, **b** longitude, **c** altitude
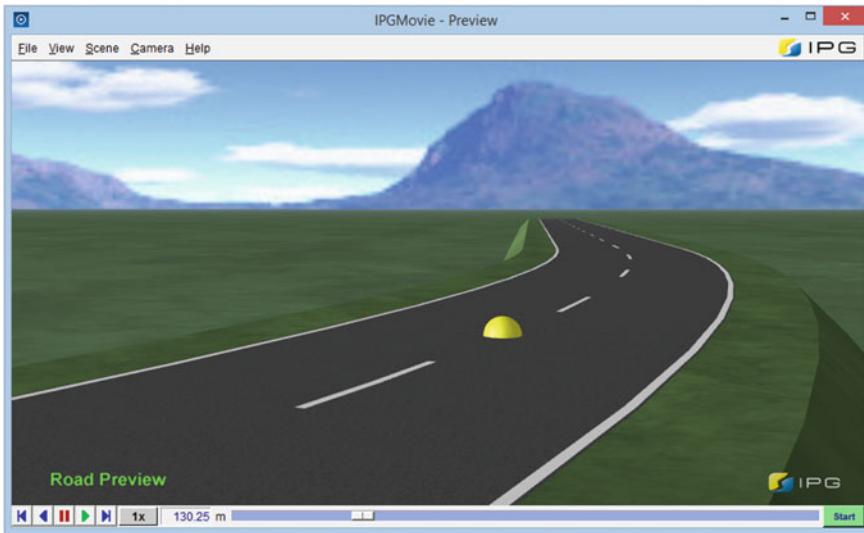
Fig. 5.17 The virtual road defined in IPGRoad

(road markings, obstacles, bumps etc.), respectively the particularities of road adjacent areas (trees, ditches, sidewalks, buildings etc.). The IPGRoad relies on two methods of road geometry parametrization, based on real road measurements (x, y, z), respectively on a virtual track with an interface created from segments [1].

The IPGRoad dialog box can be accessed from the main GUI by selecting Parameters—Road. The first tab that appears shows the general settings of the road (Fig. 5.18). The global settings are [1]:

- Start coordinates x, y, z (m) defines the origin of the road;
- Start direction (deg) defines the angle offset from the first segment regarding the x-axis;
- Car starts at (m) define at which distance the car should start;
- Driving lane should be used: the left or the right one;
- Country is option for the visualization and availability of the traffic signs;
- Track width (m) is defined on both sides of the centerline;
- Margin width (m) the margins are basically longitudinal stripes on both sides of the entire road length;
- Friction stripe (m) in order to have a variable friction coefficient along the track width up to two stripes can be defined;
- GPS coordinates representing the latitude (Lat), longitude (Long), respectively the elevation (Height) of the reference point (°);
- The file containing digitized Road.

The definition of the road geometry with a segment-based approach consists of a succession of various segments (straight lines, curve left or right) with correctly
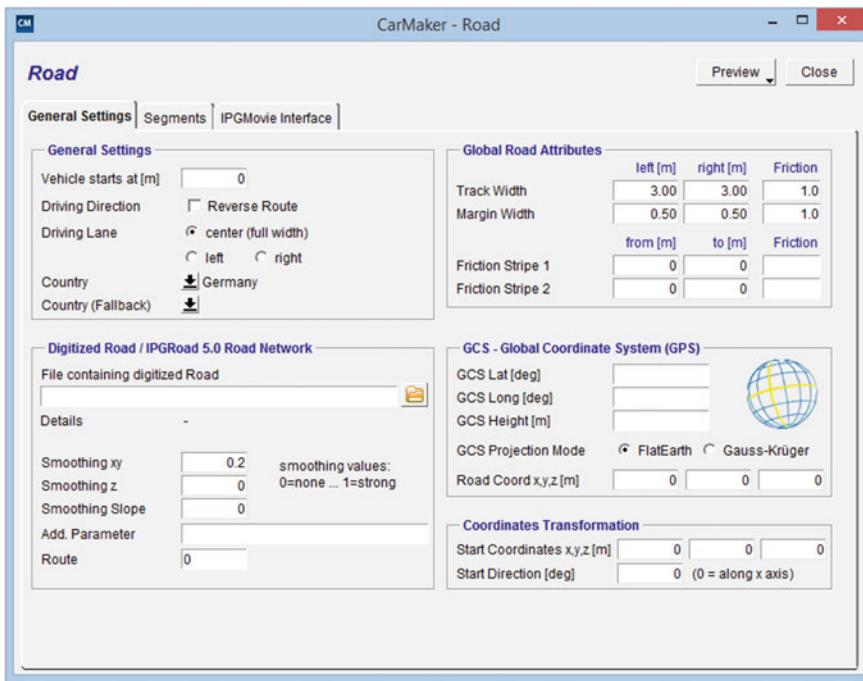
Fig. 5.18 IPGRoad—general settings

parameterized properties in order to build a complete road. To use this method, move to the second tab of the IPGRoad dialog box called Segments (Fig. 5.19).

The list of segments from which the road is defined is displayed in window (1), the 3D geometry of each segment is defined in Segment Definition window (2), and the Override selected Segment Attributes window (3) will be activated solely in the situation in which one desires to define punctual parameters (road width or friction coefficients) for one segment only [1].

After defining the road geometry by using digital road data or by defining based on segments, the road can be visualized in one panoramic image with the Bird's Eye View command or with aerial view (Fig. 5.20).

The aerial view term refers to any visualization from a greater height perpendicular on the plan or with a maximum inclination of 40°. The perspective given by the Bird's Eye View allows to observe the delimitations of the segments composing the virtual road and to identify the active roads [7].

The virtual roads loaded in the IPGRoad which were used for creating the computer simulations with the help of the bus models built are presented in the Figs. 5.21, 5.22, 5.23 and 5.24.
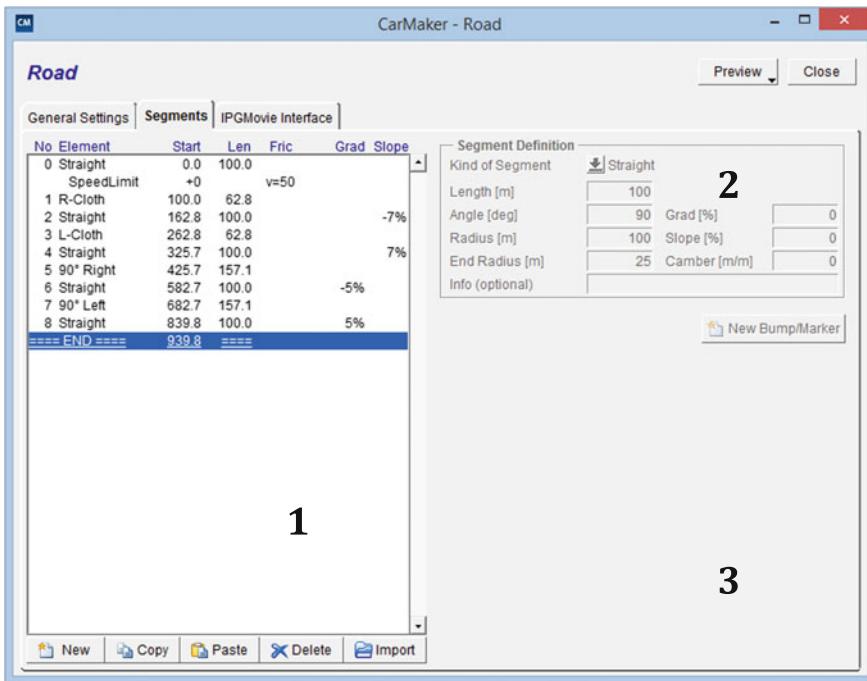
Fig. 5.19 IPGRoad—segments

With the help of IPGRoad, which is a 3D road generator, one can define simple individual elements in three dimensional format, which represents precisely all the characteristics and particularities of the simulated road. The road can be represented on obstacle sections, roads with more lanes, exits, crossroads, friction coefficients, wind conditions, road signs, obstacles, buildings, trees, bridges, respectively with other conditions which may intervene in traffic. Furthermore, the user can define points on the road which can be attributed to some road segments for shifting gears, stopping in pre-established places or any particular maneuver commands [1].

The IPGMovie Interface dialog window (Fig. 5.25) contains data which define the characteristics of the road displayed in the IPGMovie and namely the parameters generating the road geometry (Parameters for Generation of Road Geometry), the demarcation route (Borderline), respectively the dimensions for slopes (Natural Slope). Here, one can also load the files containing data related to the terrain geometry of the respective sector (User-defined Background and Terrain).
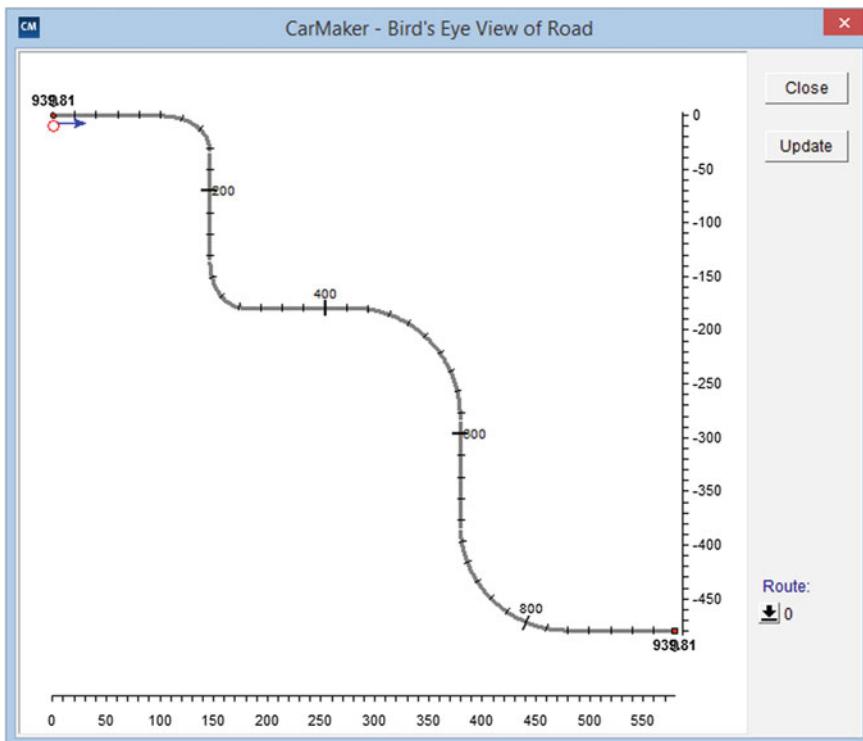
Fig. 5.20 IPGRoad—Bird's Eye View
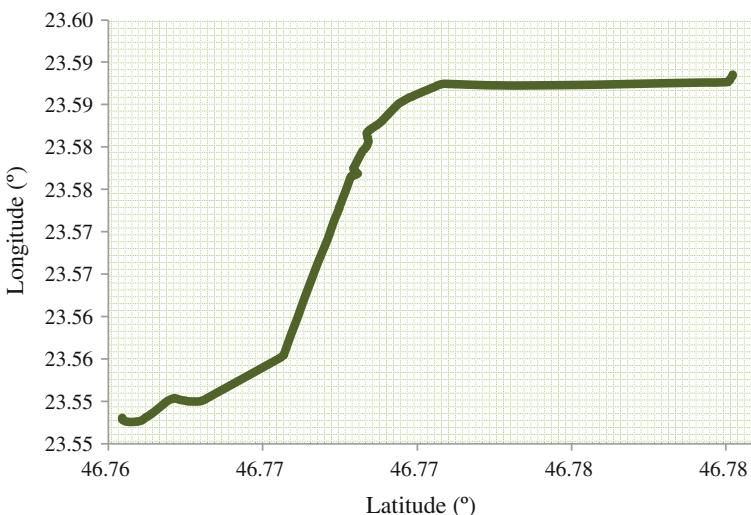
Fig. 5.21 Virtual road for bus route 27 in the IPGRoad
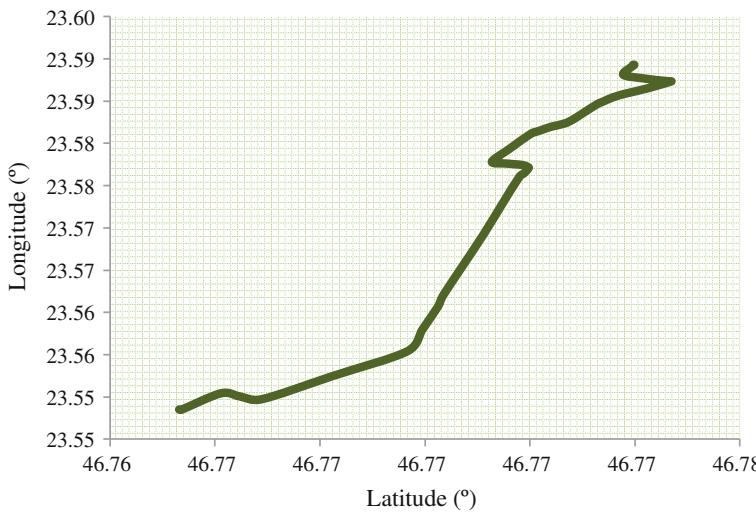
Fig. 5.22 Virtual road for bus route 28 in the IPGRoad
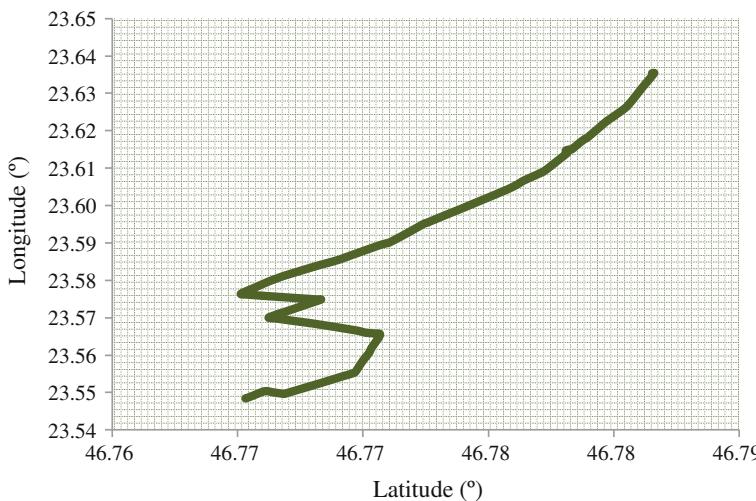
Fig. 5.23 Virtual road for bus route 30 in the IPGRoad

5.4   Parameterization of Vehicle Movement

The Maneuver application is launched from IPG TruckMaker—Parameters and it offers the possibility of defining a running scenario on a road created in IPGRoad. The scenario for Maneuver is composed of a series of operations defined on road steps, called Minimaneuvers. Each minimaneuver is composed of dynamic
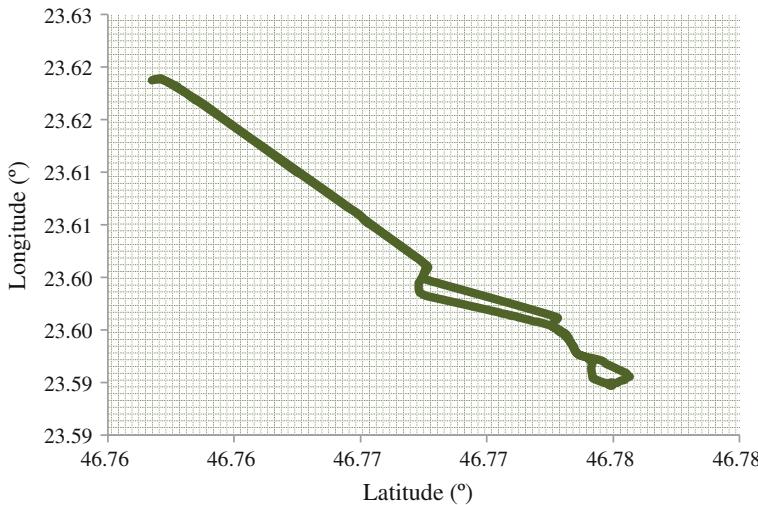
Fig. 5.24 Virtual road for bus route 32 in the IPGRoad

Fig. 5.25 IPGMovie interface

longitudinal actions (acceleration, braking, shifting gears etc.), dynamic lateral actions (changing the traveling direction etc.), and respectively supplementary actions, defined by a list of special commands known as scripts (Fig. 5.26).

To build a maneuver scenario, one must add and parameterize successively the different necessary steps for vehicle control. The list of maneuver steps is displayed in window (1), and to define every maneuver step one must add its corresponding
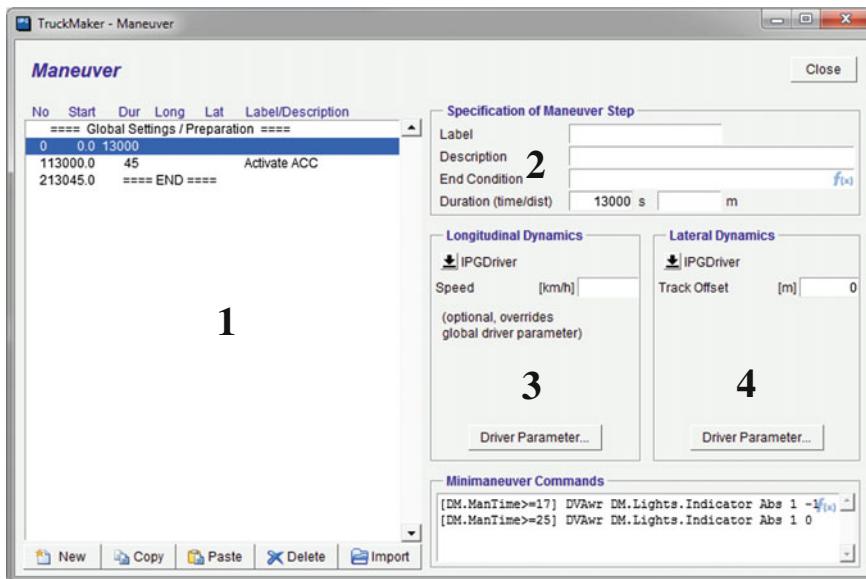
Fig. 5.26 The IPGRoad—maneuver

parameters and the action with which it is responsible in window (2), named Specification of Maneuver Step [8].

The Longitudinal Dynamics and Lateral Dynamics are defined in windows (3) and (4) and are characterized by the following parameters:

- Longitudinal Dynamics:

  - IPGDriver complete automation and detailed control of travel;
  - Speed Profile defined through measurements, Speed Control defined by the PID controller;
  - Manual for direct control of throttle;
  - Stop Vehicle stopping the vehicle, controlled by the IPGDriver;
  - Drive Backwards defining the velocity and acceleration for driving in reverse;
  - IPGDriver + User Driver using a predefined model.

- Lateral Dynamics:

  - IPGDriver complete automation and detailed control of travel;
  - Sinus Sweep entry signal with ascending amplitude for steering angle;
  - Steer Step command for modifying the steering angle;
  - Follow Course PID automation necessary for tracking the medium value of the signal.

The supplementary actions are defined by the following parameters:

- Special mini-maneuvers:

  - Set Starting Conditions the first maneuver which defines gear and acceleration;
  - Clean Up intervenes is the duration of the latest maneuver was 0 s.

- End Condition:

  - Time defined by time, Distance defined by distance;
  - Real Time Expression defining real time;
  - DrivMan Jump command for defining a minimaneuver;
  - Road Marker DrivMan Jump parameter for defining the road.

The IPGDriver is launched from IPG TruckMaker—Parameters and it is an option activating the control model over the longitudinal dynamics of the vehicle (Fig. 5.27).

The vehicle movement on the defined road can be parameterized according to the options established by the user in the User parameterized Driver (constantly maintaining the travelling direction, the velocity, the acceleration, the braking, the gear shifting etc.) [8]. The second method for vehicle movement parameterization is by using Racing Driver, which allows the optimization of travel time according to velocity and automatically adapts the vehicle driving procedure within the imposed limits. The Traffic option allows the model used in the simulation process to acknowledge the objects within the road traffic and by setting certain limit values to adapt the traveling velocity and the minimum distances towards these objects. The Misc/Additional Parameters options offers supplementary facilities to calibrate the control actions over the simulated model [8]. The IPGDriver facilities allow defining certain control actions similar to those of a human driver for the virtual vehicle (Virtual Driver) through a mathematical model. The IPG TruckMaker application integrates a Virtual Vehicle on a Virtual Road and assures its control by a Virtual Driver, thus achieving a Virtual Vehicle Environment for testing vehicles in real time, as presented in Fig. 5.28 [9].

IPGDriver is a part of the standard installation package of IPG CarMaker and TruckMaker application which defines a model for the driver with the purpose of executing complex tasks of driving a vehicle in a closed loop. IPGDriver reproduces accurately the actions and reactions of a real driver and has special options for driving trucks and buses. The facilities offered by IPGDriver include the automatic planning of the travel according to bud characteristics, automated procedures for shifting gears, braking, changing traveling direction, manual operation of some active systems like ESC, the steering systems or ADAS, road gradient start etc. [9].

To connect to the Google Earth application from the IPGMovie, one must launch the command File—Connect Google Earth, through which the virtual road created in IPGRoad is uploaded in the online environment according to the defined coordinates.
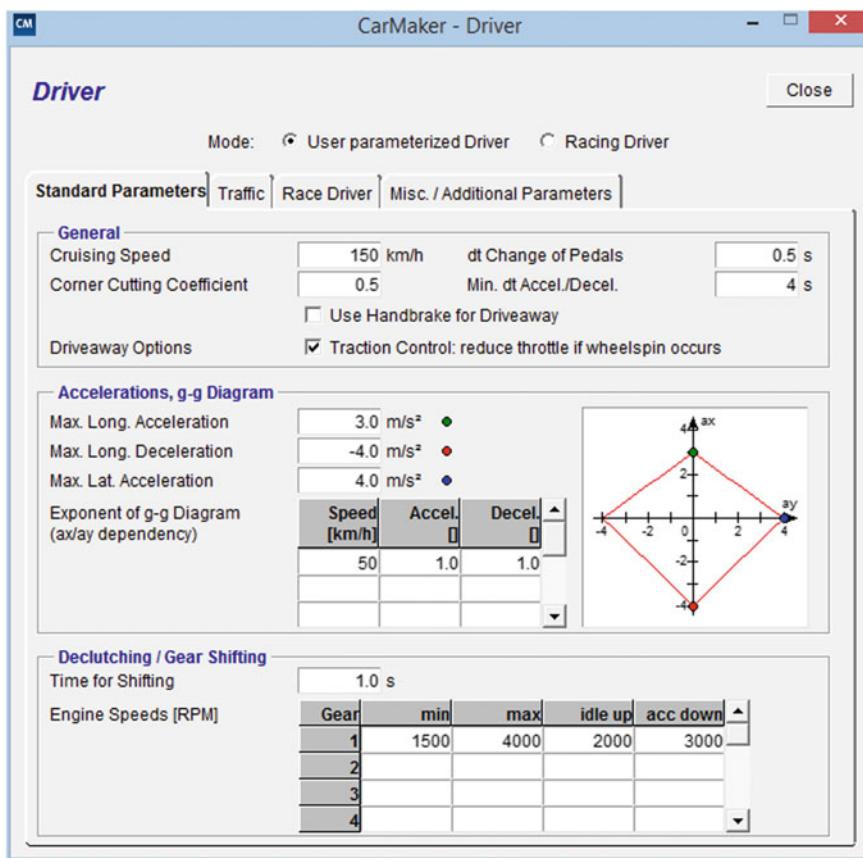
Fig. 5.27 The IPGRoad—driver
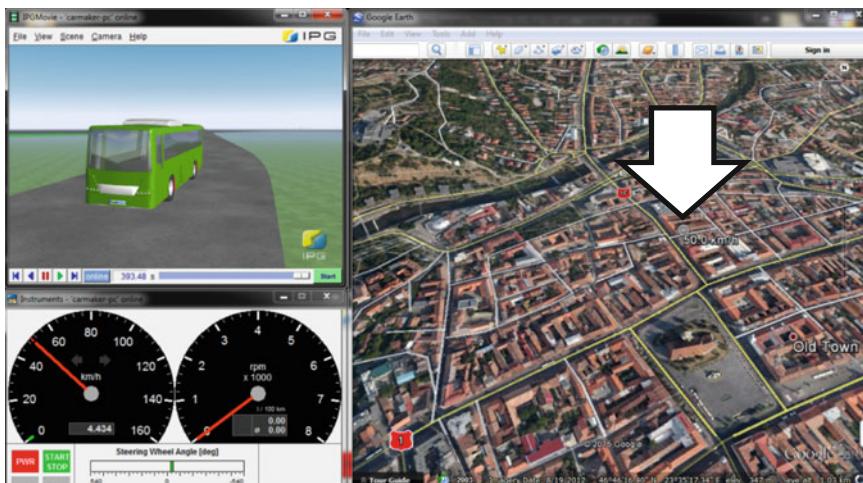
Fig. 5.28 Virtual environment for testing the vehicles in real time VVE
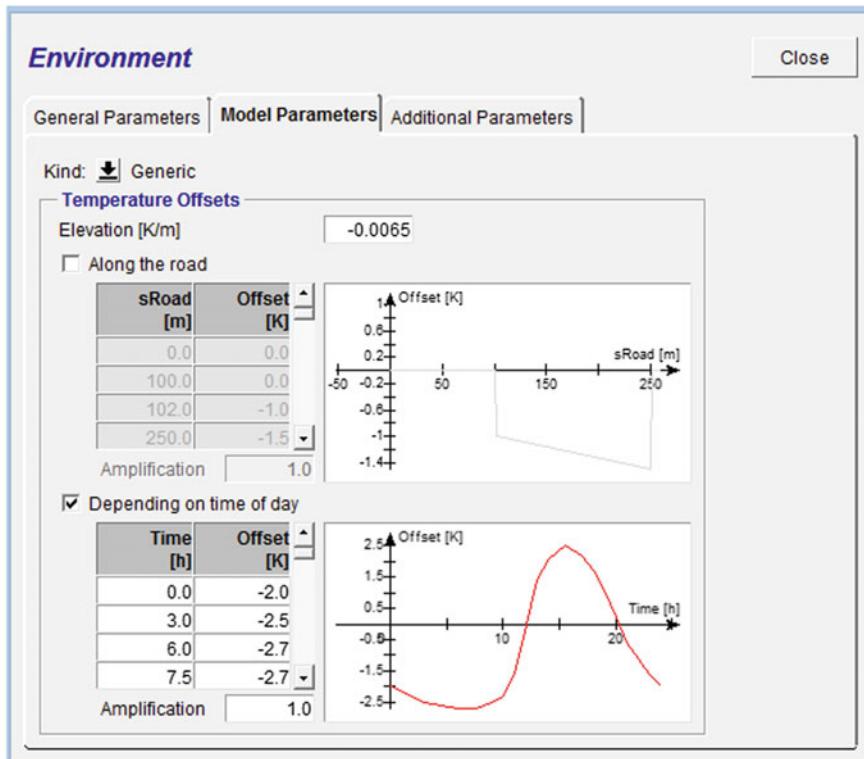
Fig. 5.29 Virtual environment GUI

Using the Environment GUI (Fig. 5.29), it is possible to define environmental conditions like the temperature, the time of day, or the wind velocity for the simulation [1]. If the model takes these parameters into account, they can influence the results of the simulation. The generic model uses a simplified approach to calculate the environmental air temperature, pressure, and density. Other environmental parameters are kept constant.

It is possible to define temperature offsets depending on the time of day and/or distance. Both offsets can be defined via the look-up tables.

References

1. Varga, B. O., Mariaşiu, F., Moldovanu, D., & Iclodean, C. (2015). *Electric and plug-in hybrid vehicles—advanced simulation methodologies, Chapter 7* (pp. 463–476). Springer International Publishing Ed. ISBN: 978-3-319-18638-2.
2. Varga, B. O. (2015). Energy efficiency of vehicles equipped with hybrid or electrical powertrain for urban public transport (in Romanian). Habilitation thesis, Technical University of Cluj-Napoca, Romania, 18 September 2015.

3. Retrieved December 2, 2015, from http://www.nearby.org.uk/elevation-kml.php.
4. Retrieved December 20, 2015, from http://activityworkshop.net/software/gpsprune.
5. Retrieved December 9, 2015, from http://ctpcj.ro/index.php/ro/ (in Romanian).
6. Retrieved December 20, 2015, from http://harti.tramclub.org/cluj-nov09.pdf (in Romanian).
7. Retrieved December 20, 2015, from http://en.wikipedia.org/wiki/Bird's-eye_view.
8. IPG CarMaker. (2014). User's Guide Version 4.5.2, IPG Automotive, Karlsruhe, Germany.
9. IPG TruckMaker. (2014). Reference Manual Version 4.5, Simulation Solutions, Test Systems, Engineering Services, IPG Automotive, Karlsruhe, Germany.

Chapter 6
Design of Hybrid and Electric Drive Systems in the IPG TruckMaker Software Application

6.1 The IPG TruckMaker Application

A virtual vehicle is a model created based on a mathematical system of a real vehicle, the model having the technical-functional characteristics identical to the model from the real world. The virtual model is build based on the parameterized data which reflect the constructive properties of the studied vehicle.

The development of vehicles with improved energy efficiency and performance targets implies ever more sophisticated powertrain sub-systems and electronic controllers being implemented, in conventional, hybrid electric and fully electric vehicles.

Vehicle modeling and simulation is a very important part in the design and development of hybrid and electric vehicles. To precisely simulate the powertrain running status, many commercial software products are applied into the development of control strategy. However, these models take too much time in the simulation analysis, which would be difficult to apply in the control strategy optimization [1].

A model is used as powertrain in CRUISE—TruckMaker co-simulation. System and sub-system architecture in CRUISE is used to prepare CRUISE powertrain model. This approach allows fast model preparation as well as better understanding of model building process for co-simulation feature. SAM Task (System Analysis Mode) in CRUISE is specially developed for co-simulation calculation demands and therefore will be used in this procedure [2].

CRUISE allows the simulation of vehicle driving performance, fuel consumption and emissions. This concept can be used for modeling all vehicle configurations with scalable fidelity. This approach allows the reuse of models or sub-systems in different optimization phases of a process in order to improve vehicle performances [3].

IPG CarMaker and TruckMaker are open integration and test platforms designed for virtual test driving. The software package consists of the Virtual Vehicle

Environment (VVE) providing models for the Vehicle, Road (inclusive Traffic), Driver and Environment. Moreover the software has open interfaces for model and hardware integration as well as a collection of tools for simulation control, model parameterization, data analysis, visualization, file management and test automation.

The VVE represents the computer modeled composition of the vehicle with all its components such as powertrain, tires, brakes and chassis as well as the VVE which can be operated on a regular office computer or on a real-time system. Real-time operation allows investigation of deterministic behavior, office operation might lack real-time capabilities but is therefore applicable on almost any host computer and allows the simulation to run slower or faster than real-time depending on system performance and model complexity and does not require special hardware.

A virtual road is a digitized or computer modeled, which is a representation of a road, track or course, which simulates a real course or one, that is generated specifically for testing. A virtual driver is chosen from the computer software, which simulates the actions of a real driver. Everything that would normally be controlled by a real driver, such as turning the steering wheel, stepping on the gas, brake and clutch pedals, shifting gears in a manual transmission vehicle etc. is controlled by the virtual driver.

The connection between the external environment and the system is achieved through the use of system parameters that characterize their input/output relationship of the presented entities [4].

The virtual vehicle contains all the component parts of a real vehicle, including the powertrain, steering, suspension, braking system etc. and it also integrates the management and control electronic elements (ABS, ESP, ACC etc.), elements which are modeled for the virtual vehicle with the help of HIL (Hardware in the Loop) or SIL (Software in the Loop) testing components [5]. Through the co-simulation process a drive system built in AVL CRUISE can be equipped on a vehicle model developed in IPG TruckMaker.

When a virtual vehicle is integrated on a virtual road and it is controlled by a virtual driver, we refer to a virtual vehicle environment (VVE) for testing vehicles in real time. The integration of the models described above can be made in the IPG TruckMaker application (Fig. 6.1) [1].

The IPG TruckMaker application contains the following utility software instruments which allow the simulation of a vehicle functioning in the virtual space:

- TruckMaker GUI (Graphical User Interface) this is the main Graphical User Interface which is used to control the actions of the VVE, select the virtual vehicle parameter data, define or select the virtual road, set the virtual driver parameters, define or load maneuvers (Fig. 6.2) [6].
- IPG Control (Fig. 6.3) is visualization and analysis tools. IPG Control can be used to view selected output quantities in real-time, load post-simulation data files, and plot and analyze the results [7].
- IPGMovie (Fig. 6.4) is real-time 3D animation of the VVE. The virtual vehicle is shown performing the specified driving maneuvers (performed by the virtual

Fig. 6.1 IPG TruckMaker—VVE (Virtual Vehicle Environment)
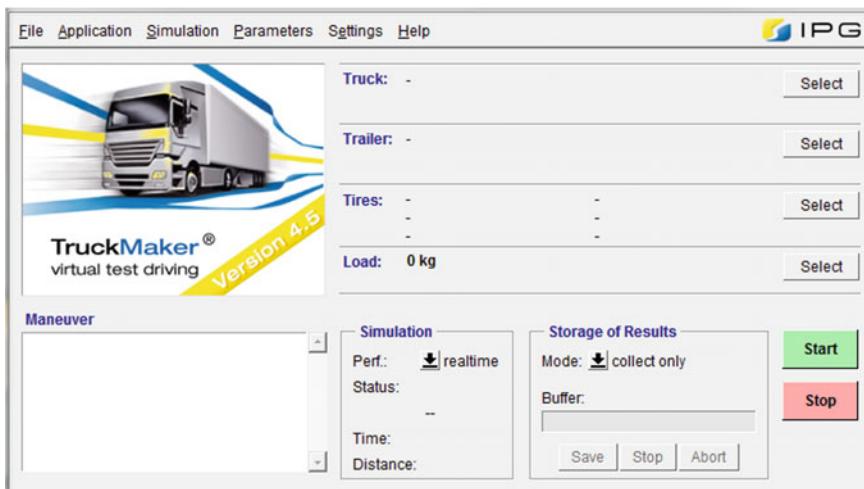
Fig. 6.2 IPG TruckMaker interface—GUI (Graphical User Interface)

driver) on the virtual road. The image captions made in real time can be exported in .jpg format at a maximum resolution of 1280 × 720 pixels, and the recording of the simulation process can be exported in AVI XviD format at a maximum resolution of 1280 × 720 pixels [7].
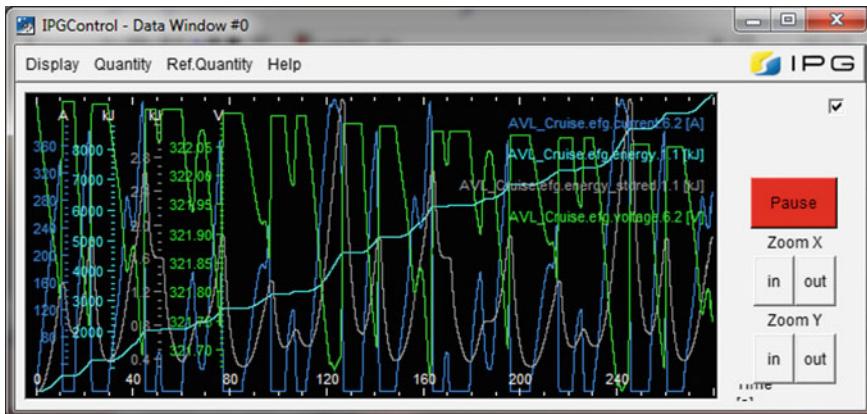
Fig. 6.3 IPG TruckMaker interface—IPG control
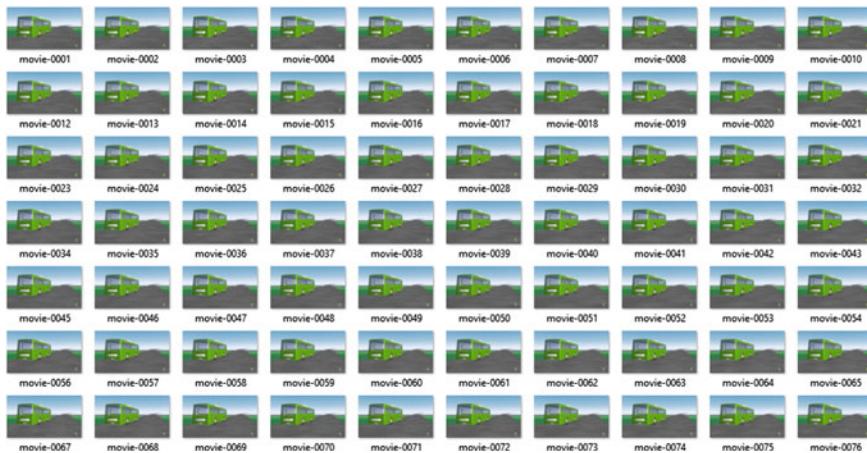
Fig. 6.4 IPG TruckMaker interface—IPGMovie

- Instruments (Fig. 6.5) display the most important instruments, dials, and information about the vehicle driving conditions like: pedal position, steering wheel angle, gear selection, ignition, speedometer, tachometer, ESP and ABS warning lamps, brake light, etc. [7].
- DVA (Fig. 6.6) (Direct Variable Access) allow simulation quantities to be read and modified interactively through a user-friendly graphical interface. The modification of parameters is made only for certain dedicated interaction point, the parameters which can be modified from the DVA menu are highlighted in the Quantity submenu [7].
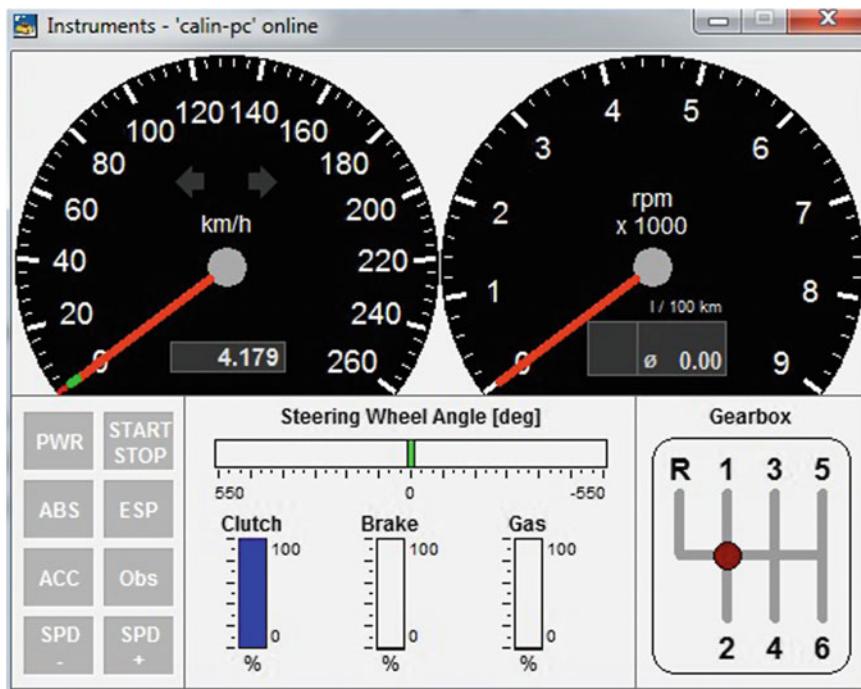
Fig. 6.5 IPG TruckMaker interface—instruments
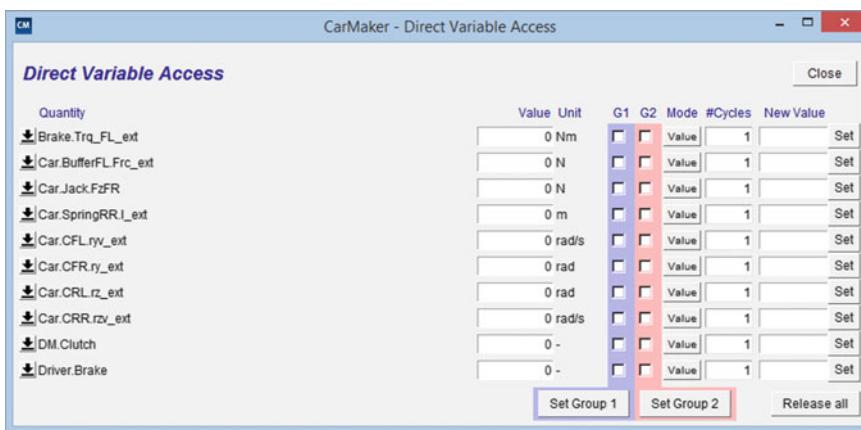
Fig. 6.6 IPG TruckMaker interface—direct variable access
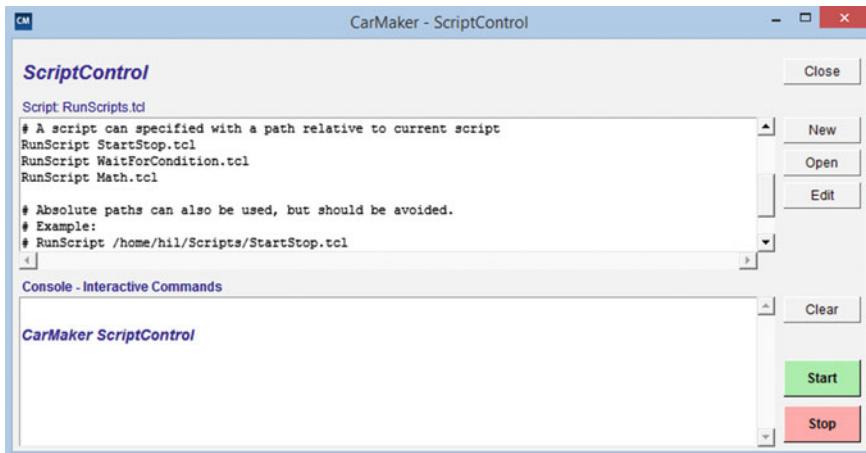
Fig. 6.7 IPG TruckMaker interface—ScriptControl

- ScriptControl (Fig. 6.7) test automation utility that allows scripts to be defined, edited, and executed. All the functions of the TIT (TruckMaker Interface Toolbox) can be controlled automatically using ScriptControl [7].
- TestManager another utility for test automation. A mixture of script and GUI based creation and execution of test series [7].

6.2 Designing a Vehicle in the IPG TruckMaker Application

To start IPG TruckMaker GUI (Graphical User Interface) under windows press the Start button and select Programs—IPG—TruckMaker.

The TruckMaker main GUI pops up and automatically loads the project folders where the user was working before last shut down of the program. Nonetheless, it can easily switch the project folder by selecting File—Project Folder and select the one project for work [5].

The main window of TruckMaker is called the main Graphical User Interface GUI (Fig. 6.8). The Truck module describes the parameters necessary for defining the vehicle model by using Vehicle Editor. The main sections used in defining the vehicle constructive parameters are the following:

The functionalities that can be found under file intend to manage the vehicle data set library. Below it can find functionalities that are available:
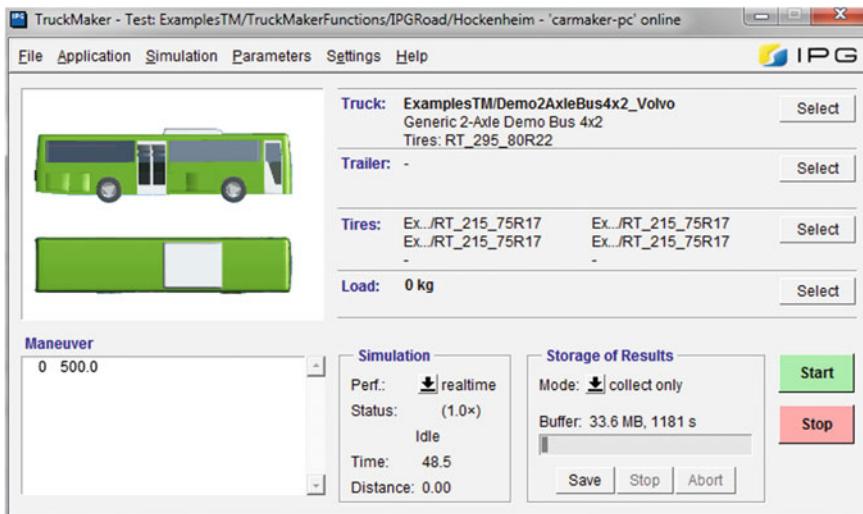
Fig. 6.8 Bus model defined in IPG TruckMaker

- To use a data set which is already built, corresponding vehicle file must be loaded via the vehicle editor;
- The user can also create a new vehicle data set from scratch. In this case, be aware that even if this option is chosen, the Vehicle Editor is filled with default values (the exception is the vehicle picture). If the vehicle parameterization not finished before closing, a comment should be added;
- Once the vehicle data set is parameterized, the changes can be saved or alternatively save them to a new file;
- Note that there is the possibility to import a part of the vehicle from another vehicle data set;
- The Vehicle Generator gives the possibility to generate a vehicle model with basic data only;
- The Vehicle Data Set Generator can generate a vehicle with basic data. This can be extremely useful if the work is dedicated on a new regulation system and on the exact vehicle parameterization itself [5].

The Vehicle Data Set parameters are:

- Vehicle Body and Bodies are the masses of the vehicle models and can be described in the Vehicle Body tabs (Fig. 6.9) and Bodies (Fig. 6.10). According to the selected vehicle model (flexible or rigid), a different number of bodies can be parameterized. In case of a flexible body mode, the main body is split into two bodies. The main body/bodies include all sprung mass of the vehicle [5].
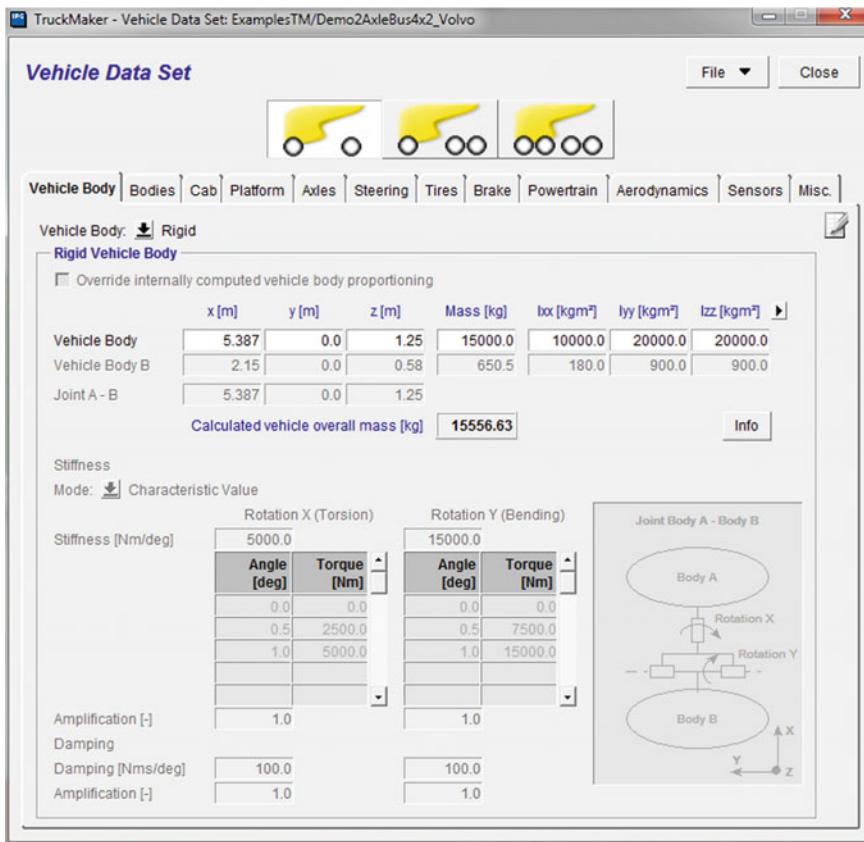
Fig. 6.9 The Truck module—vehicle bodies

- Suspensions for a given axel: the spring characteristics are the same for both
  sides of the vehicle. The Spring is modeled as a component that generates a
  force when it is compressed or stretched (Fig. 6.11). For each front and rear
  axel, the stiffness of the Secondary Spring can be defined with a simple coef-
  ficient if the secondary spring force is a linear function of the wheel travel
  variation. If the mode not specified is selected, the secondary spring is deacti-
  vated [5]. The stiffness parameter is either a simple coefficient or a table
  according to the selected parameter Mode. Amplification parameter enables to
  scale the stiffness of the secondary spring very quickly for test purposes, instead
  of modifying the whole table. It can also use this parameter to convert the values
  to fit to the units required by TruckMaker. The default value is 1.0. If the value
  is 0.0, the secondary spring is deactivated [5].
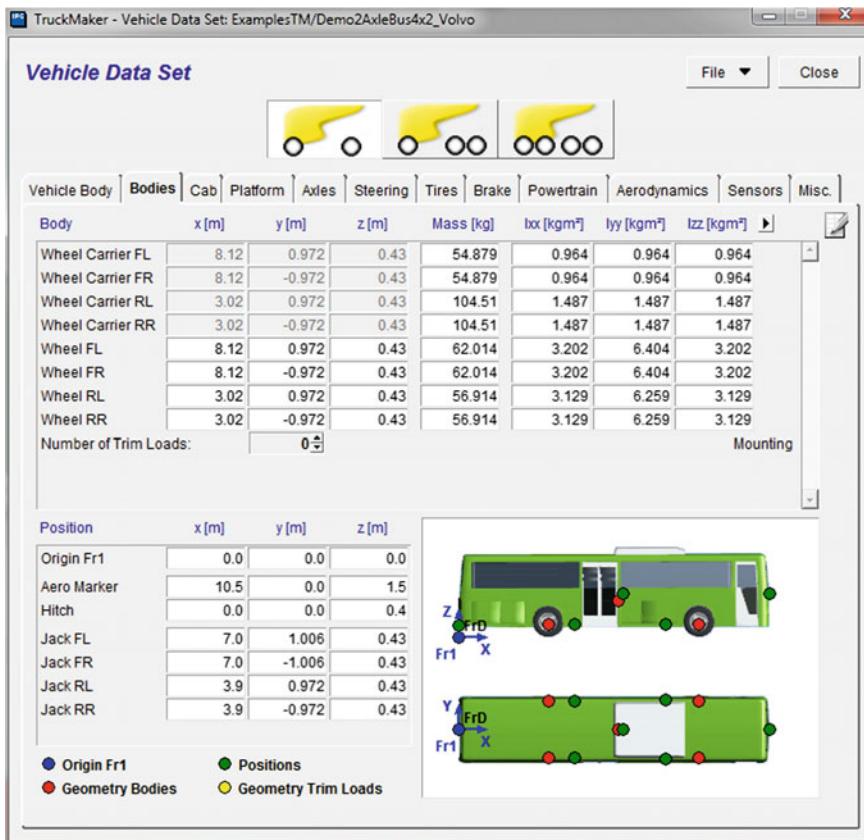
Fig. 6.10 The Truck module—bodies

- For a given axel, the Damper characteristics are the same for both sides of the vehicle (Fig. 6.12). The damper is modeled as a component that generates a force when being compressed or deflected (reaction to the change of velocity). For each front and rear axel, the damper characteristic is defined either by a coefficient or by a table of values according to the selected mode. The characteristics of the damper are split into two domains (push & pull). For each domain a different damping can be defined. The push domain corresponds to a positive damper speed [5].
- For a given axel, the Buffer characteristics are the same for both sides of the vehicle (Fig. 6.13). The buffers are used to limit the wheel travel in one direction or in both up and down. If the wheel traveled far enough to hit one of the buffers, the buffer acts like an additional spring [5]. That is why the user has
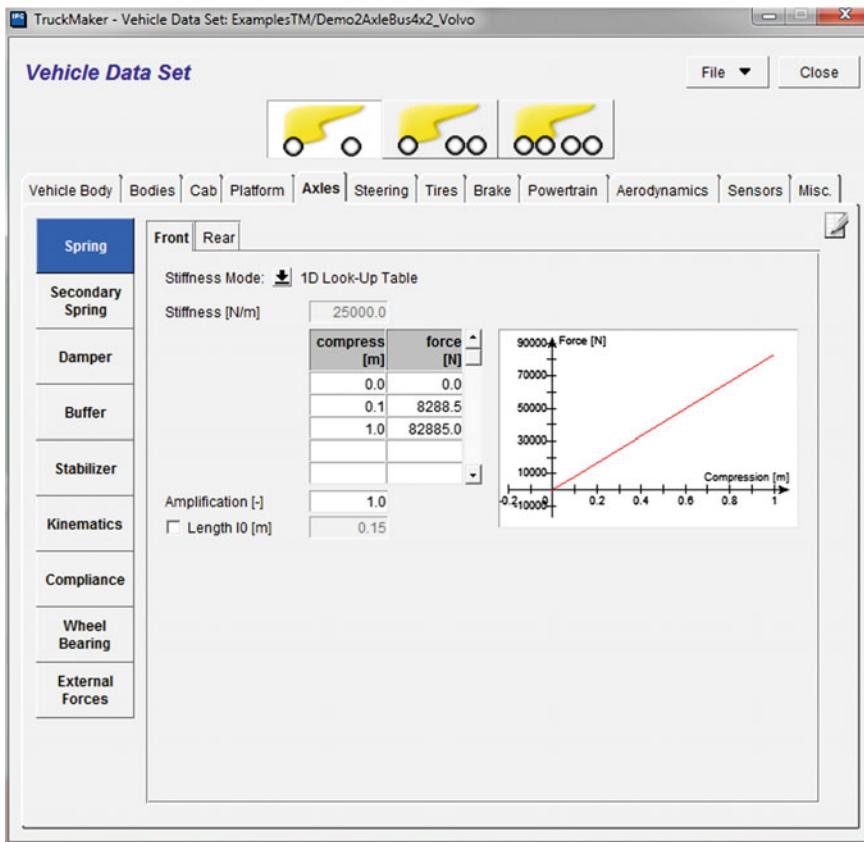
Fig. 6.11 The Truck module—suspensions

to parameterize two buffers per axel (four in total), stiffness for each buffer, and the wheel travel from which the buffers are activated in both positive and negative directions.

- In the Stabilizer tab (Fig. 6.14), only the properties of the single Anti Roll Bar (ARB) element are specified. Its angle or length variation is defined in the kinematics of the model [5]. Various Kinematics models are available (Fig. 6.15). The kinematics of the model has to be specified or each of the front and rear axels separately. The Compliance model takes into account the transition of the wheel when forces are applied due to elasticity effects of the suspension. The user can choose between the following compliance descriptions
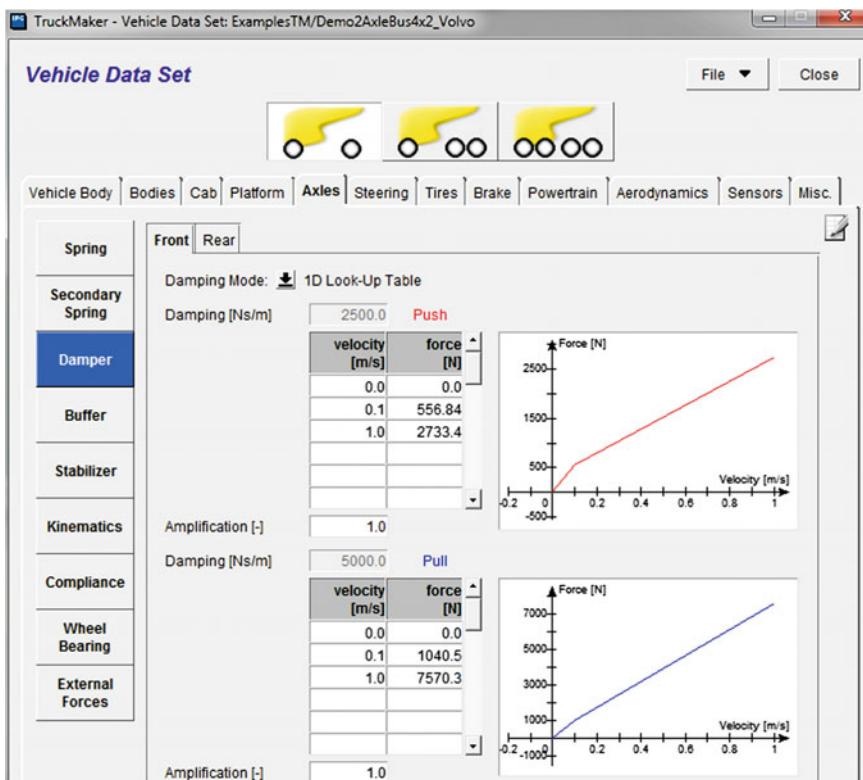
Fig. 6.12 The Truck module—damper
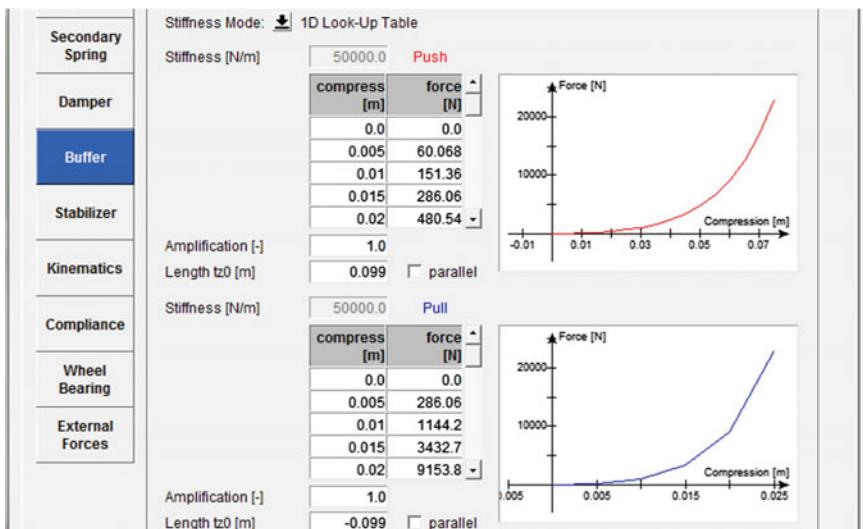
Fig. 6.13 The Truck module—buffer

that are available in the model option on the compliance tab, for others the user has to select the mode not specified and define them in an external kinematics file [5].

- Steering System consists of a mechanical module which defines the ratio between the steering wheel angle and the steering rack displacement (Fig. 6.16). Optionally, a power steering unit can be added by selecting the Pfeffer Steering model which also regards friction losses in the steering system [5].
- Tires are parametrized within the vehicle data set (Fig. 6.17). The purpose of the tire models is to calculate the slips and the stress applied to the contract point on the road (patch point) and then to convert them into stresses applied to the wheel center, since the rest of the vehicle model directly uses those efforts.
- Brake model determines the ratio between the forces at the brake pedal to the braking torque at each wheel (Fig. 6.18). The brake system consists of hydraulic models and does not contain any controller model.
- Powertrain module is a torque transmission model which transfers a torque from the engine to the wheels. In reaction to that, the wheel speeds are modified and
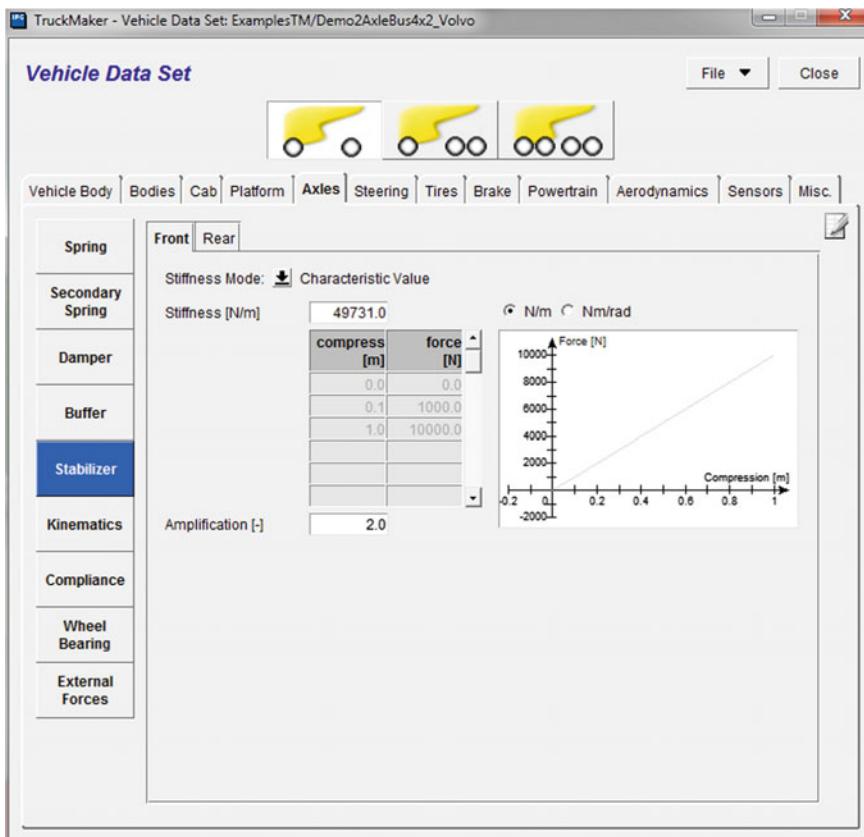
Fig. 6.14 The Truck module—stabilizer
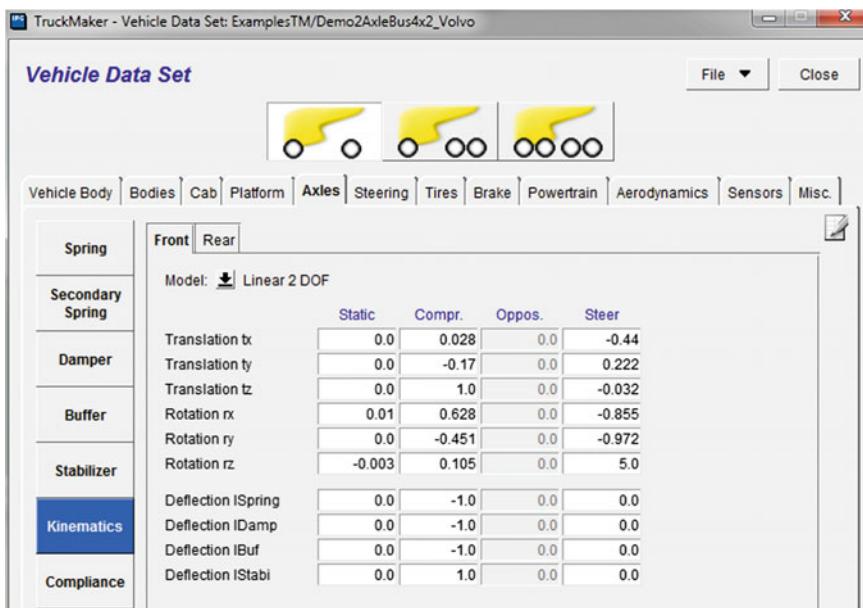
Fig. 6.15 The Truck module—kinematics
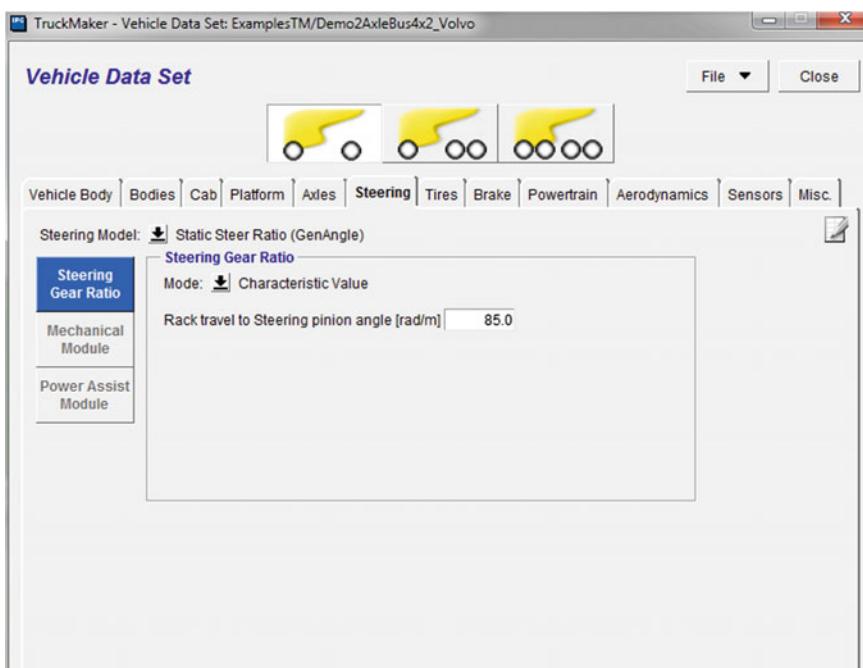
Fig. 6.16 The Truck module—steering system
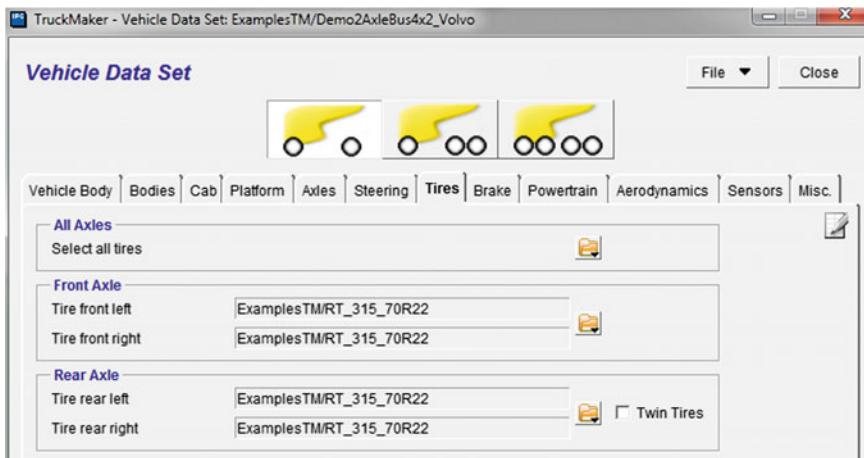
Fig. 6.17 The Truck module—tires

the rotation speed of the different components of the driveline are calculated
subsequently (Fig. 6.19). The engine is seen as a torque source producing its
output depending on the throttle position and on its speed (its speed is imposed
by the wheel speeds) [5]. The model selected for the drive system (Powertrain
Model) is AVL CRUISE to load the project developed in order to complete the
co-simulation process. Computer simulations made in real time need the
implementation of bus models built in the AVL CRUISE application. For this,
one will use the connection interface between AVL CRUISE and IPG
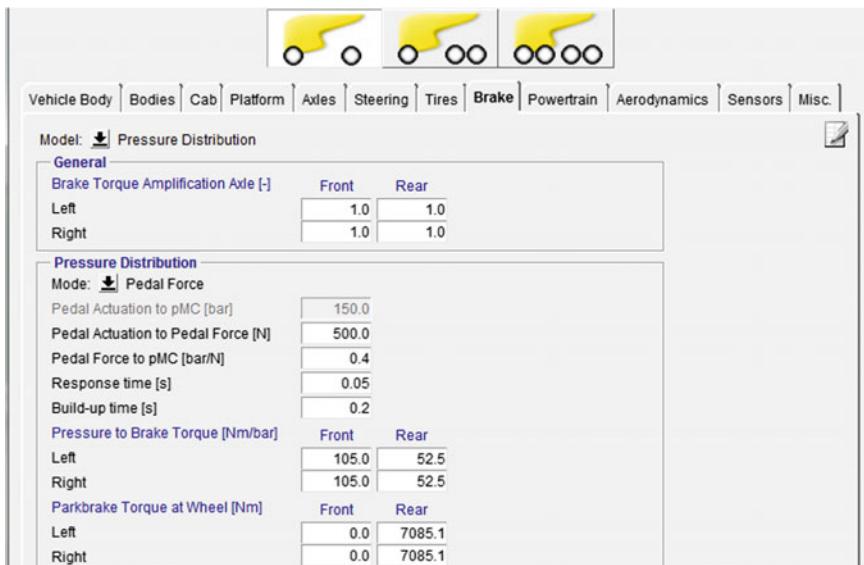
Fig. 6.18 The Truck module—brake
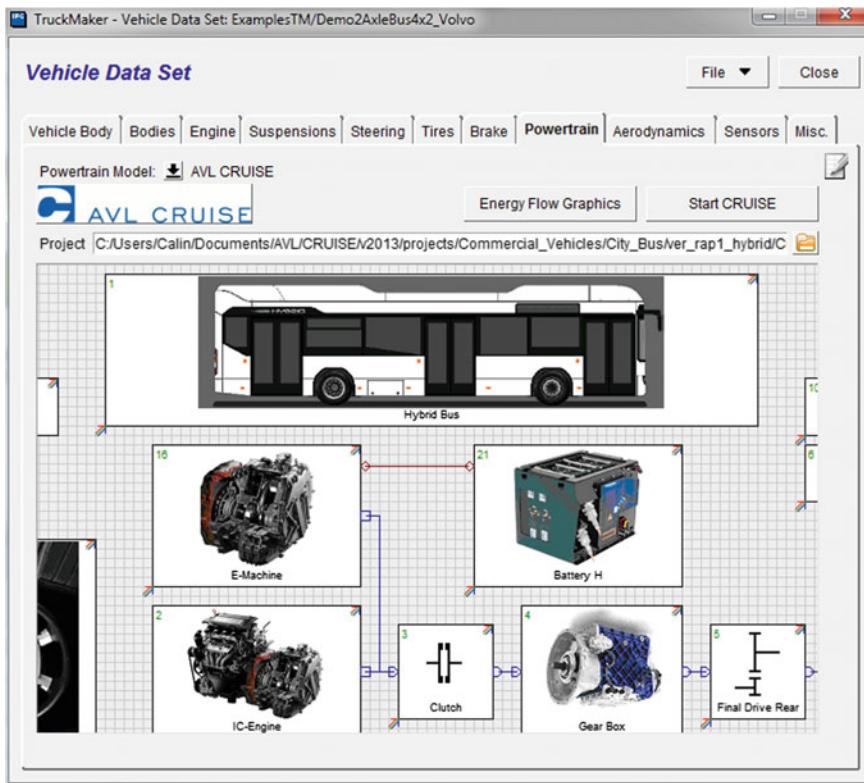
Fig. 6.19 The Truck module—Powertrain AVL CRUISE

TruckMaker (the co-simulation process) in order to implement on the presented vehicle model one of the studied drive systems. The pre-processing program is used to enter the initial data, the entry data and the technical characteristics of the vehicle which is about to be built as a model for the simulation process [5].

- The Aerodynamic model (Fig. 6.20) applies additional variable forces to the vehicle body, according to the vehicle speed. The adaptation of the map by accurate values is often not required as the aerodynamic model is of minor importance at low speeds [5].
- In the Sensors tab, there is the possibility to define four types of sensors: Sideslip Angle Sensors, Body Sensors, Driving Assistance Sensors, and Road Property Sensors (Fig. 6.21) [5]:

  - Sideslip Angle Sensors are located in the vehicle center of gravity by default.
  - A Body Sensor is an inertial sensor that can be positioned anywhere on the vehicle to measure the position, velocity, rotational velocity, acceleration and rotational acceleration. Up to 10 body sensors can be placed on the vehicle.
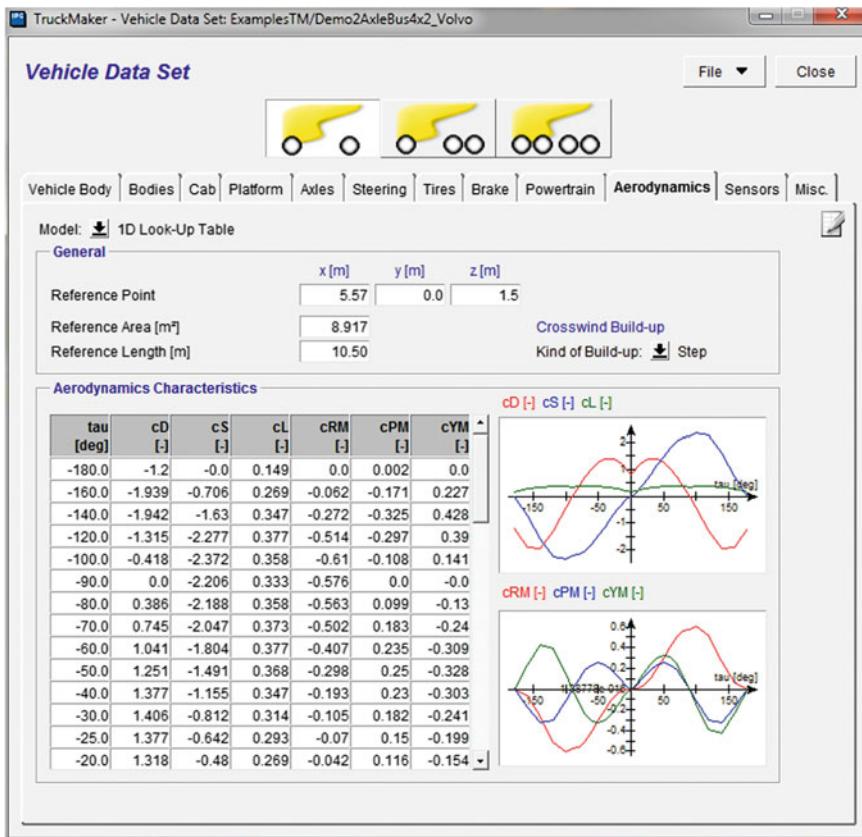
Fig. 6.20 The Truck module—aerodynamic

- Driving Assistance Sensors (DASensor) can be parameterized independently, just by selecting the sensor in the general area. The parameters that are specific to the selected sensor are displayed under the graphical representation of the vehicle.
- The Free Space Sensor Module (FSSensor) is an extended DASensor module, whose sensor beam is subdivided in equiangular horizontal and vertical segments.
- The Traffic Sign Sensor (TSSensor) detects all or preselected traffic sign which falls within its defined range and horizontal/vertical aperture angles. The sensor cross-checks if the sign faces the sensor and then sorts all detected signs in ascending order with distance.
- The Line Sensor module is used to detect lines and barriers that have been defined by the user on the road dialog using the road marking and/or traffic barrier options as a new bump or marker. It can be compared to an idealized camera.
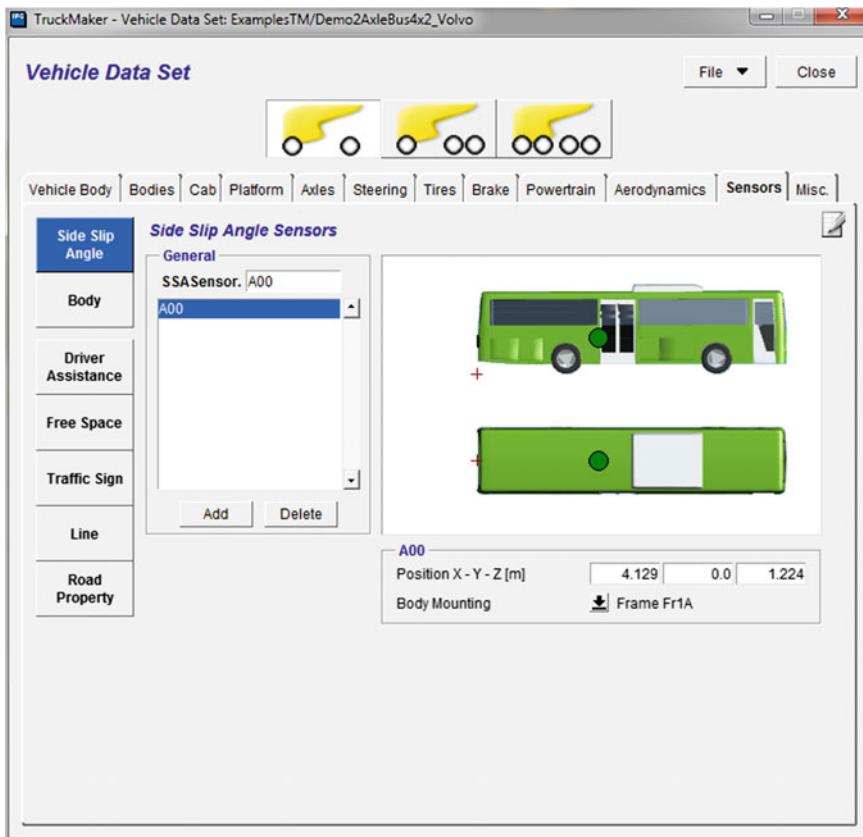
Fig. 6.21 The Truck module—sensors

- In the Miscellaneous module the user can create own vehicle graphics. Supported file types are PNG images (Fig. 6.22). Using PNG pictures, any photo can be imported. A picture of the vehicle in top view and another one in side view is required. To create a PNG using IPGMovie, the picture needs to be scaled to the length of the vehicle (1 m = 100 pixel) and saved as a PNG image. Using the graphical tool, everything around the vehicle needs to be deleted to create a transparent background. Then, select all and paste it to another file of the size of 560 × 226 pixels (72 dpi). Move the picture to the left side of the window (in case of a side view additionally aligns it vertically to the bottom). The top view should be saved in the same folder and finally the pictures can be selected in the TruckMaker GUI [5].

Loads: the following section will present information about the additional loads (Fig. 6.23). With the so-called trim loads there is the possibility to add some extra loads in order to simulate passengers, luggage, and heavy measurement equipment. Check if the static position of the vehicle using Model Check, the effects of trim,
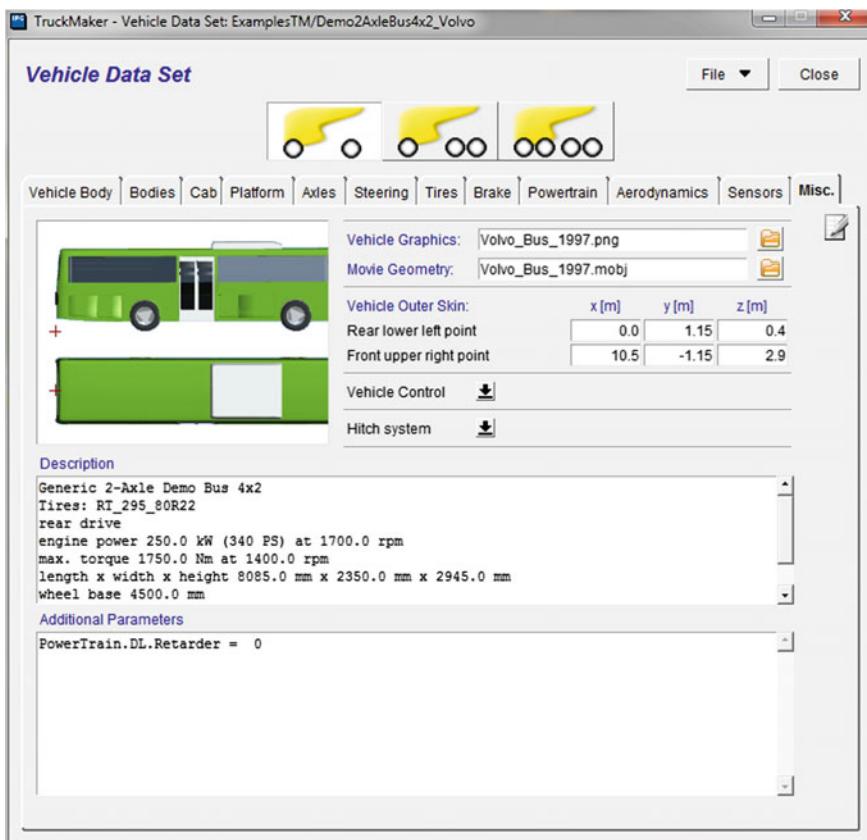
Fig. 6.22 The Truck module—miscellaneous

loads will be included in the height of the vehicle's center of gravity or the wheel positions at the start of the configuration. For some specific simulation purposes, the user may want to simulate a Test Run with an additional load on the vehicle, but still want to check the static state of the vehicle without it. The picture represents the vehicle body, defined loads (this is illustrated by a point) [5].

Maneuver is the concept of TruckMaker for the driving scenario (Fig. 6.24) and it is following maneuver definition, which is split into several maneuver steps (acceleration, braking, etc.). These maneuver steps are called mini-maneuvers. Each mini-maneuver is composed of:

- Longitudinal dynamic actions: accelerating, braking, gear shifting, etc.;
- Lateral dynamic actions: steering;
- Additional actions, defined by a very easy script language [5].
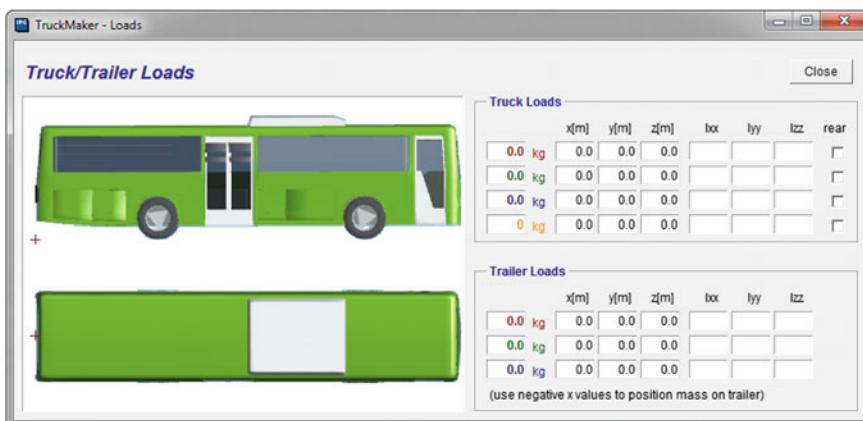
Fig. 6.23 The Truck module—load

TruckMaker offers a convenient GUI to build a great diversity of driving sce-
narios. To build a driving scenario how to add and parameterize successive and
various maneuver steps it is necessary to control the vehicle as the user wants. The
list of the maneuvers steps is displayed and can be built in box 1.

The first entry in the maneuver list serves to specify starting conditions. Possible
settings are the initial speed, the gear number, the steering wheel angle, and track
offset. A new maneuver step is added by using the New button at the bottom of box 1.
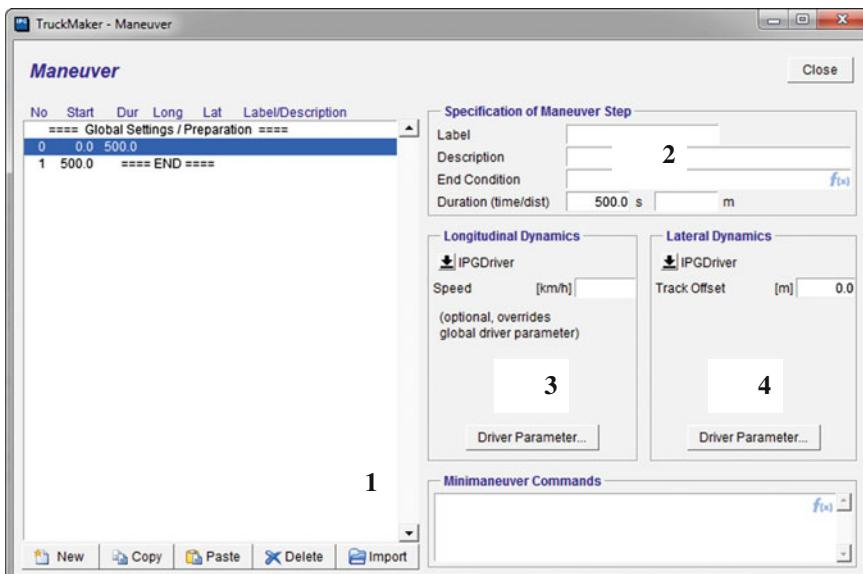
Fig. 6.24 The Truck module—maneuver

The maneuver steps are always inserted ahead of the one selected. A maneuver step can be selected by clicking on the maneuver list in box 1; it is then highlighted in blue. To add a step to the end of the list, click on the entry " ==== END ==== " to select it, and then click on the New button. Maneuver steps can also be copied and pasted, deleted, or imported from another Test Run. You can find the same functionality Import by clicking with the right mouse button anywhere in the Maneuver GUI [5].

After creating a maneuver step, the actions need to be defined. Each mini-maneuver consists of duration (box 2) and a description of the driver's task, separated in longitudinal and lateral dynamics (box 3 and 4).

On the specification of a maneuver step (box 2) the user can define an end condition for each maneuver step using real-time expressions. The classic end conditions—time or distance—can be directly entered in the duration fields.

Longitudinal dynamics (box 3) are available to fully automate and detailed speed and pedal control. To accelerate and brake the vehicle according to its dynamic limits, the option IPGDriver should be chosen (closed loop maneuver). This option activates the driver model for the longitudinal dynamics.

Possible specifications of lateral dynamics (box 4) are available to control the steering wheel [5].

Simulation the whole control of the VVE, and with this of the TruckMaker simulation, is done via the TruckMaker main GUI. The status of the simulation can be observed in the simulation box.

Storage of Results mode collects only selected data and it is temporarily stored in a ring buffer without being saved to the disk automatically. For mode saves all is selected, all data is continuously and automatically saved to the disk.

If one of the history modes is selected, the data is temporarily stored in a ring buffer. The saving process is started manually at the end of the simulation by clicking the Save button. The amount of saved data depends on the history mode that has been selected. If the mode history 10 s is selected, clicking on save at the end of the simulation will save simulation results for the last 10 s of the simulation [5].

6.3 Vehicle Models Generated for Co-simulation

The main vehicle models used in the simulation process have the technical characteristics presented in Table 6.1 [1, 8–11].

The vehicle models developed in the AVL CRUISE application are composed of component elements which can be identified with real elements from both the point of view of the constructive characteristics and the point of view of the mathematical relations which govern their functionality. Each element taking part in the composition of the three bus models developed in this project has been define through mathematical relations, which help with the calculus of processes and the characteristics of the model while the simulation process in the AVL CRUISE application is in process.

Table 6.1 Technical characteristics of the simulated vehicle models

No	Parameter	Description	Classic	Hybrid	Electric
1	Dimensions	Length (mm)	11990	12074	12267
		Width (mm)	2500	2520	2550
		Height (mm)	3304	3216	3486
		Overhang front/rear (mm)	2700/3200	2700/3450	2600/3300
		Front gauge/Rear gauge (mm)	6120	5945	6250
		Ground clearance (mm)	330	400	370
		Passenger Capacity (–)	96	95	70
2	Performances	Maximum velocity (km/h)	80	75	90
		Energy consumption (kW/h)		120	130
		Fuel consumption (l/h)	12.0	5.2	–
3	Dynamic characteristics	Gyration radius (m)	10.0	10.8	12.8
		Angle of approach (°)	7.0	7.0	8.0
		Angle of departure (°)	7.0	8.0	9
4	Mechanical characteristics	Type of suspension	Pneumatic	Pneumatic	Pneumatic
		Braking system	ABS	Regenerative	Regenerative
		Tire specifications	275/70 R22.5	275/70 R22.5	305/70 R22.5
5	Thermal engine	Maximum power (kW)	180	61	–
		Maximum power (CP)	245	216	–
		Maximum torque (Nm)	1100	800	–
6	Electric motor	Maximum power (kW)	–	120	2 * 90
		Maximum power (CP)	–	161	2 * 121
		Maximum torque (Nm)	–	800	2 * 350
7	Electric energy system and/or fuel	Type of batteries	–	Li-Ion	Li-FE
		Capacity (Ah)	–	225	324
		Life span (cycle)	–	4000	6000
		Tank capacity (l)	250	220	–
		Type of fuel (l)	Diesel	Diesel	–

<div align="right">(continued)</div>

Table 6.1 (continued)

No	Parameter	Description	Classic	Hybrid	Electric
8	Emissions according to EURO norms	CO emissions (g/kWh)	1.50	1.50	0 local
		NO_x emissions (g/kWh)	2.00	0.40	0 local
		HC emissions (g/kWh)	0.46	0.13	0 local
9	Autonomy	Partial recharge (km)	–		100
		Full recharge (km)	–		250
		Classic fuel (km)	1000	4000	–

The AVL CRUISE—IPG TruckMaker interface is based on a co-simulation of the models for the drive systems developed in the AVL CRUISE application which are equipping the vehicle models developed in the IPG TruckMaker application [5].

The preparation of a model developed AVL CRUISE for co-simulation in the IPG TruckMaker application needs the insertion of certain new components in the model built in AVL CRUISE, namely an element named interface for TruckMaker and four elements of the Hub type, which simulate the dynamometer composition which will replace the tire type elements of the model.

The Hub type elements (Fig. 6.25) represent a combination between a brake and a virtual wheel and they transmit into IPG TruckMaker the vehicle movement on the established road. The element for the interface with the TruckMaker application (Fig. 6.26) defines the connection for the co-simulation process for the model developed in AVL CRUISE.
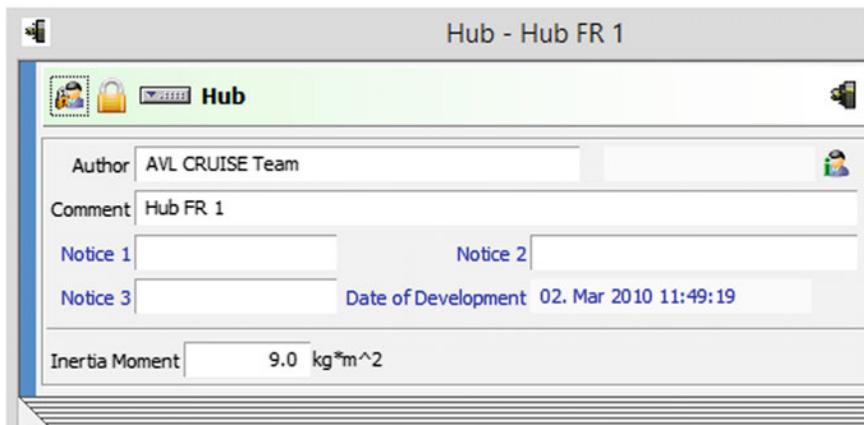
Fig. 6.25 The Hub element—the model for co-simulation
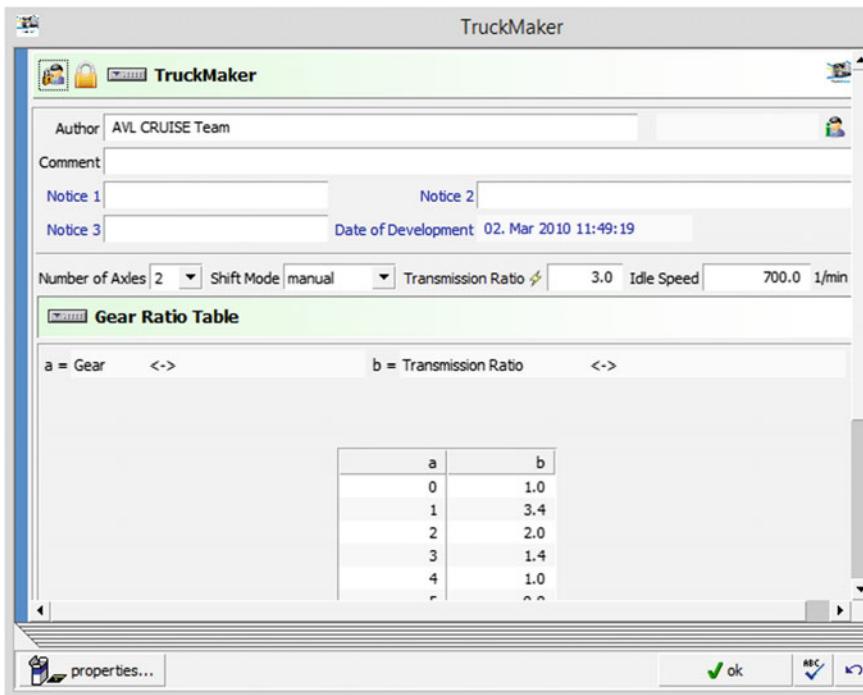
Fig. 6.26 TruckMaker interface—the model for co-simulation

The model for the drive system transmits the data selected by the user towards the corresponding input channels (Table 6.2) from the IPG TruckMaker application, where these are implemented on the selected vehicle model and the simulations results are collected and transmitted through the corresponding output channels towards AVL CRUISE (Table 6.3).

The channels 0–7 are automatically connected to the corresponding HUB elements equipping the model developed in AVL CRUISE.

The parameters which can be selected from the interface element TruckMaker are as follows [5]:

- The Shift module which transmits to the IPGDriver the model of gearbox which equips the drive system (manual or automated);
- The transmission ratio of the gearbox output speed towards the powertrain;
- The engine idle speed which is transmitted to the IPGDriver;
- The transmission ratio of the gears towards the gearbox;
- The suspension model for the vehicle chassis in front and/or rear.

The simulation system analysis SAM (System Analysis Mode) is used for investigating and recording the parameters of the transmission system components

Table 6.2 Signals transmitted from AVL CRUISE to IPG TruckMaker [2]

Channel	Signals in AVL CRUISE	Variables in IPG TruckMaker	U.M.
0	Wheel FL Angle	PowerTrain.WFL.rot	rad
1	Wheel FR Angle	PowerTrain.WFR.rot	rad
2	Wheel RL Angle	PowerTrain.WRL.rot	rad
3	Wheel RR Angle	PowerTrain.WRR.rot	rad
4	Wheel FL Speed	PowerTrain.WFL.rotv	rad/s
5	Wheel FR Speed	PowerTrain.WFR.rotv	rad/s
6	Wheel RL Speed	PowerTrain.WRL.rotv	rad/s
7	Wheel RR Speed	PowerTrain.WRR.rotv	rad/s
8	Engine On/Off	PowerTrain.Engine.on	–
9	Engine Speed	PowerTrain.Engine.rotv	rad/s
10	Engine Torque	PowerTrain.Engine.Trq	Nm
11	Fuel Volume Flow	PowerTrain.Engine.Fuel.Flow	1/s
12	GB Speed In	PowerTrain.GearBox.rotv_in	rad/s
13	GB Act Ratio	PowerTrain.GearBox.in	–
14	GB Gear No	PowerTrain.GearBox.GearNo	–
15	Supp Brake Torque FL	PowerTrain.WFL.Trq_B2W	Nm
16	Supp Brake Torque FR	PowerTrain.WFR.Trq_B2W	Nm
17	Supp Brake Torque RL	PowerTrain.WRL.Trq_B2W	Nm
18	Supp Brake Torque RR	PowerTrain.WRR.Trq_B2W	Nm
19	Drive Torque FL	PowerTrain.WFL.Trq_DL2W	Nm
20	Drive Torque FR	PowerTrain.WFR.Trq_DL2W	Nm
21	Drive Torque RL	PowerTrain.WRL.Trq_DL2W	Nm
22	Drive Torque RR	PowerTrain.WRR.Trq_DL2W	Nm
23	Front Supp2Bdy Torque X-axis	PowerTrain.Trq_Supp2Bdy1[0]	Nm
24	Front Supp2Bdy Torque Y-axis	PowerTrain.Trq_Supp2Bdy1[1]	Nm
25	Front Supp2Bdy Torque Z-axis	PowerTrain.Trq_Supp2Bdy1[2]	Nm
26	Rear Supp2Bdy Torque X-axis	PowerTrain.Trq_Supp2Bdy1B[0]	Nm
27	Rear Supp2Bdy Torque Y-axis	PowerTrain.Trq_Supp2Bdy1B[1]	Nm
28	Rear Supp2Bdy Torque Z-axis	PowerTrain.Trq_Supp2Bdy1B[2]	Nm
29	Supp Torque Engine X-axis	PowerTrain.Trq_Supp2BdyEng[0]	Nm
30	Supp Torque Engine Y-axis	PowerTrain.Trq_Supp2BdyEng[1]	Nm

and it will be used in the model built in AVL CRUISE to determine the propulsion energy flow which is necessary for the optimal functioning of the studied model [5].

The virtual vehicle contains all the component parts of a real vehicle, including the drive, steering, suspension, braking system etc. and it also integrates the management and control electronic elements (ABS, ESP, ACC etc.), elements which can be modeled for the virtual vehicle with the help of HIL (Hardware in the Loop) or SIL (Software in the Loop) testing components [2].

Table 6.3 Signals transmitted from IPG TruckMaker to AVL CRUISE [2]

Channel	Variables in IPG TruckMaker	Signals in AVL CRUISE	U.M.
0	SimCore.DeltaT	Simulation step size	s
1	SimCore.Time	Simulation time	s
2	Vehicle.PoI_Vel_1[0]	Car velocity	m/s
3	VehicleControl.Brake	Brake signal	–
4	VehicleControl.Clutch	Clutch release	–
5	VehicleControl.Gas	Load signal	–
6	VehicleControl.GearNo	Desired gear	–
7	Car.Tire[0].Trq_T2W	Resistance torque Wheel FL	Nm
8	Car.Tire[1].Trq_T2W	Resistance torque Wheel FR	Nm
9	Trq_RL	Resistance torque Wheel RL	Nm
10	Trq_RR	Resistance torque Wheel RR	Nm
11	Car.ConBdy1.atHori	Acceleration	m/s^2
12	Car.ConBdy1.atHori	Acceleration lateral	m/s^2
13	Vehicle.LongSlipFL	Longitudinal slip FL	–
14	Vehicle.LongSlipFR	Longitudinal slip FR	–
15	LongSlip_RL	Longitudinal slip RL	–
16	LongSlip_RR	Longitudinal slip RR	–
17	VehicleControl.Ignition	Ignition	–
18	VehicleControl.StarterCtrl	Starter switch	–
19	VehicleControl.EngineSwitch	Engine switch	–
20	Brake.Trq_tot[0]	Brake torque FL	Nm
21	Brake.Trq_tot[1]	Brake torque FR	Nm
22	Brake.Trq_tot[2]	Brake torque RL	Nm
23	Brake.Trq_tot[3]	Brake torque RR	Nm

The new models built for co-simulation are presented in Fig. 6.27—the bus equipped with an internal combustion engine, Fig. 6.28—the hybrid bus, respectively in Fig. 6.29—the electric bus, the introduced elements needing to be connected and defined [1].

As a supplementary option of the co-simulation process there is the AVL CRUISE RT (Real Time) application, an application which allows running the virtual tests for an AVL CRUISE model in real time, together with the IPG TruckMaker applications. The AVL CRUISE RT application is used in the situations in which the simulated cases are too many, when the costs of a physical experiment are too high or when running the application in real time, where the time factor is critical.

The constructive modification of the model in AVL CRUISE for co-simulation needs the implementation of the following steps [2]:

- The introduction of the TruckMaker type interface and of the Hub type components in the initial model;
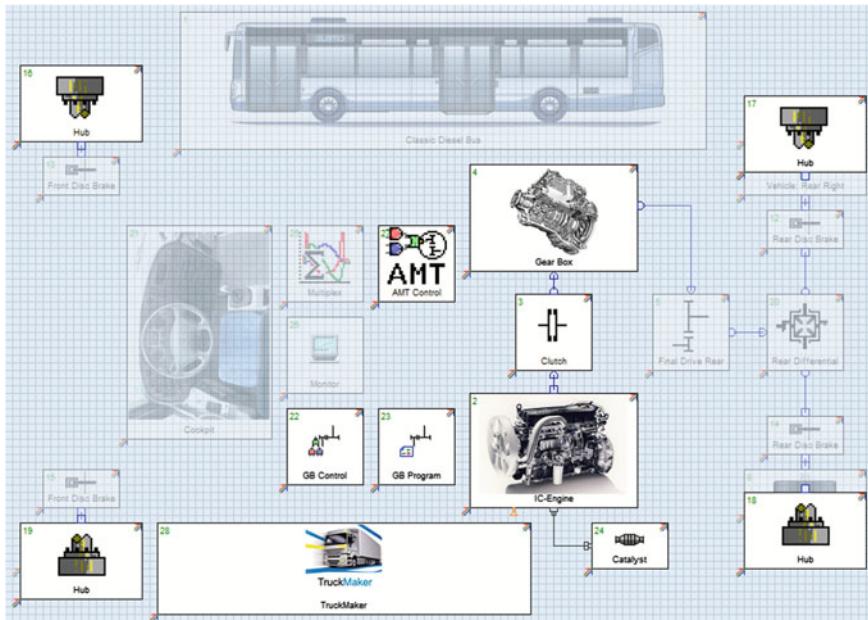
Fig. 6.27 Classic bus—the model for co-simulation
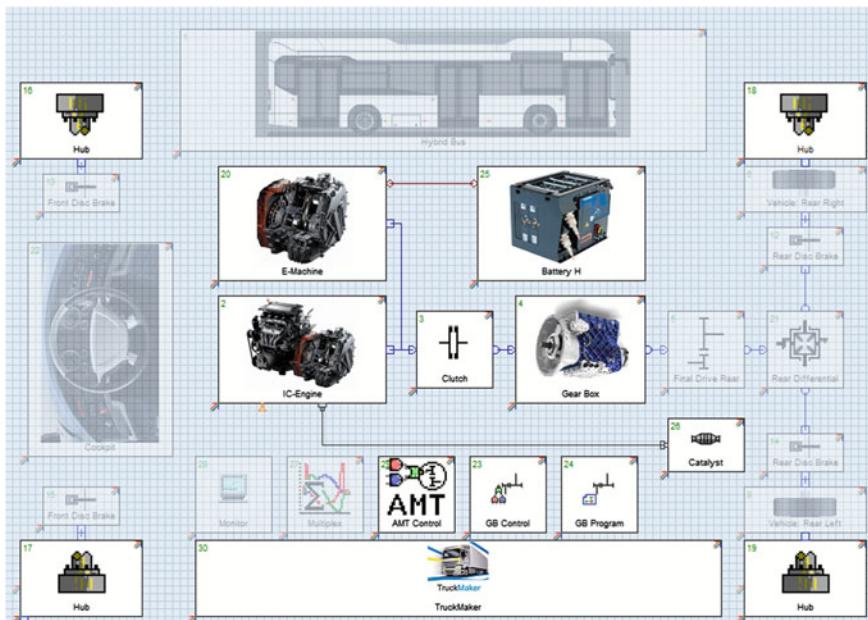
Fig. 6.28 Hybrid bus—the model for co-simulation
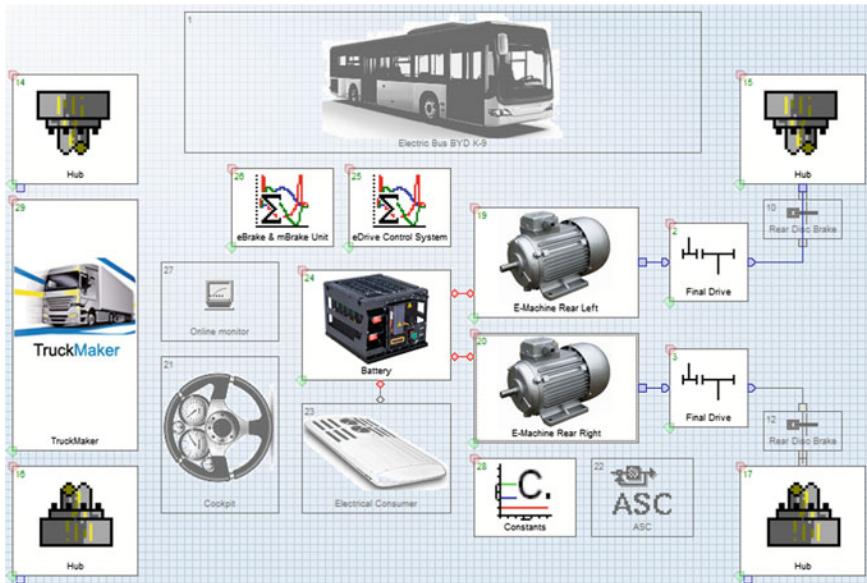
Fig. 6.29 Electric bus—the model for co-simulation

- The definition of a hierarchy of the sub-system type by grouping the components forming the model in order to commute between the modes used in the simulation (Drivetrain, CRUISE, TruckMaker);
- The definition of SAM (System Analysis Mode) for the calculus of the co-simulation process;
- The exclusion of certain components used in the simulation in AVL CRUISE (Vehicle, Cockpit, Monitor etc.) from the co-simulation process in IPG TruckMaker (for the model built in AVL CRUISE, in IPG TruckMaker only the powertrain is exported which is implemented on a vehicle model existing in IPG TruckMaker).

The model with interface for co-simulation, defined in AVL CRUISE corresponding to the drive system will be loaded in IPG TruckMaker to equip the vehicle model simulated in this application.

References

1. Varga, B. O. (2015). *Energy efficiency of vehicles equipped with hybrid or electrical powertrain for urban public transport (in Romanian)*. Habilitation thesis, Technical University of Cluj-Napoca, Romania, 18 September 2015.
2. AVL CRUISE. (2010). CRUISE—CarMaker/TruckMaker Co-Simulation", AVL List GmbH, Graz, Austria, Document no. 04.0115.2010, Edition 07.2010.

3. AVL CRUISE. (2011). Users Guide, AVL List GmbH, Graz, Austria, Document no. 04.0104.2011, Edition 06.2011.
4. Varga, B. O., & Iclodean, C. (2015). Advanced research methods of hybrid electric vehicles' performances. *Acta Electrotehnica Journal* (Cluj-Napoca), (1–2), 111–116. ISSN: 2344–5637.
5. Varga, B. O., Mariaşiu, F., Moldovanu, D., & Iclodean, C. (2015). *Electric and plug-in hybrid vehicles—advanced simulation methodologies, chapter7* (pp. 477–524). Springer International Publishing Ed., ISBN: 978-3-319-18638-2.
6. IPG TruckMaker. (2014). Reference Manual Version 4.5, Simulation Solutions, Test Systems, Engineering Services, IPG Automotive, Karlsruhe, Germany.
7. IPG CarMaker. (2014). User's Guide Version 4.5.2, IPG Automotive, Karlsruhe, Germany.
8. Retrieved December 20, 2015, from http://ibb.iveco.com/Bus%20Drawings/CITELIS/BODYBUILDER%20INSTRUCTIONS/chassis%20Citelis%2060393821-2C(GB).pdf.
9. Retrieved December 20, 2015, from http://ibb.iveco.com/Bus%20Drawings/CITELIS/COMMERCIAL%20SHEETS/Citelis%20Diesel%2012%20chassis%20E5%20INT%20oct2011.pdf.
10. Retrieved December 20, 2015, from http://www.volvobuses.com/bus/germany/de-de/products/stadtbusse/volvo-7700-hybrid/Pages/Volvo-7700-Hybrid.aspx.
11. Retrieved December 20, 2015, from http://www.byd.com/ap/images/ebus/download/k9%20brochure.pdf.

Chapter 7
Co-simulation of Buses Equipped with Hybrid and Electric Drive Systems

7.1 Development of Co-simulation Models CRUISE—TruckMaker

The CRUISE—TruckMaker interface is based on the co-simulation process of the models for drive systems developed in the AVL CRUISE application, which equip the vehicle models developed in the IPG TruckMaker application [1].

If a AVL CRUISE powertrain is chosen in the vehicle data set TruckMaker starts the AVL CRUISE simulation program during the initialization phase of the Test Run simulation.

A TruckMaker working directory is created over main menu File—Project Folder—Create Project (Fig. 7.1). Selecting TruckMaker working directory over main menu: File—Project Folder—Select.

Preparing a AVL CRUISE powertrain for TruckMaker co-simulation requires the introduction of several new components in AVL CRUISE (TM-Car and Hub component) as well as usage of system GUI feature and SAM calculation task.

On AVL CRUISE side the preparation for co-simulation are [1]:

- Building model with specific components—modules for co-simulation (TM-Car and Hub module);
- Using system/sub-system to switch between AVL CRUISE stand-alone simulation and co-simulation with TruckMaker;
- Setup SAM calculation task of co-simulation;
- Some special modules needed for AVL CRUISE stand-alone simulation must be excluded in co-simulation model (Vehicle, Cockpit, Monitor, etc.).

On TruckMaker side the preparation for co-simulation are:

- Creating CRUISE working directory inside a directory TruckMaker;
- Copying and renaming the calculation kernel file (CRUISE\bin\CRUISE_m.dll in TruckMaker\lib\CRUISENT.dll);
- Selecting AVL CRUISE powertrain and Project Folder for co-simulation.
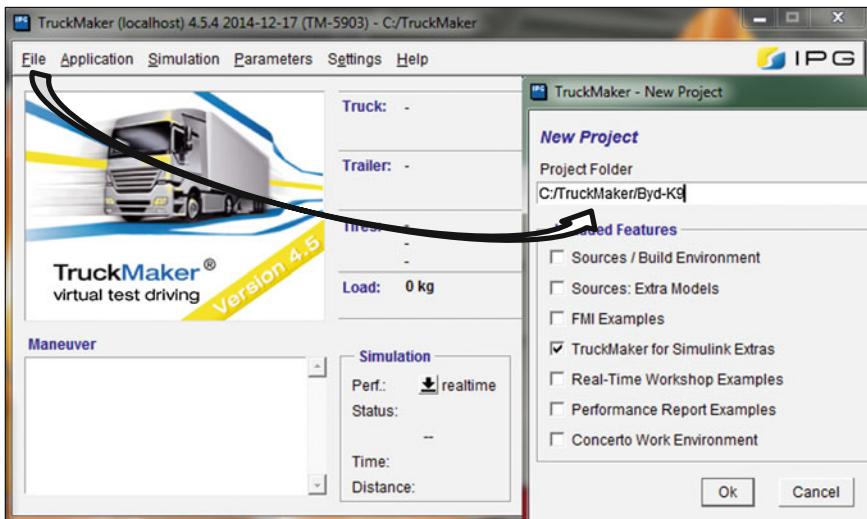
Fig. 7.1 Defining a new project as new project

On both AVL CRUISE and TruckMaker the preparations for co-simulation are:

- Harmonizing SimParameters and Memory Management.

The model with interface for co-simulation defined in AVL CRUISE corresponding to the powertrain will be loaded in IPG TruckMaker in order to equip the vehicle model simulated in this application. From the Powertrain menu of the vehicle configuration system (Vehicle Data Set) in IPG TruckMaker, the AVL CRUISE option is chosen, following that through selection, the project model for co-simulation built in AVL CRUISE will open on the Project line of command.

The new models built for co-simulation are presented in Fig. 7.2 (bus equipped with thermal engine), Fig. 7.3 (hybrid bus), respectively in Fig. 7.4 (electric bus), the data entered will then be connected and defined [2].

The TM-Car component defines the interface in co-simulation between AVL CRUISE powertrain models calculated by SAM calculation task and TruckMaker simulation package [1].

The interface component is exchanging the information between AVL CRUISE and TruckMaker and there must be one TM-Car module in the vehicle model.

At every time step, AVL CRUISE data will go to the TruckMaker application through Data Bus input channels CRUISE to TruckMaker, and from there, the data comes back to AVL CRUISE through output channels TruckMaker to CRUISE which can be connected with AVL CRUISE components [1].

This interface allows the user to easily establish a working AVL CRUISE powertrain model for CRUISE—TruckMaker co-simulation. The main settings to be entered in the CM-Car interface are the following:
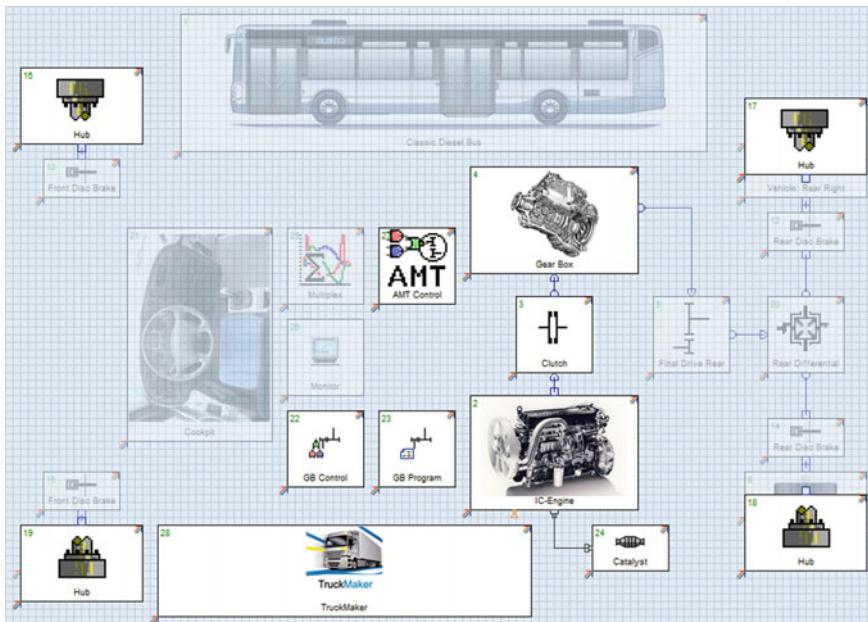
Fig. 7.2 Classic bus—the model for co-simulation
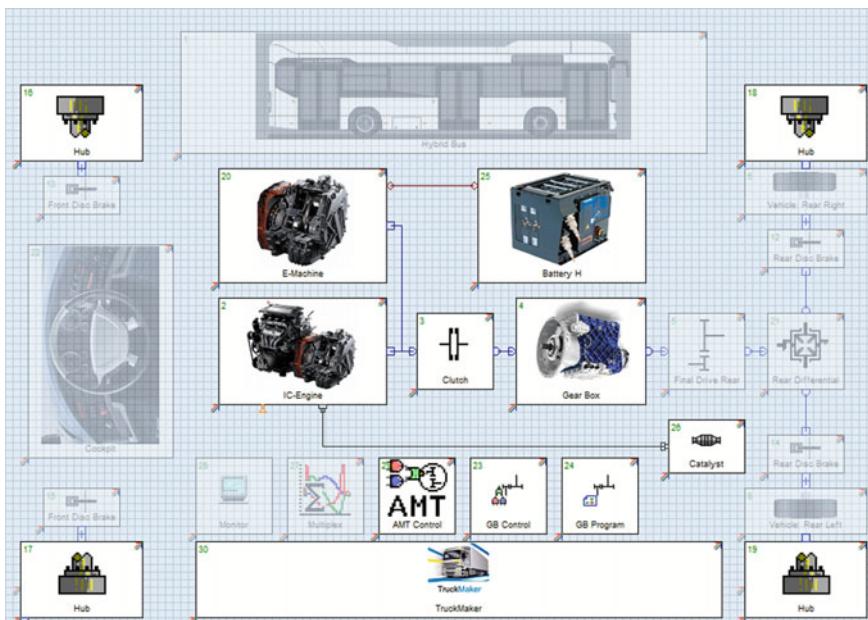
Fig. 7.3 Hybrid bus—the model for co-simulation
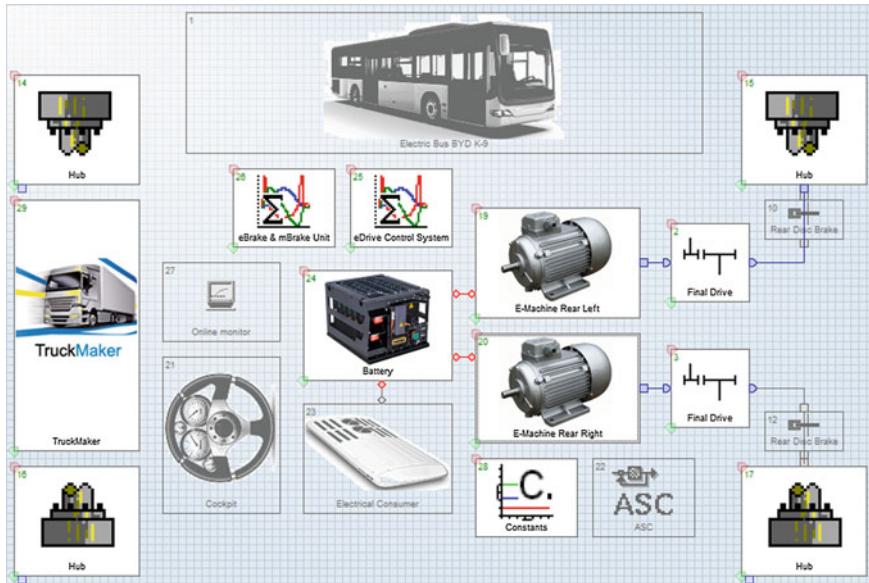
Fig. 7.4 Electric bus—the model for co-simulation

- Manual or Automatic Shift Mode—information about using gearbox in vehicle model and it is needed by the IPGDriver;
- Transmission Ratio—the complete transmission ratio between the gearbox output speed and wheel speed and it is needed by the IPGDriver;
- Idle Speed—the value has to be consistent with the engine idle speed inside the engine module;
- Gear Ratio Table—value of the transmission ratio for complete gearbox and supposed to be consistent with transmission ratio values in gear ratio table of gearbox module;
- Body—the drive torque is supported by the car chassis.

The first step is dividing the initial model in three sub-systems. In order to highlight the supplementary actions in the sub-systems structure, all the components which are not part of the powertrain (Vehicle, Wheel, Brake, Cockpit, ASC, Monitor) will be selected and allocated to the CRUISE sub-system.

First step is to add two sub-systems in the current system. These will be renamed Drivetrain, CRUISE, respectively TruckMaker. The result of this procedure should be one system with three sub-systems (sub-system 001, sub-system 002, and sub-system 003) [1].

Table 7.1 Data Bus Connection for the TruckMaker system (classic bus)

Component requires	Input information	Component delivering	Output information
AMT Control	**Current Gear**	Gearbox	Current Gear
	Desired Gear	GB Control	Desired Gear
	Input Speed	Clutch	Input Speed
	Load Signal	Cockpit	Load Signal
	Output Speed	Clutch	Output Speed
	Velocity	Cockpit	Velocity
Clutch	**Desired Clutch Release**	AMT Control	Desired Clutch
IC Engine	**Load Signal**	TruckMaker	Load Signal
	Start Switch	TruckMaker	Start Switch
Gearbox	**Desired Gear**	GB Control	Desired Gear
GB Control	**Current Gear**	Gearbox	Current Gear
	Desired Gear (Cockpit)	TruckMaker	Desired Gear
	Desired Gear (GB)	GB Program	Desired Gear
	Gear Selection Down	Cockpit	Gear Select Down
	Gear Selection Up	Cockpit	Gear Selection Up
	Operation Control	IC Engine	Operation Control
	Reference Speed	IC Engine	Engine Speed
	Velocity	TruckMaker	Vehicle Velocity
GB Program	**Current Gear**	Gearbox	Current Gear
	Load Signal	TruckMaker	Load Signal
	Speed	Gearbox	Output Speed
Hub FR	Braking Torque	TruckMaker	Braking FR
	Resistance Torque	TruckMaker	Resistance FR
Hub RR	Braking Torque	TruckMaker	Braking RR
	Resistance Torque	TruckMaker	Resistance RR
Hub FL	Braking Torque	TruckMaker	Braking FL
	Resistance Torque	TruckMaker	Resistance FL
Hub RL	Braking Torque	TruckMaker	Braking RL
	Resistance Torque	TruckMaker	Resistance RL
TruckMaker	Engine On/Off	IC Engine	Operation Control
	Engine Speed	IC Engine	Engine Speed
	Engine Torque	IC Engine	Behind Flywheel
	Fuel Consumption	IC Engine	Fuel Consumption
	GB Speed In	Gearbox	Input Speed
	GB Act Gear No	Gearbox	Current Gear
	Supp Brake Torque FL	Hub Front Left	Support Torque
	Supp Brake Torque FR	Hub Front Right	Support Torque
	Supp Brake Torque RL	Hub Rear Left	Support Torque
	Supp Brake Torque RR	Hub Rear Right	Support Torque
	Drive Torque FL	Differential	Output Torque 1
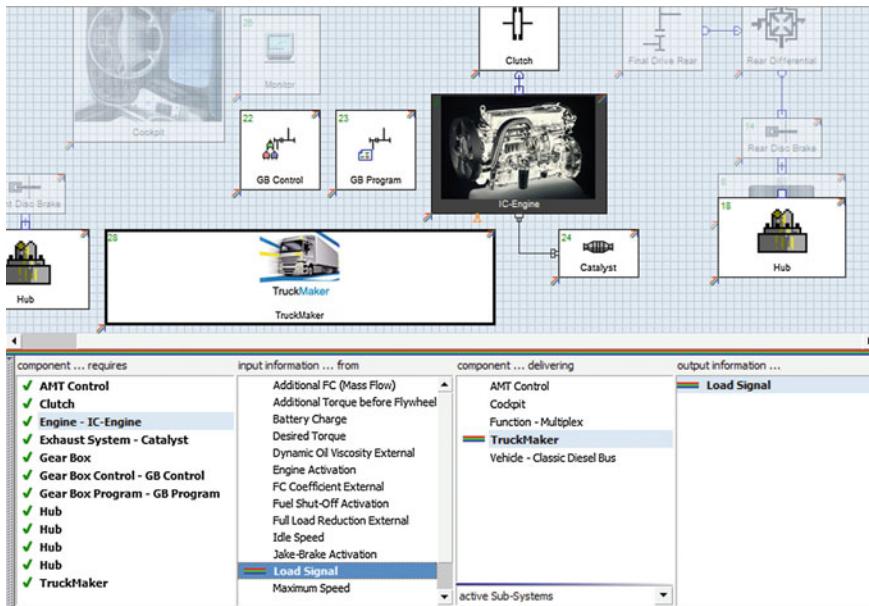
Fig. 7.5 Data Bus Connection for the TruckMaker system (classic bus)

The components of the powertrain (Engine, Torque Converter, Gearbox, Final Drive, Differential, GB Control, GB Program, Catalyst) will be allocated to the Drivetrain sub-system. In order to define the TruckMaker sub-system one will select the elements entered for creating the co-simulation interface (Hub, TruckMaker) [2, 3].

The Data Bus Connection for the TruckMaker sub-system are described in Table 7.1 and Fig. 7.5 for the bus equipped with a thermal engine, Table 7.2 and Fig. 7.6 for the hybrid bud, respectively in Table 7.3 and Fig. 7.7 for the electric bus.

The Data Bus Connection for the CRUISE sub-system are described in Table 7.4 and Fig. 7.8 for the bus equipped with a thermal engine, Table 7.5 and Fig. 7.9 for the hybrid bus, respectively in Table 7.6 and Fig. 7.10 for the electric bus.

In the first column of the Data Bus Connection dialog box (component requires) are included all the elements of the built model, elements whose functionality depends on the information received from other elements.

In the second column (input information from) are displayed all the data channels which are available for the element selected from the first column.

After selecting a data channel from the second column, in the third column (component delivering) will be highlighted all the elements which can provide information for the elements selected in the first two columns.

Table 7.2 Data Bus Connection for the TruckMaker system (hybrid bus)

Component requires	Input information	Component delivering	Output information
Clutch	**Desired Clutch**	AMT Control	Desired Clutch
E-Machine	Ambient Temperature	Cockpit	Course Temperature
	Load Signal	IC Engine	Actual Load Signal
	Temperature External	Cockpit	Course Temperature
IC Engine	**Load Signal**	TruckMaker	Load Signal
	Start Switch	TruckMaker	Engine Start Switch
Multiplex	Vehicle_brake_pressure	Cockpit	Brake Pressure
Gearbox	**Desired Gear**	GB Control	Desired Gear
GB Control	**Current Gear**	Gearbox	Current Gear
	Desired Gear Cockpit	TruckMaker	Desired Gear
	Desired Gear (GB)	GB Program	Desired Gear
	Gear Selection Down	Cockpit	Gear Selection Down
	Gear Selection Up	Cockpit	Gear Selection Up
	Operation Control	IC Engine	Operation Control
	Reference Speed	IC Engine	Engine Speed
	Velocity	Cockpit	Vehicle Velocity
GB Program	**Current Gear**	Gearbox	Current Gear
	Load Signal	TruckMaker	Load Signal
	Speed	IC Engine	Engine Speed
Hub FR	Braking Torque	TruckMaker	Braking FR
	Resistance Torque	TruckMaker	Resistance FR
Hub RR	Braking Torque	TruckMaker	Braking RR
	Resistance Torque	TruckMaker	Resistance RR
Hub FL	Braking Torque	TruckMaker	Braking FL
	Resistance Torque	TruckMaker	Resistance FL
Hub RL	Braking Torque	TruckMaker	Braking RL
	Resistance Torque	TruckMaker	Resistance RL
TruckMaker	Engine On/Off	IC Engine	Operation Control
	Engine Speed	IC Engine	Engine Speed
	Engine Torque	IC Engine	Behind Flywheel
	Fuel Consumption	IC Engine	Fuel Consumption
	GB Speed In	Gearbox	Input Speed
	GB Act Gear No	Gearbox	Current Gear
	Supp Brake Torque FL	Hub FL	Support Torque
	Supp Brake Torque FR	Hub FR	Support Torque
	Supp Brake Torque RL	Hub Rear Left	Support Torque
	Supp Brake Torque RR	Hub Rear Right	Support Torque
	Drive Torque FL	Differential	Output Torque 1
	Drive Torque FR	Differential	Output Torque 2
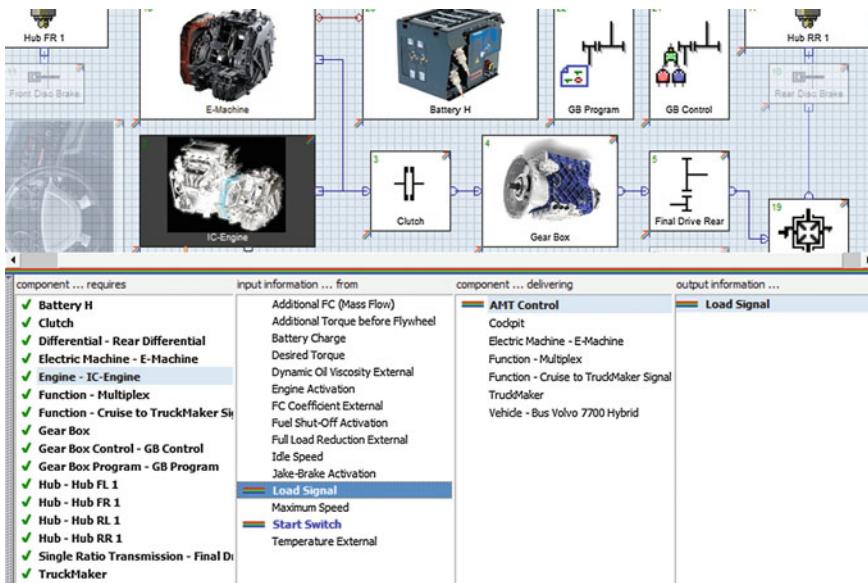
Fig. 7.6 Data Bus Connection for the TruckMaker system (hybrid bus)

In the fourth column (output information) the output channels will become active, channels which can provide information for the selections from the first three columns.

To visualize the data bus connection it is sufficient to place the Mouse cursor over the colored arrow from the left bottom corner of the selected element (the validation of connections marked with bold characters is compulsory for the model to function).

The input channels highlighted with bold in the Data Bus Connection dialog box are essential for the model to function, because it is compulsory to establish a connection between them and their corresponding output channels.

To visualize the Data Bus Connection between the elements of the model, the Mouse will be positioned on the tricolor arrow of the selected element and the informational channels will be nominally highlighted, alongside the corresponding connection.

After creating the connections between the elements of the Data Bus Connection, the three bus models were validated with the Teim-Model Reporter utility from AVL CRUISE (Fig. 7.11), which verifies the model topology and the information regarding the defined initial data [2, 4]. The validation reports of the models built in AVL CRUISE are presented in Figs. 7.12, 7.13 and 7.14.

Table 7.3 Data Bus Connection for the TruckMaker system (electric bus)

Component requires	Input information	Component delivering	Output information
Battery H	**Temperature External**	Cockpit	Course Temperature
E-Machine	**Load Signal**	eDrive CS	Mod Load Signal
	Temperature External	Battery H	Temperature
Consumer	Set Value X	Battery H	Net Voltage
eDrive CS	Max Brake Pressure	Constants	Max Brake Pressure
	Bremsfactor	Constants	Brake Factor
E&M-Brake	eDrive_Torque	E-Machine	Torque
	iFD	Constants	iFD
	iTR	Constants	iTR
	Brake_Factor_Front	Constants	Brake_Factor_Front
	Brake_Factor_Rear	Constants	Brake_Factor_Rear
Hub FR	Braking Torque	TruckMaker	Braking FR
	Resistance Torque	TruckMaker	Resistance FR
Hub RR	Braking Torque	TruckMaker	Braking RR
	Resistance Torque	TruckMaker	Resistance RR
Hub FL	Braking Torque	TruckMaker	Braking FL
	Resistance Torque	TruckMaker	Resistance FL
Hub RL	Braking Torque	TruckMaker	Braking RL
	Resistance Torque	TruckMaker	Resistance RL

Fig. 7.7 Data Bus Connection for the TruckMaker system (electric bus)

Table 7.4 Data Bus Connection for the CRUISE system (classic bus)

Component requires	Input information	Component delivering	Output information
AMT	**Current Gear**	Gearbox	Current Gear
	Desired Gear	GB Control	Desired Gear
	Input Speed	Clutch	Input Speed
	Load Signal	Cockpit	Load Signal
	Output Speed	Clutch	Output Speed
	Velocity	Vehicle	Velocity
Clutch	**Desired Clutch Release**	AMT Control	Desired Clutch
IC Engine	**Load Signal**	AMT Control	Load Signal
	Start Switch	Cockpit	Start Switch
Gearbox	**Desired Gear**	GB Control	Desired Gear
GB Control	**Current Gear**	Gearbox	Current Gear
	Desired Gear (Cockpit)	Cockpit	Desired Gear
	Gear Select Down	Cockpit	Gear Select Down
	Gear Select Up	Cockpit	Gear Select Up
	Operation Control	Cockpit	Operation Control
	Reference Speed	IC Engine	Engine Speed
	Velocity	Cockpit	Velocity
GB Program	**Current Gear**	Gearbox	Current Gear
	Load Signal	Cockpit	Load Signal
	Speed	IC Engine	Engine Speed

Fig. 7.8 Data Bus Connection for the CRUISE system (classic bus)

Table 7.5 Data Bus Connection for the CRUISE system (hybrid bus)

Component requires	Input information	Component delivering	Output information
AMT	**Current Gear**	Gearbox	Current Gear
	Desired Gear	GB Control	Desired Gear
	Input Speed	Clutch	Input Speed
	Load Signal	Cockpit	Load Signal
	Output Speed	Clutch	Output Speed
	Velocity	Vehicle	Velocity
Cockpit	**Gear Indicator**	E-Machine	Operating Mode
	Operation Control 0	E-Machine	Operation Control
	Speed	IC Engine	Engine Speed
Rear Brake	**Brake Pressure**	Multiplex	cockpit_brake_pressure
Front Brake	**Brake Pressure**	Multiplex	cockpit_brake_pressure
Rear Brake	**Brake Pressure**	Multiplex	cockpit_brake_pressure
Front Brake	**Brake Pressure**	Multiplex	cockpit_brake_pressure
Monitor	**Vehicle Acceleration**	Vehicle	Acceleration
	Vehicle Velocity	Vehicle	Velocity
	Vehicle Distance	Vehicle	Distance
	Engine Load Signal	IC Engine	Actual Load Signal
	Engine Speed	IC Engine	Engine Speed

Fig. 7.9 Data Bus Connection for the CRUISE system (hybrid bus)

Table 7.6 Data Bus Connection for the CRUISE system (electric bus)

Component requires	Input information	Component delivering	Output information
ASC	Clutch Release	Cockpit	Course Ambient
	Load Signal	Cockpit	Load Signal
	Slip Signal FL	Wheel FR	Slip Signal
	Slip Signal FR	Wheel FL	Slip Signal
	Slip Signal RL	Wheel FR	Slip Signal
	Slip Signal RR	Wheel FL	Slip Signal
Rear Brake	**Brake Pressure**	E&M-Brake	BRK_dp_Recup
Front Brake	**Brake Pressure**	E&M-Brake	BRK_dp_Recup
Rear Brake	**Brake Pressure**	E&M-Brake	BRK_dp_Recup
Front Brake	**Brake Pressure**	E&M-Brake	BRK_dp_Recup
Cockpit	**Gear Indicator**	E-Machine	Operating Mode
	Operation Control 0	E-Machine	Operation Control
	Speed	E-Machine	Speed
Monitor	LoadSignal_Cockpit	Cockpit	Load Signal
	Velocity	Cockpit	Velocity
	Torque eDrive	E-Machine	Torque
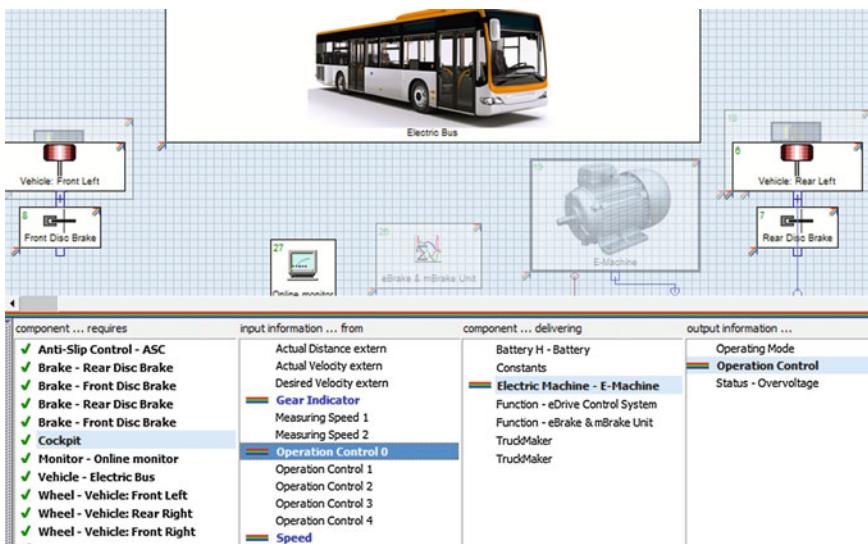
Fig. 7.10 Data Bus Connection for the CRUISE system (electric bus)
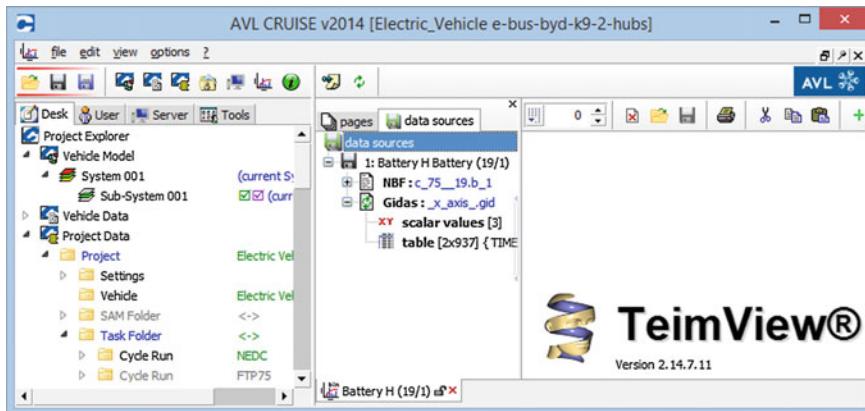
Fig. 7.11 Teim-Model Reporter in AVL CRUISE
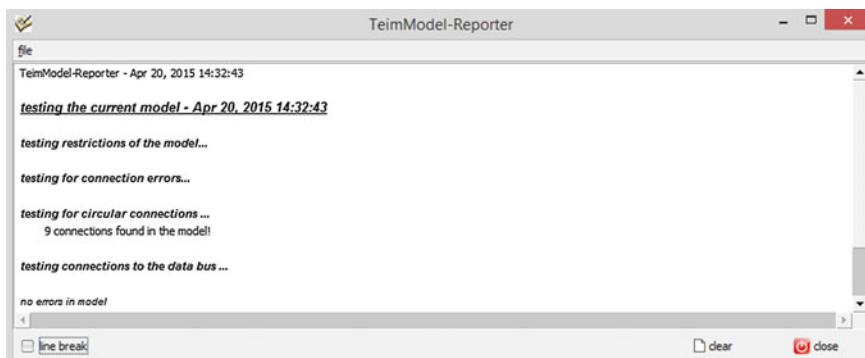
Fig. 7.12 The validation report Teim-Model Reporter for the classic bus
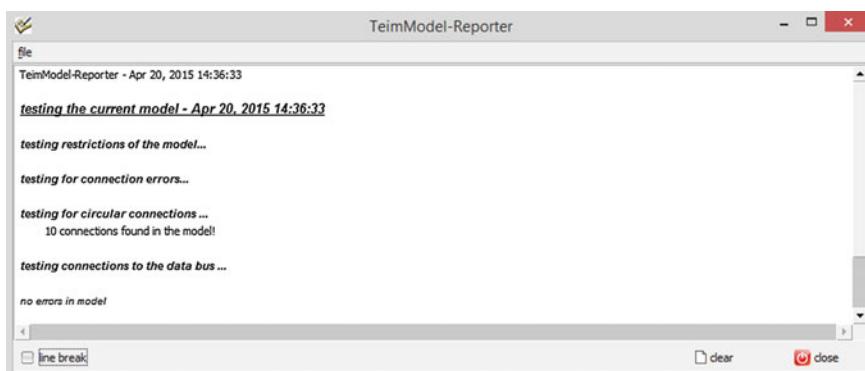
Fig. 7.13 The validation report Teim-Model Reporter for the hybrid bus
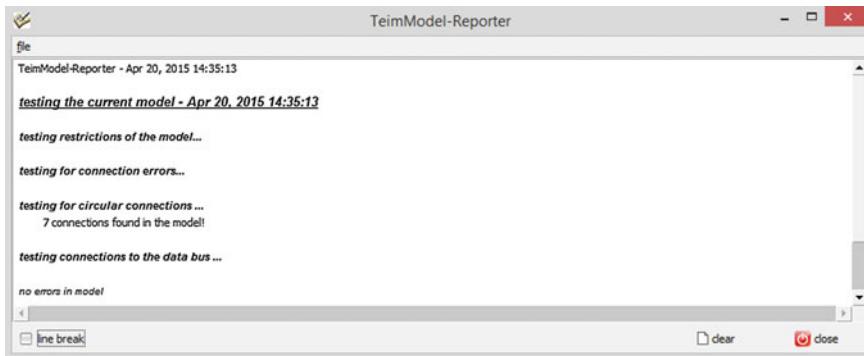
Fig. 7.14 The validation report Teim-Model Reporter for the electric bus

7.2   Computer Simulation for the Developed Models

The model with the co-simulation interface defined in AVL CRUISE of the drive system was loaded in IPG TruckMaker to equip the bus model simulated in this simulation environment. In order to monitor the energy flow the Energy Flow Graphics utility was used, where the data sets resulted from the co-simulation process were loaded (Fig. 7.15).
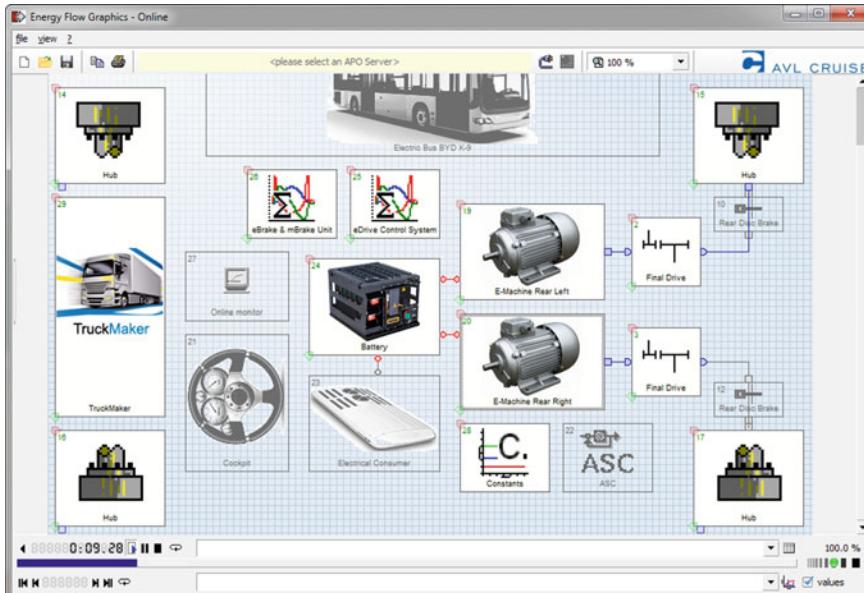
Fig. 7.15 The energy flow—Energy Flow Graphics
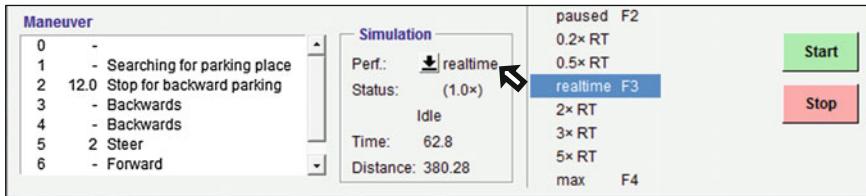
Fig. 7.16 Establishing the running speed for the computer simulation period

Fig. 7.17 Collecting the computer simulations results

To run the simulation, first the model must be connected with AVL CRUISE, (connection with the desired model must be checked), and then the road must be loaded, with the desired maneuvers.

After defining the virtual model, the simulation process can be configured from the Simulation dialog box, from where the running speed of the simulations is set having as reference RT (Real Time).

The configuration options are: paused F2, 0.2 * RT, 0.5 * RT, real time F3, 2 * RT, 3 * RT, 5 * RT, respectively maximum (max) F4 (Fig. 7.16).

The unfolding of the computer simulation process is made from the Start button and it can be stopped at any time with the Stop button. The results obtained from the computer simulations are saved in a buffer memory allocated by the application, which is managed from the GUI interface of the IPG TruckMaker application (Fig. 7.17) [5].

In order to save and archive the results obtained from the computer simulations, the following options are available [5, 6]:

- Collect Only, the results are temporarily stocked in a buffer memory, without being physically saved on the memory of the computer;
- Save All, all the results are physically saved continuously and automatically on the memory;
- History, the results are temporarily stocked on the buffer memory for a selected period of time.

In the Data Storage dialog box there is the possibility of setting the parameters to be saved after the simulation process (Fig. 7.18).
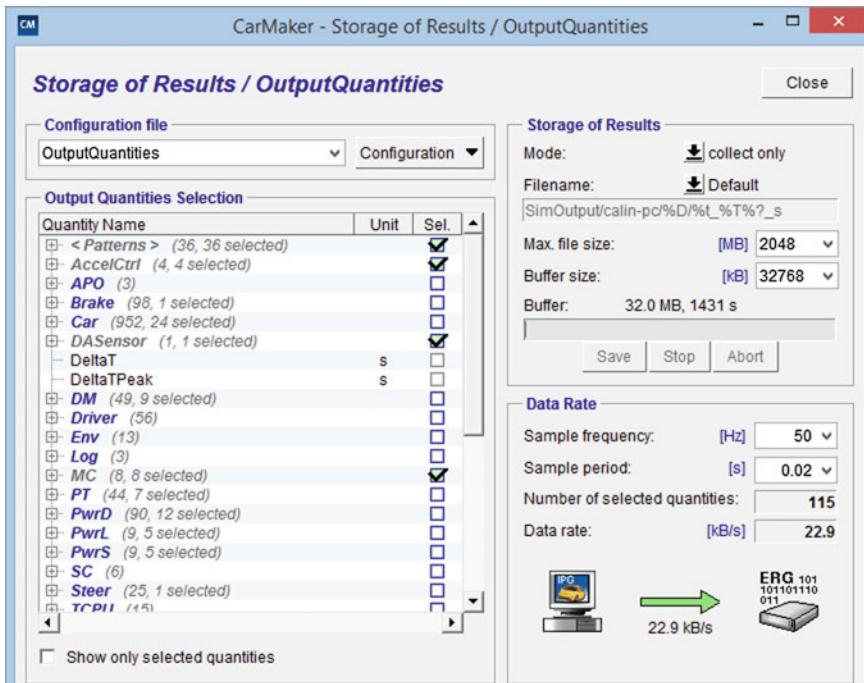
Fig. 7.18 Stocking the results of the simulations Data Storage

The post-processing of the computer simulations results can be made by using the following applications: IPG Control and AVL CONCERTO™. The export of the selected results is made using the Export to File command, which opens a dialog box which allows the selection of the format in which the data will be exported, respectively the systems of measurement units.

IPG Control is an instrument which allows to visualize the selected results in real time, to save the files containing the post-simulations data and which facilitates the analysis and interpretation of the results via an online management process with the simulation process. The data flows are provided in real time, which allows the display and visualization of the diagrams for the selected parameters directly during the simulation process (Fig. 7.19).

After pressing the start button, the simulation starts. In the IPG Control data window, the user can monitor any parameters by selecting them from the quantities tab. For the electric model the four main monitored properties are: the Current [A], the Voltage [V], Energy [kJ], and Energy Stored [kJ].

By exporting the Current [A], the Voltage [V], Energy [kJ] and Energy Stored [kJ], the user can analyze the state of the battery, the recovered energy either versus elapsed time, or by the track. Basically, the user can conclude which is the optimal track for recovered energy or underline the optimal range.
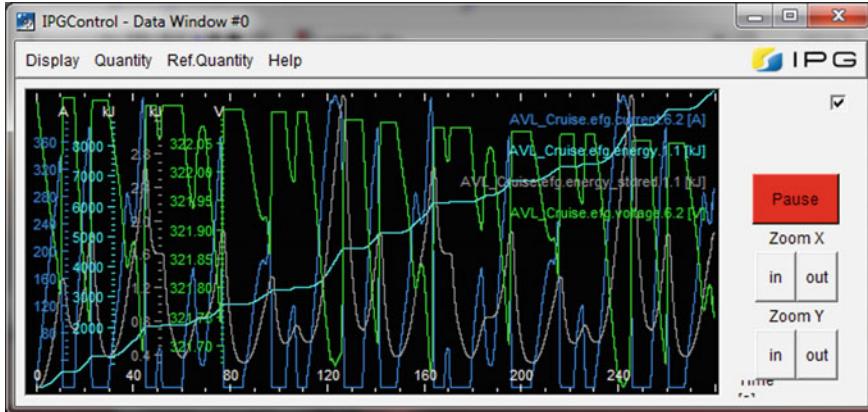
Fig. 7.19   Post-processing the results with the IPG Control application

The bus routes selected for making the computer simulations which were implemented in the IPGRoad (Fig. 7.20) are the following: 27, 28, 30 and 32 [2].

The virtual roads used in computerized and parameterized simulations using the AVL Road Importer application have been digitized in formats compatible with the applications used for computer simulations (.WAY for AVL CRUISE, respectively.BIN for IPGRoad), and these roads have been implemented in the IPG TruckMaker application in order to define some real traffic conditions, namely: atmospheric conditions, roads geometries, routes particularities, road particularities, respectively particularities of adjacent areas (Fig. 7.21a–d).
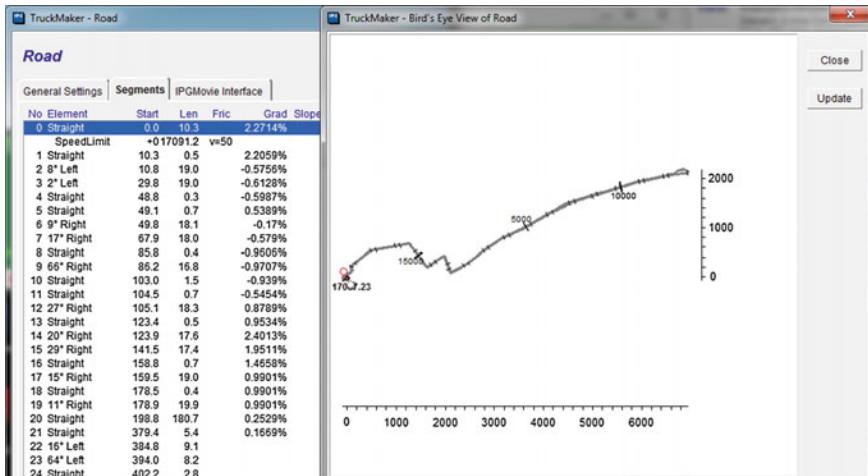
Fig. 7.20   The selected bus routes IPGRoad

Fig. 7.21 Virtual road for the bus routes in IPGRoad application: **a** route 27, **b** route 28, **c** route 30 and **d** route 32
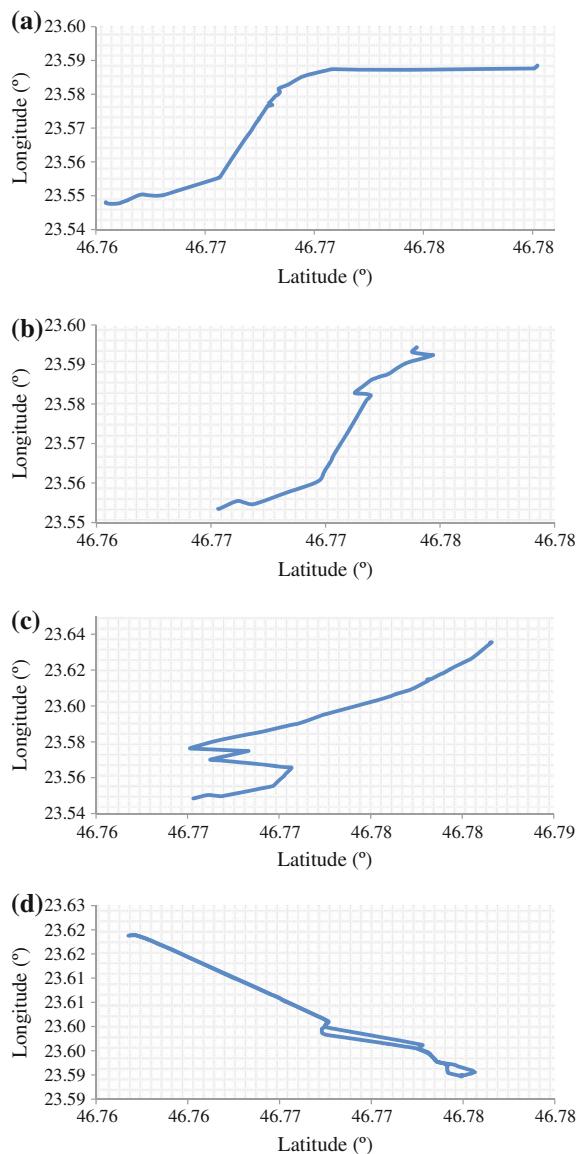
The CRUISE—TruckMaker co-simulation process was made starting from the initial characteristics of the bus models developed in the AVL CRUISE application, on the established routes (Table 7.7) [2]

In order to reach the main objectives established in the research project, certain constructive parameters have been modified, namely the charge capacity of the batteries of the hybrid and electric bus, respectively the supplementary passengers loading capacity of the buses over their own mass.

Table 7.7 Technical characteristics of the simulated bus models [2]

Simulation	Description	U.M.	Classic	Hybrid	Electric
Step I of the simulation Partial charge	Maximum velocity in Cluj-Napoca	km/h	40.0	40.0	40.0
	Medium velocity in Cluj-Napoca	km/h	13.2	13.2	13.2
	Energy consumption	kWh/km	–	0.15	1.2
	Fuel consumption	l/km	34	26	–
	Tires specifications	–	275/70 R22.5	275/70 R22.5	275/70 R22.5
	Capacity of batteries	Ah	–	200	600
	IC Engine power	kW	210	150	–
	IC Engine torque	Nm	1080	800	–
	Electric motor power	kW	–	120	150
	Electric motor torque	Nm	–	800	700
	CO emissions	g/kWh	1.50	1.50	0 local
	NO_x emissions	g/kWh	2.00	0.40	0 local
	HC emissions	g/kWh	0.46	0.13	0 local
	Partial charge	kg	13,150	15,450	16,250
	Full charge	kg	14,300	17,900	18,000
Step II of the simulation Full charge	Maximum velocity in Cluj-Napoca	km/h	40.0	40.0	40.0
	Medium velocity in Cluj-Napoca	km/h	13.2	13.2	13.2
	Energy consumption	kW/km	–	0.15	1.2
	Fuel consumption	l/km	34	26	–
	Tires specifications	–	275/70 R22.5	275/70 R22.5	275/70 R22.5
	Capacity of batteries	Ah	–	100	300
	IC Engine power	kW	210	150	–
	IC Engine torque	Nm	1080	800	–
	Electric motor power	kW	–	120	150
	Electric motor torque	Nm	–	800	700
	CO emissions	g/kWh	1.50	1.50	0 local
	NO_x emissions	g/kWh	2.00	0.40	0 local
	HC emissions	g/kWh	0.46	0.13	0 local
	Partial charge	kg	13,150	15,450	16,250
	Full charge	kg	14,300	17,900	18,000

The methodology of the simulation process for making the determinations used within the researches regarding the estimation of the energy consumption for the hybrid and electric drive systems and their comparison to the classic drive system is presented in Fig. 7.22.
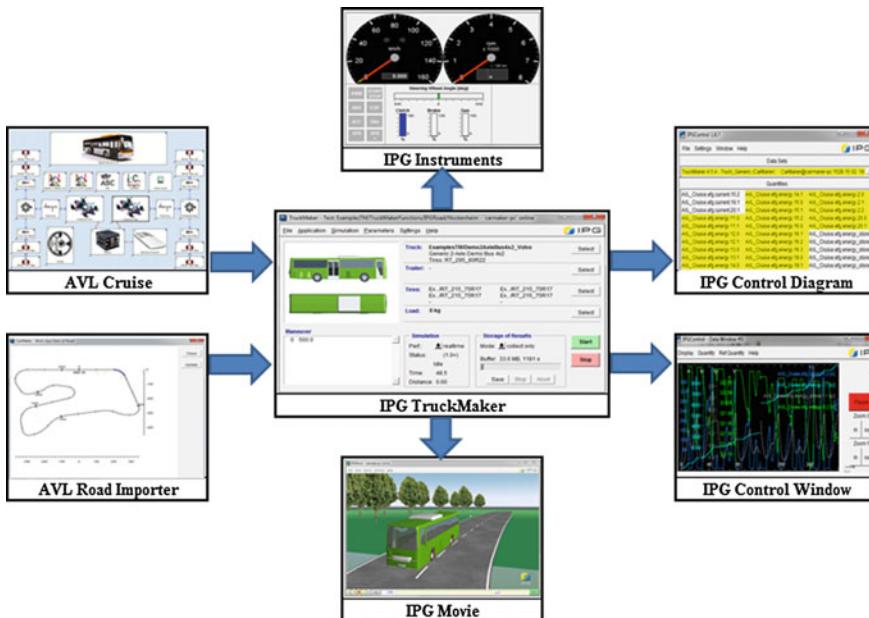
Fig. 7.22 Methodology of the simulation process

In order to evaluate the functioning of the vehicles from the point of view of energetic consumption, many analysis methods are used amongst which the average operating point method, the quasi-static method and the dynamic modelling. In this step, first are evaluated the model requirements and restrictions, and then the system components are designed.

The computer simulation is a methodology used for optimizing vehicles performances, and the computer simulation instruments are also used by vehicle manufacturers to reduce the production costs of prototypes and the time necessary for designing a prototype [2].

7.3   Evaluation of the Energetic Efficiency of the Simulated Drive Systems

After running the computer simulations on the models developed in the AVL CRUISE, IPG TruckMaker applications, respectively in the CRUISE—TruckMaker co-simulation application, the validation of the established routes was followed to assure a maximum autonomy by recovering kinetic energy and through a dosed energetic consumption corresponding according to an optimal established route.

At the same time, it was taken into account the evaluation of pollutant emissions and of CO_2 emissions by simulating some real routes for the buses used for urban passenger transport.

The energy consumption is influenced by a series of factors, namely the increase of total mass, the consumption generated by auxiliary systems which determines a significant increase in the energy consumed by the batteries, some of these factors depending on the traveled distance.

At the same time, the track configuration can influence the electric energy consumption by rising up on acceleration periods or while climbing slides and by lowering down while descending slopes or while decelerating, because it can reach negative values (the energy is transferred from the electric motor towards the battery).

The distribution of the operating time for each simulated route throughout the efficiency maps corresponding to the fuel consumption according to torque is presented in Fig. 7.23a–d—Driving Time Distribution, Fig. 7.24a–d—Portion of Fuel Consumption for the classic bus, respectively in Fig. 7.25a–d—Driving Time Distribution, Fig. 7.26a–d—Portion of Fuel Consumption for the hybrid bus.

The static distribution of the operating regimes is presented in Fig. 7.27a–d—Abundance, Fig. 7.28a–d—Condensation for the classic bus, respectively in Fig. 7.29a–d—Abundance, Fig. 7.30a–d—Condensation for the hybrid bus.

By comparing the graphics for the operating regimes statistic and for the operating time distribution it can be noted that the thermal engine runs in a higher efficiency regime for the hybrid bus and in a lower efficiency regime for the classic bus.

The mechanical power generated by the classic bus is presented in Fig. 7.31a–d, the mechanical power generated by the hybrid bus is presented in Fig. 7.32a–d, the electric power generated by the hybrid bus is presented in Fig. 7.33a–d, respectively the electric power generated by the electric bus is presented in Fig. 7.34a–d.

Thermal engine torque generated by the classic bus is presented in Fig. 7.35a–d, thermal engine torque generated by the hybrid bus is presented in Fig. 7.36a–d, electric motor torque generated by the hybrid bus is presented in Fig. 7.37a–d, respectively the electric motor torque generated by the electric bus is presented in Fig. 7.38a–d.

Because the engine speed is directly proportional to the velocity established for the traveled route and because the hybrid bus is powered by a thermal engine and an electric motor, the torque for the hybrid bus is smaller thus resulting a reduced fuel consumption.

During acceleration periods the electric motor torque is positive and it helps to propel the hybrid and electric bus, and during deceleration periods the electric motor torque is negative and it creates the conversion of mechanical energy into electric energy and it charges the batteries.
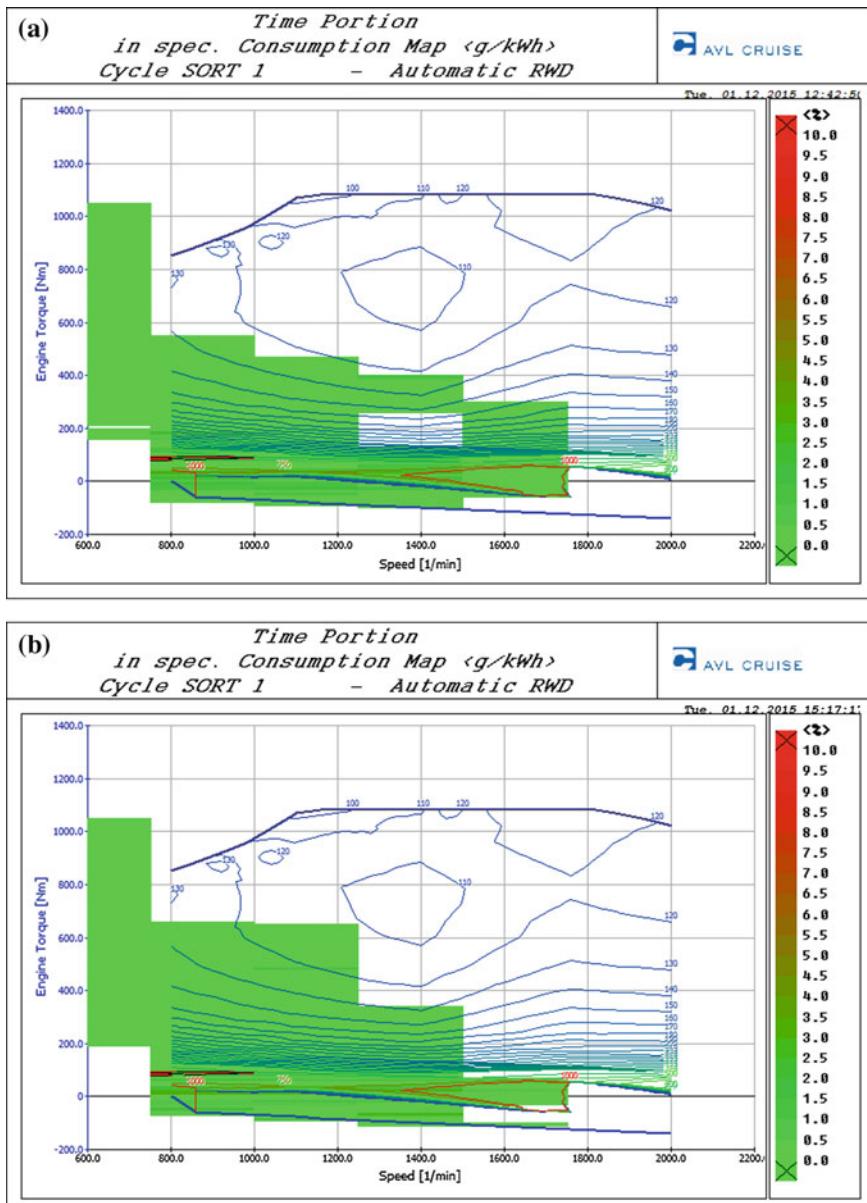
Fig. 7.23 Driving Time Distribution for the classic bus: **a** route 27, **b** route 28, **c** route 30 and **d** route 32
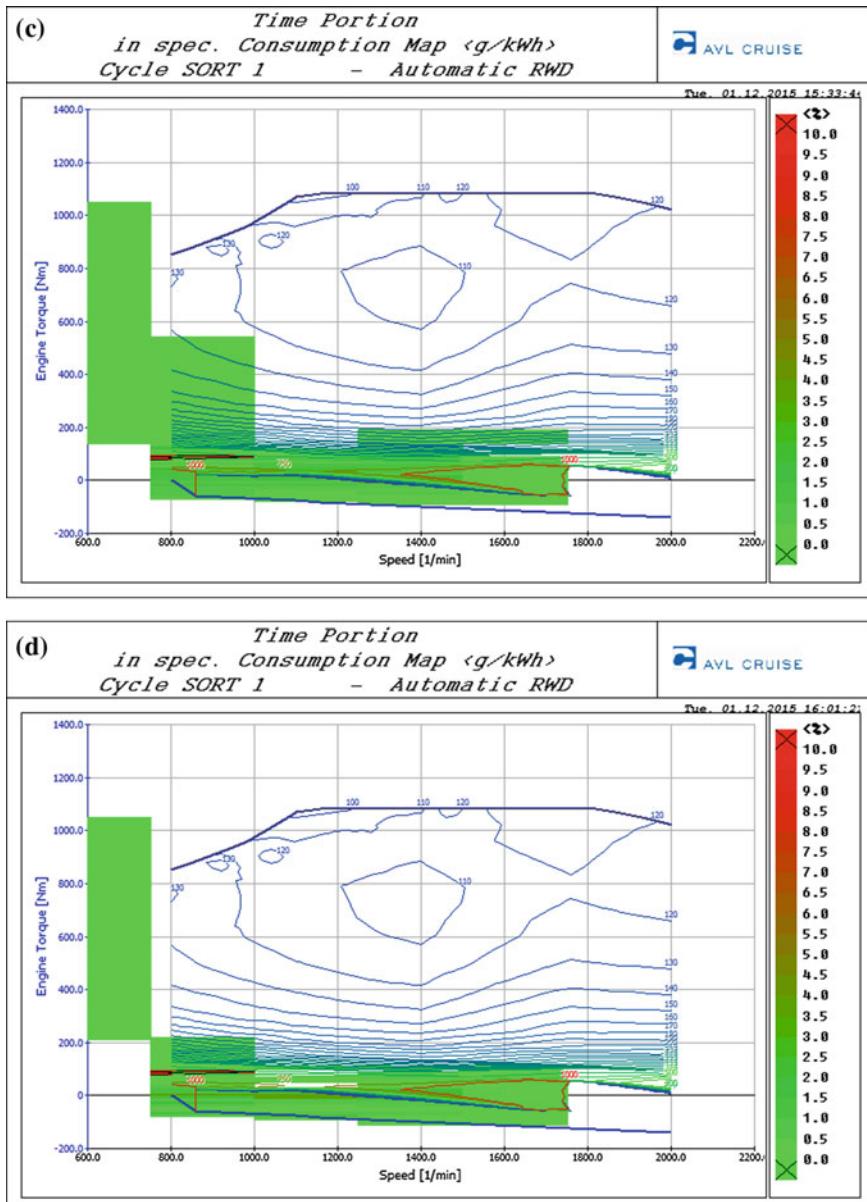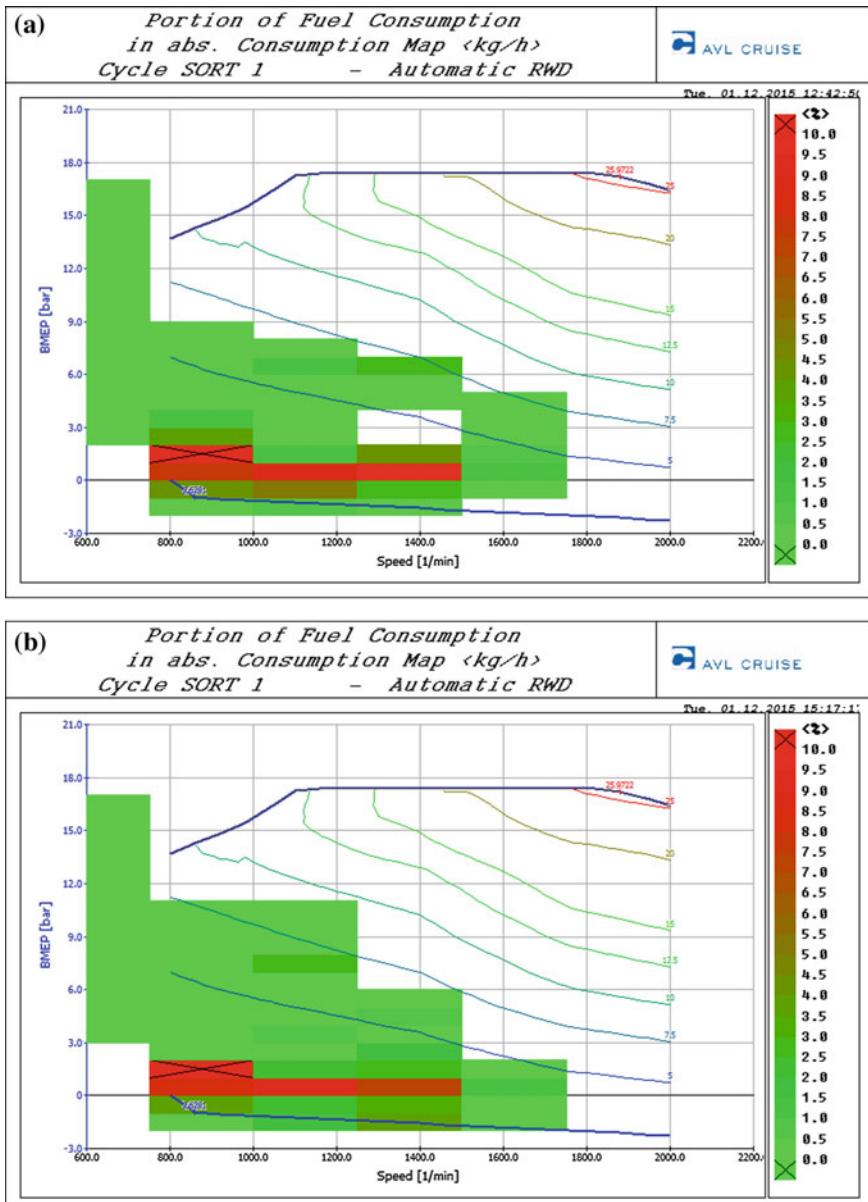
Fig. 7.23 (continued)

Fig. 7.24 Portion of fuel consumption for the classic bus: **a** route 27, **b** route 28, **c** route 30 and **d** route 32
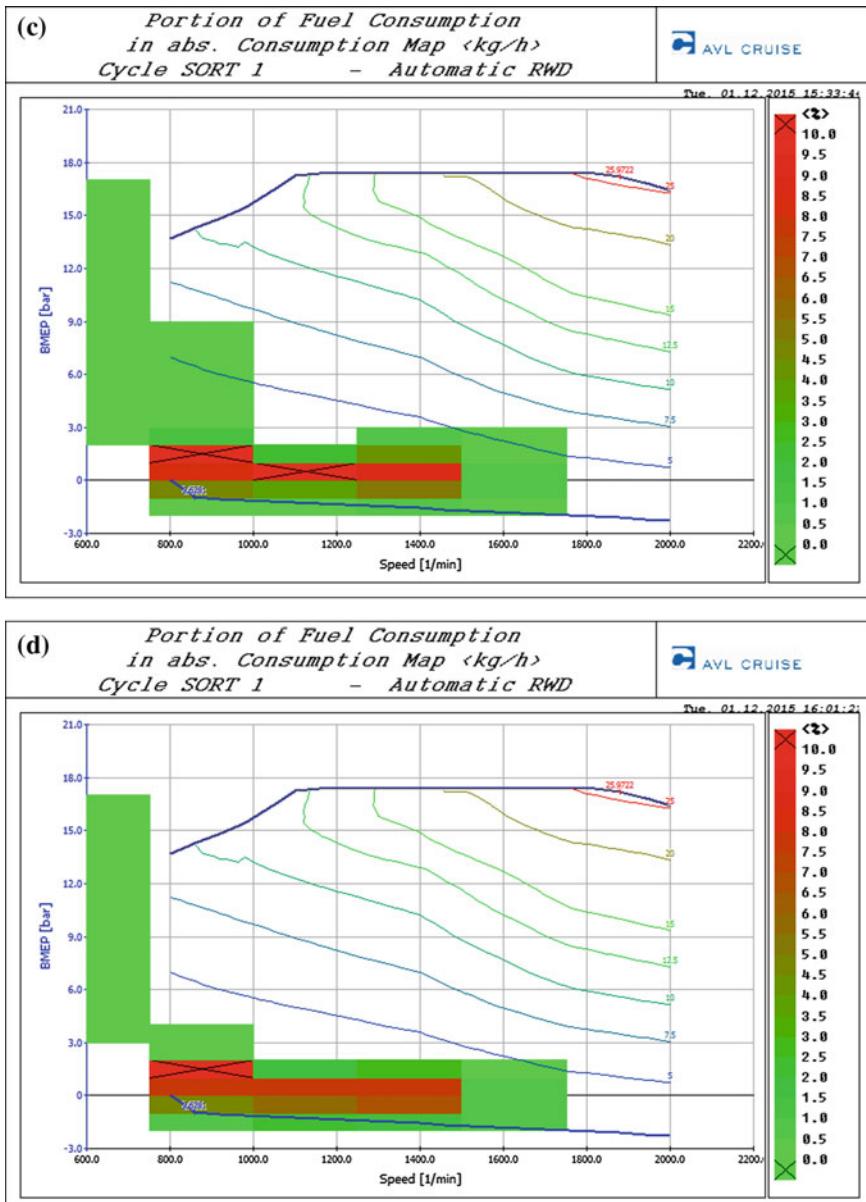
Fig. 7.24 (continued)
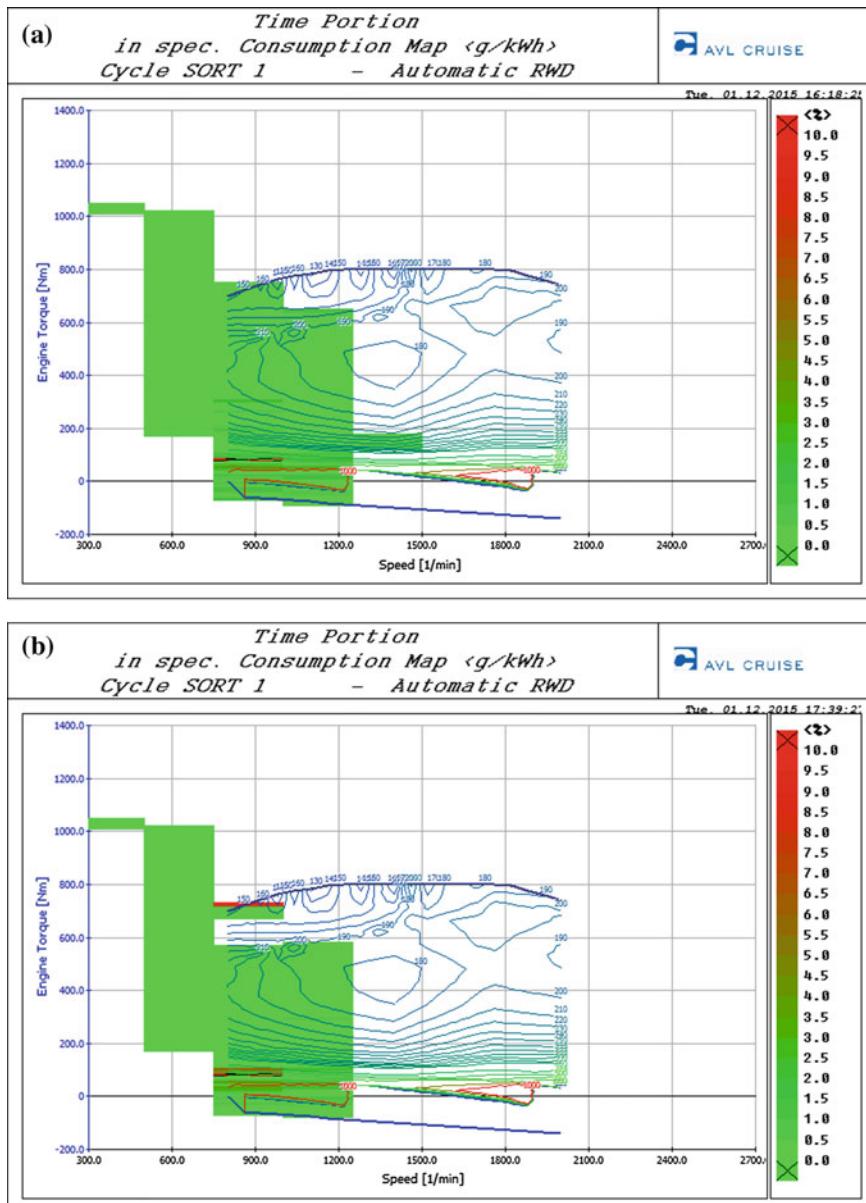
Fig. 7.25 Driving time distribution for the hybrid bus: **a** route 27, **b** route 28, **c** route 30 and **d** route 32
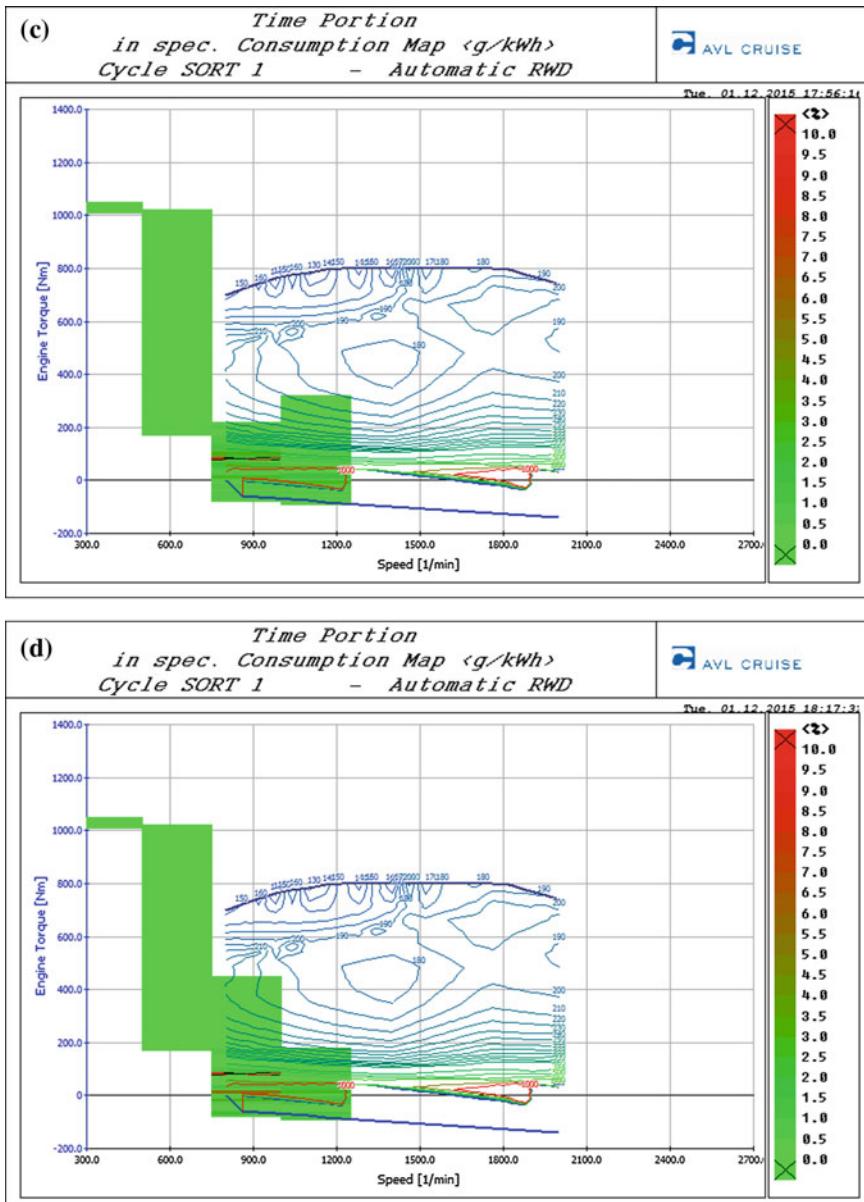
Fig. 7.25 (continued)
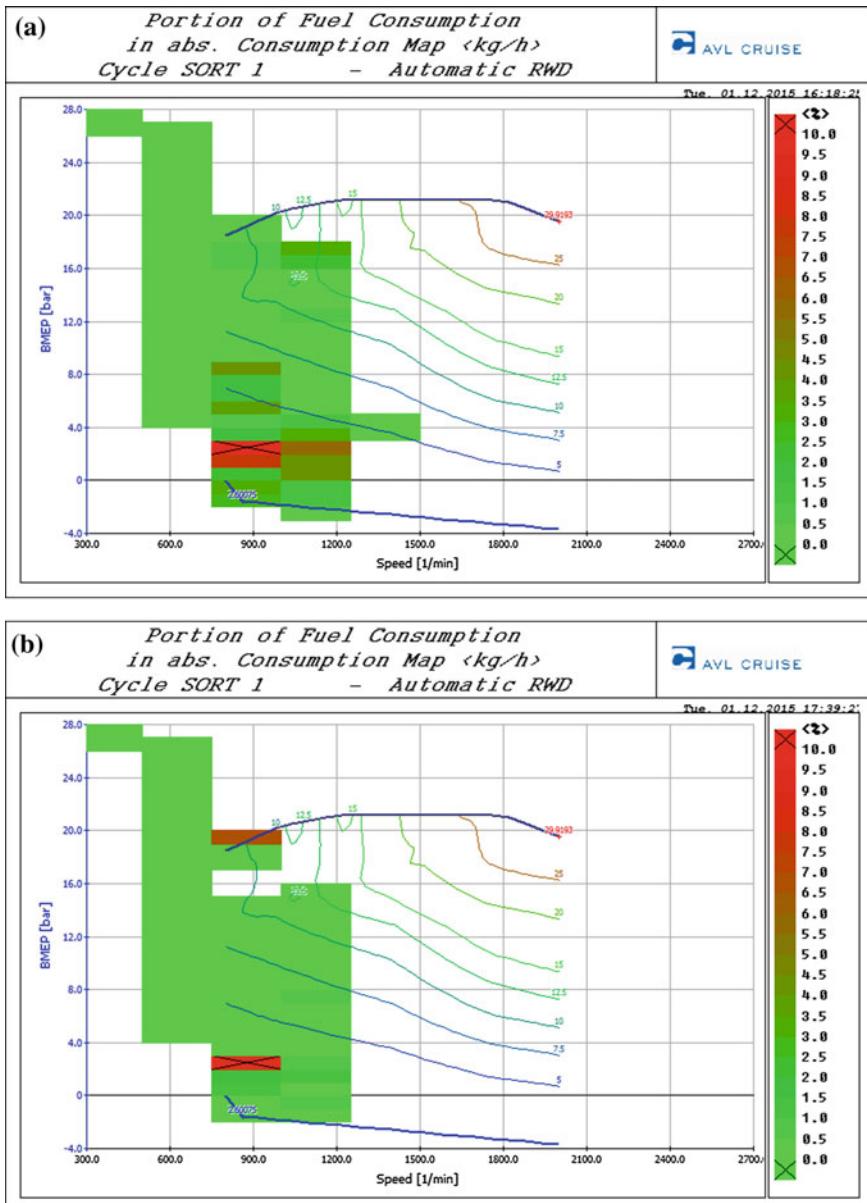
Fig. 7.26 Portion of fuel consumption for the hybrid bus: **a** route 27, **b** route 28, **c** route 30 and **d** route 32

Fig. 7.26 (continued)

(a)

SORT 1
Automatic RWD

AVL CRUISE

Tue. 01.12.2015 12:4.

CHARACTERISTIC DATA
Curb Weight   <kg>: 12080.0
Vehicle Mass   <kg>: 14300.0
Frontal Area   <m2>:   7.500
Drag Coefficient   <->:   0.520
Displacement   <l>:   7.800
Number of Cylinders   <->:   6
stat. Rolling Radius   <mm>:   436.0
dyn. Rolling Radius   <mm>:   464.0
Calculation Mode   : Simulation 2
Slip   : Off

Fig. 7.27 Abundance—classic bus: **a** route 27, **b** route 28, **c** route 30 and **d** route 32

(b)

SORT 1
Automatic RWD

AVL CRUISE

Tue. 01.12.2015 15:1

CHARACTERISTIC DATA
Curb Weight   <kg>: 12080.0
Vehicle Mass   <kg>: 14300.0
Frontal Area   <m2>:   7.500
Drag Coefficient   <->:   0.520
Displacement   <l>:   7.800
Number of Cylinders   <->:   6
stat. Rolling Radius   <mm>:   436.0
dyn. Rolling Radius   <mm>:   464.0
Calculation Mode   : Simulation 2
Slip   : Off

Fig. 7.27 (continued)

Fig. 7.27 (continued)

(d)

SORT 1
Automatic RWD

AVL CRUISE

Tue. 01.12.2015 16:0

CHARACTERISTIC DATA
Curb Weight   <kg>: 12080.0
Vehicle Mass   <kg>: 14300.0
Frontal Area   <m2>:   7.500
Drag Coefficient   <->:   0.520
Displacement   <l>:   7.800
Number of Cylinders   <->:   6
stat. Rolling Radius   <mm>:   436.0
dyn. Rolling Radius   <mm>:   464.0
Calculation Mode   : Simulation 2
Slip   : Off

Fig. 7.27 (continued)

(a)

SORT 1
Automatic RWD
Tue, 01.12.2015 12:42:50

AVL CRUISE

CHARACTERISTIC DATA		
Curb Weight	<kg>:	12080.0
Vehicle Mass	<kg>:	14300.0
Frontal Area	<m2>:	7.500
Drag Coefficient	<->:	0.520
Displacement	<l>:	7.800
Number of Cylinders <->:		6
Number of Strokes	<->:	4
stat. Roll. Radius <mm>:		436.0
dyn. Roll. Radius <mm>:		464.0
Calculation Mode: Simulation 2		
Slip	: Off	

Speed	Torque	Abund.	Abund.
[1/min]	[Nm]	[%]	[s]
875.0	89.15	48.63	1113.63
1125.0	31.68	8.5	194.66
875.0	27.72	8.04	184.06
1375.0	35.09	7.23	165.66
1125.0	-31.56	6.35	145.33
875.0	-21.32	4.75	108.86
874.78	171.56	4.05	92.69
1375.0	-17.5	3.95	90.53
1375.0	80.5	3.74	85.55
1375.0	380.71	1.45	33.23
1625.0	13.02	1.27	29.11
1125.0	105.6	1.03	23.57
1124.35	395.56	0.51	11.68
1625.0	126.15	0.5	11.42

Fig. 7.28 Condensation—classic bus: **a** route 27, **b** route 28, **c** route 30 and **d** route 32

(b)

SORT 1
Automatic RWD
Tue, 01.12.2015 15:17:17

AVL CRUISE

CHARACTERISTIC DATA		
Curb Weight	<kg>:	12080.0
Vehicle Mass	<kg>:	14300.0
Frontal Area	<m2>:	7.500
Drag Coefficient	<->:	0.520
Displacement	<l>:	7.800
Number of Cylinders <->:		6
Number of Strokes	<->:	4
stat. Roll. Radius <mm>:		436.0
dyn. Roll. Radius <mm>:		464.0
Calculation Mode: Simulation 2		
Slip	: Off	

Speed	Torque	Abund.	Abund.
[1/min]	[Nm]	[%]	[s]
874.97	86.84	53.6	961.55
1375.0	38.41	8.43	151.26
875.0	22.0	8.25	147.93
1125.0	10.71	7.9	141.66
1125.0	48.33	4.82	86.39
1375.0	-71.58	3.94	70.67
875.0	-37.28	3.7	66.37
1375.0	-12.77	2.56	45.93
1125.0	-79.5	2.0	35.92
1375.0	194.95	1.44	25.88
1625.0	27.81	1.35	24.22
1119.76	487.14	1.25	22.44
1125.0	233.62	0.4	7.2
1625.0	-105.0	0.37	6.56

Fig. 7.28 (continued)

(c)   SORT 1
                                Automatic RWD
                         Tue, 01.12.2015 15:33:44   AVL CRUISE

CHARACTERISTIC DATA			Speed	Torque	Abund.	Abund.
			[1/min]	[Nm]	[%]	[s]
Curb Weight	<kg>:	12080.0	875.0	87.66	49.06	1920.68
Vehicle Mass	<kg>:	14300.0	1375.0	3.9	7.57	296.44
Frontal Area	<m2>:	7.500	1125.0	49.81	7.24	283.59
Drag Coefficient	<->:	0.520	1125.0	11.07	5.85	229.22
Displacement	<l>:	7.800	875.0	12.42	4.69	183.45
Number of Cylinders	<->:	6	875.0	-35.63	4.5	176.14
Number of Strokes	<->:	4	875.0	45.84	4.43	173.57
stat. Roll. Radius	<mm>:	436.0	1375.0	50.72	4.4	172.2
dyn. Roll. Radius	<mm>:	464.0	1125.0	-33.88	3.27	127.89
Calculation Mode: Simulation 2			874.8	117.78	2.83	110.81
Slip	: Off		1375.0	104.79	2.29	89.62
			1375.0	-44.59	2.14	83.92
			1625.0	-8.06	1.32	51.64
			1625.0	104.34	0.4	15.85

Fig. 7.28 (continued)

(d)

SORT 1
Automatic RVD
Tue, 01.12.2015 16:01:21

AVL CRUISE

CHARACTERISTIC DATA

Curb Weight	<kg>:	12080.0
Vehicle Mass	<kg>:	14300.0
Frontal Area	<m2>:	7.500
Drag Coefficient	<->:	0.520
Displacement	<l>:	7.800
Number of Cylinders <->:		6
Number of Strokes <->:		4
stat. Roll. Radius <mm>:		436.0
dyn. Roll. Radius <mm>:		464.0
Calculation Mode: Simulation 2		
Slip	: Off	

Speed	Torque	Abund.	Abund.
[1/min]	[Nm]	[%]	[s]
875.0	84.55	39.6	588.88
874.92	95.54	12.97	192.94
875.0	10.44	8.85	131.62
1125.0	11.26	6.61	98.29
1375.0	14.78	6.34	94.25
1375.0	-14.55	5.63	83.68
1125.0	-10.25	5.28	78.56
875.0	-39.01	4.11	61.14
1125.0	-69.92	2.65	39.43
1375.0	86.74	2.23	33.15
1375.0	-71.59	2.14	31.9
1125.0	89.49	1.85	27.52
1625.0	-59.14	0.92	13.72
1625.0	49.76	0.8	11.93

Fig. 7.28 (continued)

(a)

SORT 1
Automatic RWD

AVL CRUISE

Tue. 01.12.2015 16:1

```
CHARACTERISTIC DATA
Curb Weight           <kg>: 12000.0
Vehicle Mass          <kg>: 18900.0
Frontal Area          <m2>:    7.500
Drag Coefficient      <->:     0.520
Displacement          <l>:     4.760
Number of Cylinders   <->:     4
stat. Rolling Radius  <mm>:   436.0
dyn.  Rolling Radius  <mm>:   464.0
Calculation Mode       : Simulation 2
Slip                   : Off
```


Fig. 7.29 Abundance—hybrid bus: **a** route 27, **b** route 28, **c** route 30 and **d** route 32

Fig. 7.29 (continued)

Fig. 7.29 (continued)

Fig. 7.29 (continued)

Fig. 7.30 Condensation—hybrid bus: **a** route 27, **b** route 28, **c** route 30 and **d** route 32

(b)
SORT 1
Automatic RWD
Tue, 01.12.2015 17:39:27

AVL CRUISE

CHARACTERISTIC DATA		
Curb Weight	<kg>:	12000.0
Vehicle Mass	<kg>:	18900.0
Frontal Area	<m2>:	7.500
Drag Coefficient	<->:	0.520
Displacement	<l>:	4.760
Number of Cylinders <->:		4
Number of Strokes <->:		4
stat. Roll. Radius <mm>:		436.0
dyn. Roll. Radius <mm>:		464.0
Calculation Mode: Simulation 2		
Slip : Off		

Speed	Torque	Abund.	Abund.
[1/min]	[Nm]	[%]	[s]
875.0	84.97	54.51	977.88
875.0	102.04	9.18	164.64
875.0	724.6	9.11	163.37
1125.0	46.44	7.11	127.53
875.0	28.85	6.03	108.14
875.0	55.81	3.85	69.11
1125.0	-13.09	2.77	49.61
1125.0	105.91	2.42	43.38
875.0	-26.1	2.39	42.95
1125.0	290.68	1.09	19.47
1125.0	-67.95	0.64	11.4
874.43	172.94	0.49	8.77
1125.0	429.04	0.33	5.97
624.73	679.32	0.1	1.78

Fig. 7.30 (continued)

(c)

SORT 1
Automatic RWD
Tue, 01.12.2015 17:56:16

AVL CRUISE

CHARACTERISTIC DATA		
Curb Weight	<kg>:	12000.0
Vehicle Mass	<kg>:	18900.0
Frontal Area	<m2>:	7.500
Drag Coefficient	<->:	0.520
Displacement	<l>:	4.760
Number of Cylinders <->:		4
Number of Strokes	<->:	4
stat. Roll. Radius <mm>:		436.0
dyn. Roll. Radius <mm>:		464.0
Calculation Mode: Simulation 2		
Slip	: Off	

Speed	Torque	Abund.	Abund.
[1/min]	[Nm]	[%]	[s]
875.0	85.3	57.26	2241.73
875.0	16.97	5.67	221.85
875.0	111.4	5.32	208.31
875.0	57.84	4.4	172.26
1125.0	-7.0	4.27	167.19
875.0	149.77	3.77	147.46
1125.0	20.34	3.65	143.0
875.0	-39.0	3.42	133.89
1125.0	98.28	2.69	105.43
1125.0	-60.24	2.52	98.82
1125.0	61.05	2.5	97.71
1125.0	149.49	2.04	79.76
874.73	202.73	2.0	78.22
1125.0	273.29	0.49	19.36

Fig. 7.30 (continued)

(d)

SORT 1
Automatic RWD
Tue, 01.12.2015 18:17:31

AVL CRUISE

CHARACTERISTIC DATA		
Curb Weight	<kg>:	12000.0
Vehicle Mass	<kg>:	18900.0
Frontal Area	<m2>:	7.500
Drag Coefficient	<->:	0.520
Displacement	<l>:	4.760
Number of Cylinders <->:		4
Number of Strokes <->:		4
stat. Roll. Radius <mm>:		436.0
dyn. Roll. Radius <mm>:		464.0
Calculation Mode: Simulation 2		
Slip	: Off	

Speed	Torque	Abund.	Abund.
[1/min]	[Nm]	[%]	[s]
875.0	84.89	62.1	923.37
875.0	14.94	6.16	91.62
875.0	-17.2	5.15	76.64
1125.0	-17.27	4.92	73.22
1125.0	18.26	4.43	65.81
1125.0	-73.75	3.87	57.55
875.0	-62.32	2.59	38.47
1125.0	40.64	2.2	32.66
875.0	166.21	2.14	31.88
875.0	100.84	1.88	27.97
875.0	39.29	1.87	27.86
1125.0	174.86	1.35	20.04
1125.0	111.63	1.33	19.82
619.17	506.2	0.01	0.08

Fig. 7.30 (continued)

Fig. 7.31 Mechanical power generated by the classic bus: **a** route 27, **b** route 28, **c** route 30 and **d** route 32

Fig. 7.31 (continued)

Fig. 7.32 Mechanical power generated by the hybrid bus: **a** route 27, **b** route 28, **c** route 30 and **d** route 32
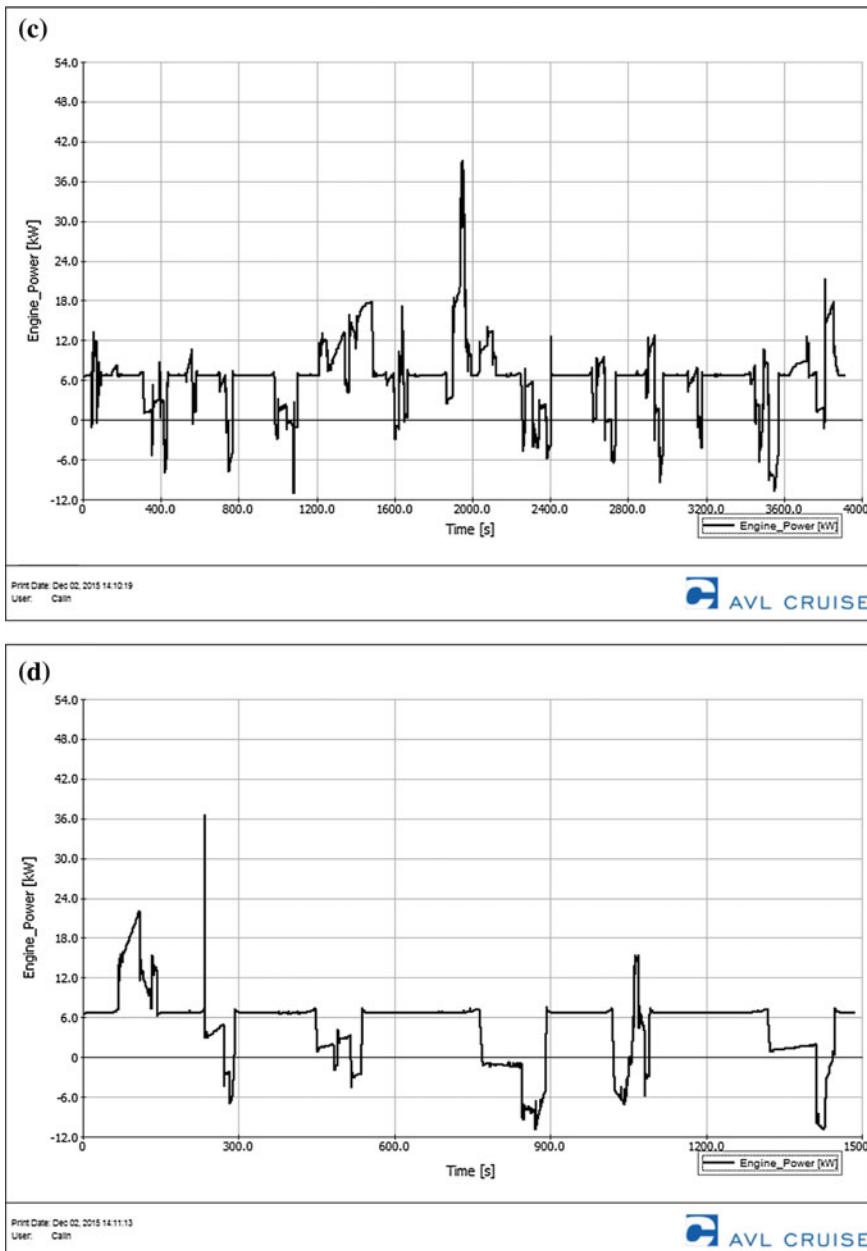
Fig. 7.32 (continued)
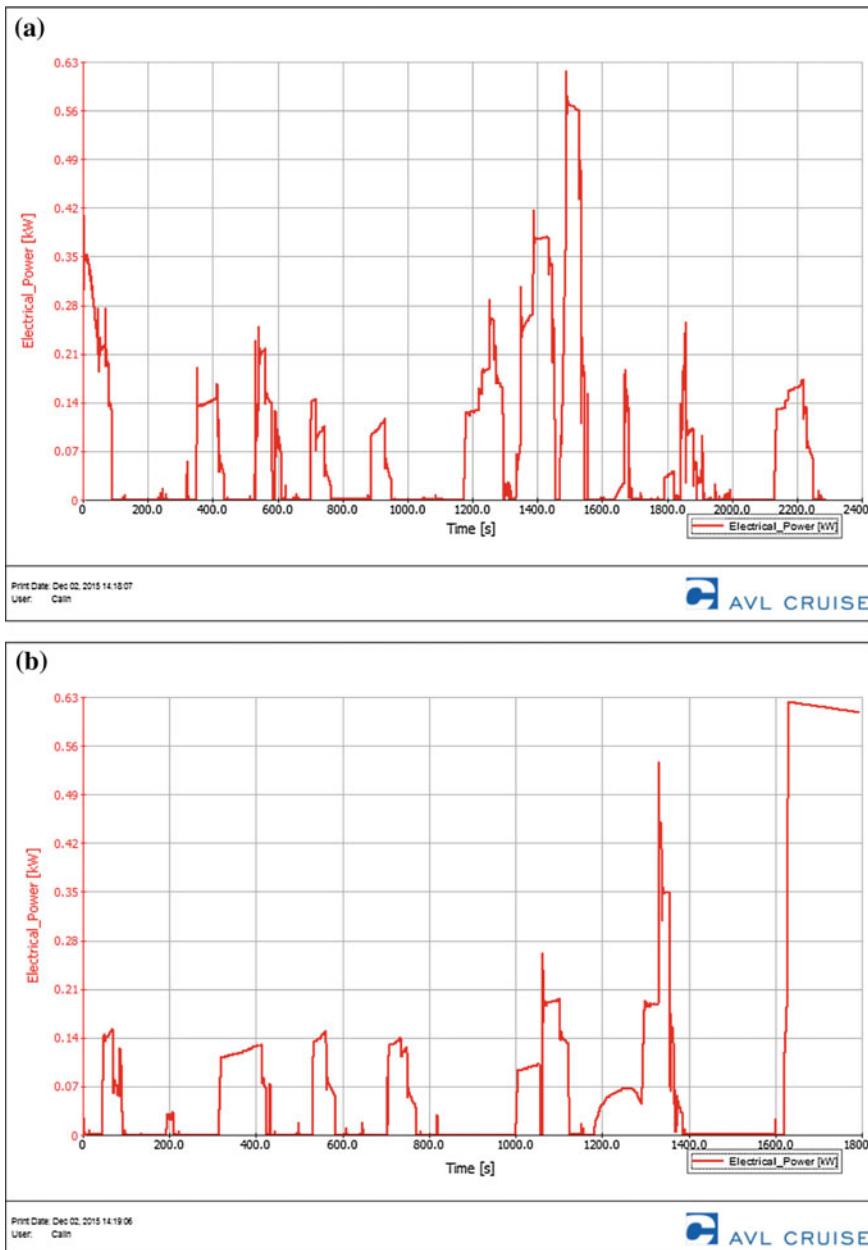
Fig. 7.33 Electric power generated by the hybrid bus: **a** route 27, **b** route 28, **c** route 30 and **d** route 32
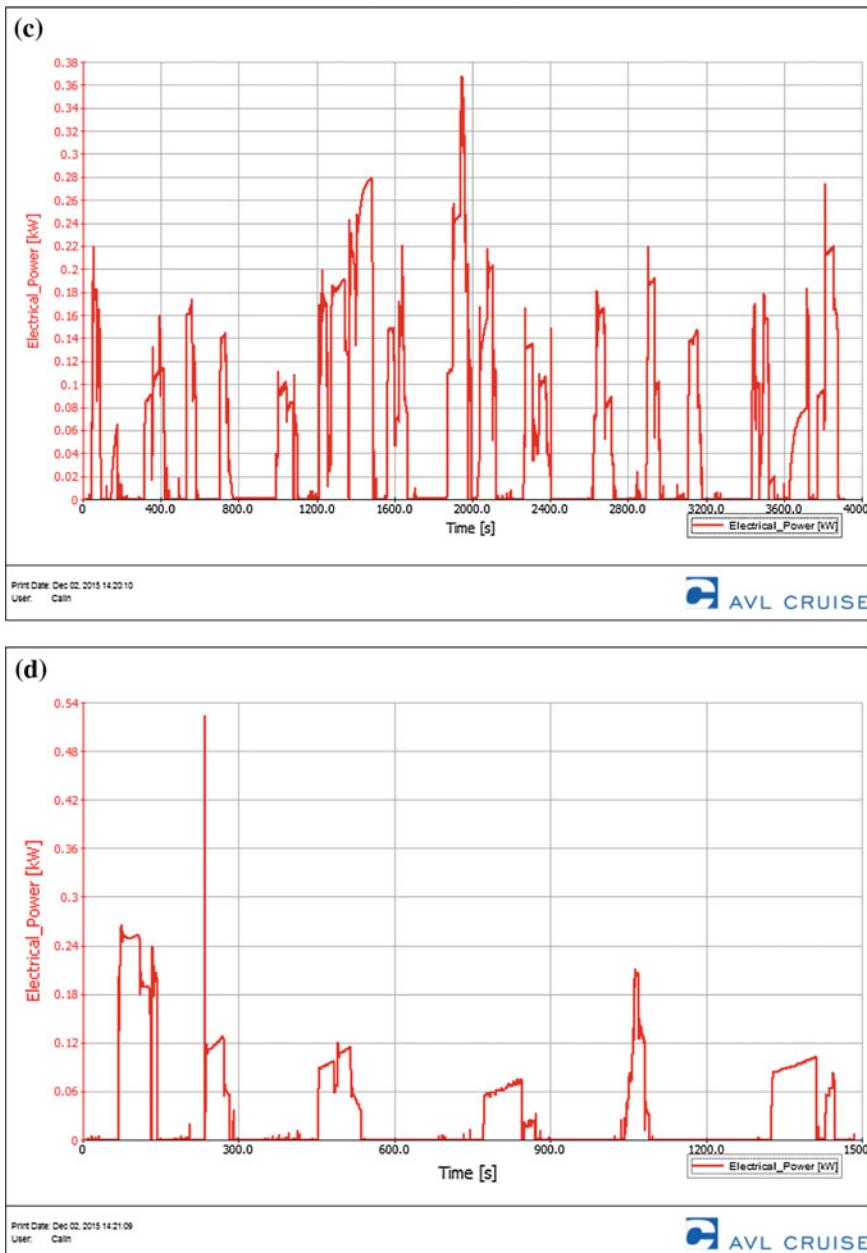
Fig. 7.33 (continued)
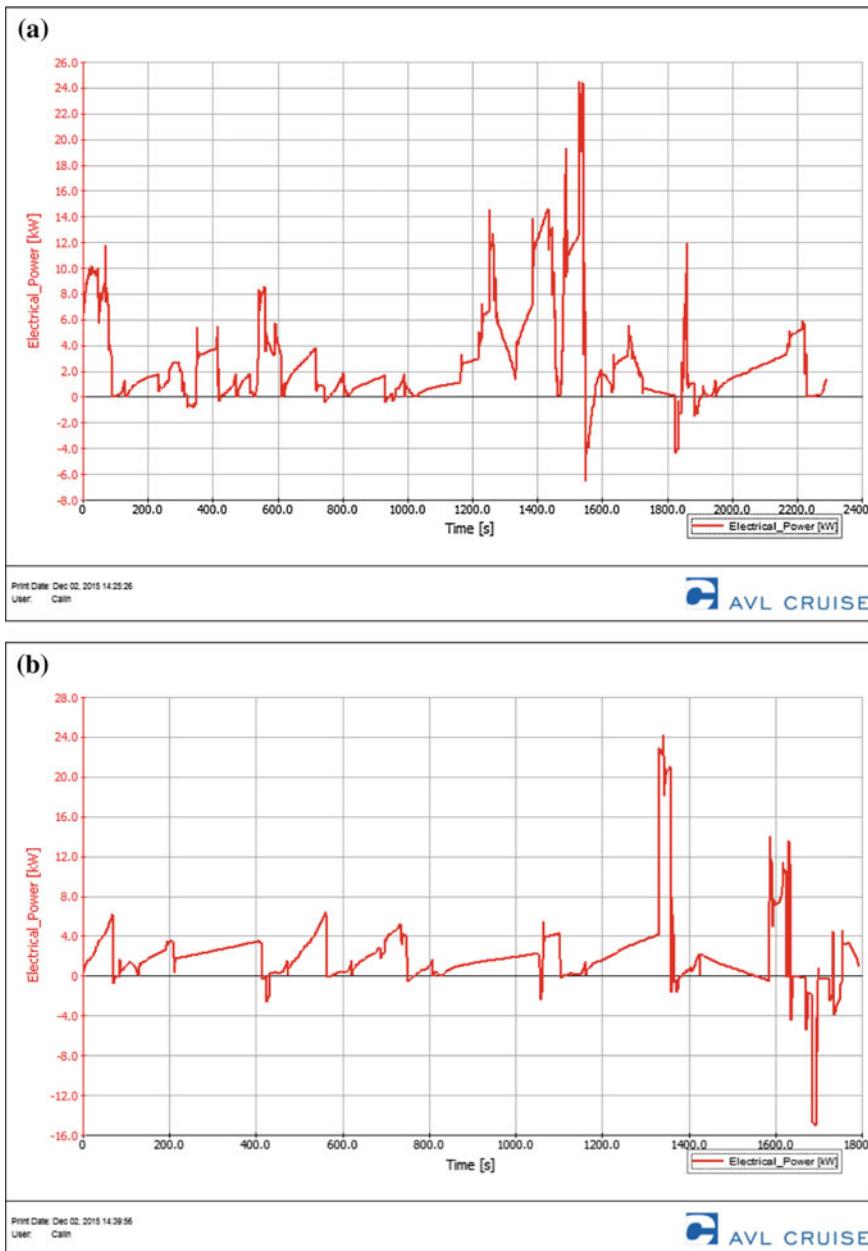
Fig. 7.34 Electric power generated by the electric bus: **a** route 27, **b** route 28, **c** route 30 and **d** route 32
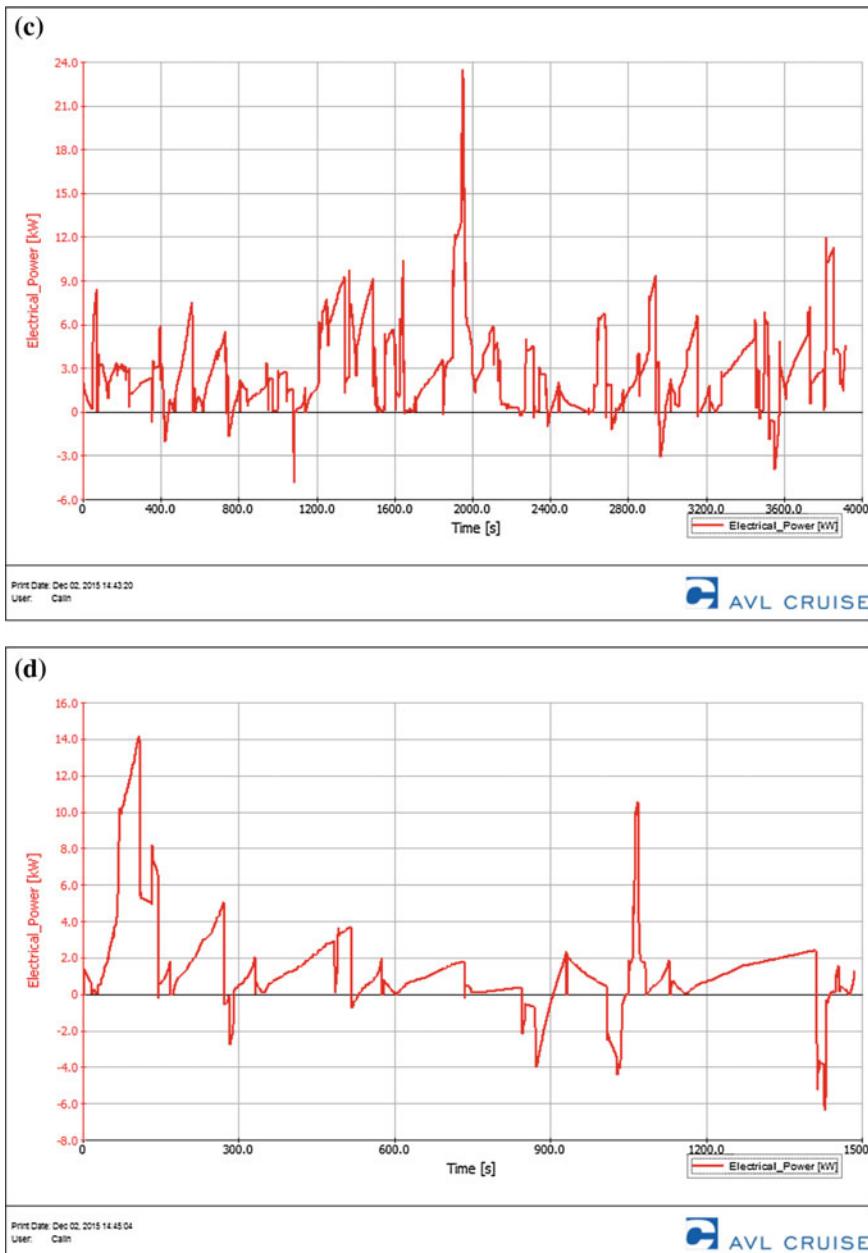
Fig. 7.34 (continued)
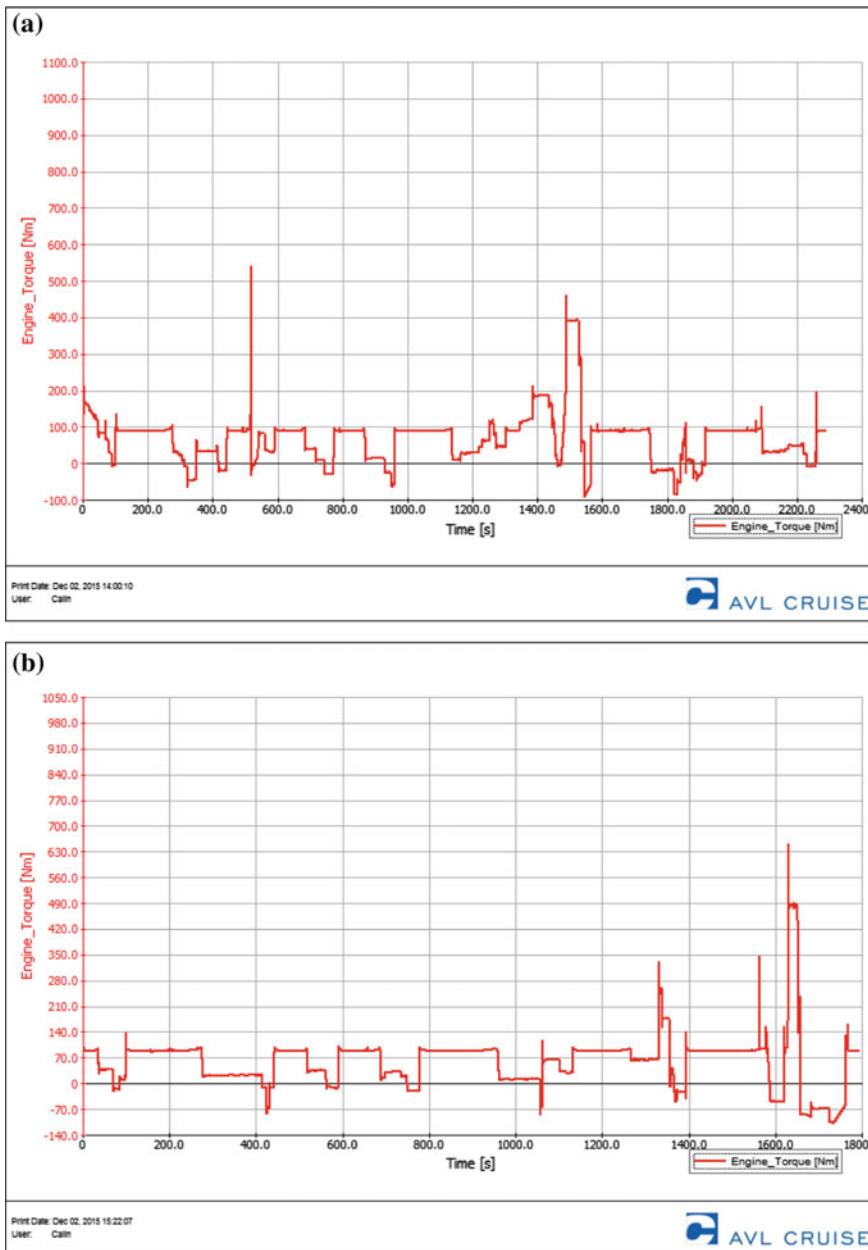
Fig. 7.35 Thermal engine torque generated by the classic bus: **a** route 27, **b** route 28, **c** route 30 and **d** route 32
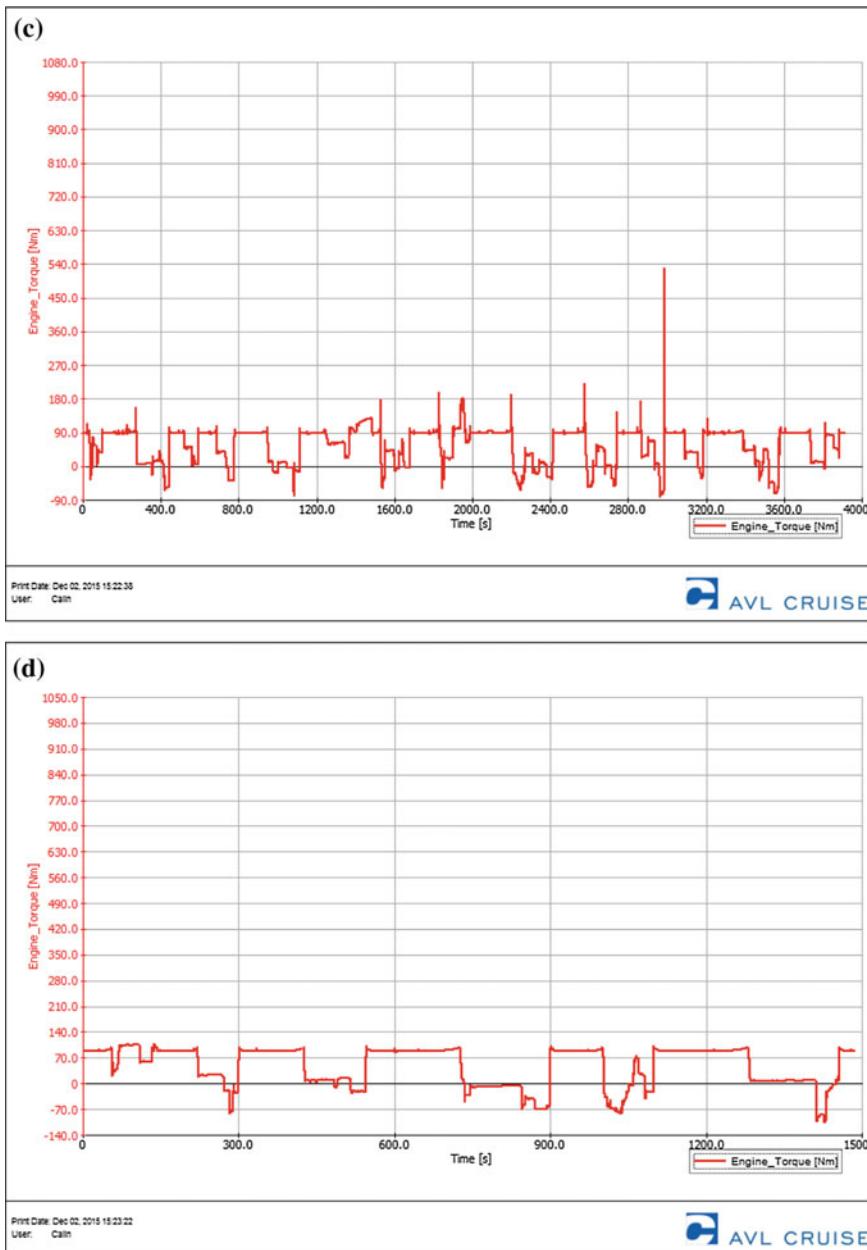
Fig. 7.35 (continued)
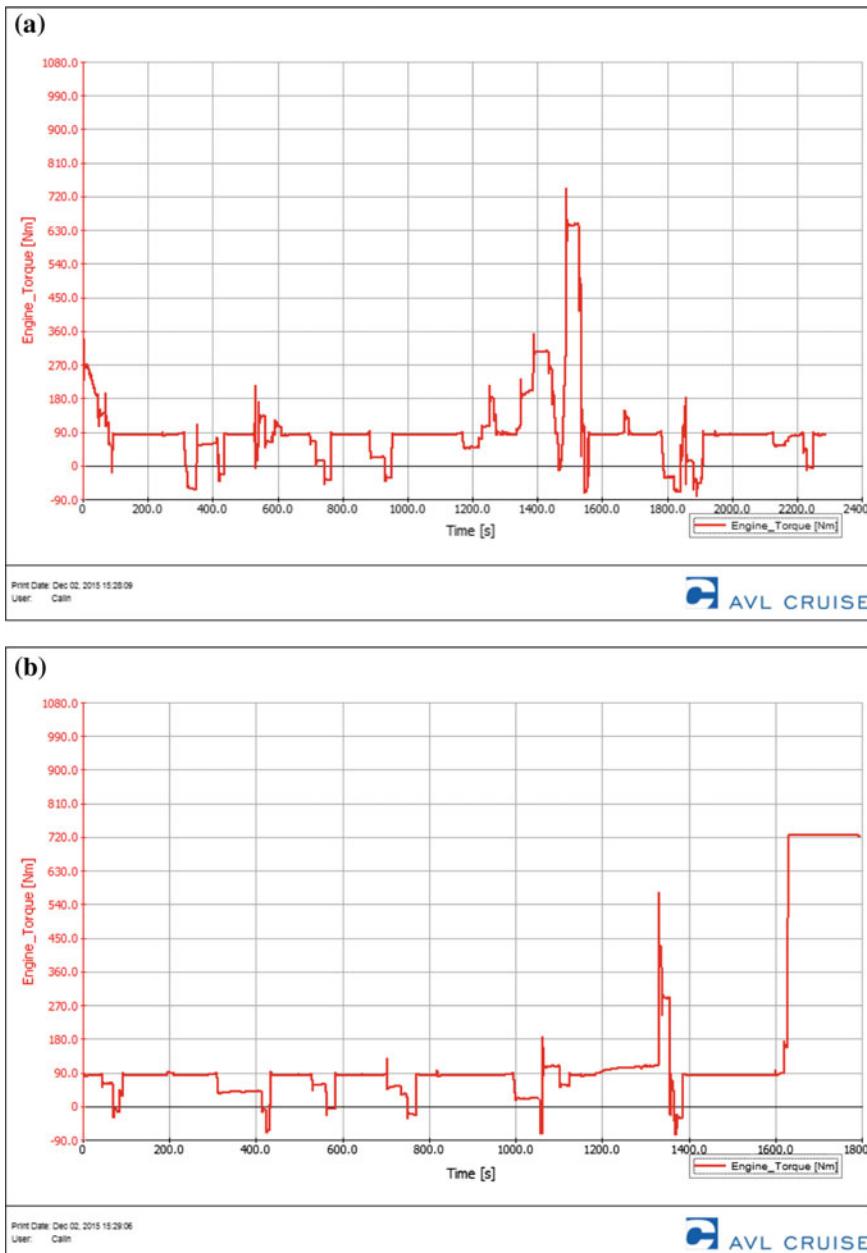
Fig. 7.36 Thermal engine torque generated by the hybrid bus: **a** route 27, **b** route 28, **c** route 30 and **d** route 32

Fig. 7.36 (continued)

(a)

(b)
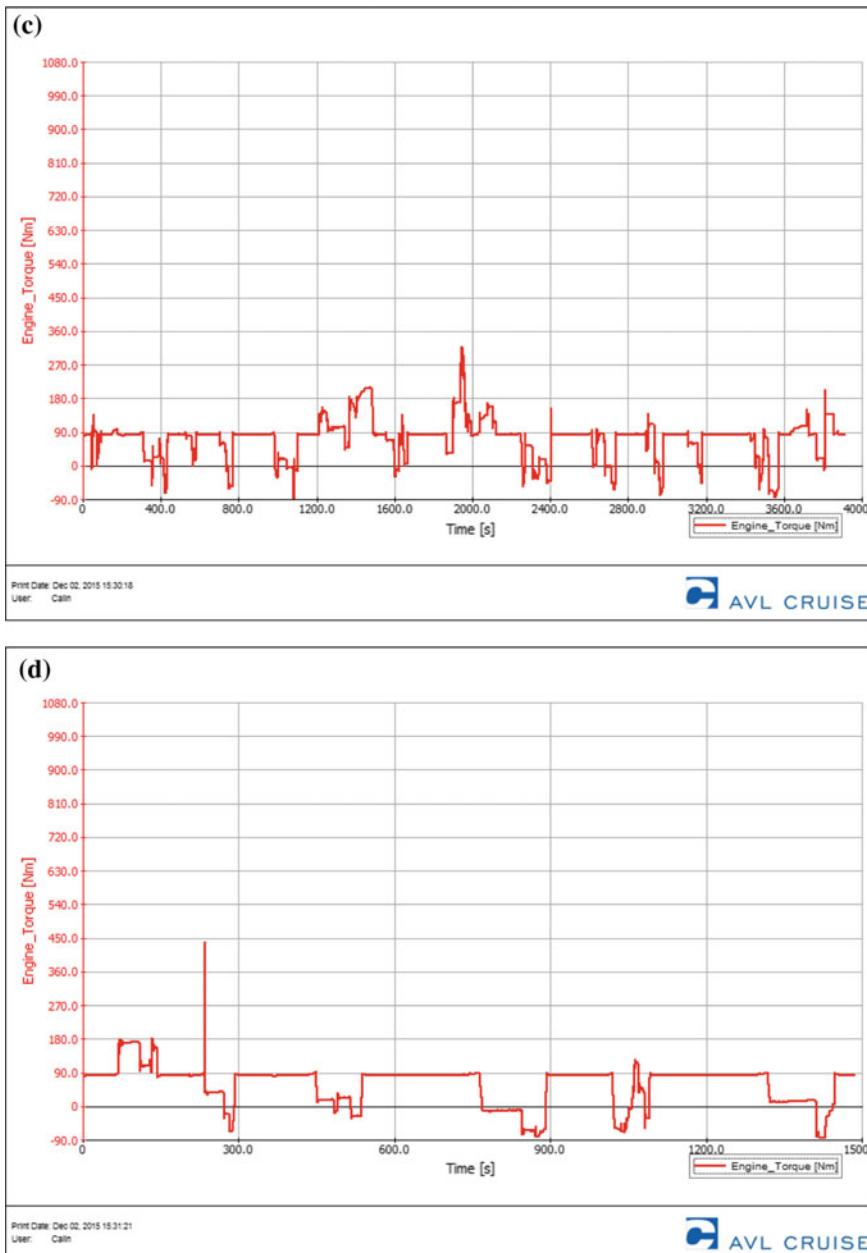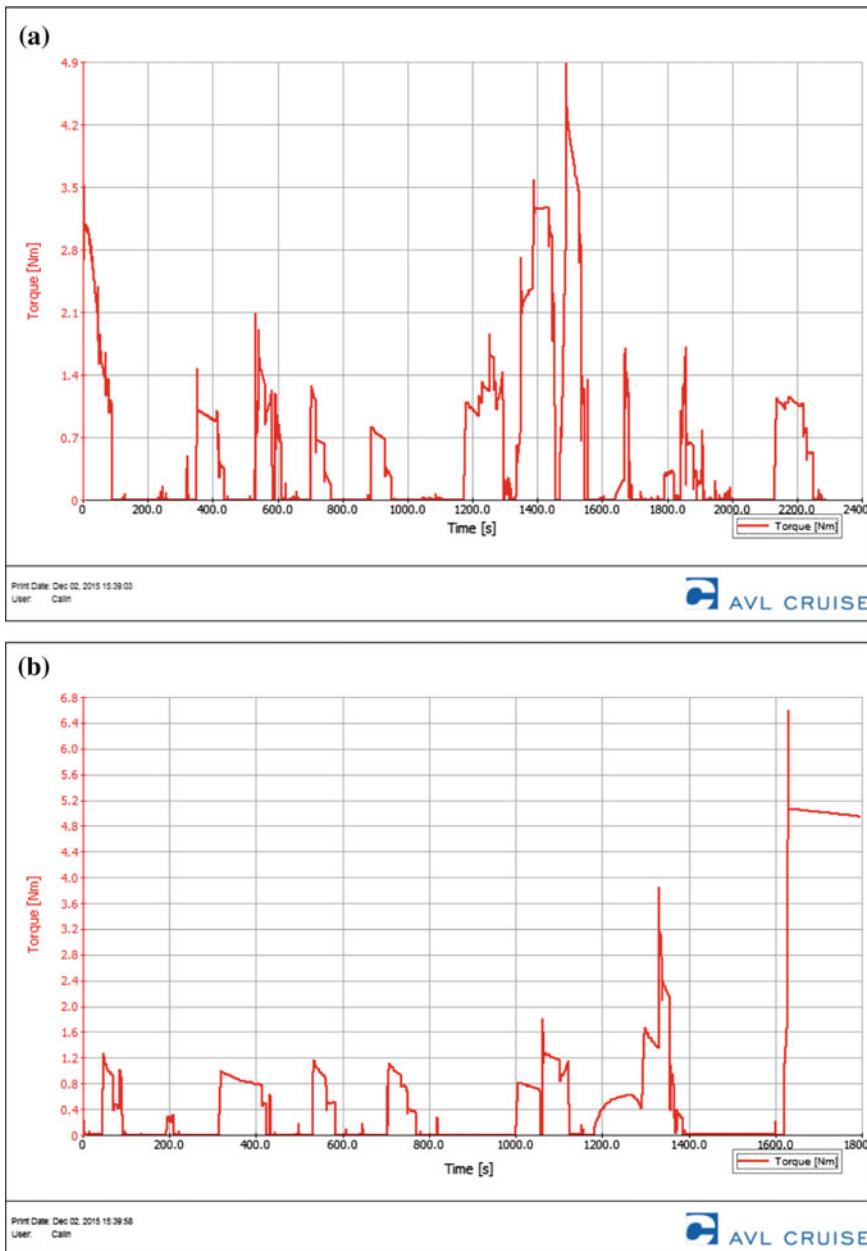
Fig. 7.37 Electric motor torque generated by the hybrid bus: **a** route 27, **b** route 28, **c** route 30 and **d** route 32
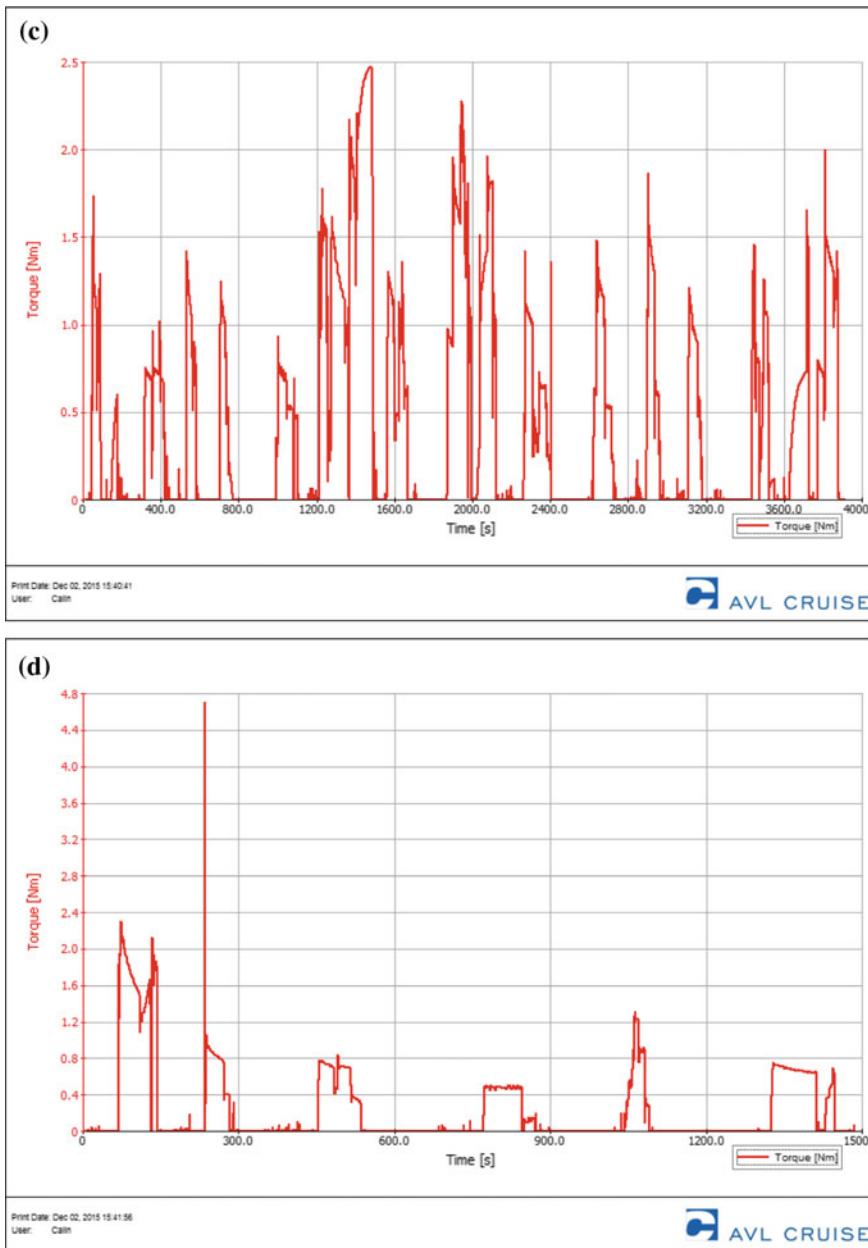
Fig. 7.37 (continued)
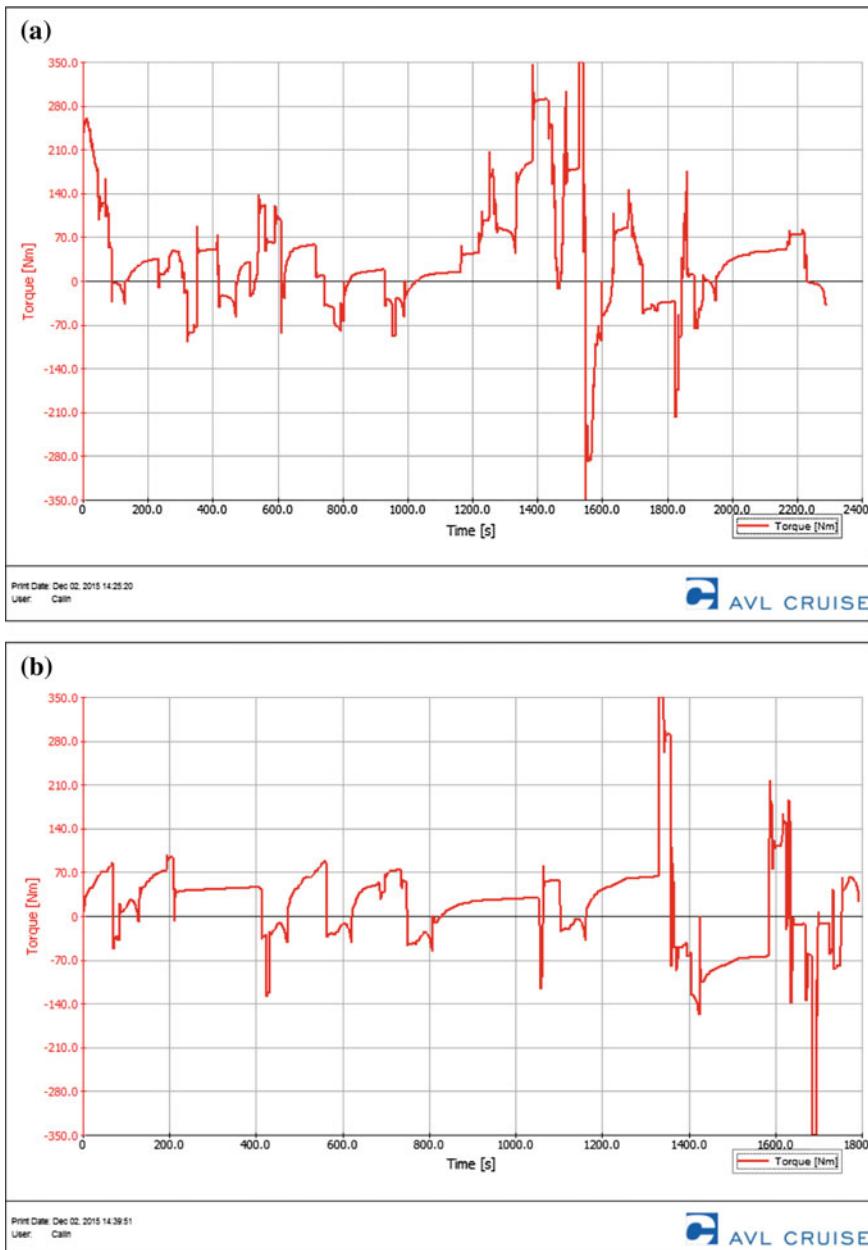
Fig. 7.38 Electric motor torque generated by the electric bus: **a** route 27, **b** route 28, **c** route 30 and **d** route 32
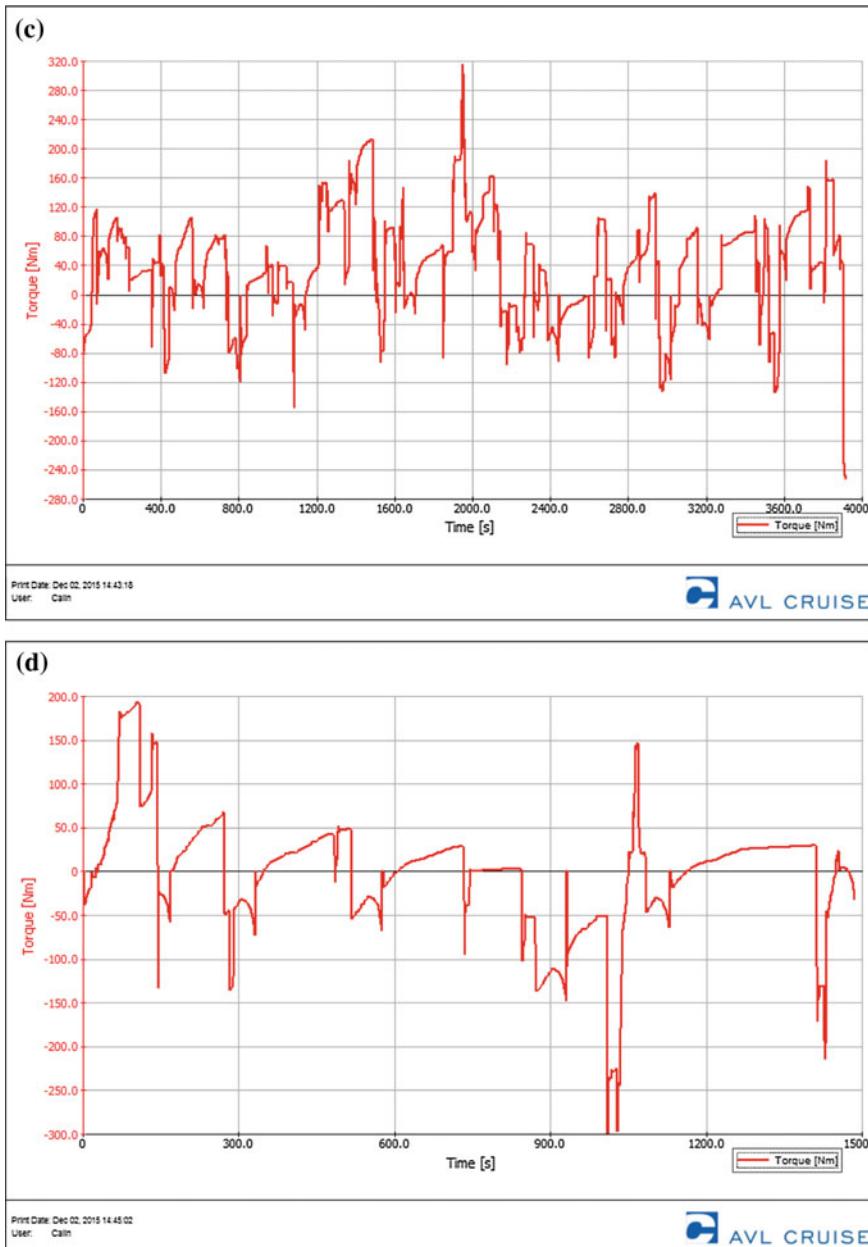
Fig. 7.38 (continued)

The electric motor equipping hybrid and electric buses creates a maximum torque even from the start, fact which leads to high maneuverability and characteristics for departure from place [2].

The effective mean pressure for the thermal engine generated by the classic bus is presented in Fig. 7.39a–d, respectively the effective mean pressure for the thermal engine generated by the hybrid bus is presented in Fig. 7.40a–d. The brake power for the thermal engine generated by the classic bus is presented in Fig. 7.41a–d, respectively the brake power for the thermal engine generated by the hybrid bus is presented in Fig. 7.42a–d. The braking torque for the thermal engine generated by the classic bus is presented in Fig. 7.43a–d, respectively the braking torque for the thermal engine generated by the hybrid bus is presented in Fig. 7.44a–d. The fuel consumption for the thermal engine generated by the classic bus is presented in Fig. 7.45a–d, respectively the fuel consumption for the thermal engine generated by the hybrid bus is presented in Fig. 7.46a–d.

The quality of the transformation process of the heat resulting from the combustion process from the thermal engine in specific mechanical work actually usable for bus drive is appreciated by the value of the actual engine efficiency, defined as the rapport between the usable mechanical work and the energy consumed for obtaining this mechanical work [2].

The thermal engine converts only a part of the energy obtained from fuel combustion effectively into mechanical work. The efficiency of such an engine is from 30 % up to 40 %, the higher values being for diesel engine, and the lower ones for gasoline engine. The rest of the energy is lost through friction and heat release, the largest share being represented by heat losses via exhaust gases.

The pollutant emissions generated by the classic bus are presented in Fig. 7.47a–d for NO_x, Fig. 7.48a–d for CO and Fig. 7.49a–d for HC. The emissions generated by the hybrid bus are presented in Fig. 7.50a–d for NO_x, Fig. 7.51a–d for CO, Fig. 7.52a–d for HC. The electric bus generates zero local emissions.

From the NO_x emissions analysis it can be observed that in the case of the hybrid bus the maximum values of NO_x emissions are 50 % lower, and the CO emissions are reduced with up to 30 % and the HC emissions are reduced with up to 15 % due to the fast that the thermal engine equipping this type of bus has a lower cylindrical capacity than the classic bus, and the operating period for the thermal engine is reduced by up to 70 % for the same route due to its use in parallel with the electric motor.

By using hybrid and electric vehicles, compared to classic drive systems, the level of pollutant emissions decreases by up to 35 % for hybrid vehicles, respectively by up to 100 % for the electric ones (zero local emissions) due to the existence of the electric motor which for the urban environment is used in proportion of 70 % for hybrid models, respectively permanently for electric models.

The acceleration generated by the classic bus is presented in Fig. 7.53a–d, the acceleration generated by the hybrid bus is presented in Fig. 7.54a–d, respectively the acceleration generated by the electric bus is presented in Fig. 7.55a–d. The load signal for the classic bus is presented in Fig. 7.56a–d, the load signal for the hybrid bus is presented in Fig. 7.57a–d, respectively the load signal for the electric bus is
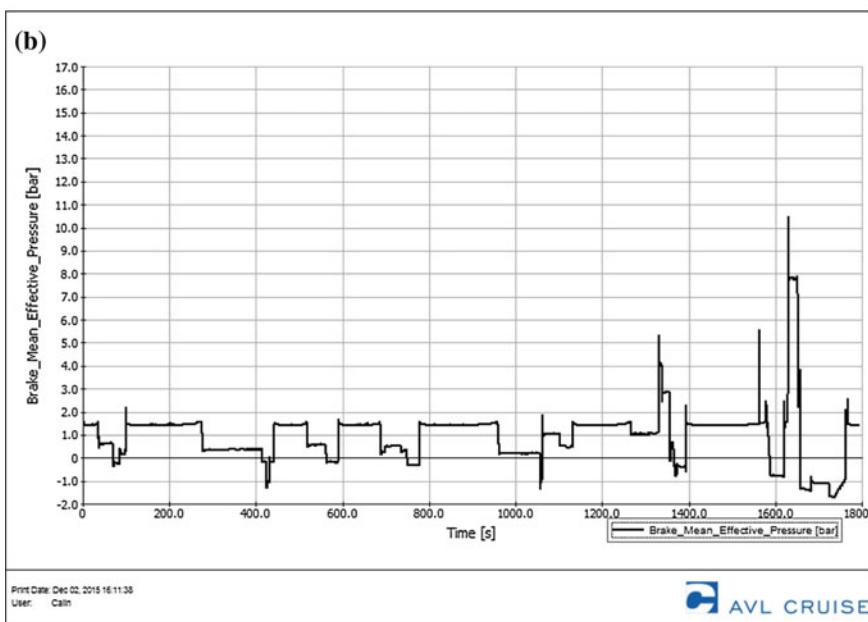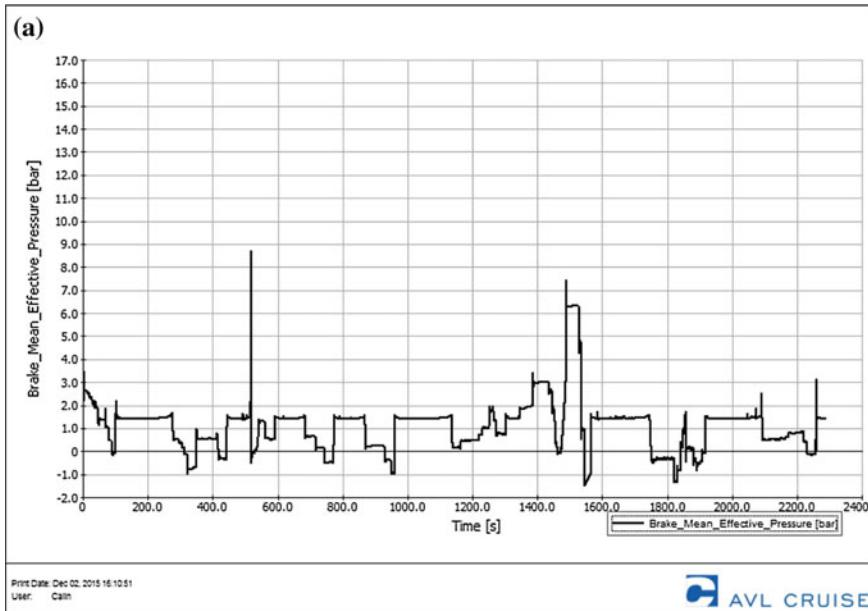
Fig. 7.39 Effective Mean Pressure generated by the classic bus: **a** route 27, **b** route 28, **c** route 30 and **d** route 32
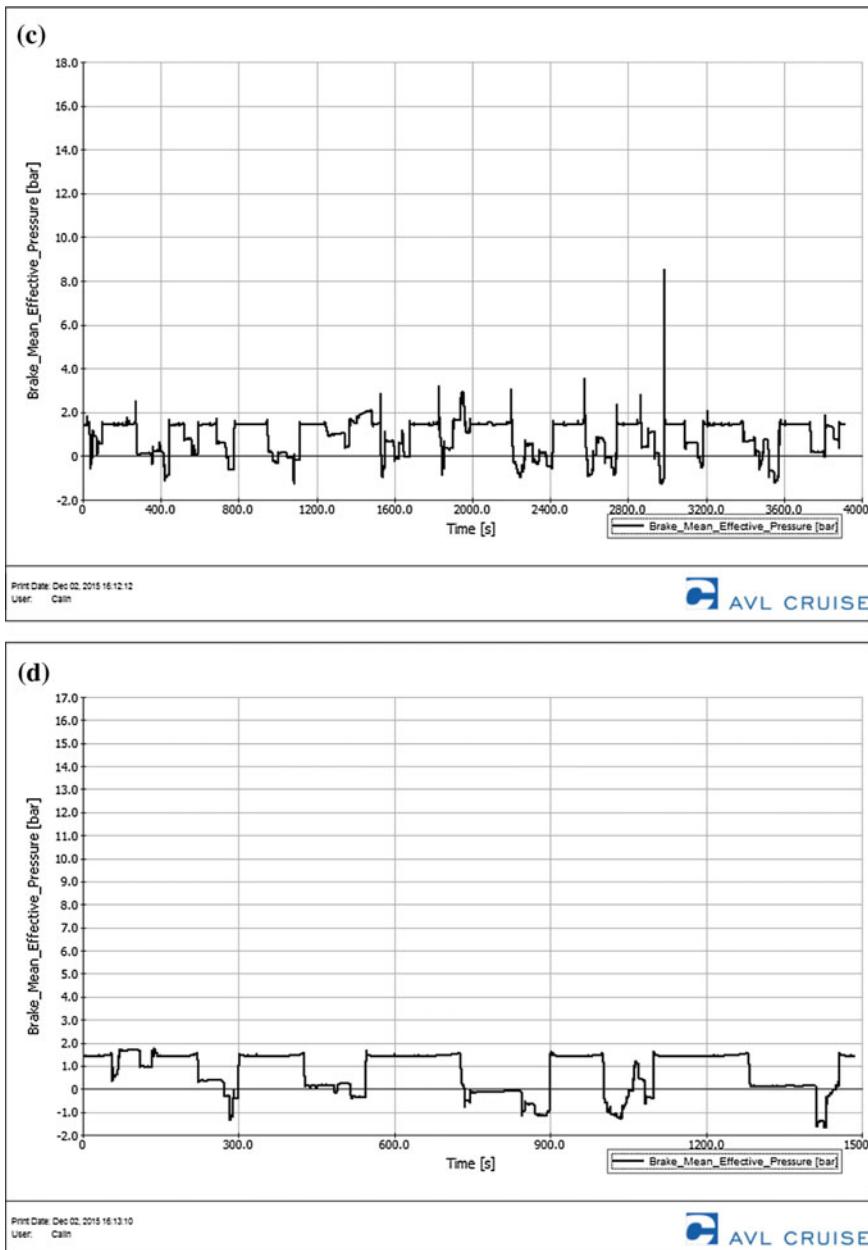
Fig. 7.39 (continued)
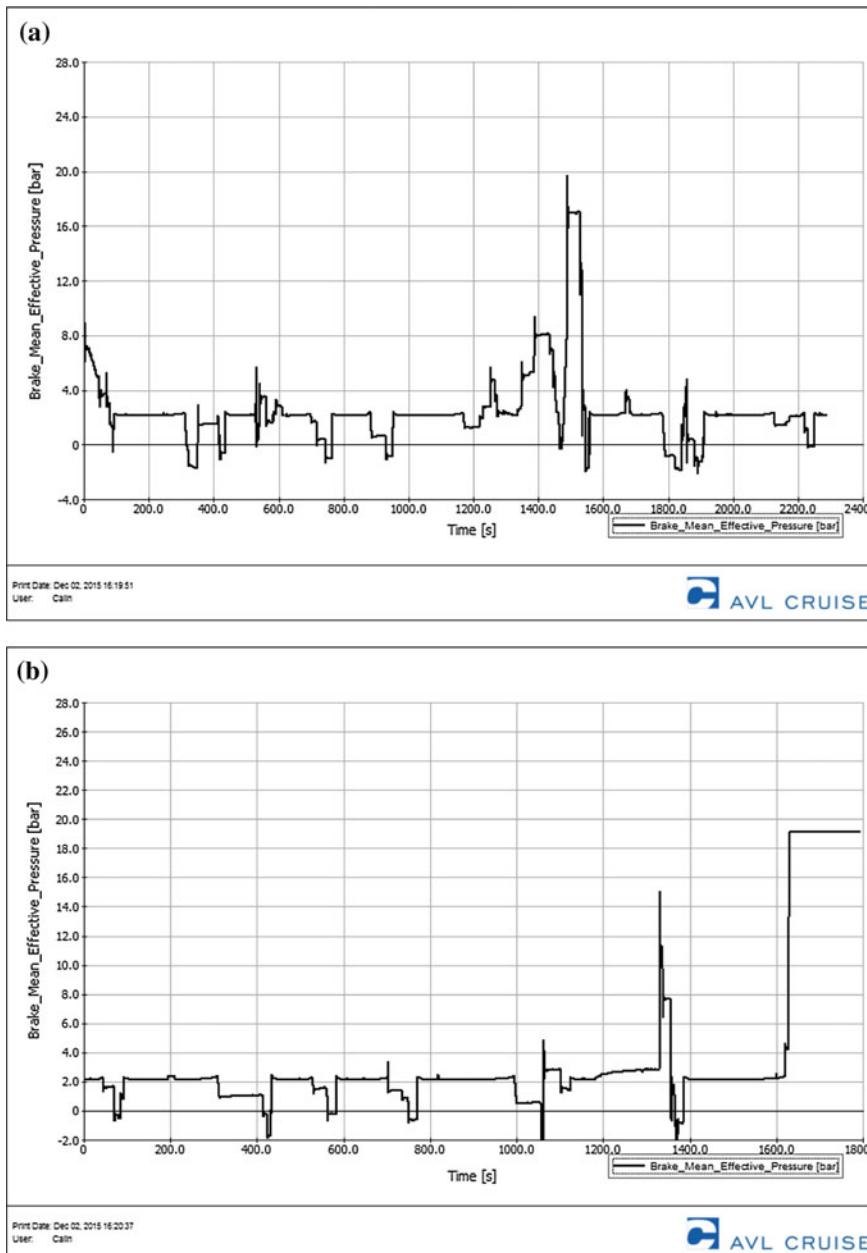
Fig. 7.40 Effective Mean Pressure generated by the hybrid bus: **a** route 27, **b** route 28, **c** route 30 and **d** route 32
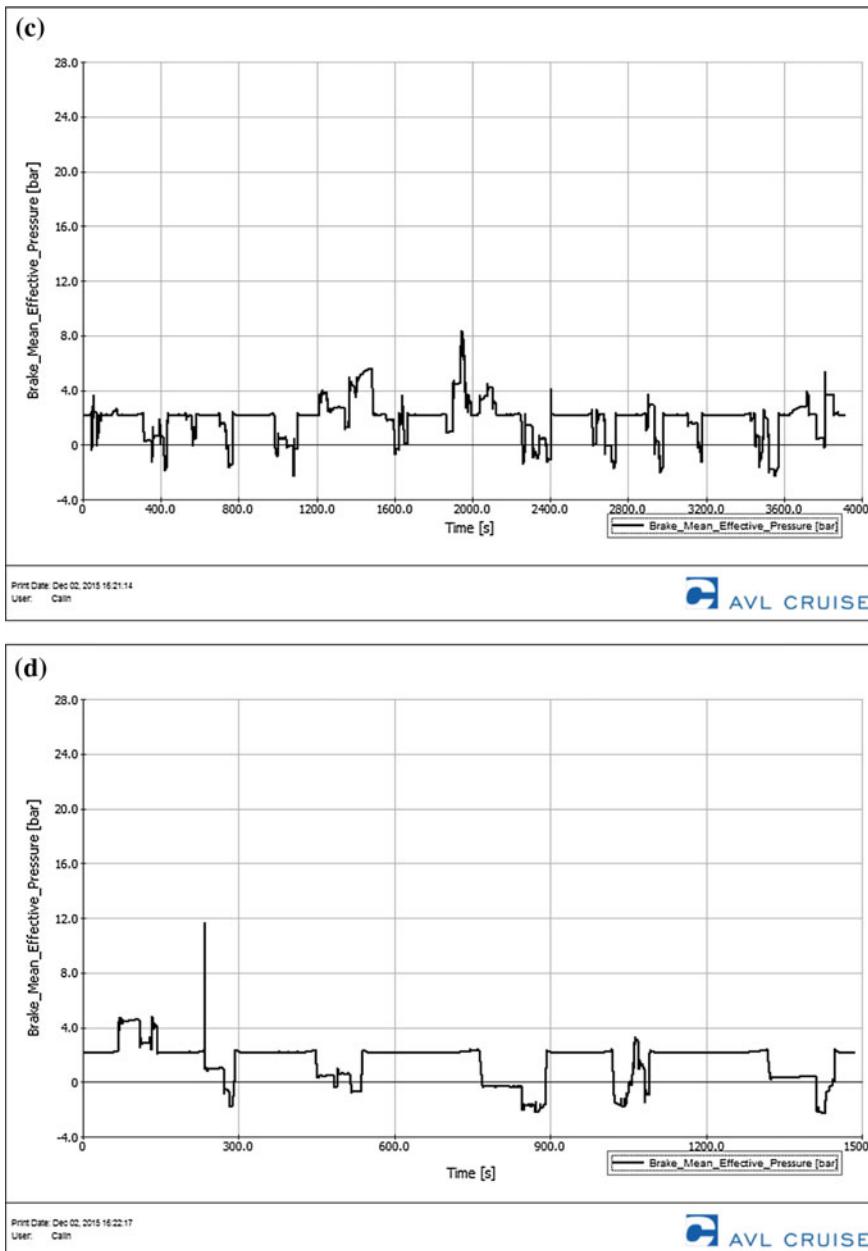
Fig. 7.40 (continued)
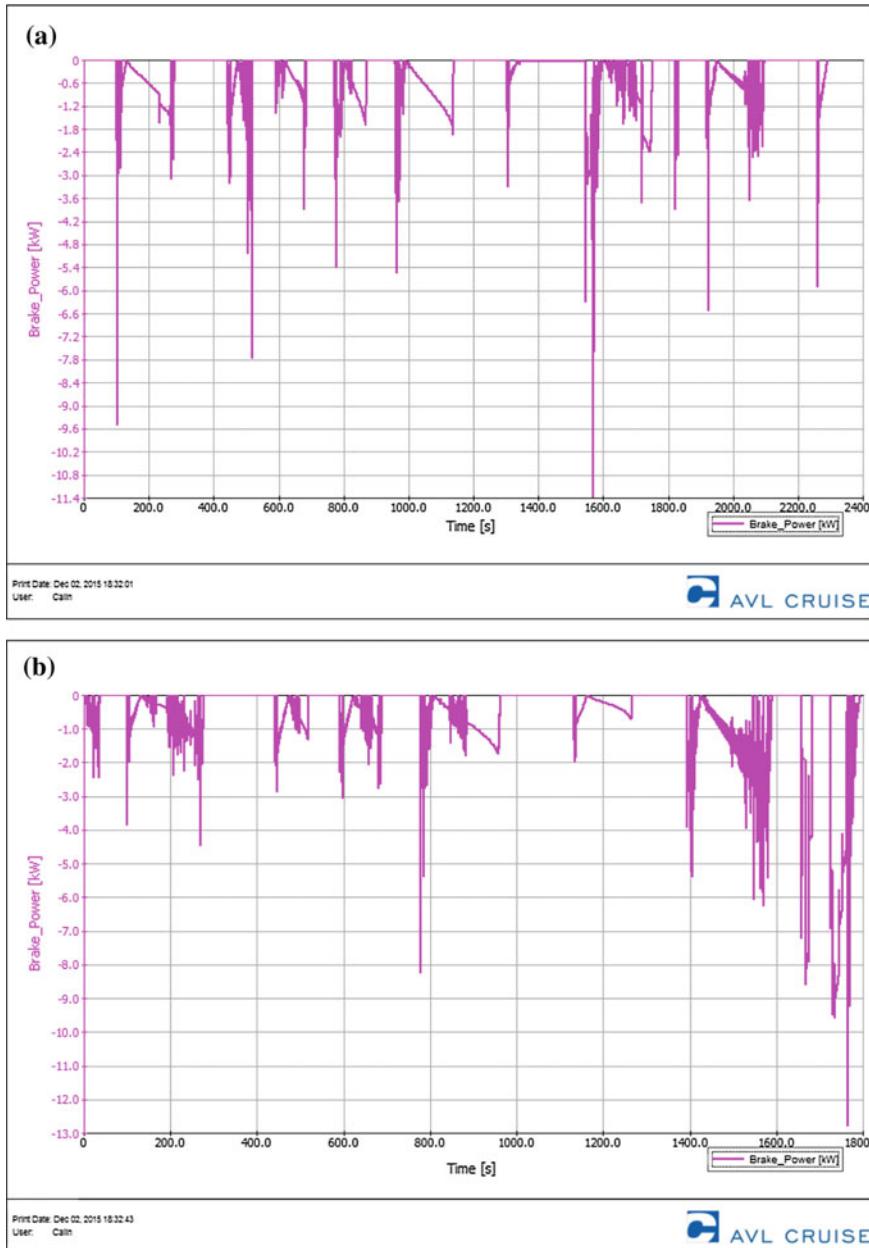
Fig. 7.41 Brake Power generated by the classic bus: **a** route 27, **b** route 28, **c** route 30 and **d** route 32
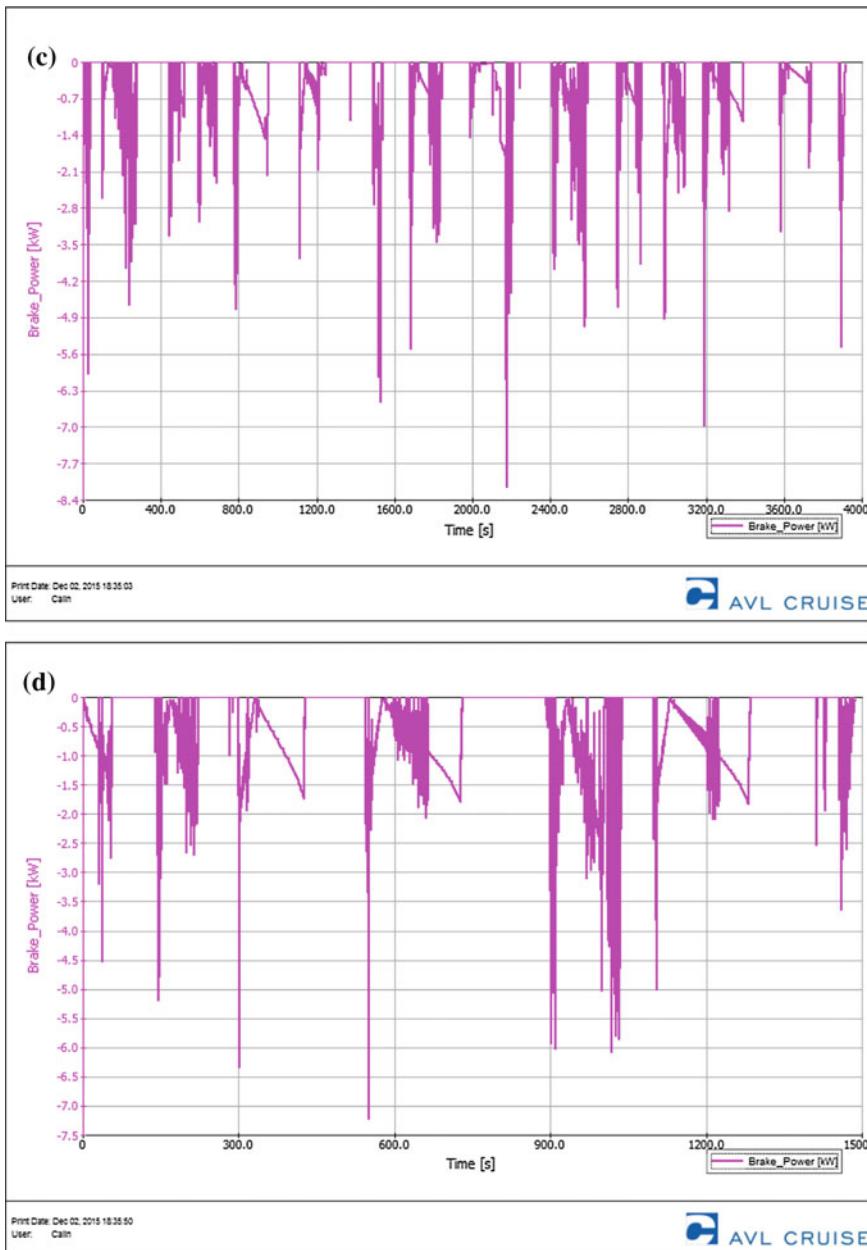
Fig. 7.41 (continued)
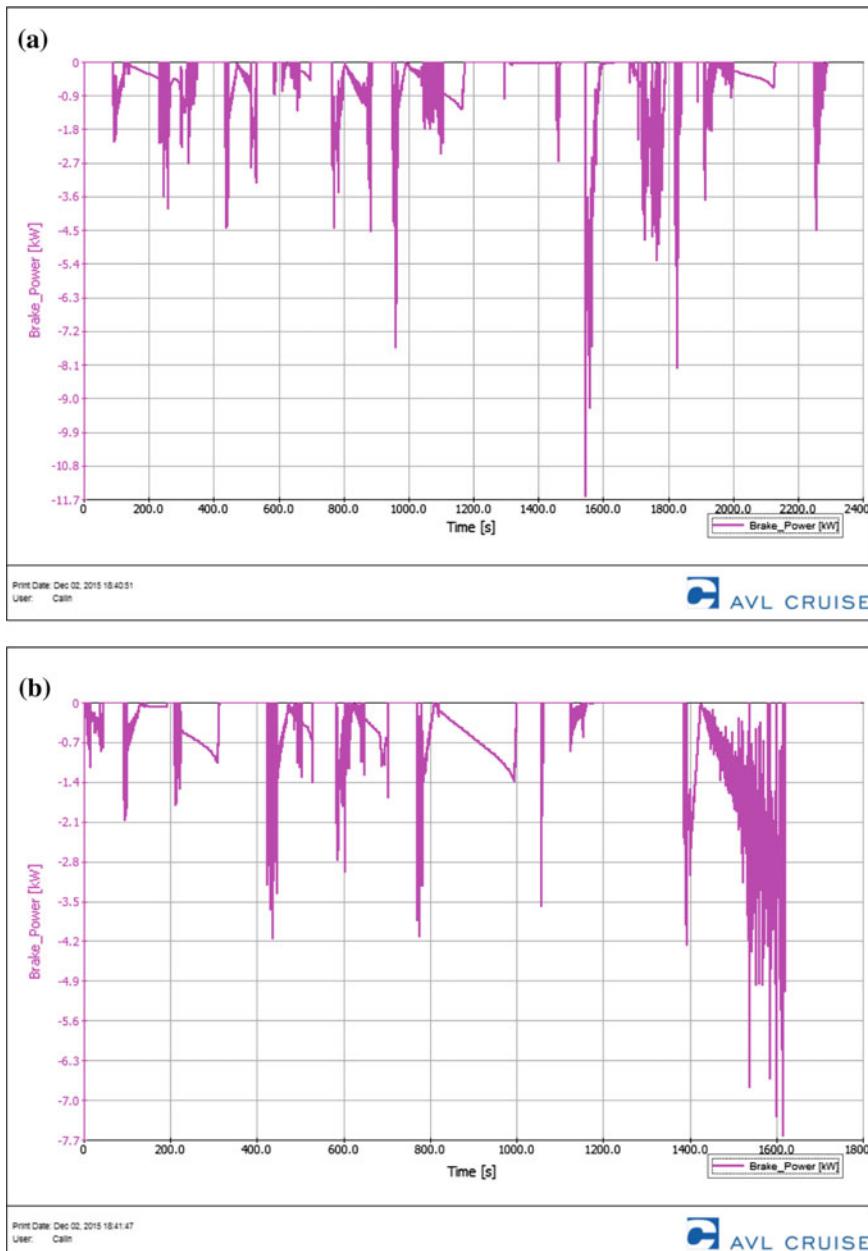
Fig. 7.42 Brake Power generated by the hybrid bus: **a** route 27, **b** route 28, **c** route 30 and **d** route 32
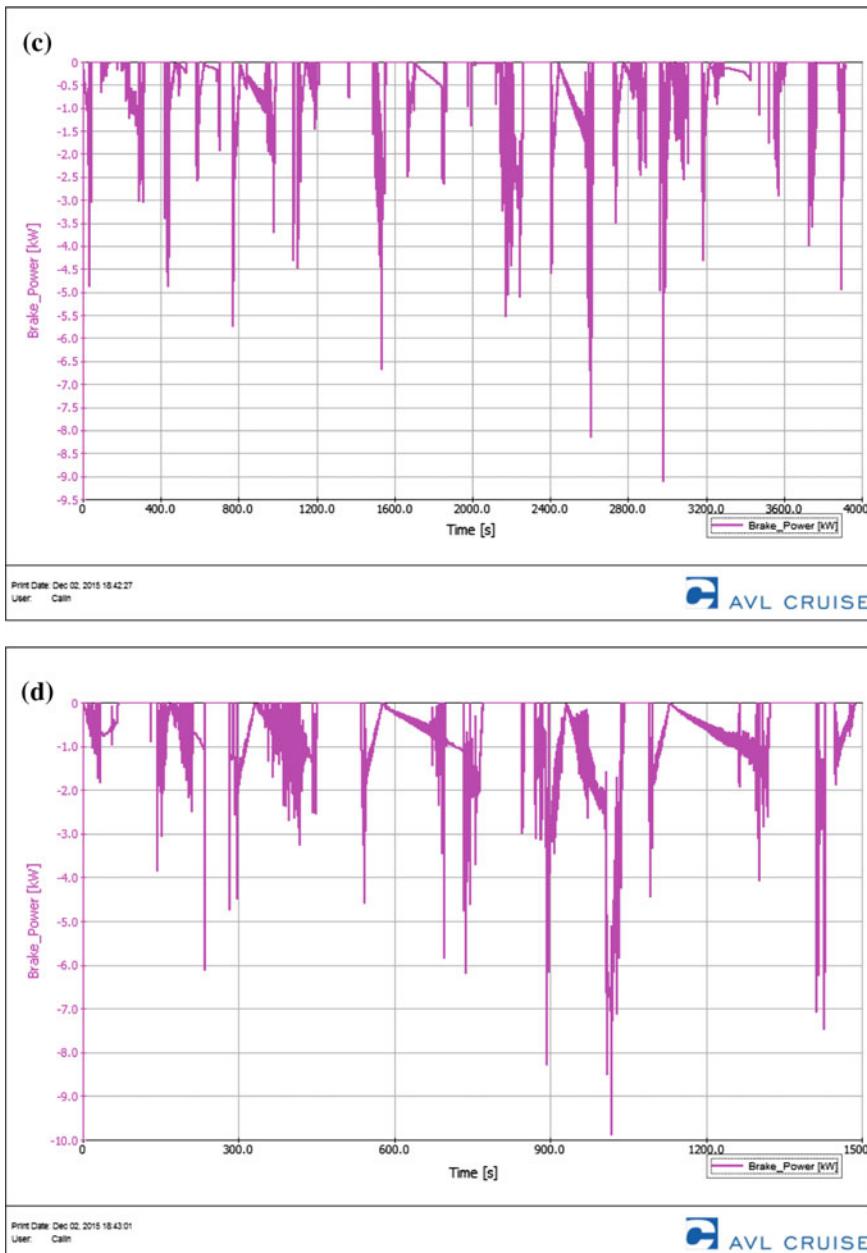
Fig. 7.42   (continued)
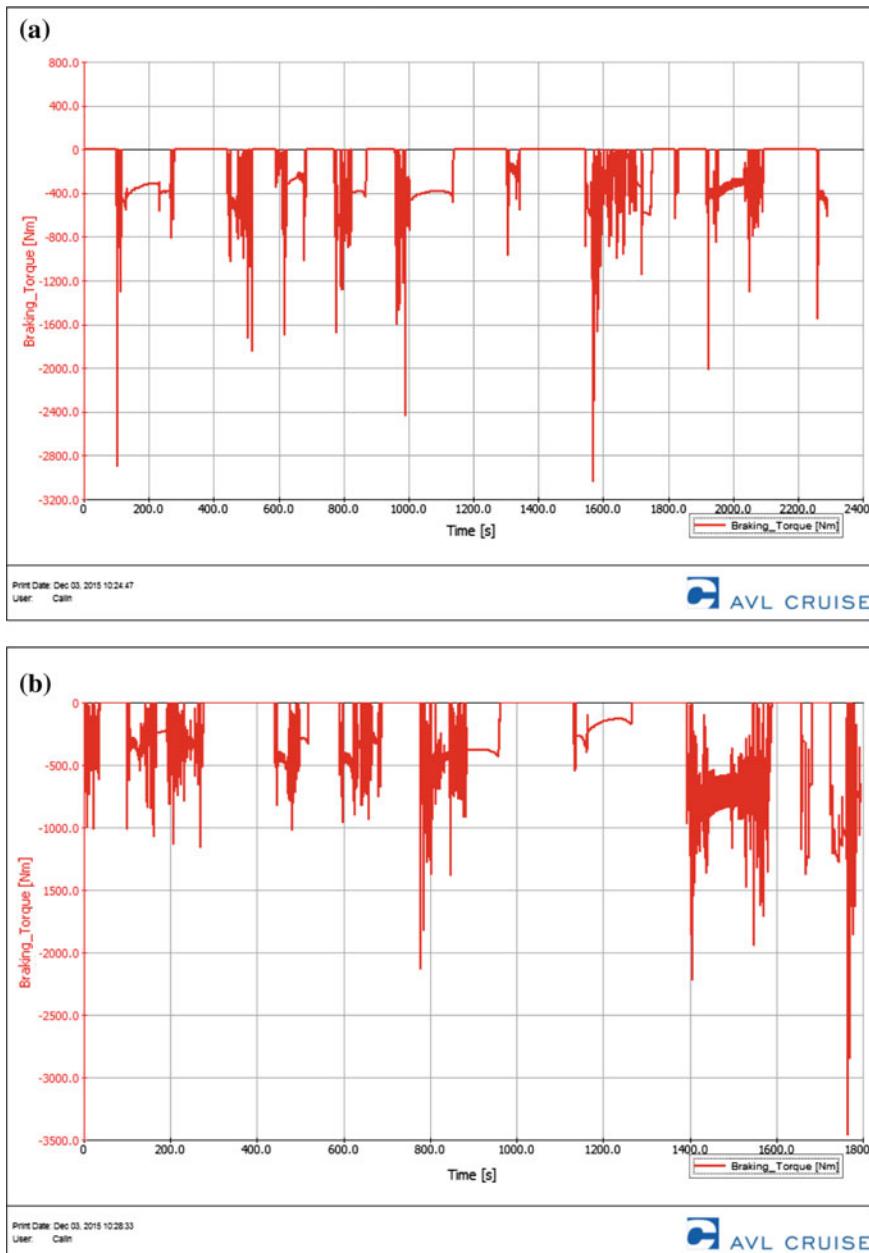
Fig. 7.43 Braking Torque generated by the classic bus: **a** route 27, **b** route 28, **c** route 30 and **d** route 32
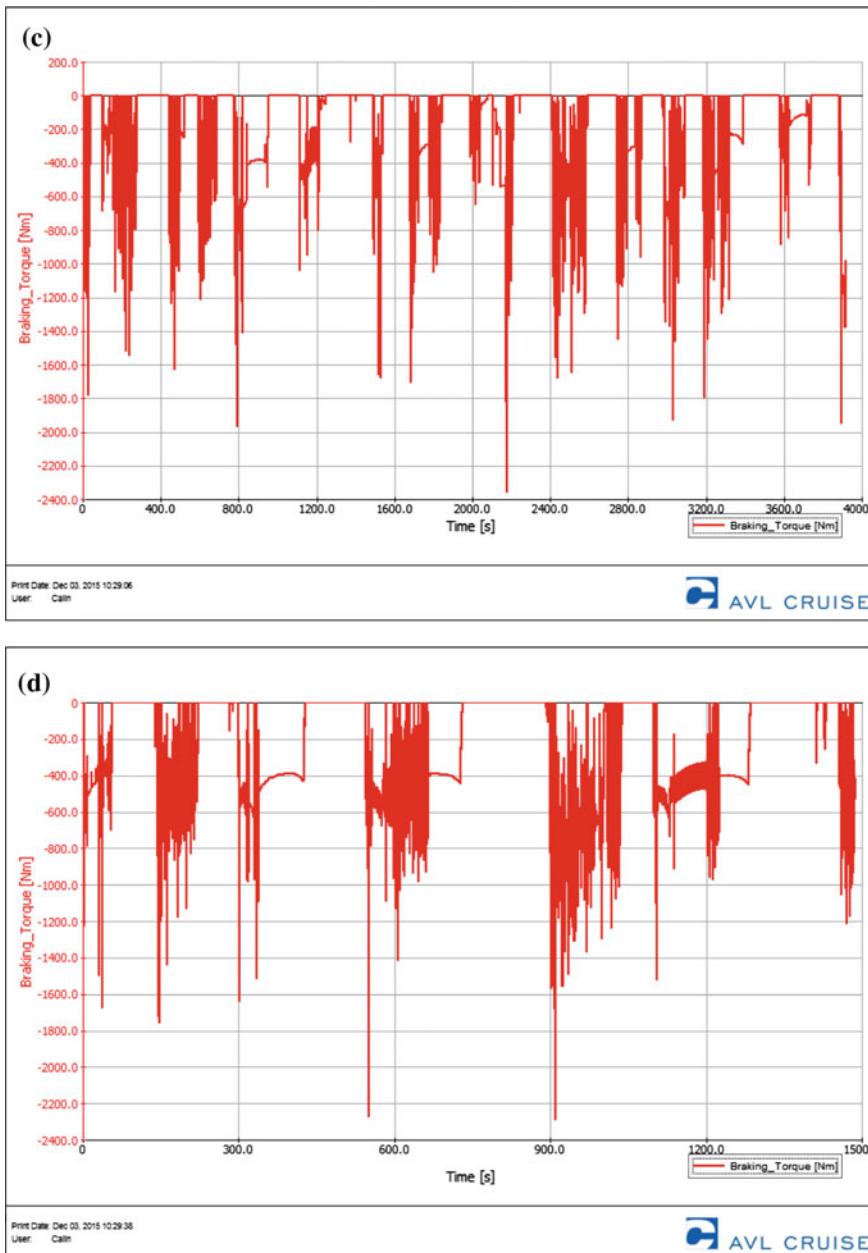
Fig. 7.43   (continued)
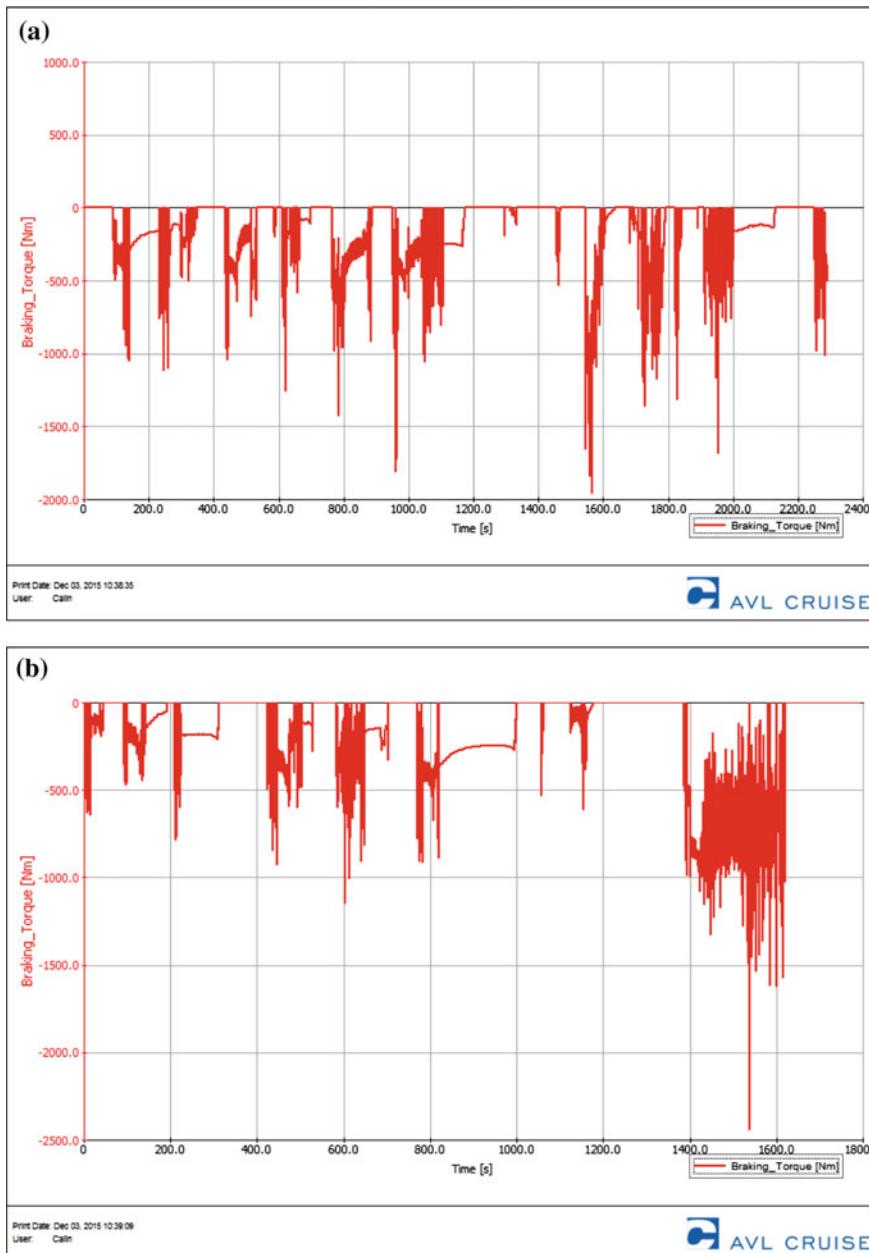
Fig. 7.44 Braking Torque generated by the hybrid bus: **a** route 27, **b** route 28, **c** route 30 and **d** route 32
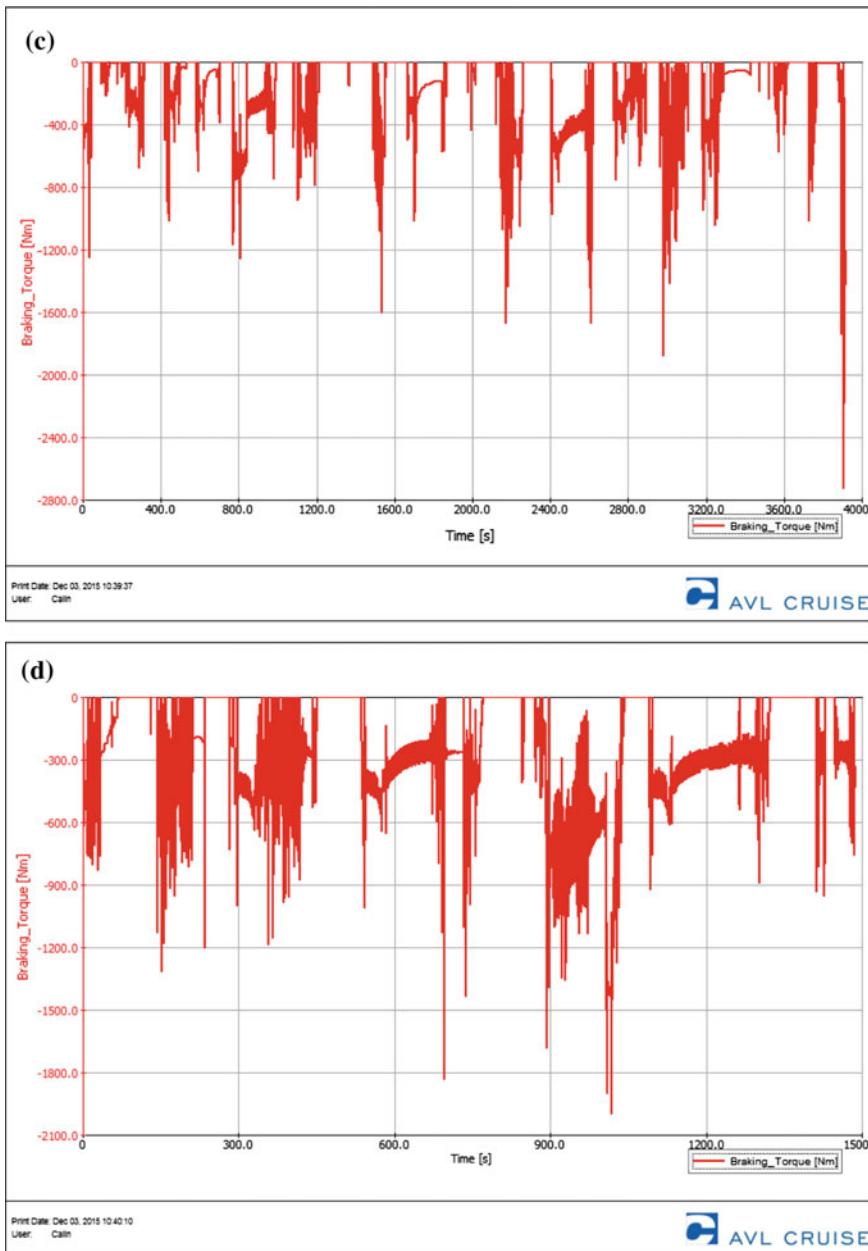
Fig. 7.44 (continued)
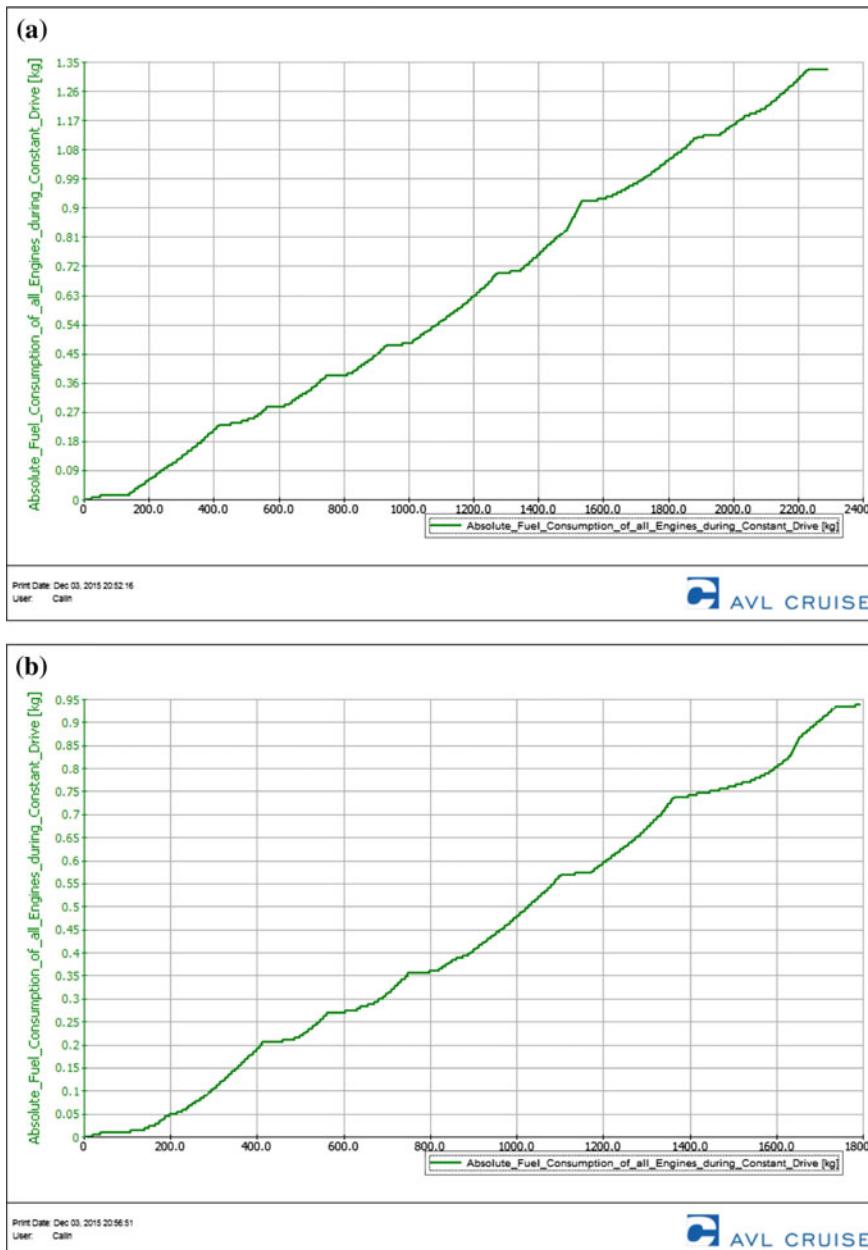
Fig. 7.45 Fuel consumption generated by the classic bus: **a** route 27, **b** route 28, **c** route 30 and **d** route 32
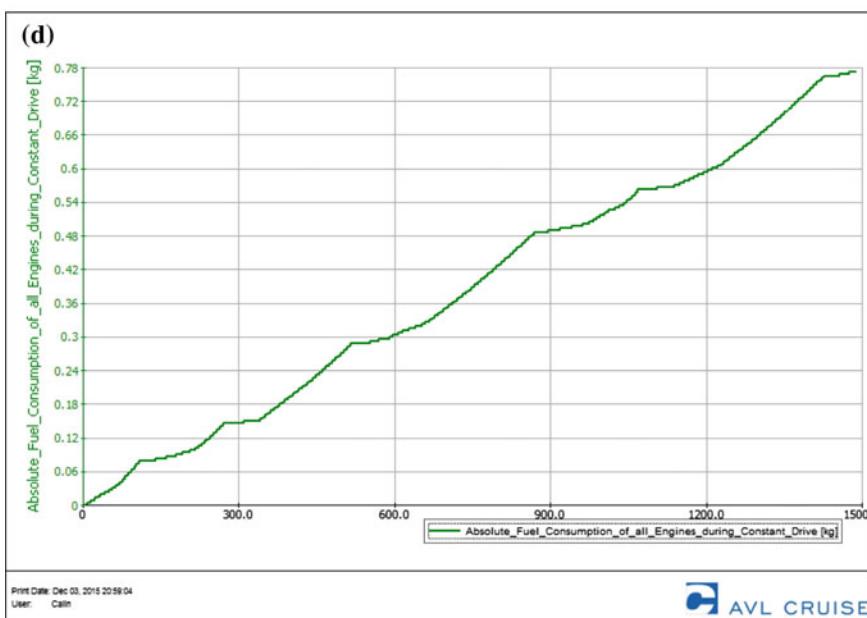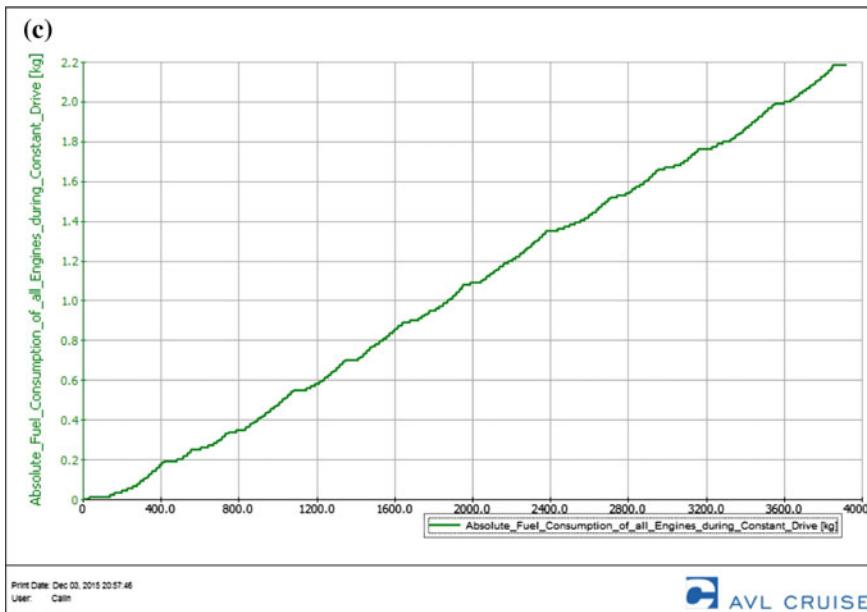
Fig. 7.45 (continued)
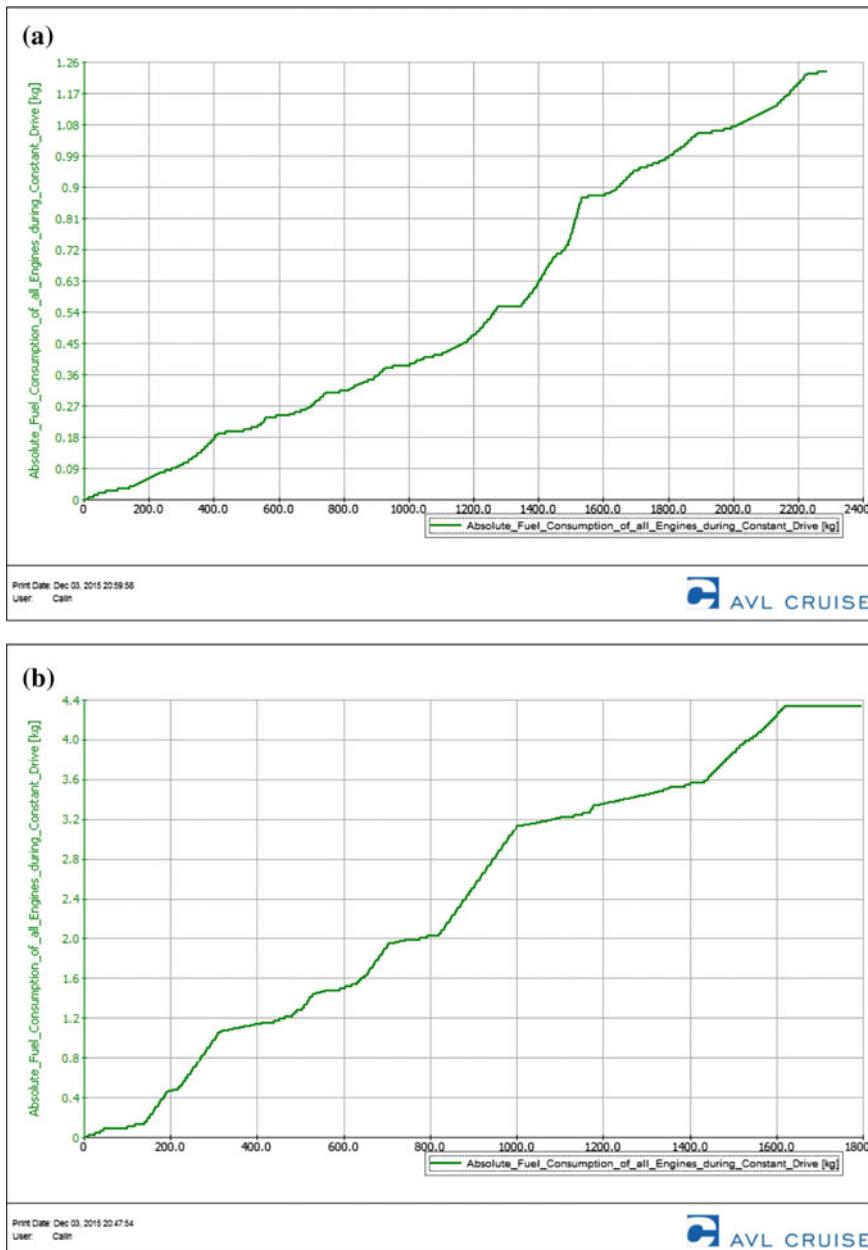
Fig. 7.46 Fuel consumption generated by the hybrid bus: **a** route 27, **b** route 28, **c** route 30 and **d** route 32
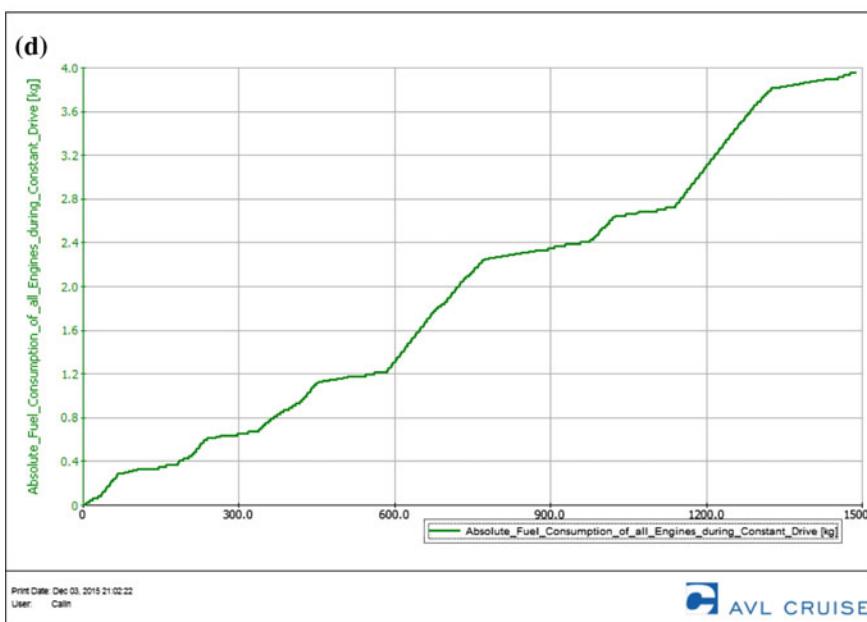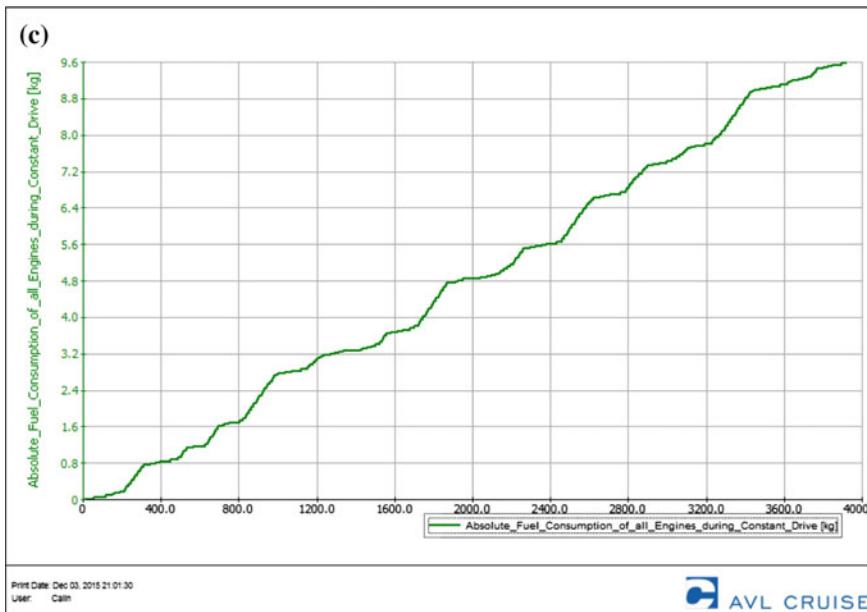
Fig. 7.46 (continued)
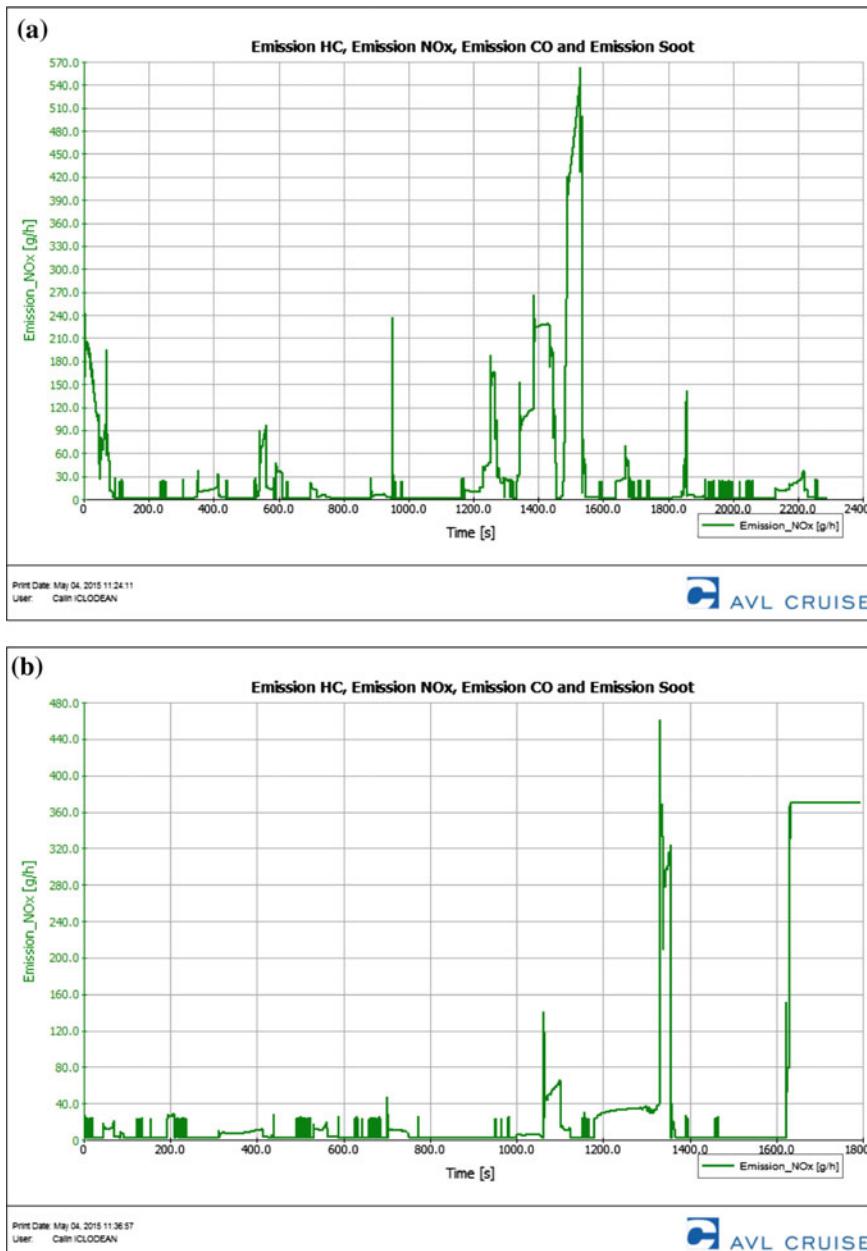
Fig. 7.47 NO$_x$ emissions generated by the classic bus: **a** route 27, **b** route 28, **c** route 30 and **d** route 32
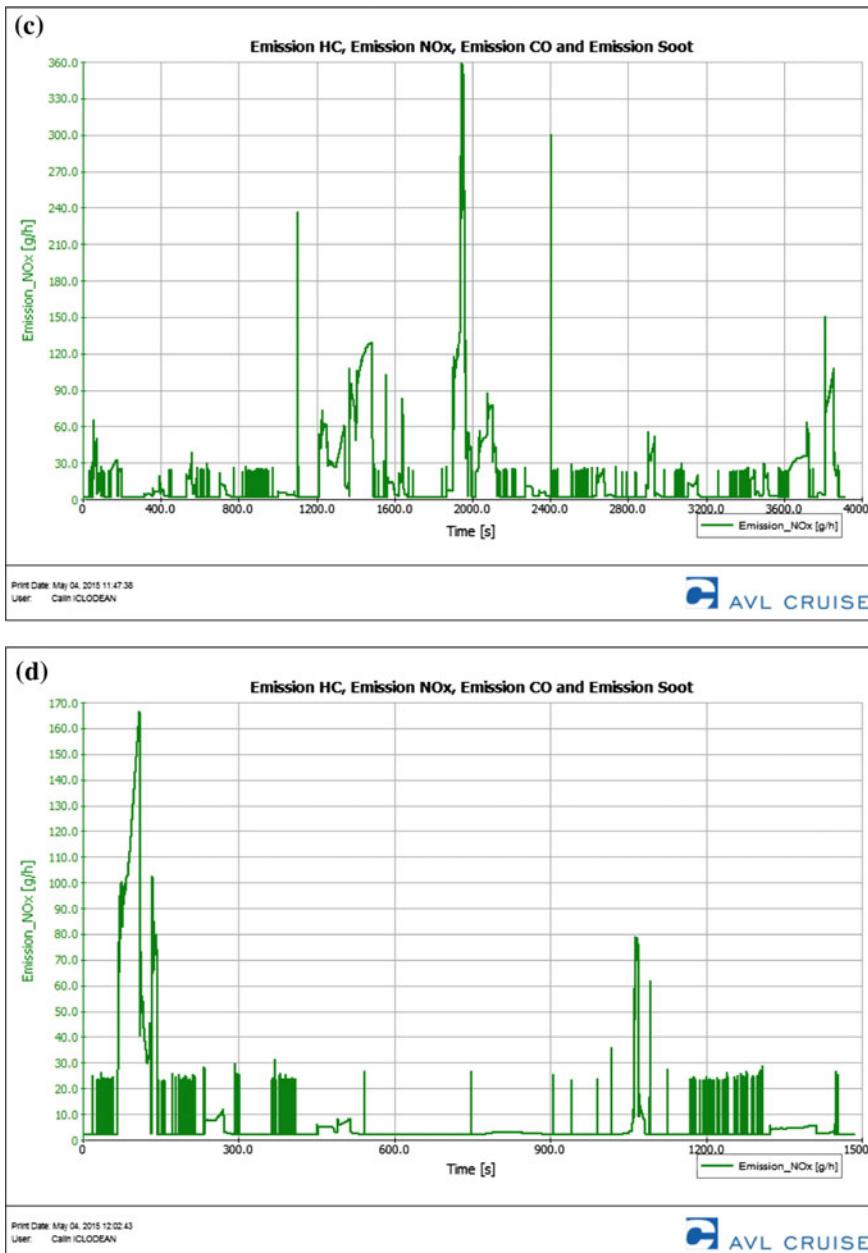
Fig. 7.47 (continued)
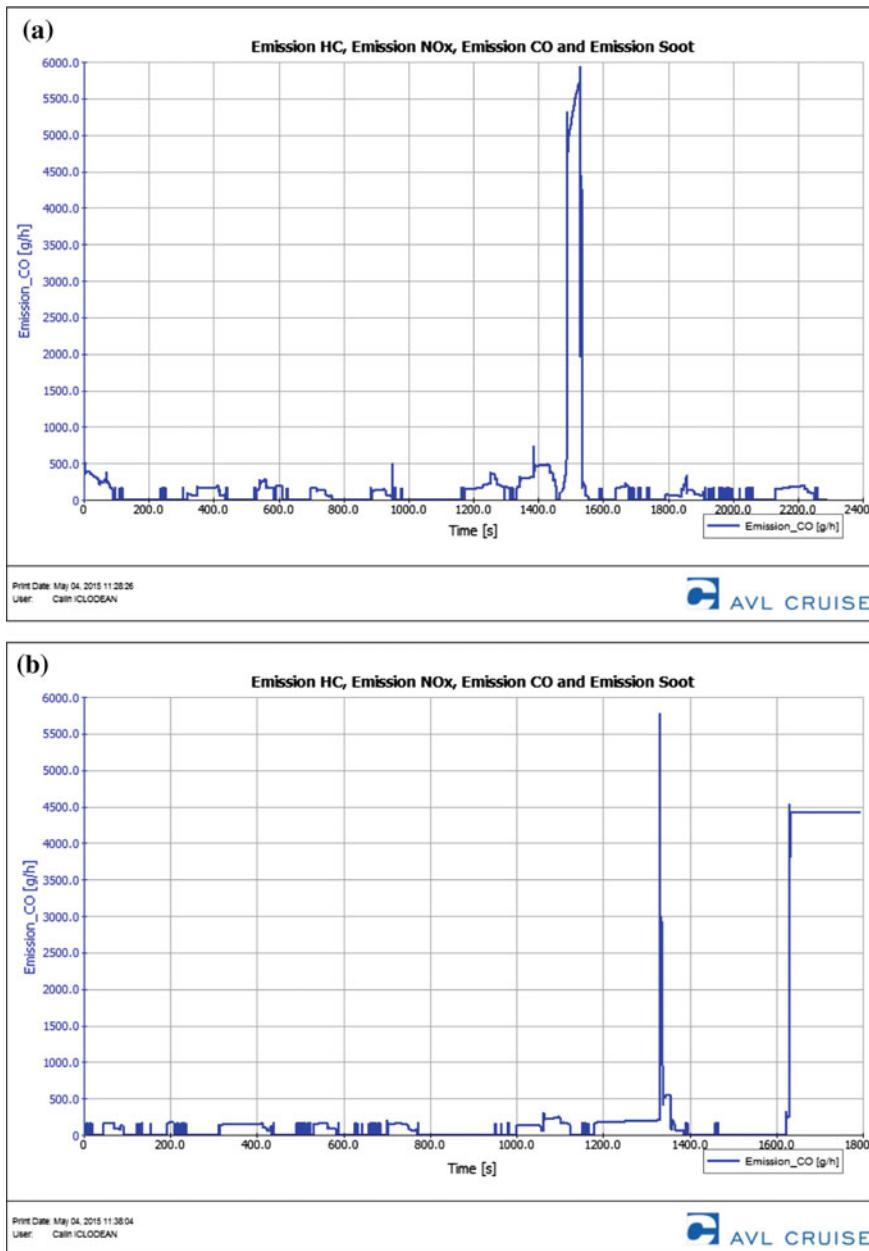
Fig. 7.48 CO emissions generated by the classic bus: **a** route 27, **b** route 28, **c** route 30 and **d** route 32
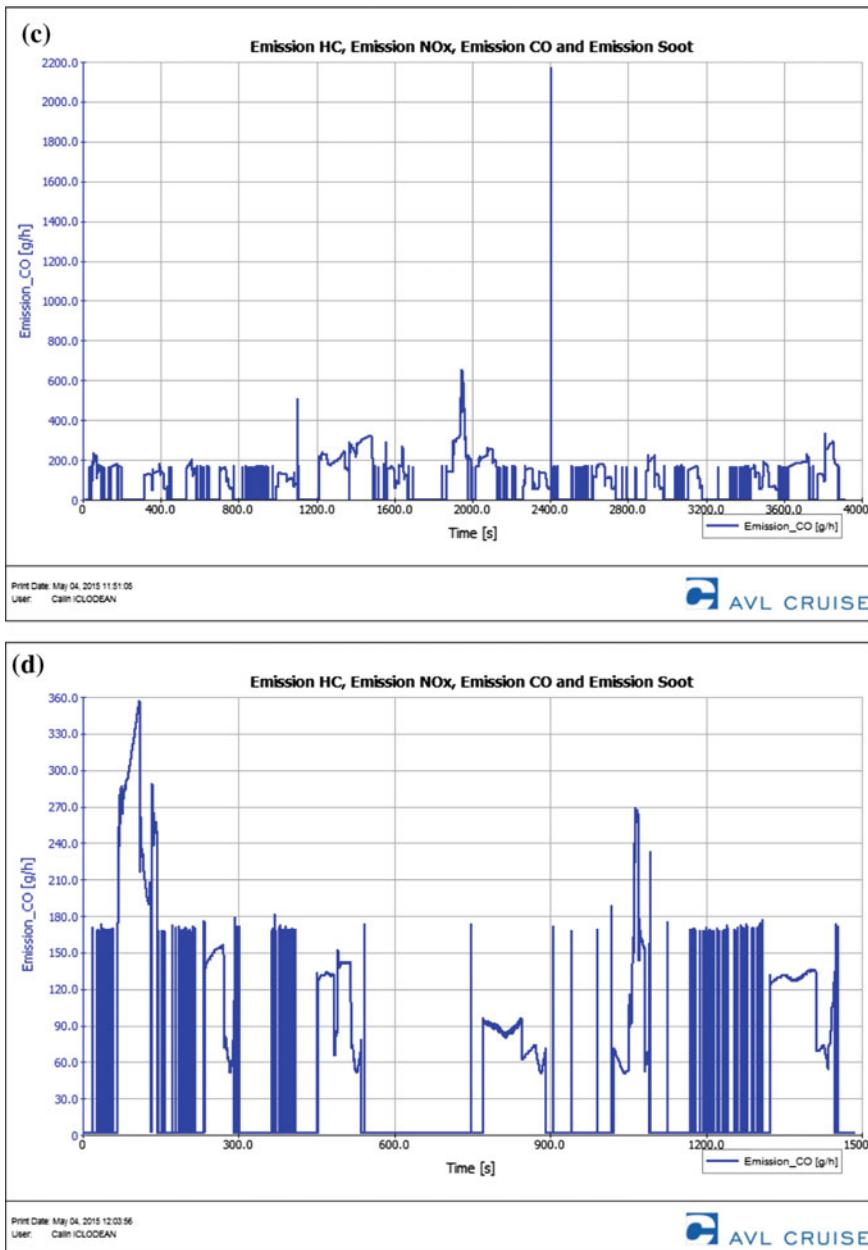
Fig. 7.48 (continued)
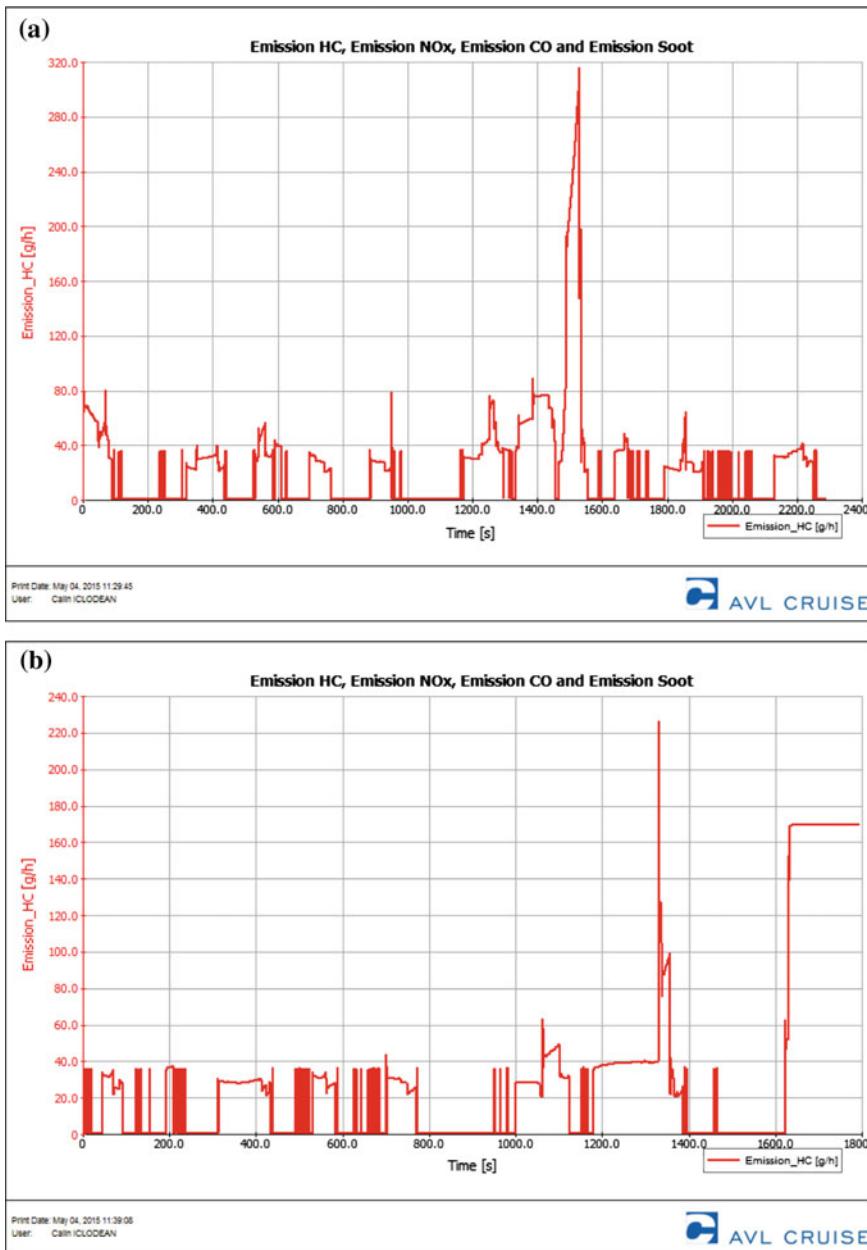
Fig. 7.49 HC emissions generated by the classic bus: **a** route 27, **b** route 28, **c** route 30 and **d** route 32

Fig. 7.49   (continued)
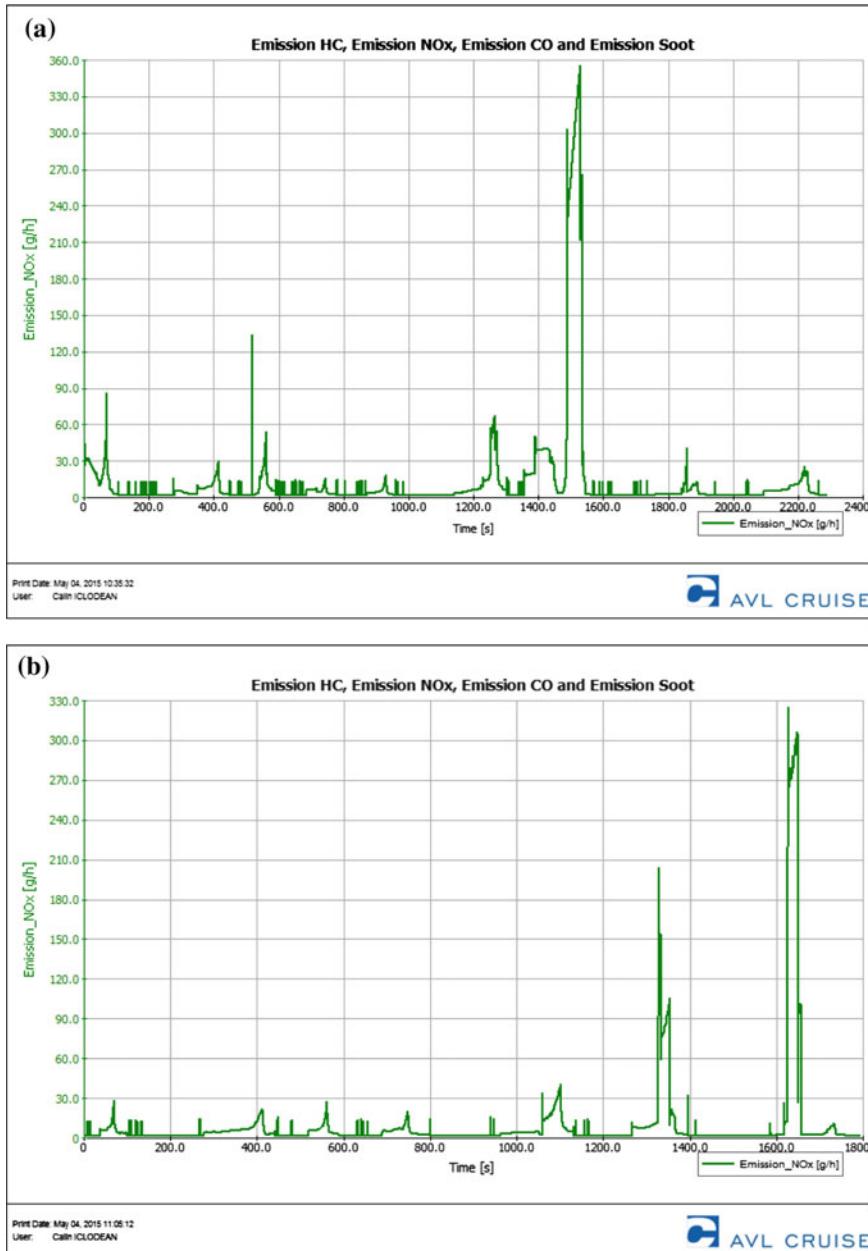
Fig. 7.50 NO$_x$ emissions generated by the hybrid bus: **a** route 27, **b** route 28, **c** route 30 and **d** route 32
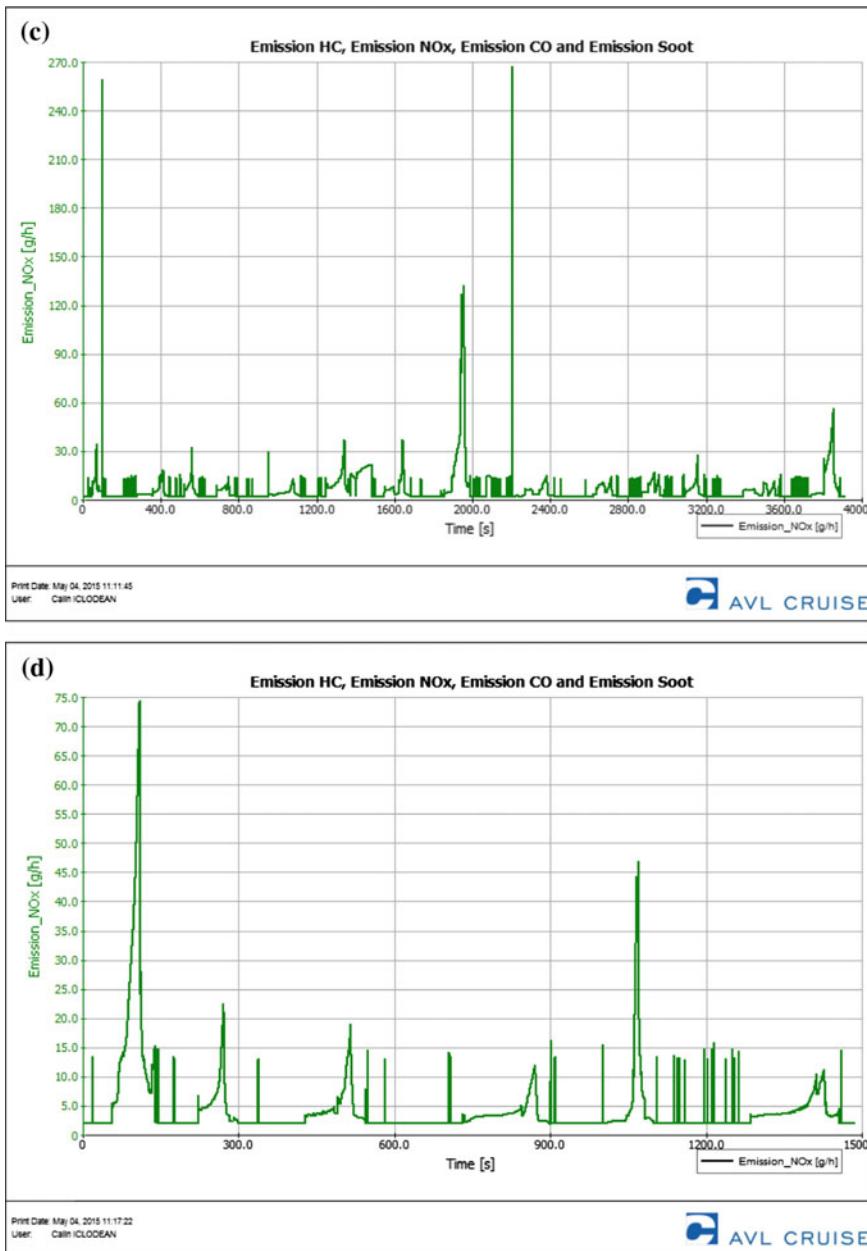
Fig. 7.50 (continued)
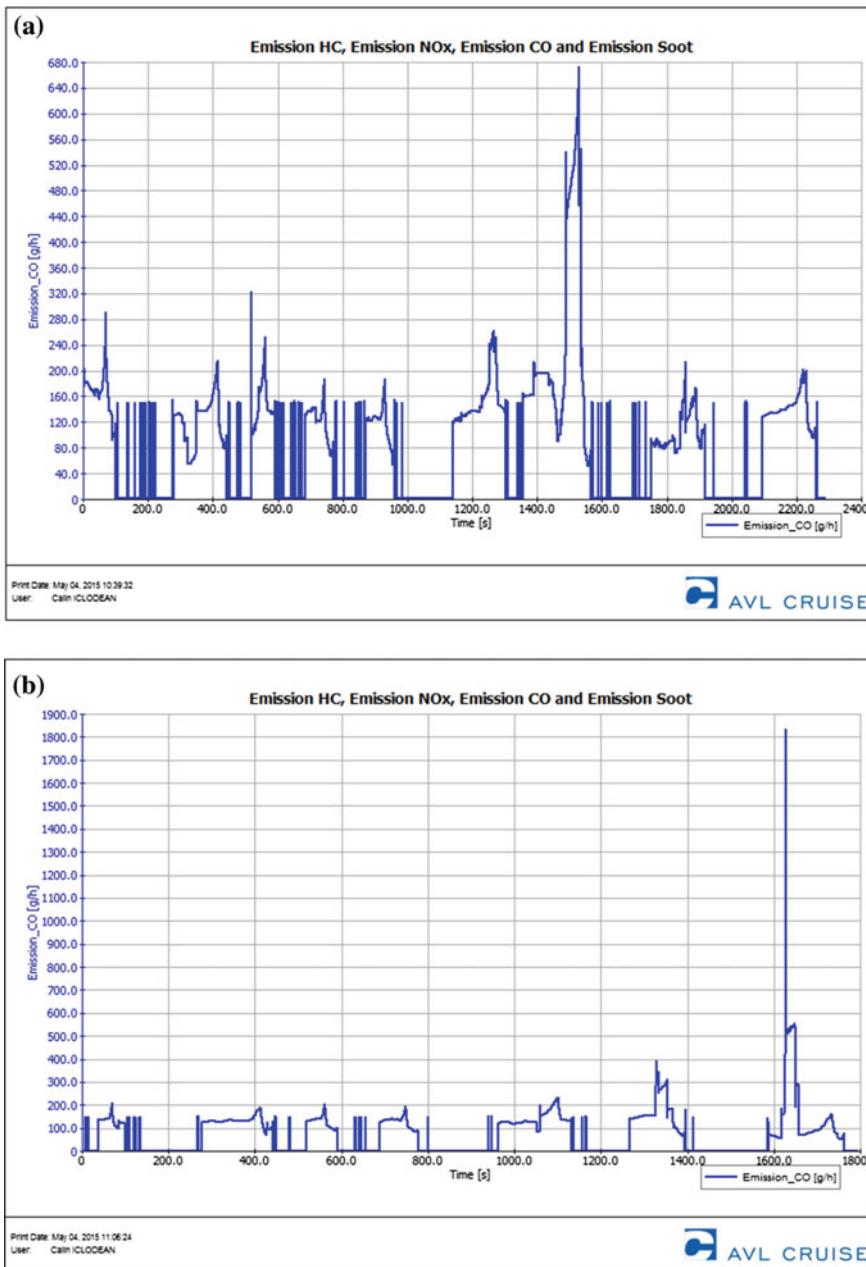
Fig. 7.51 CO emissions generated by the hybrid bus: **a** route 27, **b** route 28, **c** route 30 and **d** route 32
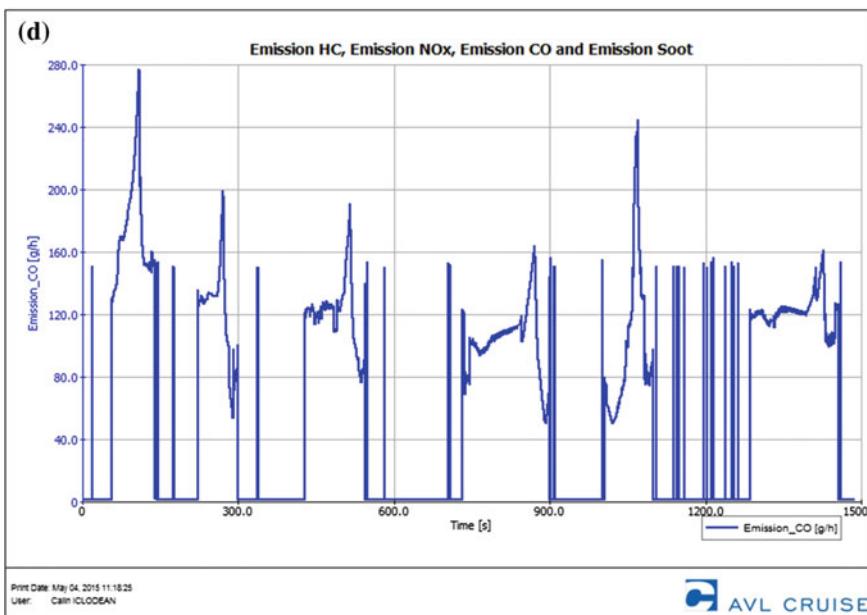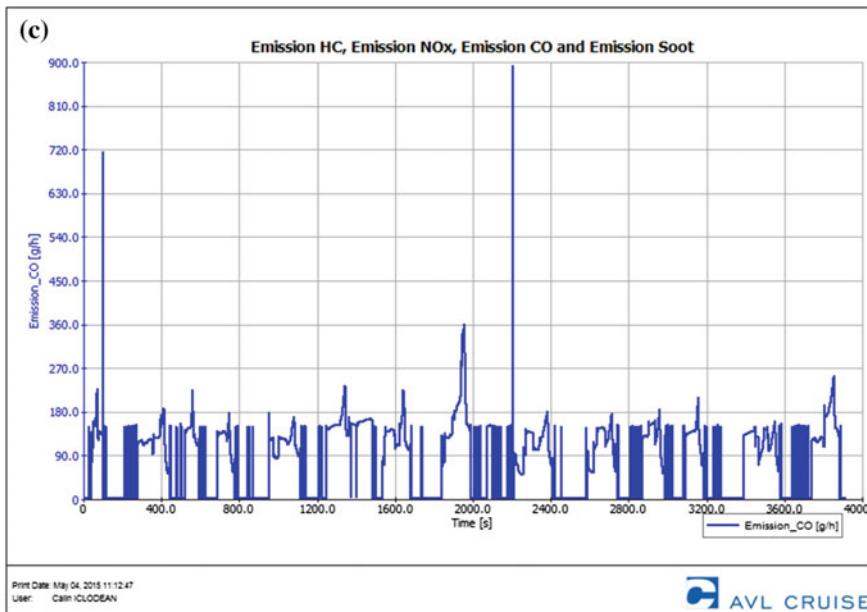
Fig. 7.51   (continued)
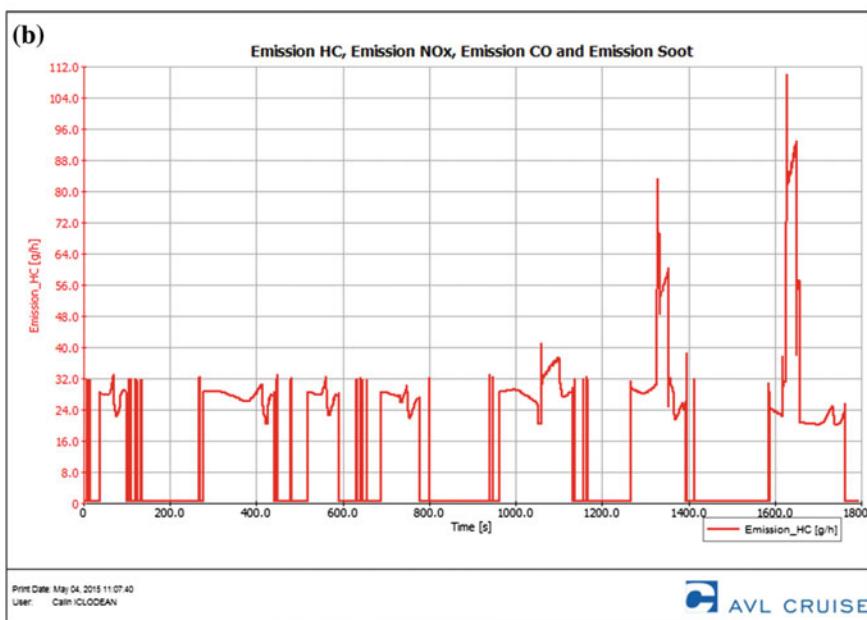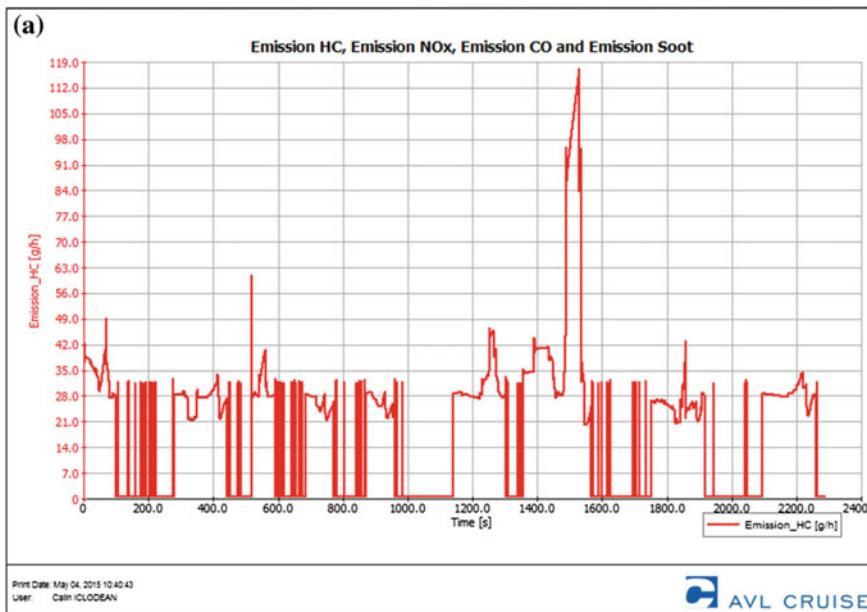
Fig. 7.52 HC emissions generated by the hybrid bus: **a** route 27, **b** route 28, **c** route 30 and **d** route 32
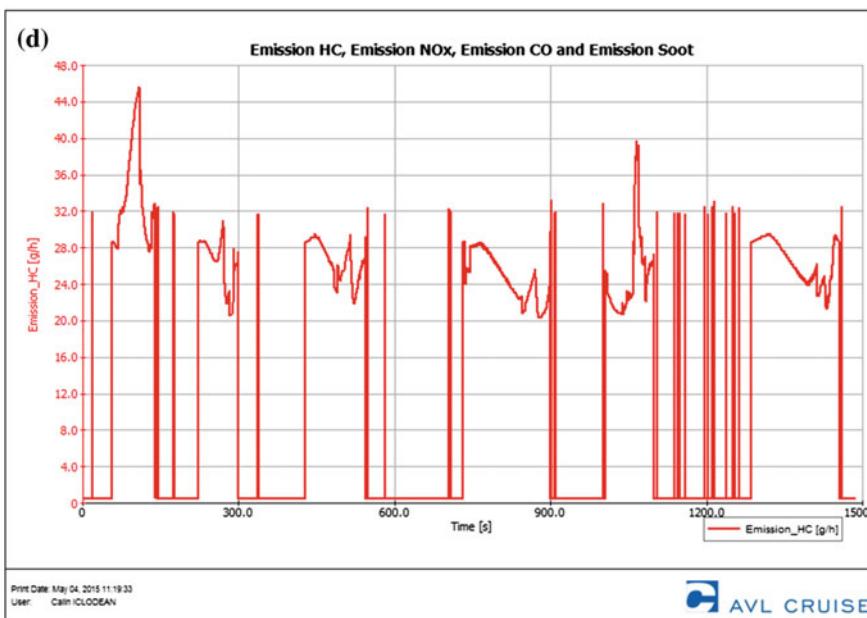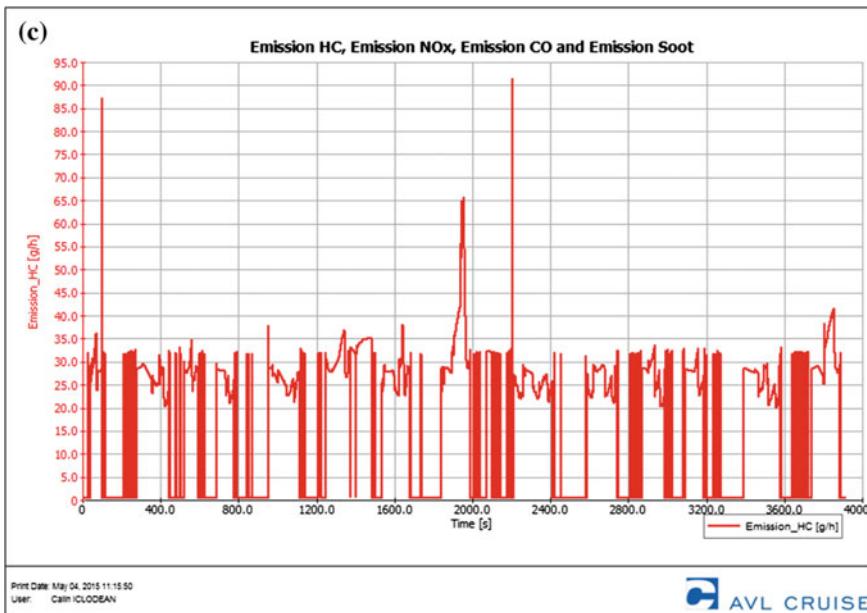
Fig. 7.52 (continued)
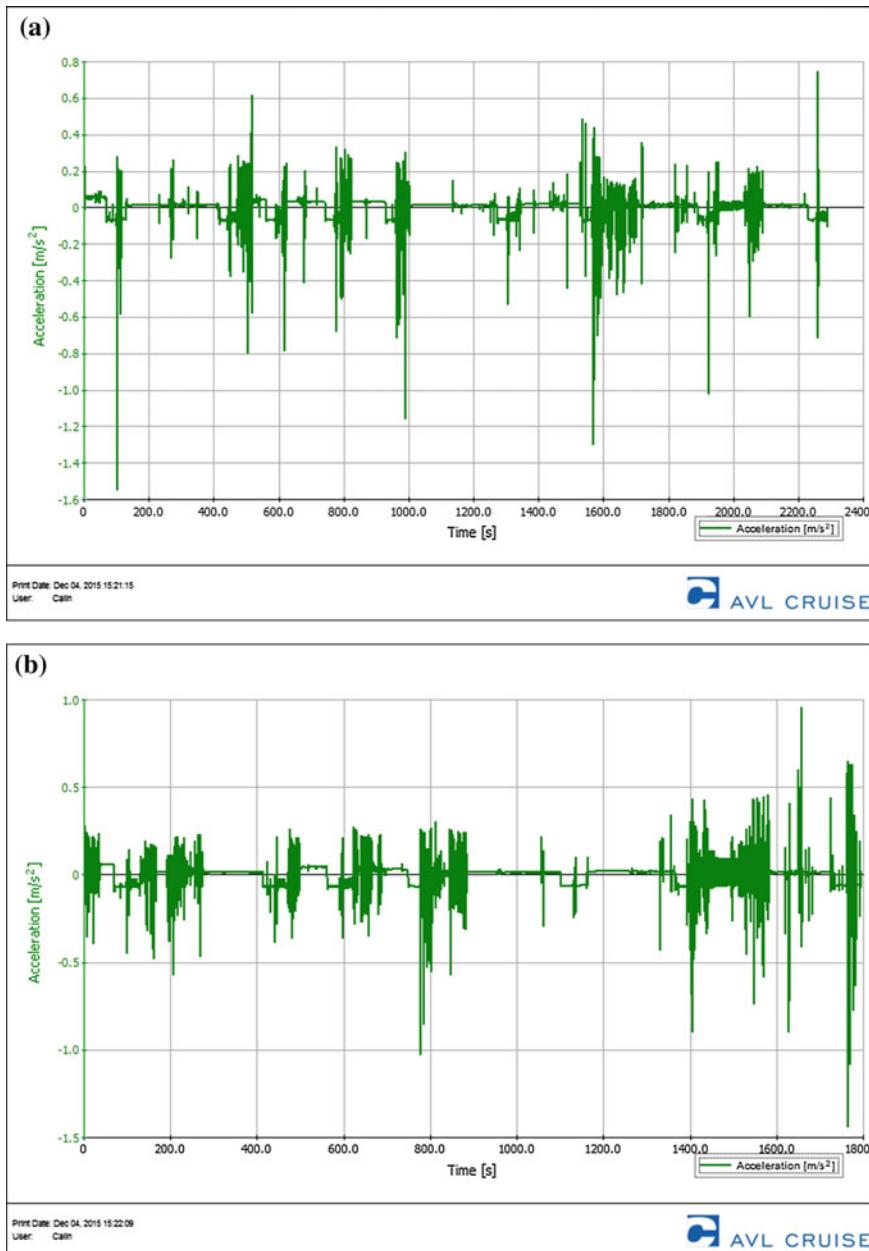
Fig. 7.53 Acceleration generated by the classic bus: **a** route 27, **b** route 28, **c** route 30 and **d** route 32
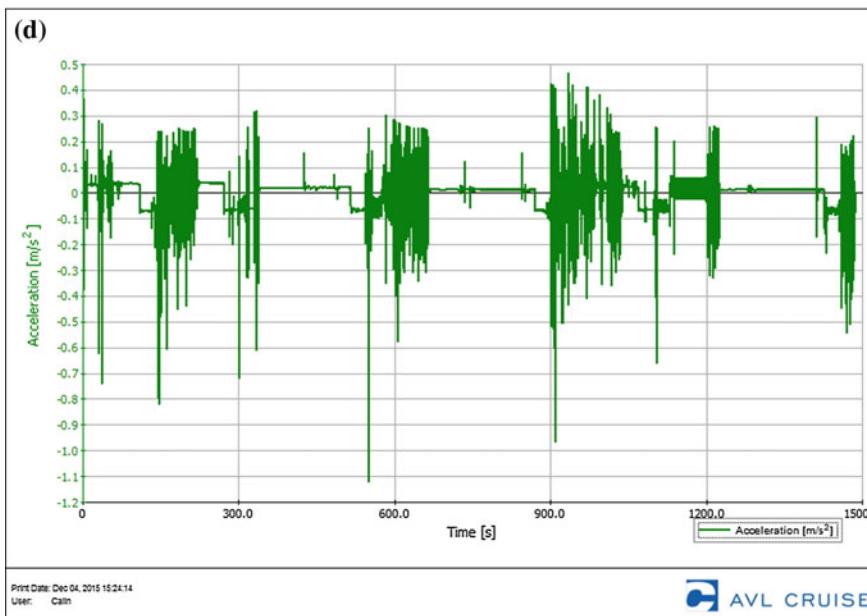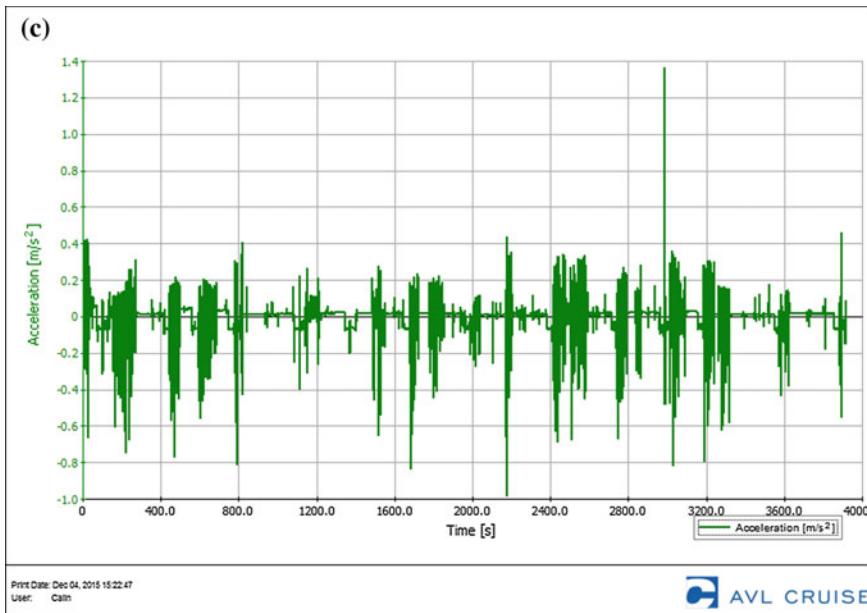
Fig. 7.53 (continued)

Fig. 7.54 Acceleration generated by the hybrid bus: **a** route 27, **b** route 28, **c** route 30 and **d** route 32
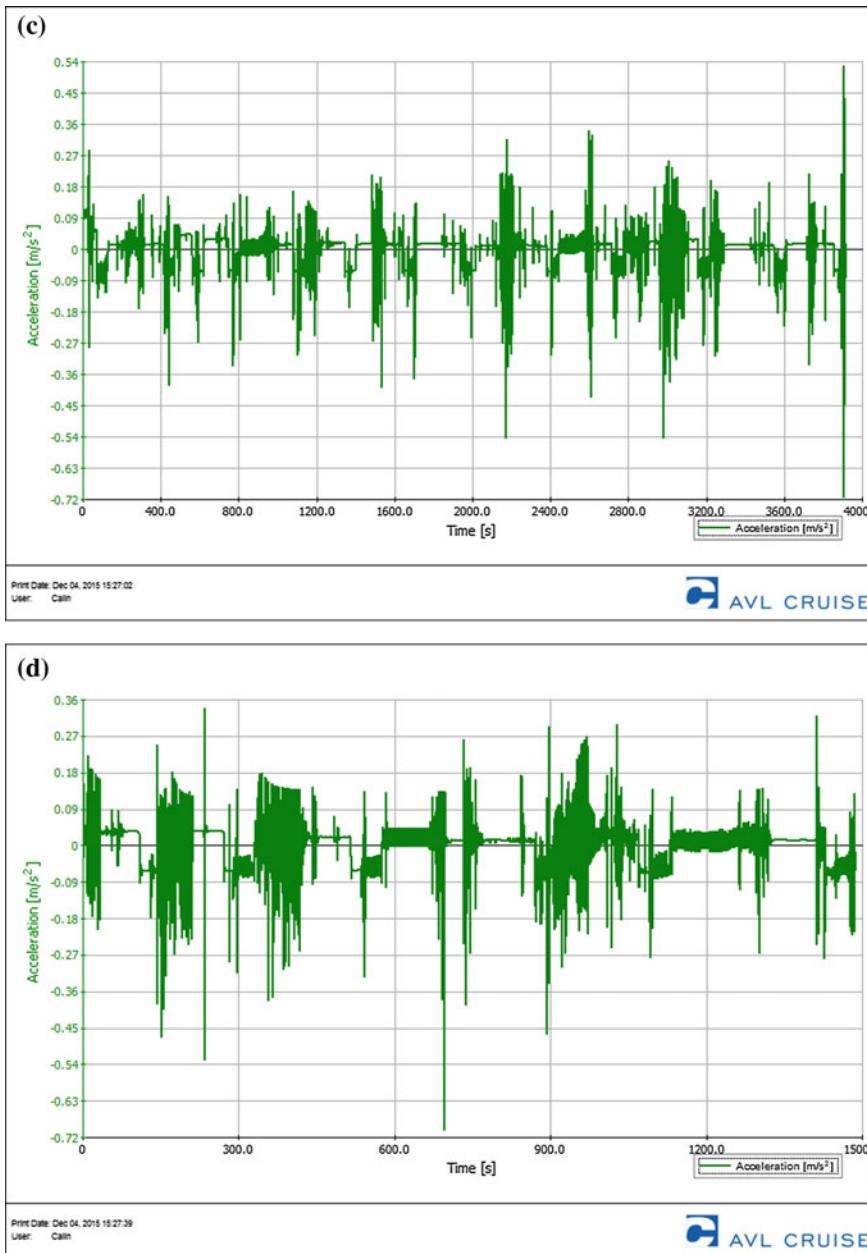
Fig. 7.54 (continued)

Fig. 7.55 Acceleration generated by the electric bus: **a** route 27, **b** route 28, **c** route 30 and **d** route 32
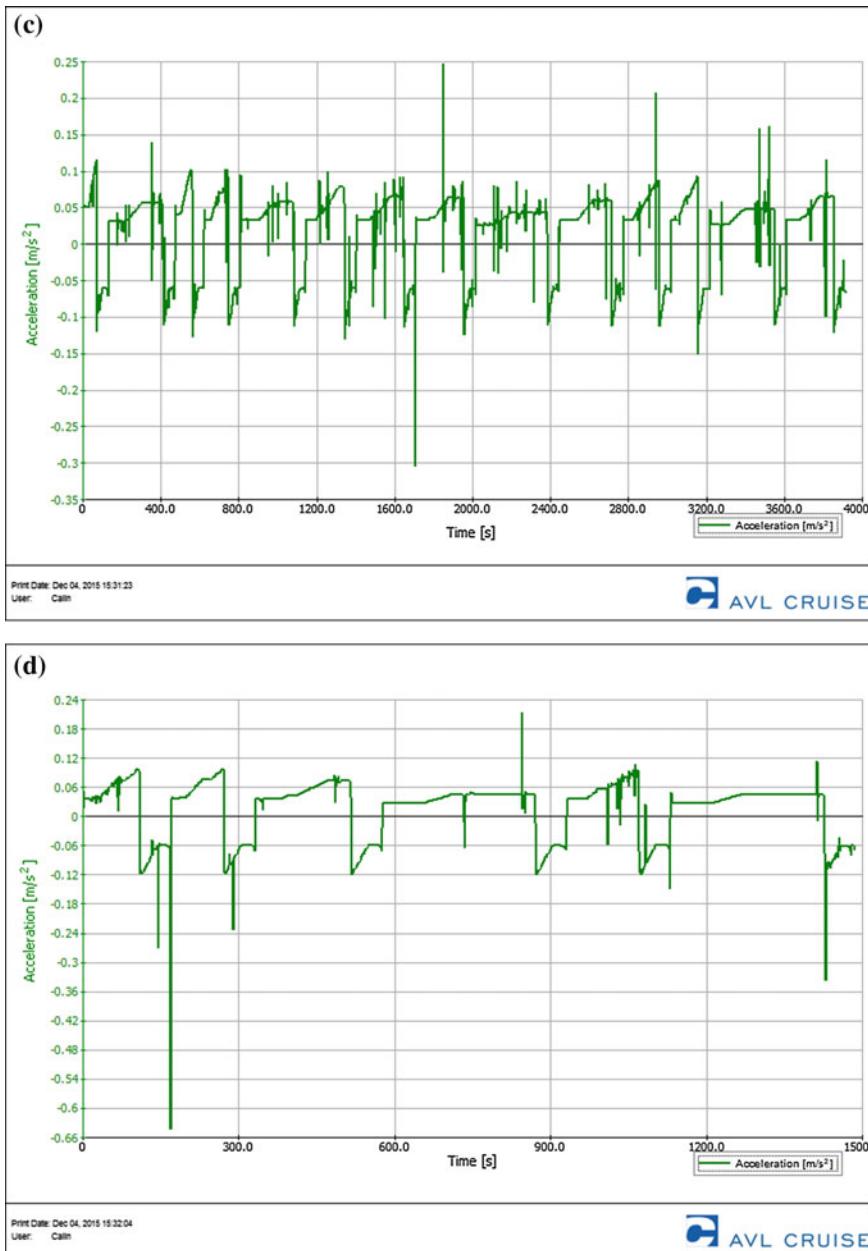
Fig. 7.55 (continued)
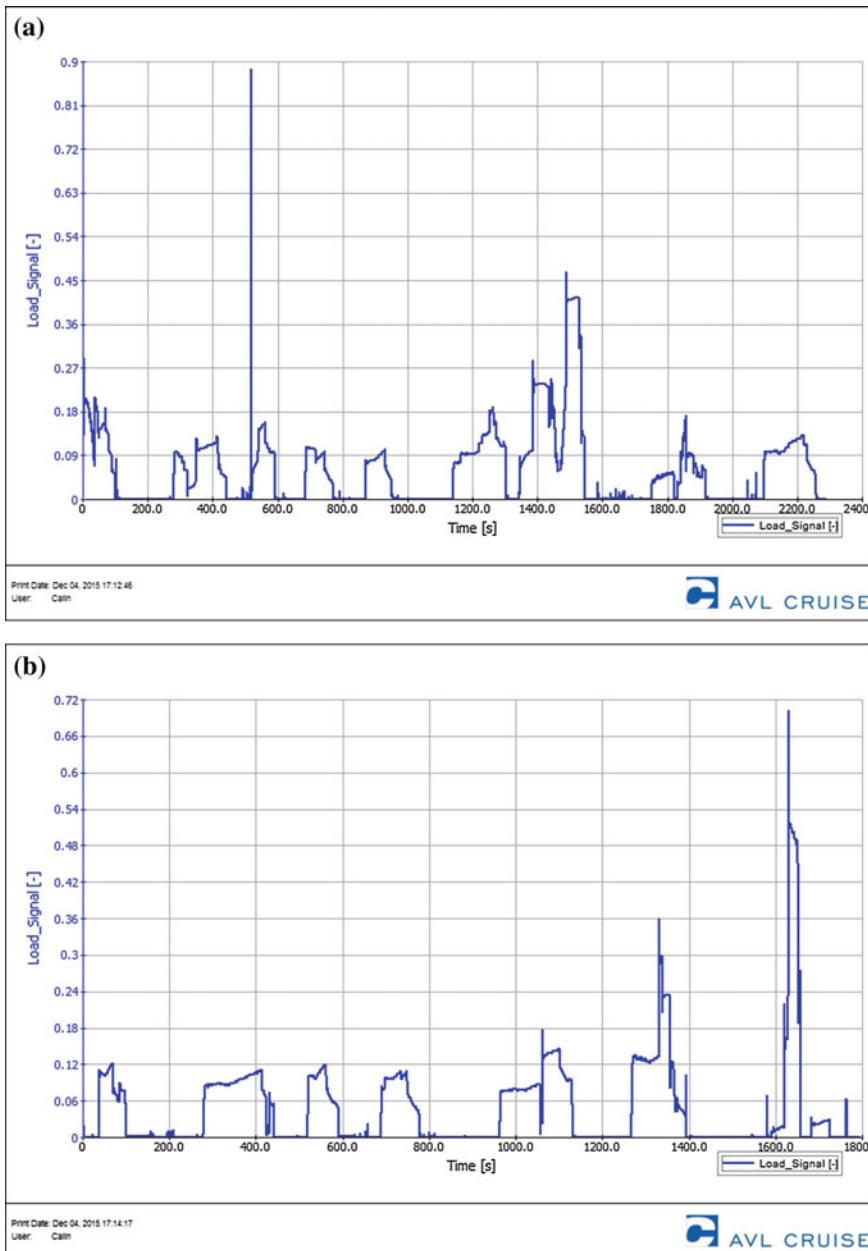
Fig. 7.56 Load Signal for the classic bus: **a** route 27, **b** route 28, **c** route 30 and **d** route 32
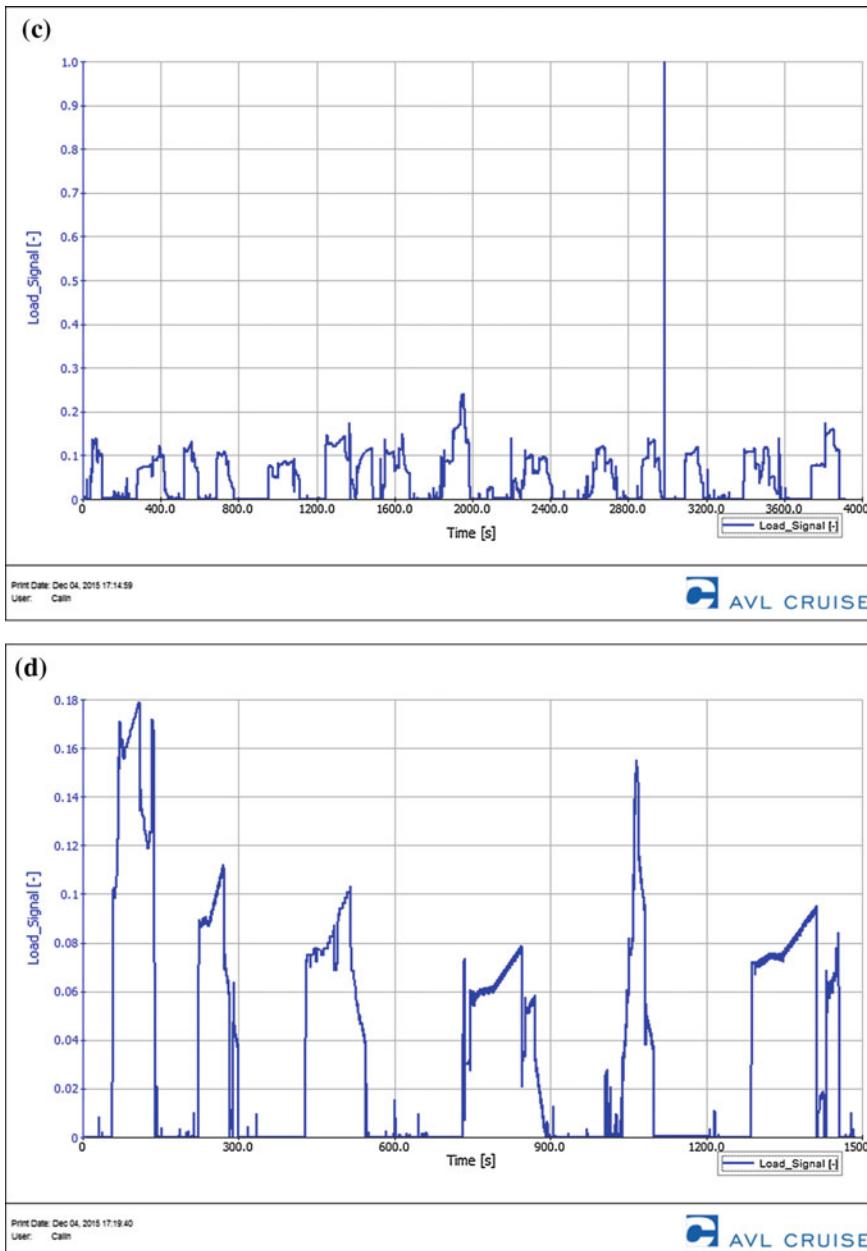
Fig. 7.56 (continued)

presented in Fig. 7.58a–d. The traction force of the classic bus is presented in Fig. 7.59a–d, the traction for of the hybrid bus is presented in Fig. 7.60a–d, respectively the traction force of the electric bus is presented in Fig. 7.61a–d.

Due to the electric motor which has a maximum torque even from the start off and it stays constant until the bus reaches a high speed value (7000–8000 min^{-1}), the hybrid and electric buses have a maximum start off acceleration. While braking a part of the braking energy assures the battery recharge, a process which is known as energy regenerative braking. In the case of traffic in agglomerated urban areas, this energy recovery reduces considerably the fuel consumption and the values of pollutant emissions [7].

Due to the electronic control and automation systems which are integrated in the electric motor, the motor has an efficiency of over 80 % and this efficiency increase proportionally with the motor nominal power and it is maintained for a long interval within the functioning domain.

The total raw emissions for the classic bus are presented in Fig. 7.62a–d, and the ones for the hybrid bus are presented in Fig. 7.63a–d.

Compared to the classic buses, the hybrid and electric buses have a higher acceleration value and they need a shorter amount of time to reach maximum velocity, thus resulting increased fuel savings, a reduced quantity of pollutant emissions and the reach of superior dynamic performances for these bus models.

The savings generated by electric buses depend on the way in which the electric power is obtained, namely starting from 30 % in the case of generating electricity from the national network with CO_2 emissions, up to 100 % in the case of generating electricity from renewable electricity sources [8].

Electric buses do not produce emissions at the exhaust pipe, which means zero local emissions. Although they require a greater initial investment, electric buses offer the advantages of saving money with fuel and reducing maintenance costs due to the smaller amount of moving components.

The presented analysis comprises the comparative study of total values regarding pollutant emissions in the atmosphere, for which was taken into consideration and highlighted the pollutant quantity in kg, calculated according to the emissions factor afferent to the simulated bus models, according to the type of engine equipping the buses and according to the distance traveled for each route individually.

In the presented graphics it can be observed that there is a considerable diminution of pollutant concentration between buses equipped with thermal engine and hybrid buses. In the case of buses with electric drive, all emission indicators analyzed were considered zero (locally).

Also, a comparative representation of greenhouse gases emissions (GHG) was made between the analyzed drive systems, more precisely for CO_2 emissions, by using the afferent emission factors according to fuel consumption for 100 km traveled, for which the total quantity of consumed fuel for the traveled distance is divided by the afferent emission factors.
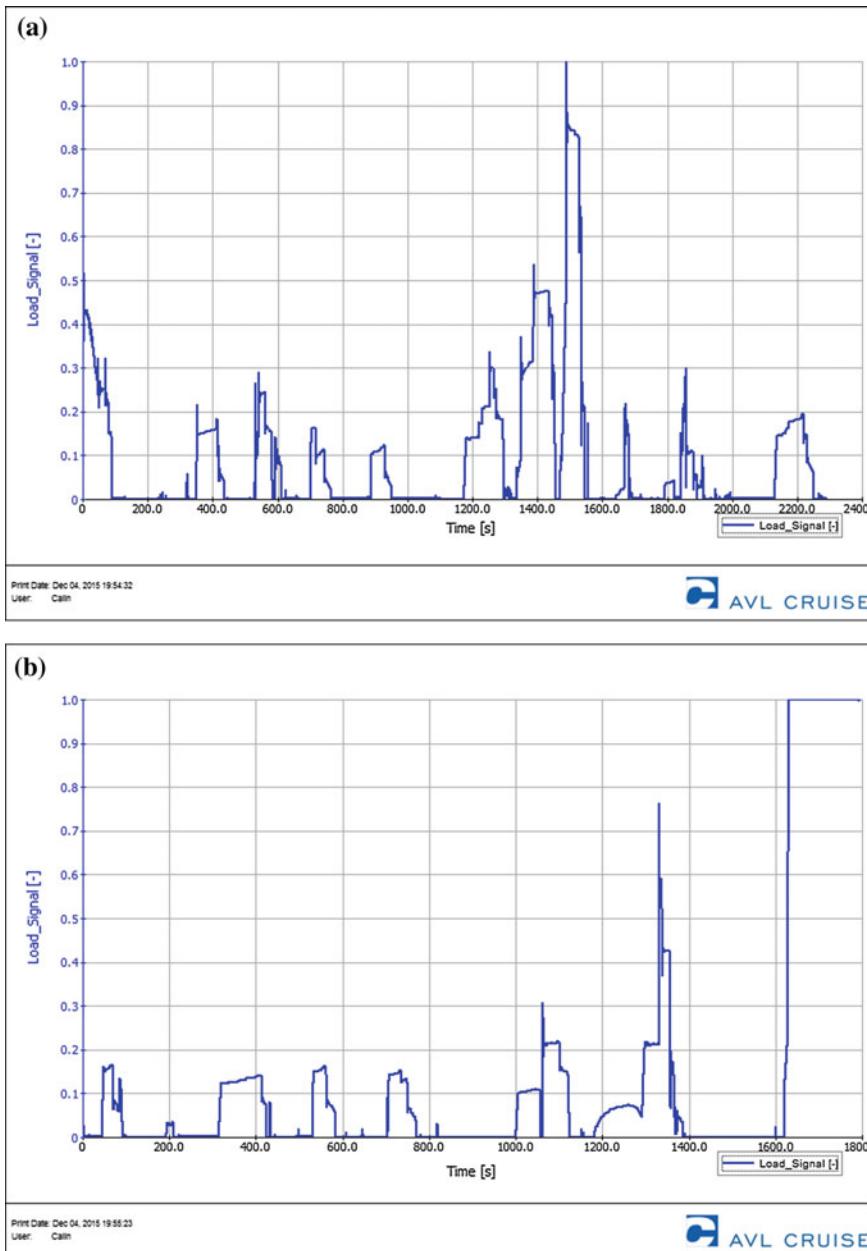
Fig. 7.57 Load Signal for the hybrid bus: **a** route 27, **b** route 28, **c** route 30 and **d** route 32
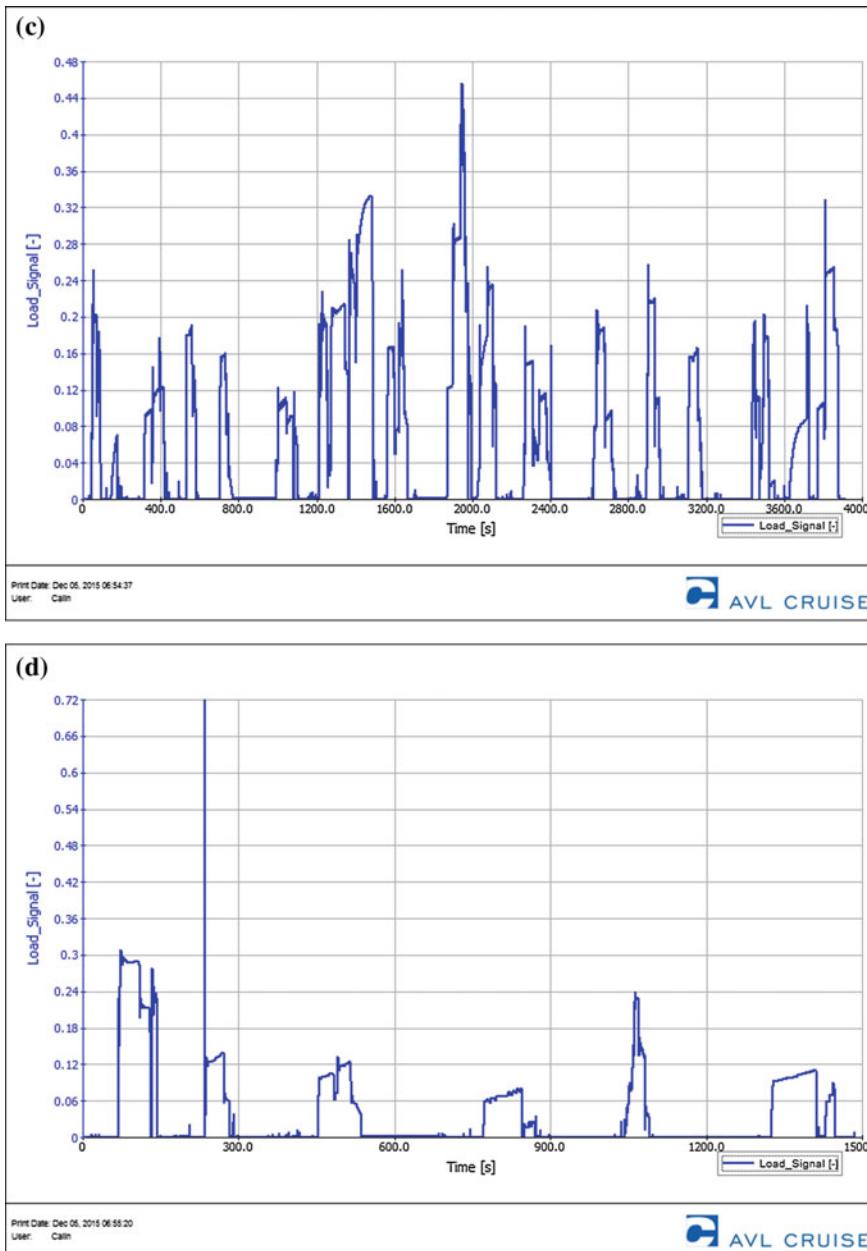
Fig. 7.57   (continued)
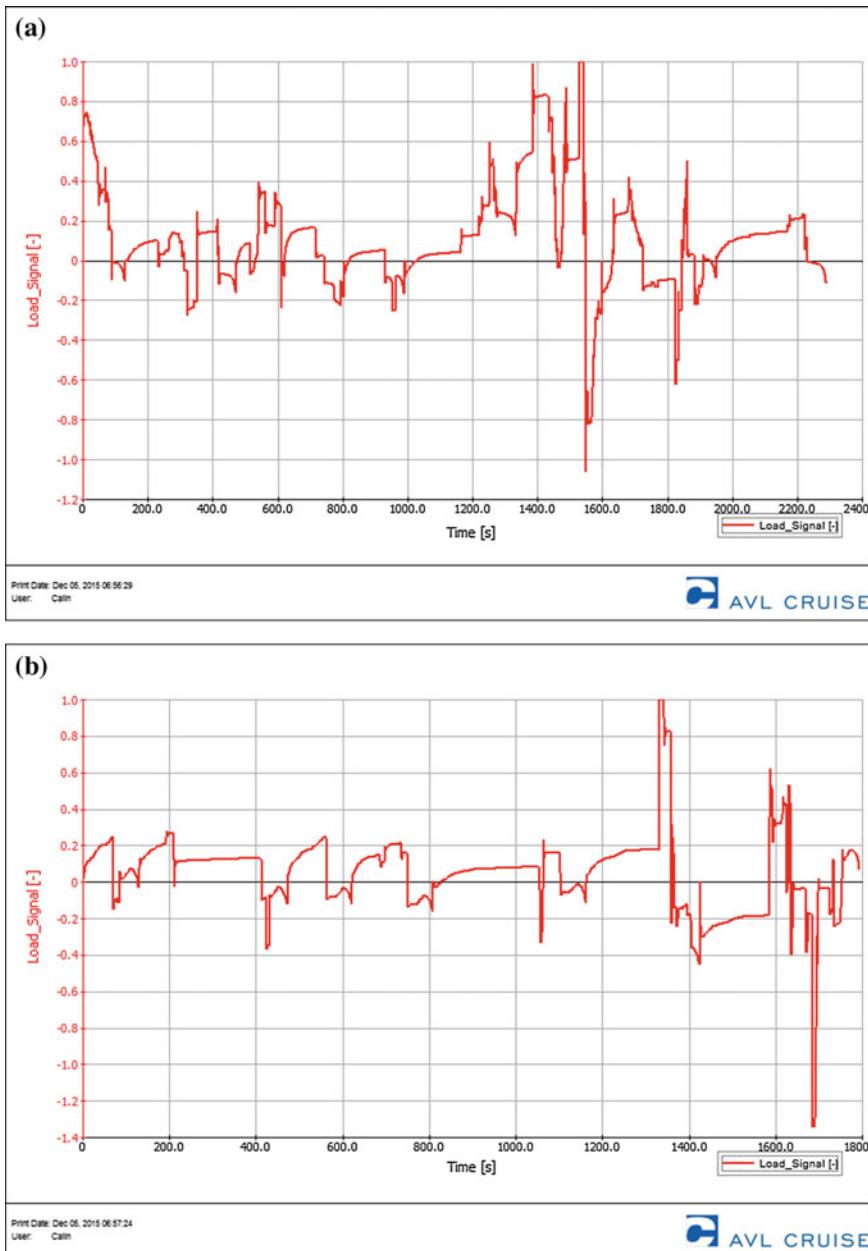
Fig. 7.58 Load Signal for the electric bus: **a** route 27, **b** route 28, **c** route 30 and **d** route 32
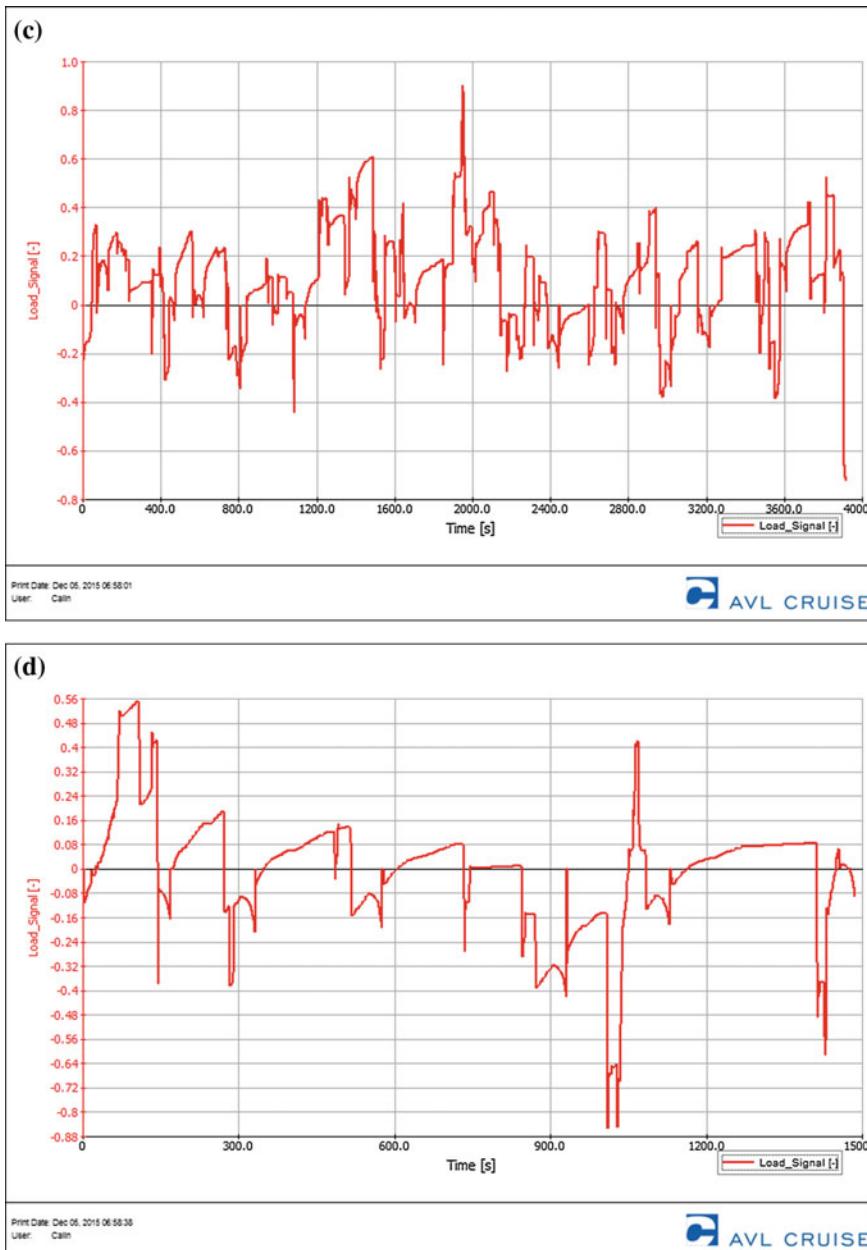
Fig. 7.58   (continued)
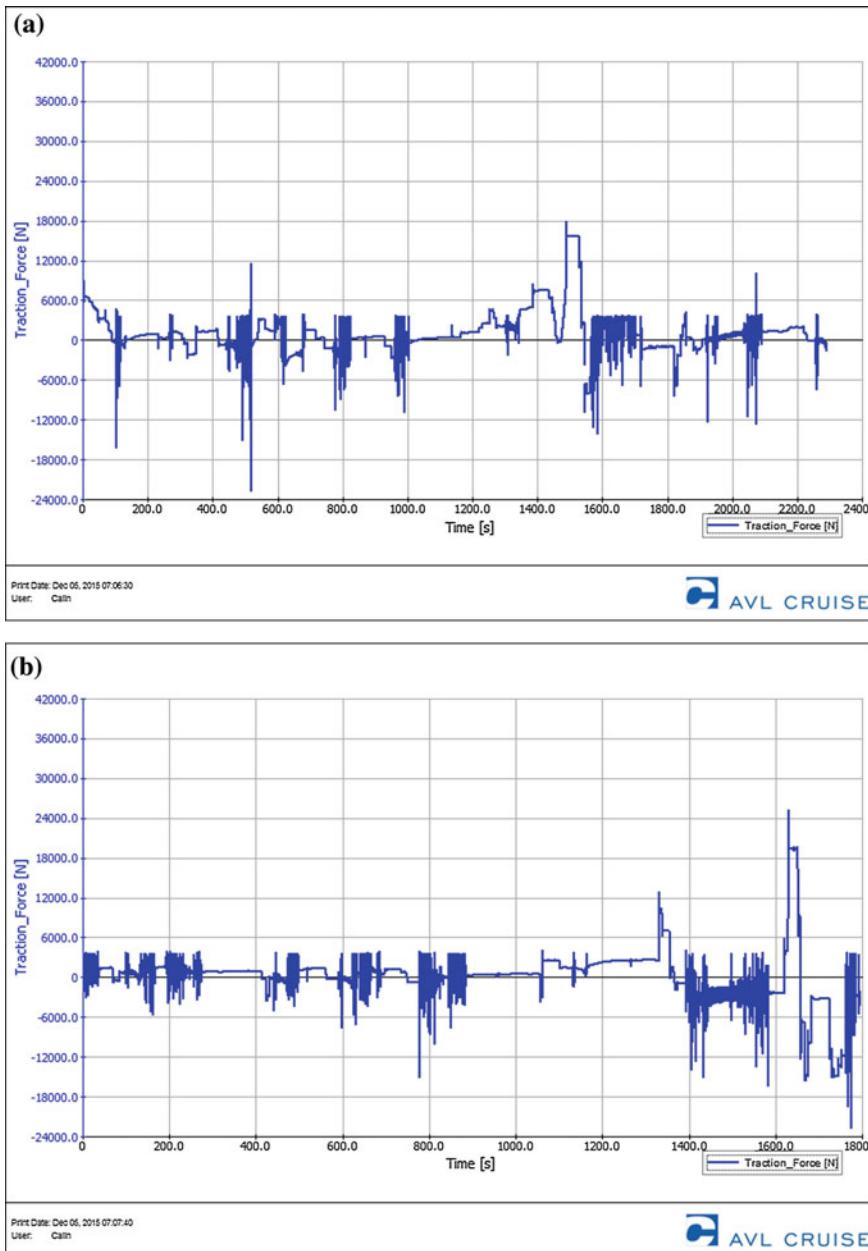
Fig. 7.59 Traction force of the classic bus: **a** route 27, **b** route 28, **c** route 30 and **d** route 32
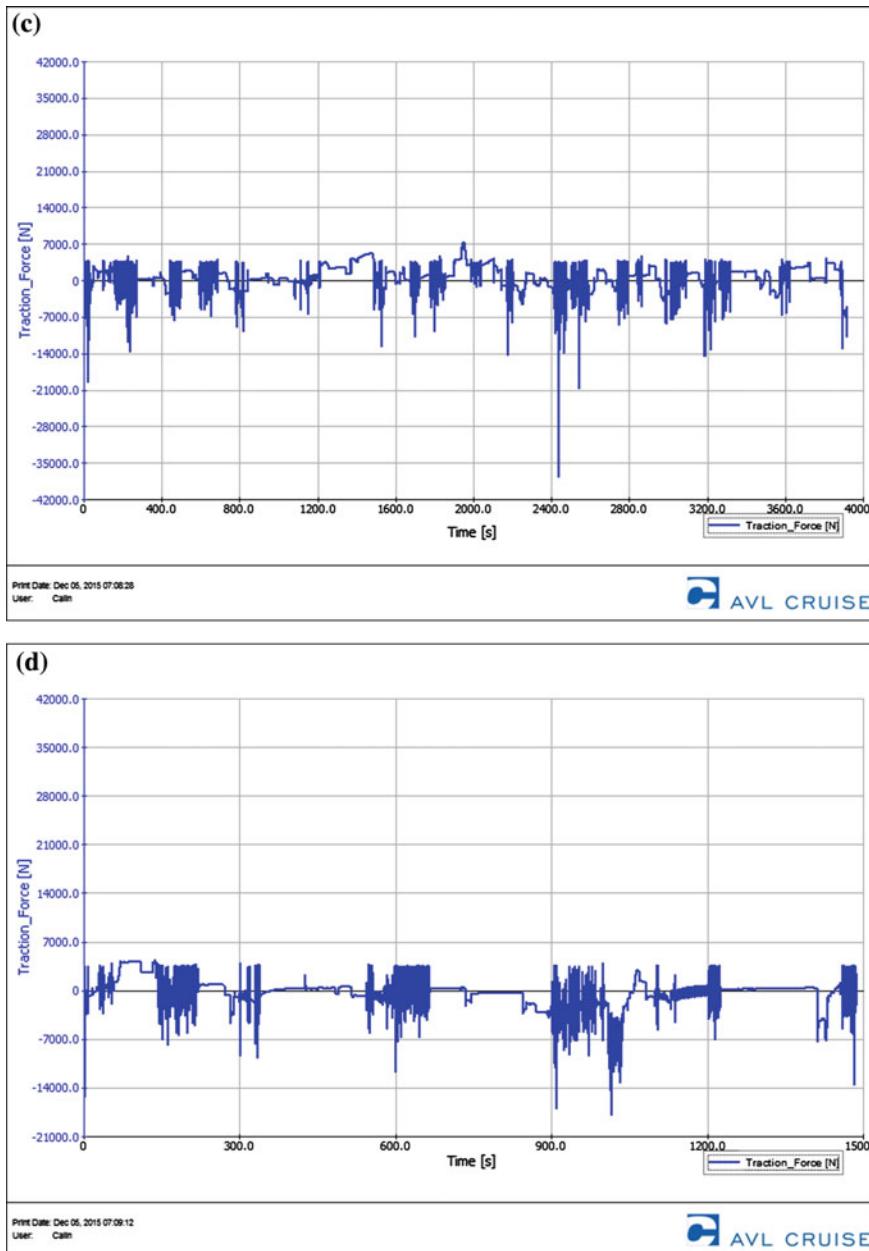
Fig. 7.59   (continued)
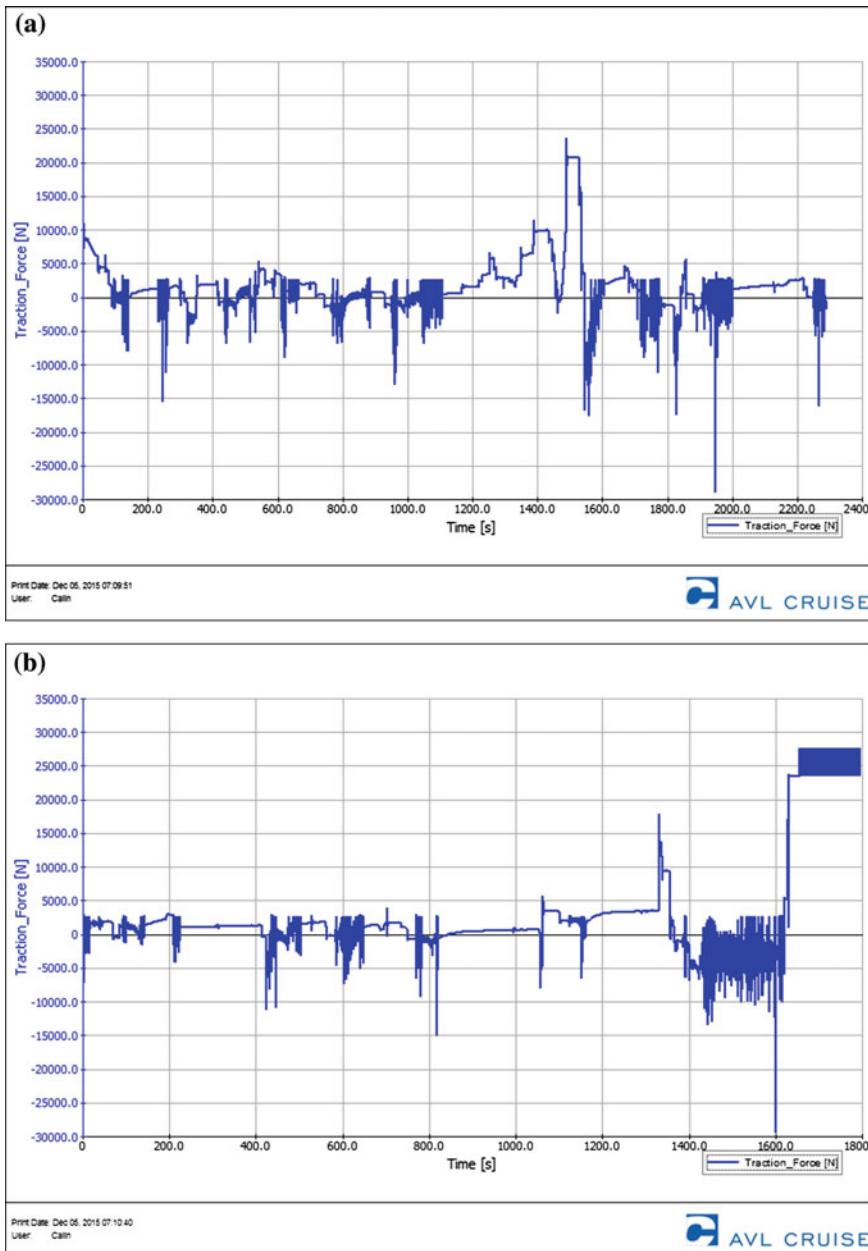
Fig. 7.60 Traction force of the hybrid bus: **a** route 27, **b** route 28, **c** route 30 and **d** route 32
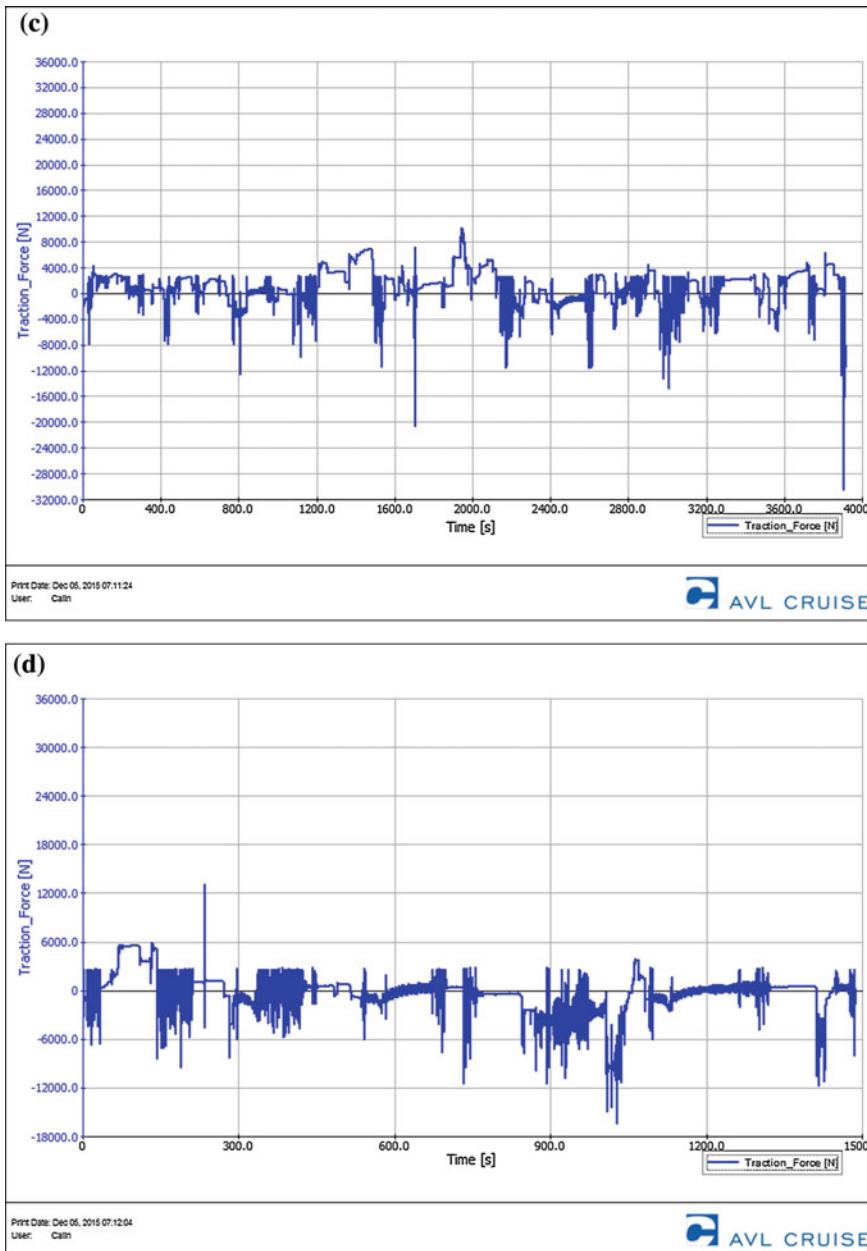
Fig. 7.60 (continued)
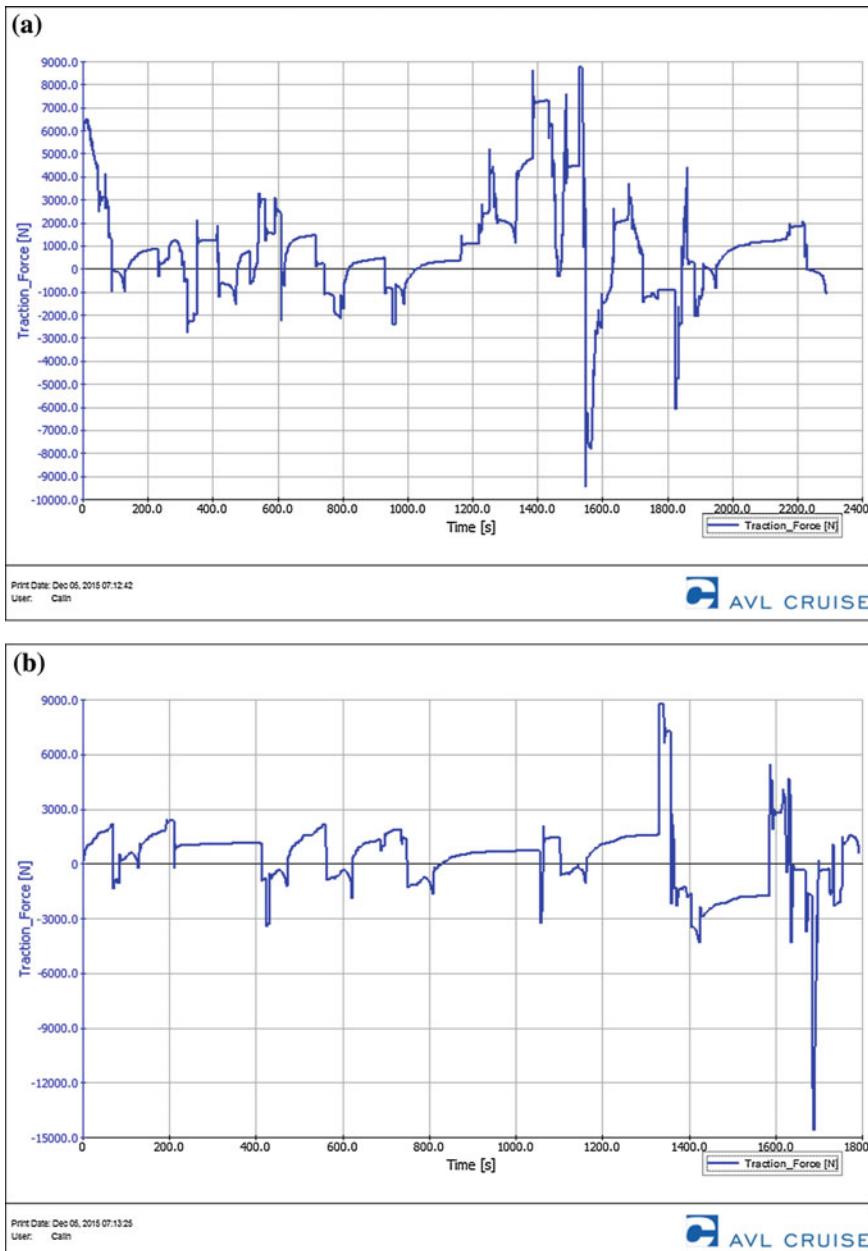
Fig. 7.61 Traction force of the electric bus: **a** route 27, **b** route 28, **c** route 30 and **d** route 32
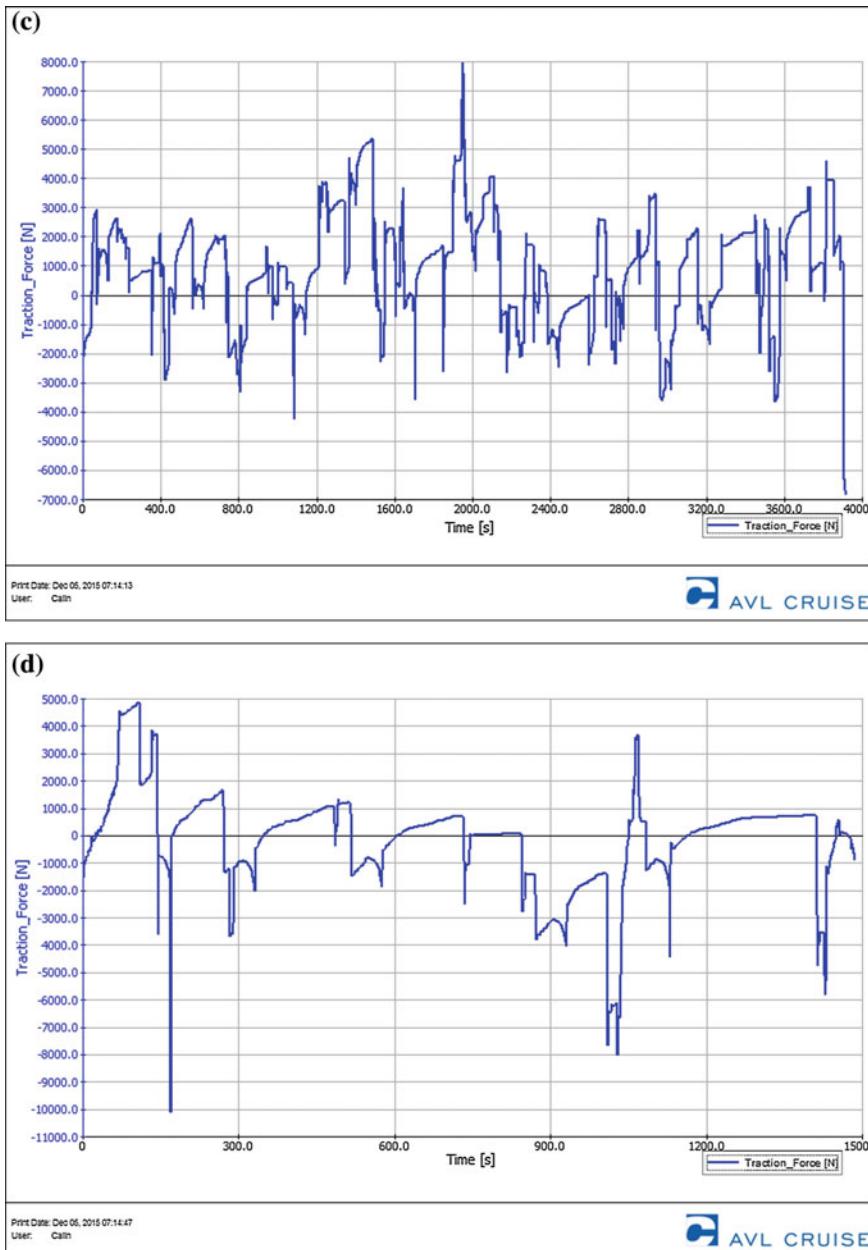
Fig. 7.61 (continued)
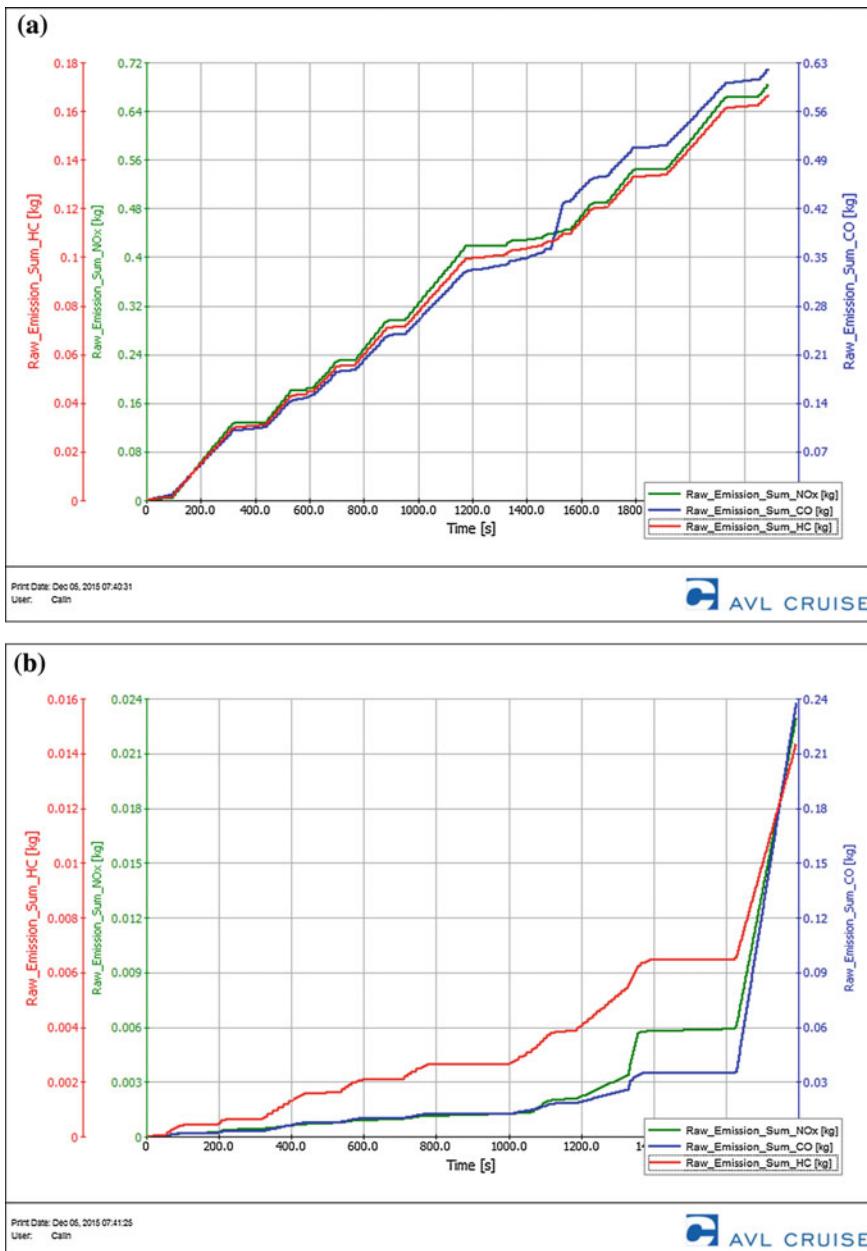
Fig. 7.62 Total Raw Emission for the classic bus: **a** route 27, **b** route 28, **c** route 30 and **d** route 32

Fig. 7.62   (continued)

(a)

(b)
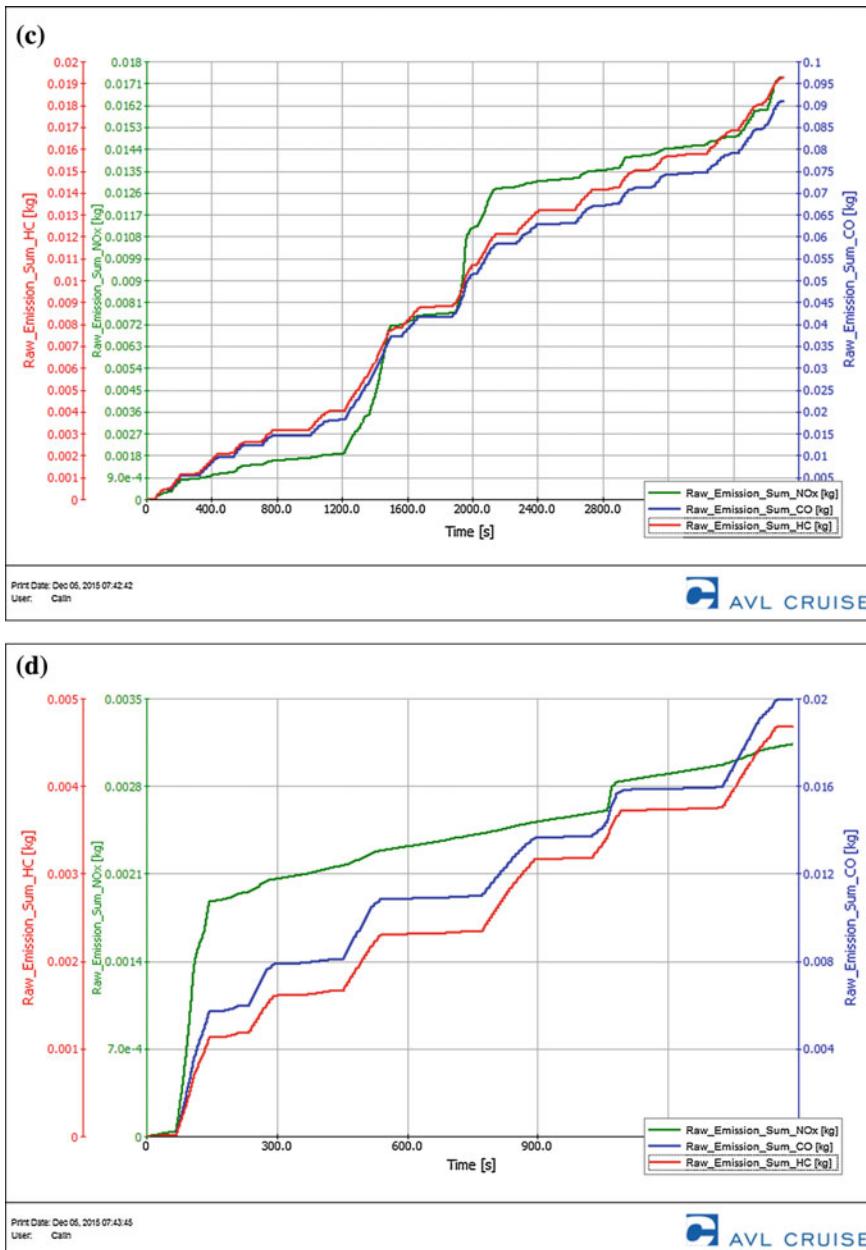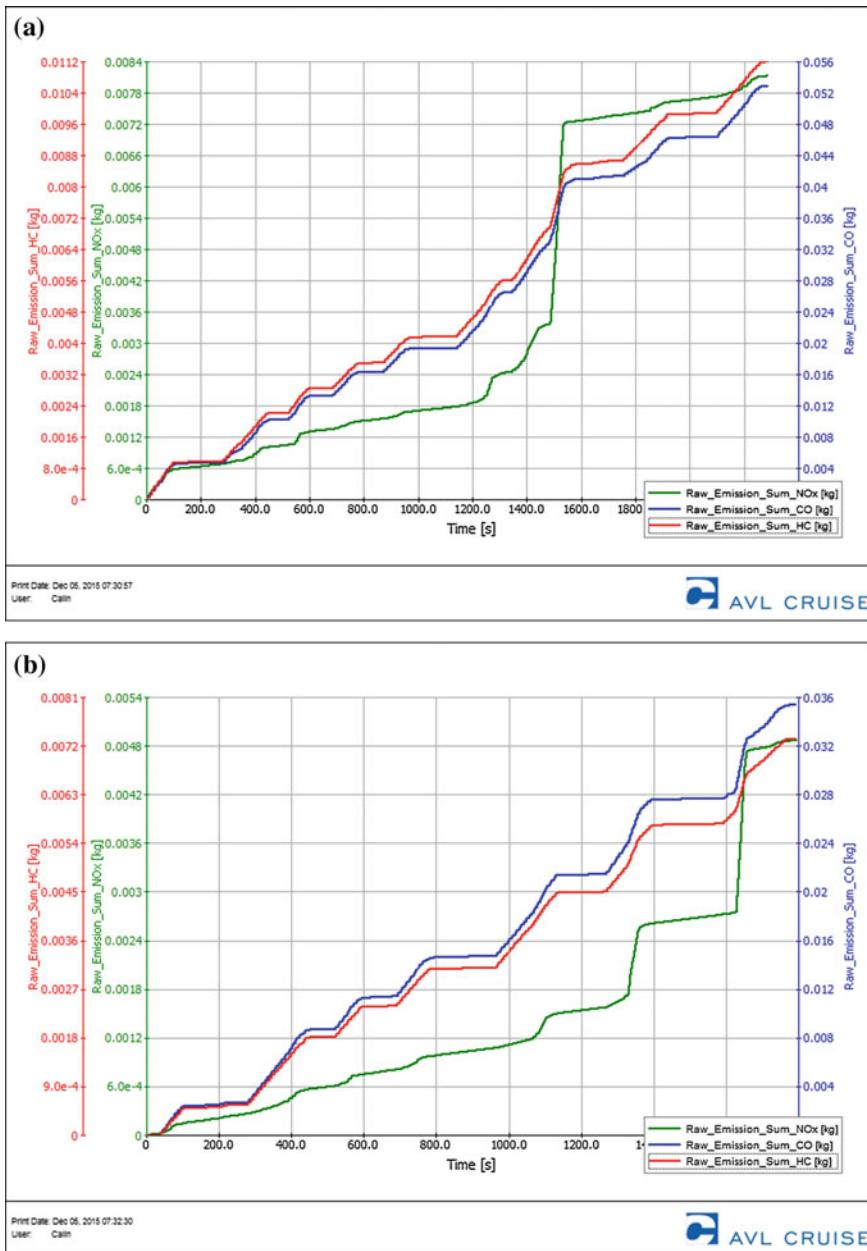
Fig. 7.63 Total Raw Emission for the hybrid bus: **a** route 27, **b** route 28, **c** route 30 and **d** route 32
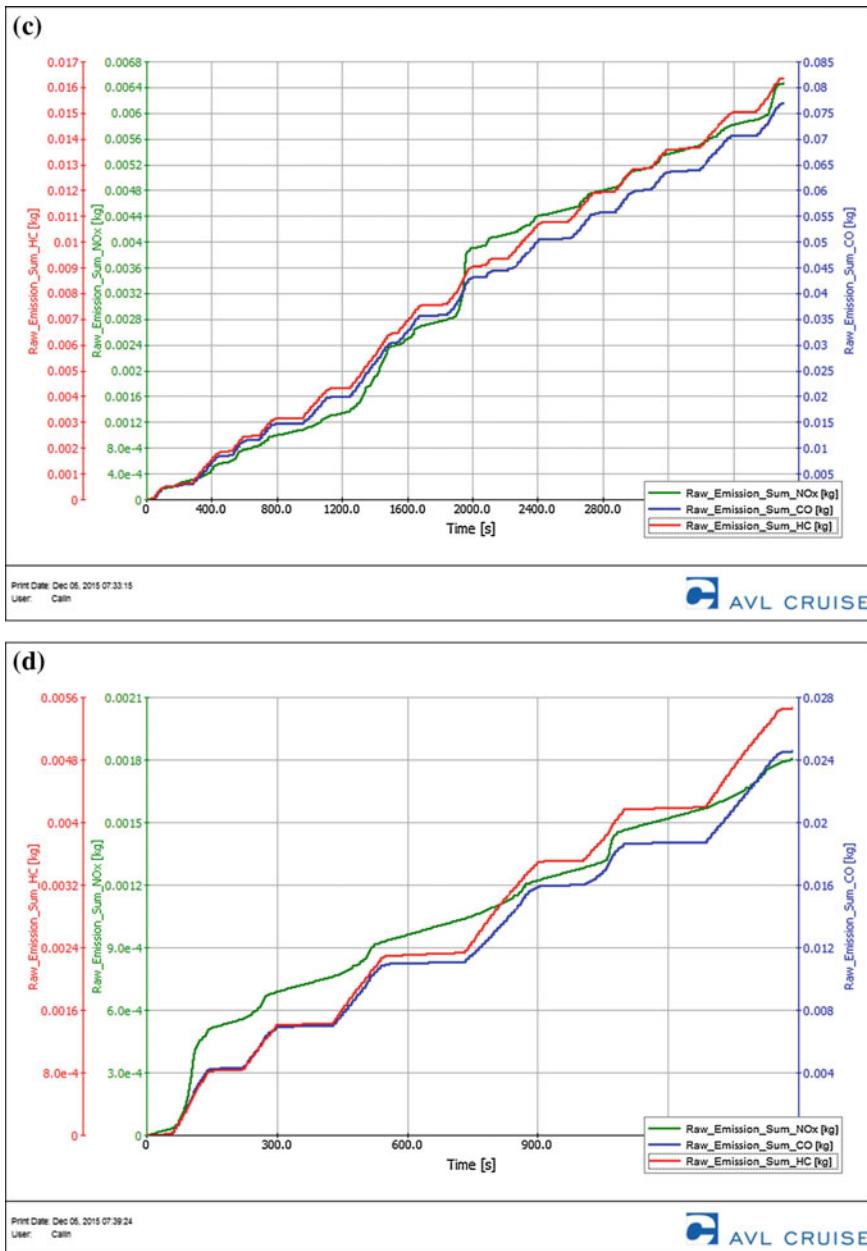
Fig. 7.63   (continued)

The graphic analysis reflects the diminution of greenhouse gas emissions, mainly of CO_2 emissions according to the studied drive system and in this case for the electric bus the CO_2 emissions have a zero value (locally).

The battery discharge current variation for the hybrid but on the selected routes is presented in Fig. 7.64a–d, respectively for the classic bus on the selected routes is presented in Fig. 7.67a–d. The power supply voltage variation for the hybrid bus on the selected routes is presented in Fig. 7.66a–d, respectively for the electric bus on the selected routes is presented in Fig. 7.69a–d (Fig. 7.65).

By tracking the profile and the elevations of the digitized routes which were used in creating the computer simulations, it can be observed that the increase in altitude difference is made simultaneously with the increase of the electric battery discharge current value with which are equipped the hybrid and electric buses.

Even though during the descent of a slope the electric motor is less used and in most descending cases intervenes the energy regenerative braking, the battery discharge current for electric motor functioning is greater that the recovered value. For hybrid buses in these situations the thermal engine action intervenes which starts and assures together with the electric motor the bus movement and the energy necessary for charging the batteries.

The electric buses have an autonomy limited by the charging capacity of the batteries and the energy provided during regenerative braking, but in the situation of battery discharge under a critical level it is imposed to remain stationary at the end of the route to recharge the batteries.

In Fig. 7.65a–d and in Fig. 7.68a–d are presented the graphic regarding the evolution of energy consumption while the electric motor functions, respectively the graphic for the variation of electric battery discharge voltage for the hybrid bus and for the electric bus, data provided after the CRUISE—TruckMaker co-simulation process (Fig. 7.69).

The most economic routes in relation to the vehicles equipped with classic drive systems are significantly different from the exploitation concept of maximum energetic efficiency, corroborated with kinetic energy retrieval, which is one of the base principles for the concepts of hybrid or electric drive group, implicitly supporting their autonomy (Table 7.7).

Thus of all the selected routes for creating computer simulations, the ones having a maximum efficiency regarding electric energy consumption are the bus routes 28 and 30, which have the lowest difference in altitude variation between the ends of the route, fact which results from Table 7.8.

By analyzing the graphics from Fig. 7.51a–d, respectively Fig. 7.52a–d, one can observe that electric buses consume a larger quantity of electric energy due to the fact that for the entire traveled route only the electric motor was used, while the only recharging source while running was the energy regenerative braking. Hybrid buses use the electric motor for speeds of under 40 km/h and the thermal engine starts to function when these speeds are exceeded or when the energy from the batteries has reached a critical low level which imposes their recharging.
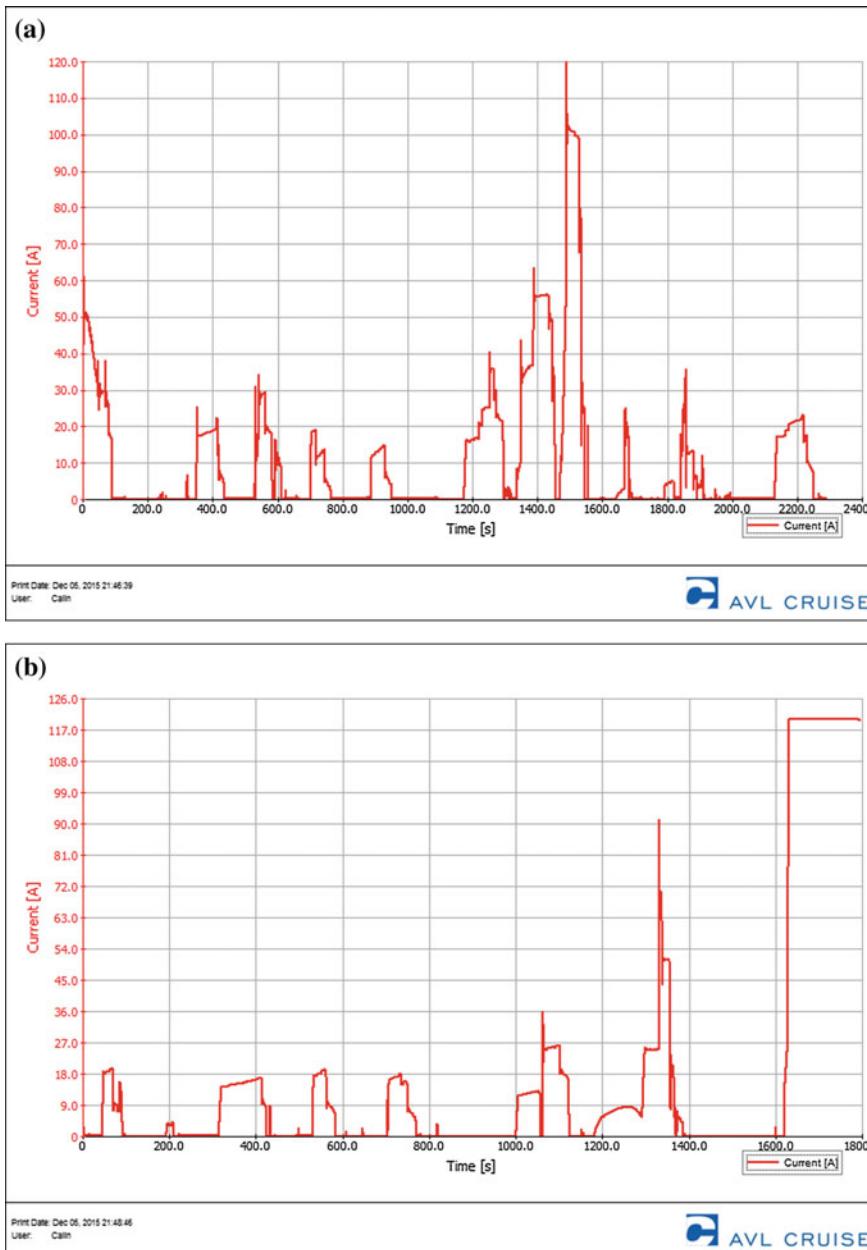
Fig. 7.64 Current consumption for the hybrid bus: **a** route 27, **b** route 28, **c** route 30 and **d** route 32
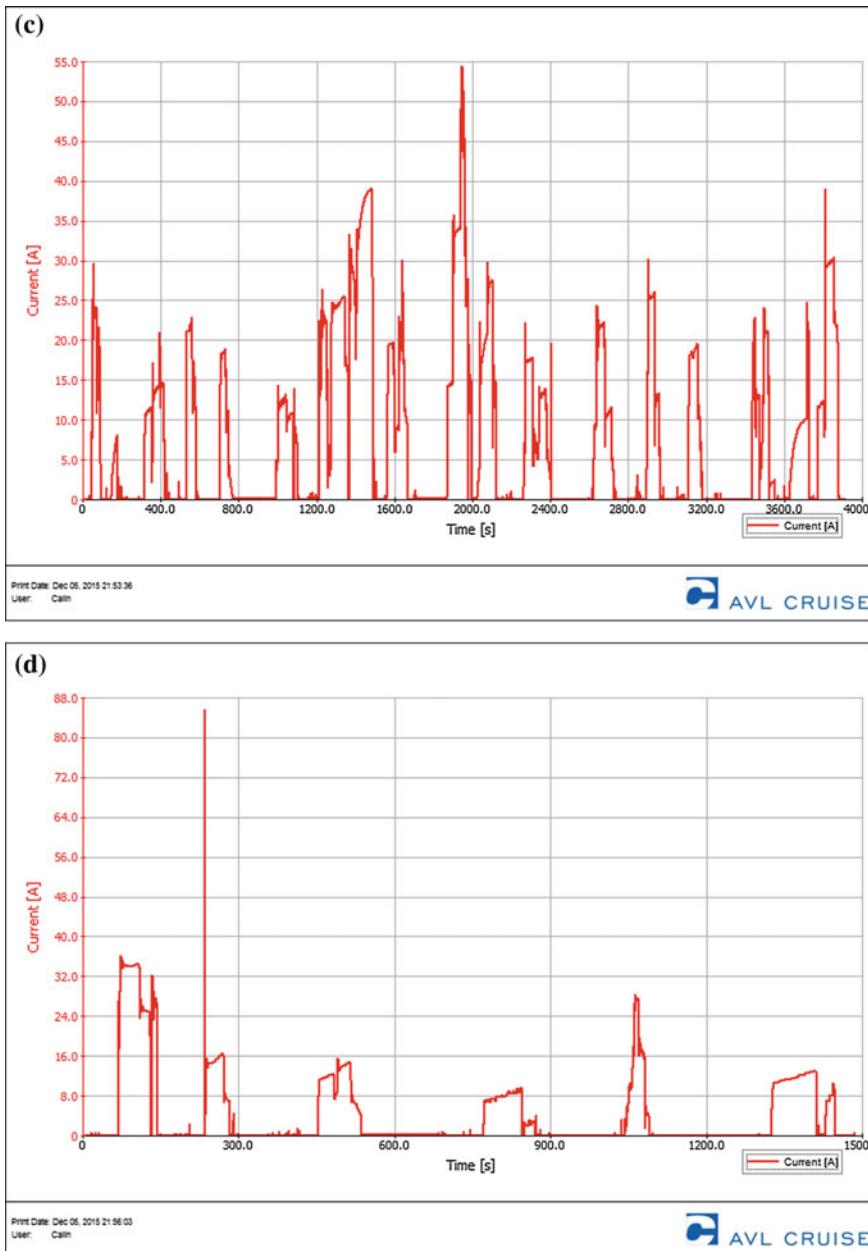
Fig. 7.64 (continued)
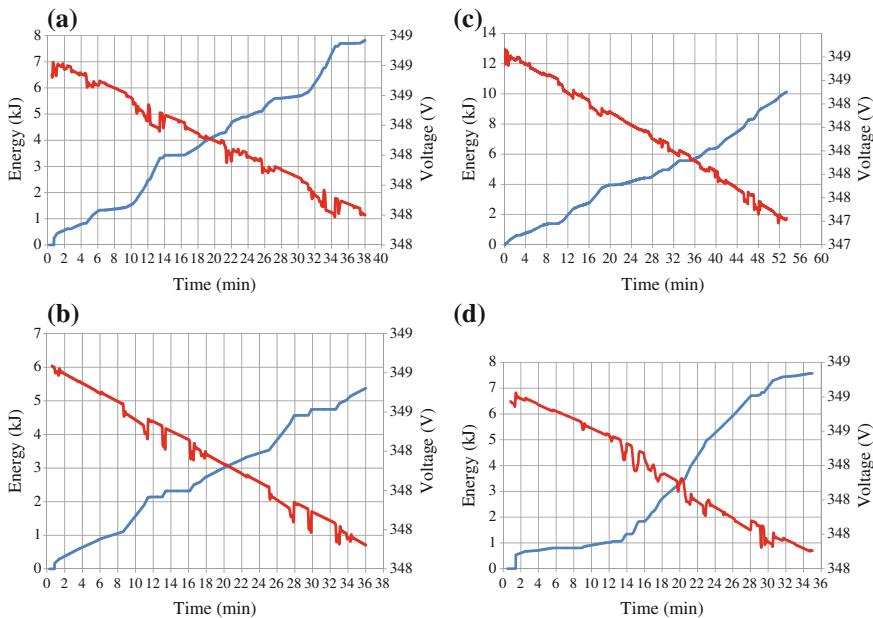
Fig. 7.65 Energetic consumption for the hybrid bus: **a** route 27, **b** route 28, **c** route 30 and **d** route 32

These differences between hybrid buses as compared to electric buses depend on many factors, such as route geometry (electric buses are more advantageous for routes where there are little altitude fluctuations), traffic conditions (heavy traffic with many traffic lights are disadvantageous for both types of bus models due to repeated stops and starts), season (during the cold season the state of charge of the batteries increases) etc.

Thus for route 27, which is characterized by an altitude difference of 25 m, the electric bus consumes 35 % more electric energy than the hybrid bus, for route 28, which is characterized by an altitude difference of 30 m, the electric bus consumes 47 % more electric energy than the hybrid bus, for route 30, which is characterized by an altitude difference of 25 m, the electric bus consumes 52 % more electric energy than the hybrid bus, respectively for route 32, which is characterized by an altitude difference of 40 m, the electric bus consumes 20 % more electric energy than the hybrid bus.

The electric voltage variation for traveled routes presents a decreasing characteristic with a decrease of approximately 1 V for each 1 KWh of energy consumed. Unlike the electric bus for which the electric voltage decreases linearly as the energy is consumed by the electric motor, for the hybrid bus this variation of electric voltage presents fluctuations characterized through voltage increase in the moments when the thermal engine starts, due to the fact that the electric motor commutes in the generator regime and charges the battery. This can also be
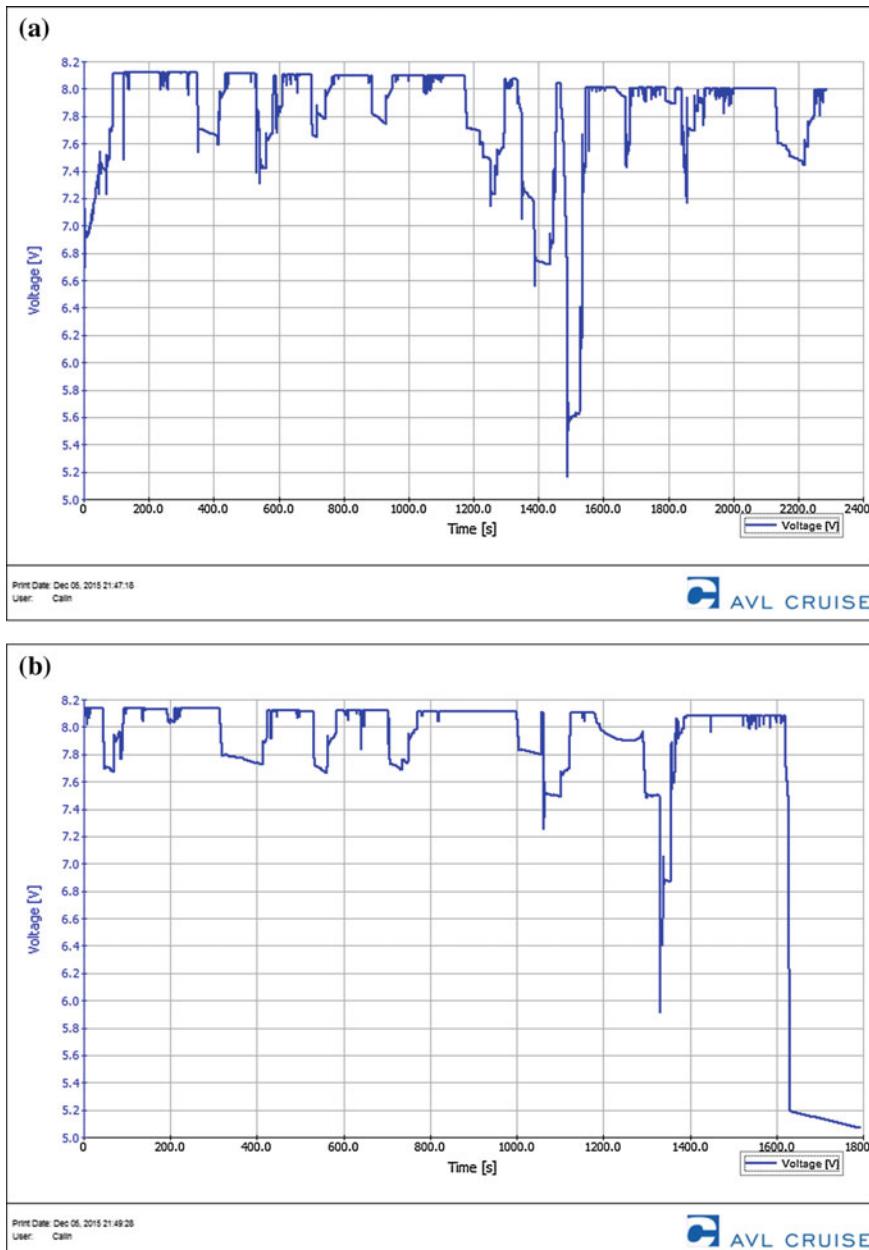
Fig. 7.66 Electric voltage variation for the hybrid bus: **a** route 27, **b** route 28, **c** route 30 and **d** route 32
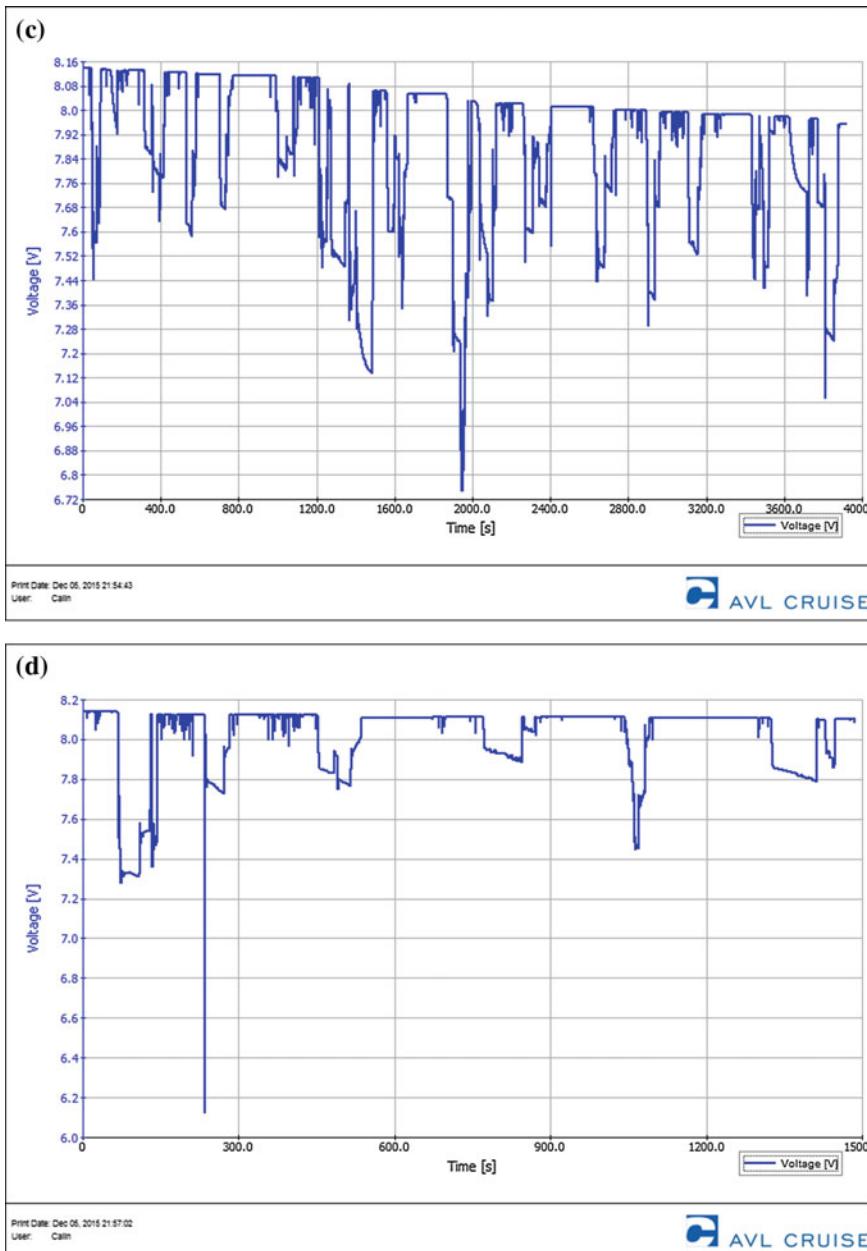
Fig. 7.66 (continued)
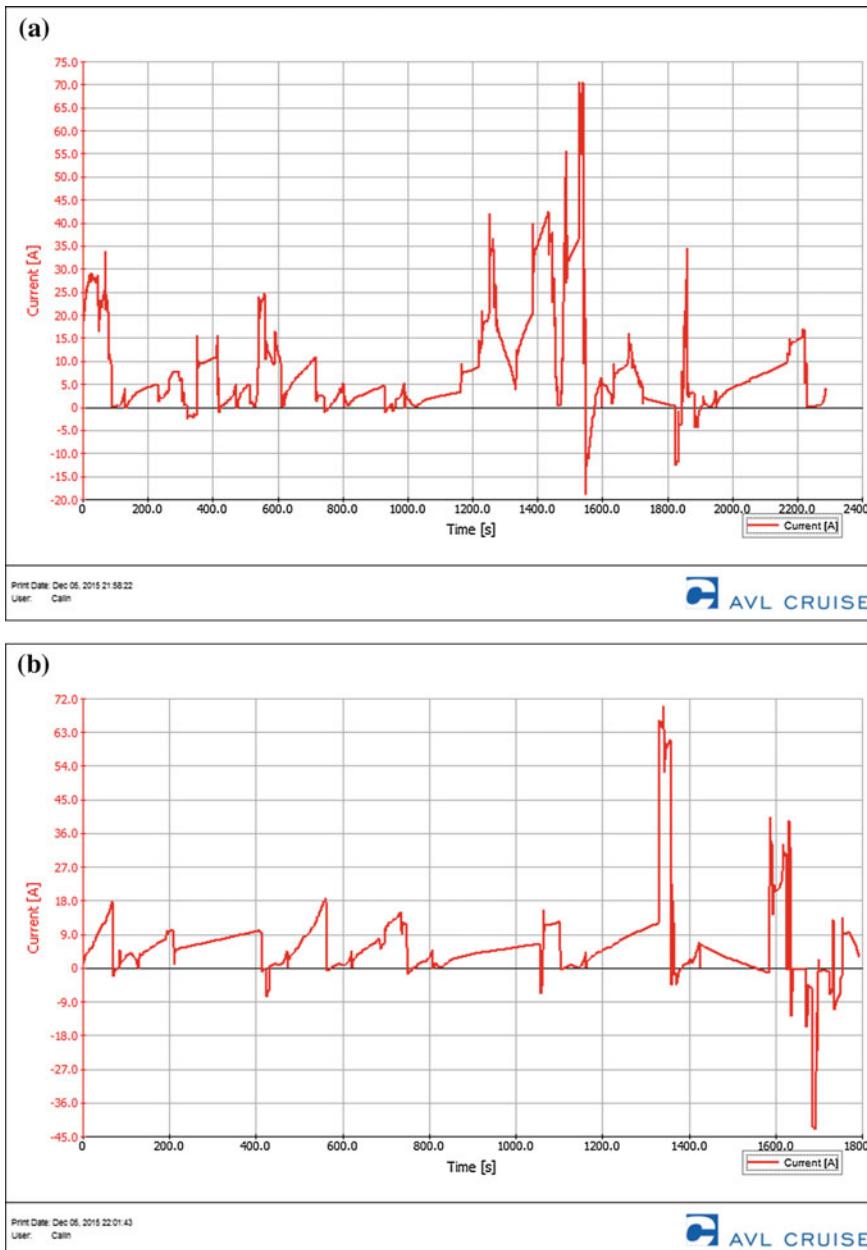
Fig. 7.67 Current consumption for the electric bus: **a** route 27, **b** route 28, **c** route 30 and **d** route 32
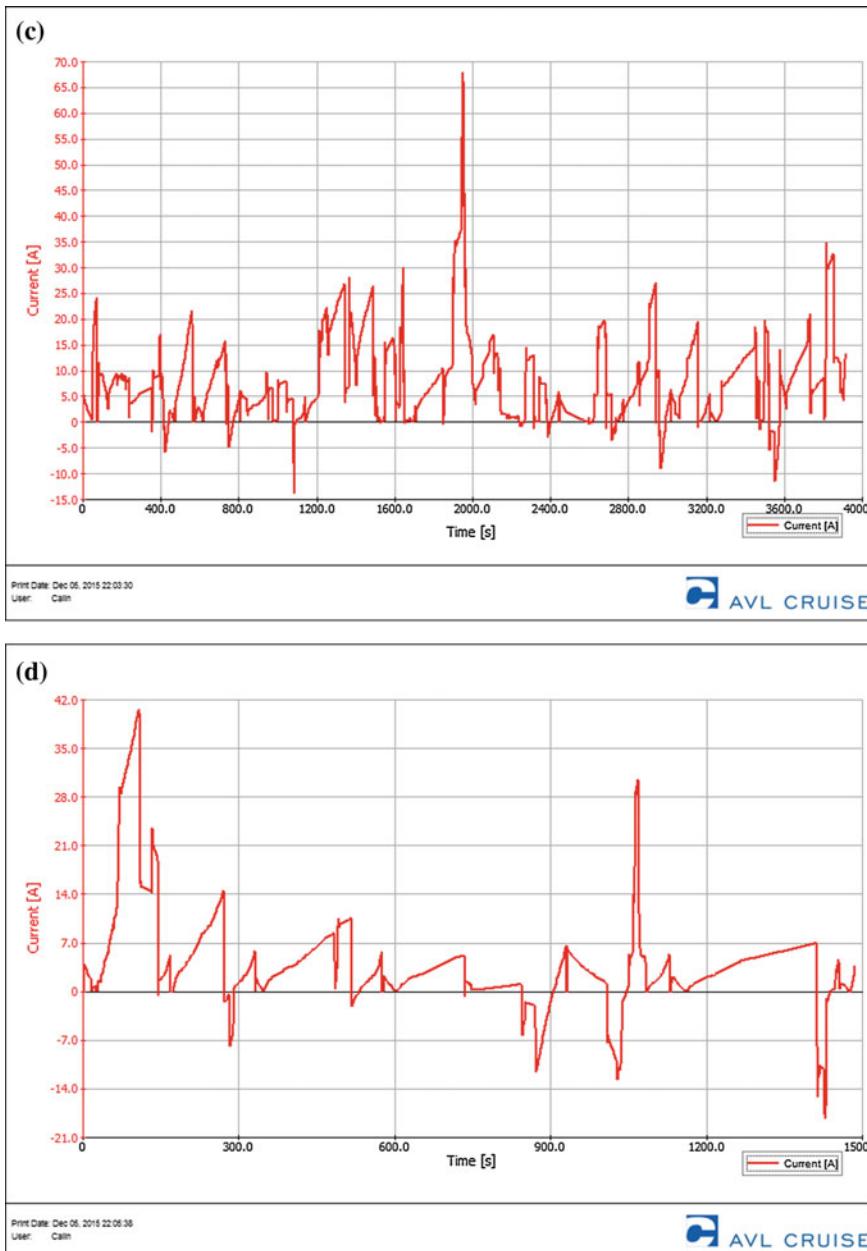
Fig. 7.67 (continued)
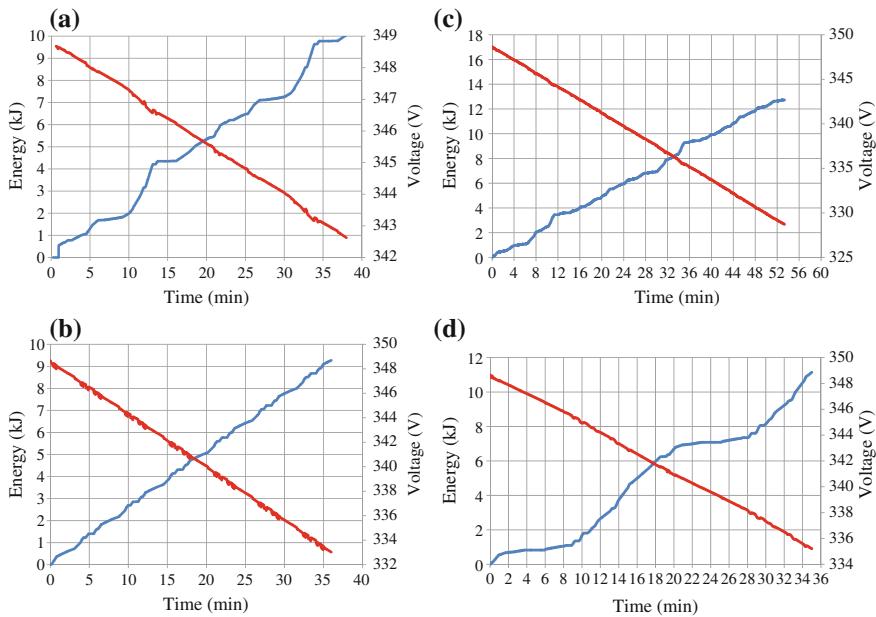
Fig. 7.68 Energetic consumption for the electric bus: **a** route 27, **b** route 28, **c** route 30 and **d** route 32

observed on the graphic for electric energy consumption which is characterized by a constant level when the thermal engine functions, thus resulting in a reduced energy consumption.

This constant level can also be observed for the electric bus, but for lower values and is due to energy regenerative braking, when the electric motor functions as a generator.

The running thermal engine assures a decrease in electric energy consumption of up to 40 %, while the energy regenerative braking assures the generation of a quantity of electric energy directly proportional with the altitude differences which are characteristic for the route.

Thus, in the case of the hybrid bus for route 27 the energy regenerative braking assures the recovery of a value of up to 2.8 % from the consumed energy, for route 28 the energy regenerative braking assures the recovery of a value of up to 3.3 % from the consumed energy, for route 30 the energy regenerative braking assures the recovery of a value of up to 2.1 % from the consumed energy, respectively for route 32 the energy regenerative braking assures the recovery of a value of up to 6.7 % from the consumed energy.

In the case of the electric bus for route 27 the energy regenerative braking assures the recovery of a value of up to 2.1 % from the consumed energy, for route 28 the energy regenerative braking assures the recovery of a value of up to 2.3 % from the consumed energy, for route 30 the energy regenerative braking assures the
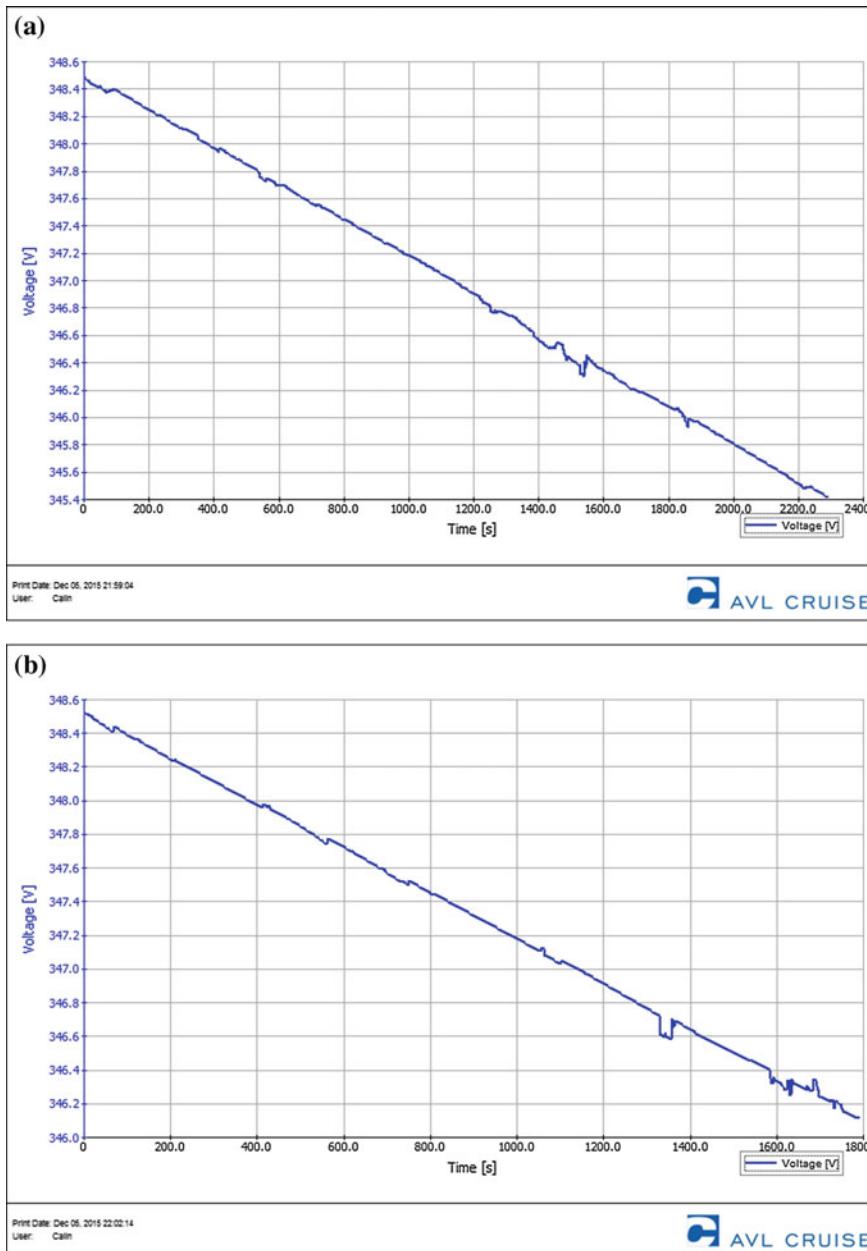
Fig. 7.69 Electric voltage variation for the electric bus: **a** route 27, **b** route 28, **c** route 30 and **d** route 32
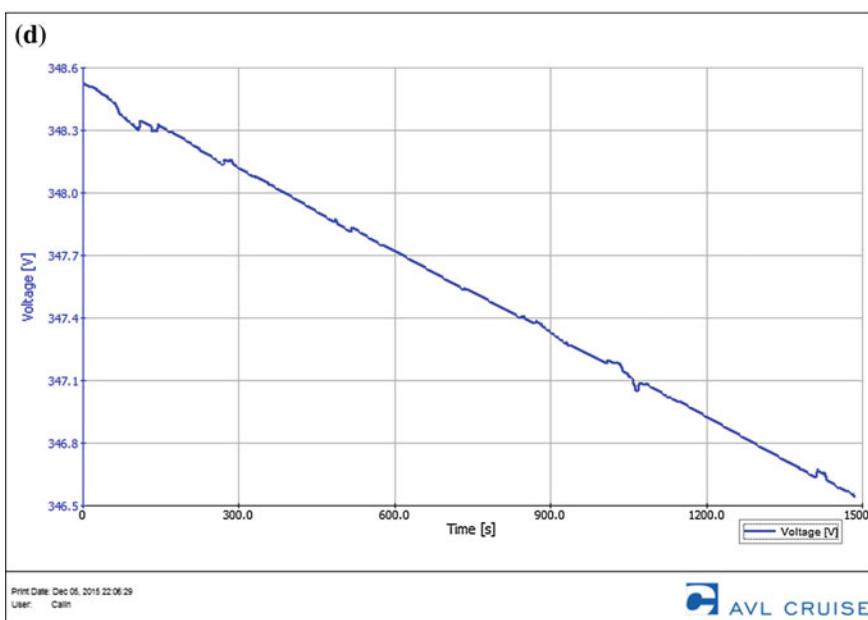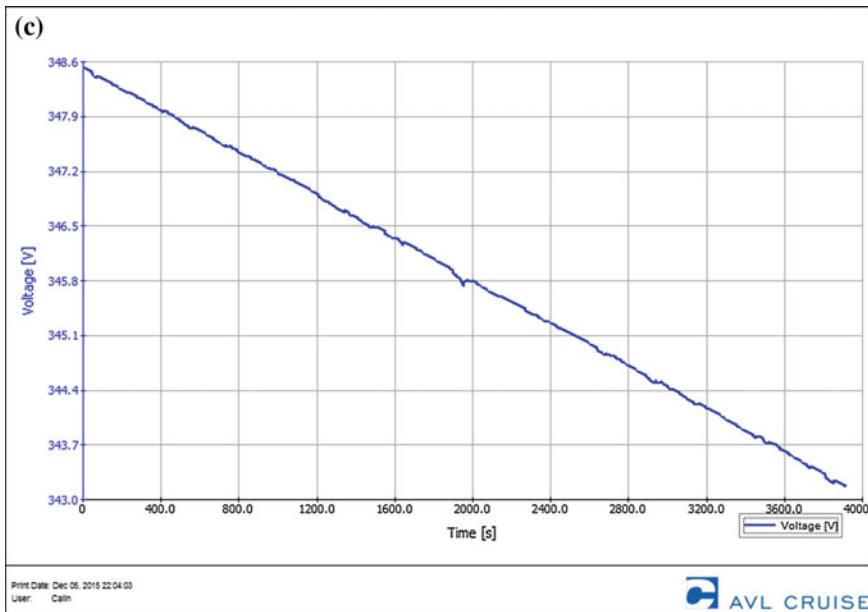
Fig. 7.69 (continued)

Table 7.8 Energetic parameters for the selected routes

Parameters	U.M.	Route 27	Route 28	Route 30	Route 32
Classic bus					
Traveled distance	m	4597	3642	7928	3246
Total travel time, stops	s	2290	1790	3915	1490
Medium urban velocity	km/h	13.20	13.20	13.20	13.20
Fuel consumption	l/100 km	37.00	37.00	37.00	37.00
Fuel consumption/route	l	1.70	1.35	2.93	1.20
Total NO_x emissions/route	g	27.58	21.85	47.57	19.48
Total CO emissions/route	g	9.19	7.28	15.86	6.49
Total HC emissions/route	g	2.30	1.82	3.96	1.62
Total CO_2 emissions/route	g	4597	3642	7928	3246
Diesel fuel cost	Euro	2.21	1.75	3.81	1.56
Hybrid bus					
Traveled distance	m	4597	3642	7928	3246
Total travel time, stops	s	2290	1790	3915	1490
Medium urban velocity	km/h	13.20	13.20	13.20	13.20
Total consumed energy	kJ	7820	6375	19,858	6423
Total recovered energy	kJ	215	206	431	423
Consumed energy/time	kWh	4.63	4.87	6.59	6.00
Recovered energy/time	kWh	0.13	0.16	0.14	0.40
Consumed energy/km	kWh/km	1.01	1.34	0.83	1.85
Energy balance/km	kWh/km	0.98	1.29	0.81	1.73
Fuel consumption	l/100 km	26.00	26.00	26.00	26.00
Fuel consumption/route	l	1.20	0.95	2.06	0.84
Total NO_x emissions/route	g	18.39	14.57	31.71	12.98
Total CO emissions/route	g	4.60	3.64	7.93	3.25
Total HC emissions/route	g	1.61	1.27	2.77	1.14
Total CO_2 emissions/route	g	2758	2185	4757	1948
Electric energy cost	Euro	1.55	1.23	2.68	1.10
Diesel fuel cost	Euro	0.46	0.49	0.66	0.60
Electric bus					
Traveled distance	m	4597	3642	7928	3246
Total travel time, stops	s	2290	1790	3915	1490
Medium urban velocity	km/h	13.20	13.20	13.20	13.20
Total consumed energy	kJ	10,500	9270	29,840	7575
Total recovered energy	kJ	215	206	431	423
Consumed energy/time	kWh	6.21	7.08	9.90	7.08
Recovered energy/time	kWh	0.13	0.16	0.14	0.40
Consumed energy/km	kWh/km	1.35	1.94	1.25	2.18
Energy balance/km	kWh/km	1.32	1.90	1.23	2.06
Electric energy cost	Euro	0.62	0.71	0.99	0.71
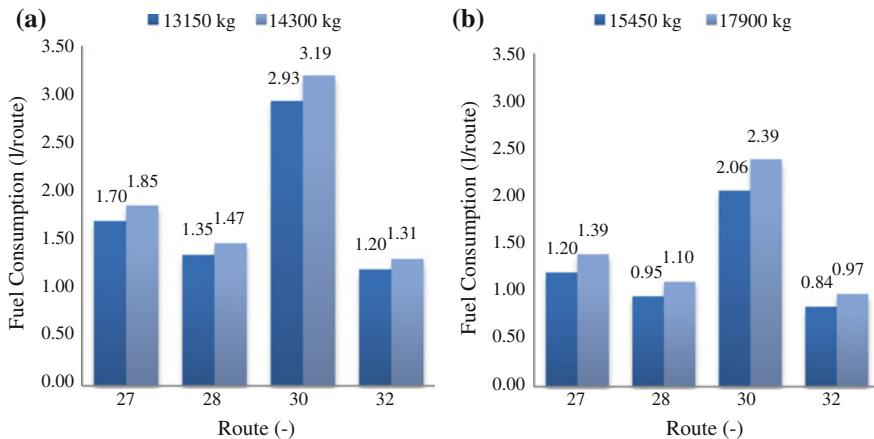
Fig. 7.70 Fuel consumption on the simulated routes: **a** classic bus, **b** hybrid bus

recovery of a value of up to 1.4 % from the consumed energy, respectively for route 32 the energy regenerative braking assures the recovery of a value of up to 5.7 % from the consumed energy.

The fuel consumption on the simulated routes for the classic bus as compared to the hybrid bus are presented in the graphic from Fig. 7.70.

Due to the electric motor which supplements the torque realizing the movement, one can observe that for the hybrid bus the consumption is lower than for the classic bus, with a percentage of 30 % when the two bus models are loaded to half the maximum capacity of passengers to be transported (13,150 kg for the classic bus, 15,450 kg for the hybrid bus), respectively lower with a 40 % percentage when the two bus models are loaded to full capacity of passengers to be transported (14,300 kg for the classic bus, 17,900 kg for the hybrid bus).

The total NO_x emissions on the simulated routes for the classic bus as compared to the hybrid bus are presented in the graphic from Fig. 7.71.

Due to the thermal engine which functions throughout the entire time the classic bus moves, the emissions are lower for the hybrid bus with a percentage of 50 % when the two bus models are loaded to half the maximum capacity of passengers to be transported (13,150 kg for the classic bus, 15,450 kg for the hybrid bus), respectively lower with a 40 % percentage when the two bus models are loaded to full capacity of passengers to be transported (14,300 kg for the classic bus, 17,900 kg for the hybrid bus).

The total CO emissions on the simulated routes for the classic bus as compared to the hybrid bus are presented in the graphic from Fig. 7.72.

Due to the thermal engine which functions throughout the entire time the classic bus moves, the emissions are cut in half for the hybrid bus when the two types of bus models are loaded to half the maximum capacity of passengers to be transported (13,150 kg for the classic bus, 15,450 kg for the hybrid bus), respectively lower
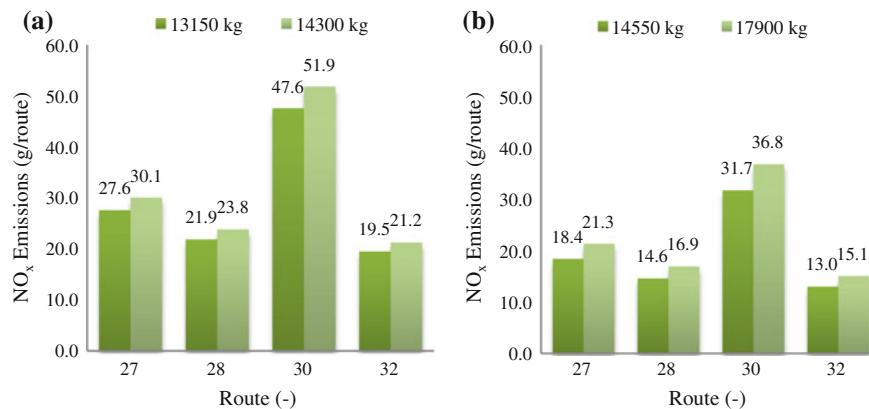
Fig. 7.71 Total NO$_x$ emissions on the simulated routes: **a** classic bus, **b** hybrid bus
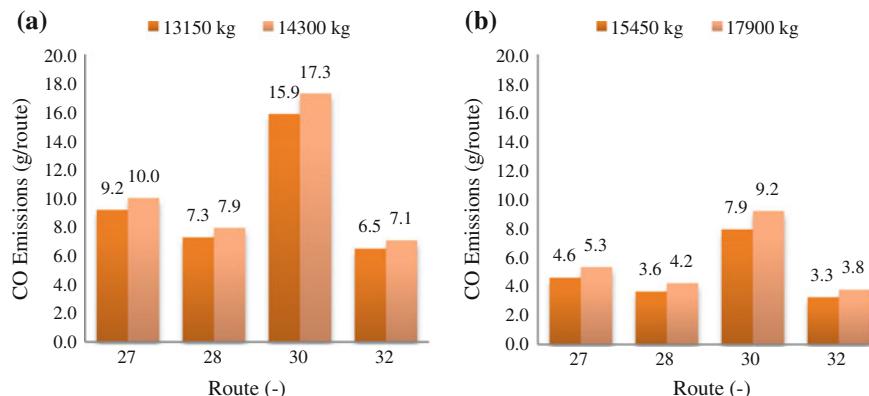
Fig. 7.72 Total CO emissions on the simulated routes: **a** classic bus, **b** hybrid bus

with an 80 % percentage when the two bus models are loaded to full capacity of passengers to be transported (14,300 kg for the classic bus, 17,900 kg for the hybrid bus).

The values for HC emissions on the simulated routes for the classic bus as compare to the hybrid bus are presented in the graphic from Fig. 7.73.

Due to the thermal engine which functions throughout the entire time the classic bus moves, the emissions are lower for the hybrid bus with a percentage of 45 % when the two bus models are loaded to half the maximum capacity of passengers to be transported, respectively lower with a 40 % percentage when the two bus models are loaded to full capacity of passengers to be transported.

The total CO$_2$ emissions on the simulated routes for the classic bus as compared to the hybrid bus are presented in the graphic from Fig. 7.74.
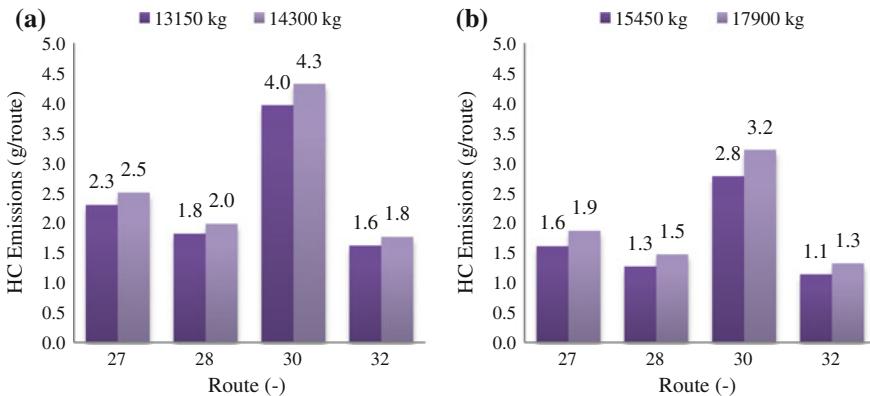
Fig. 7.73 Total HC emissions on the simulated routes: **a** classic bus, **b** hybrid bus
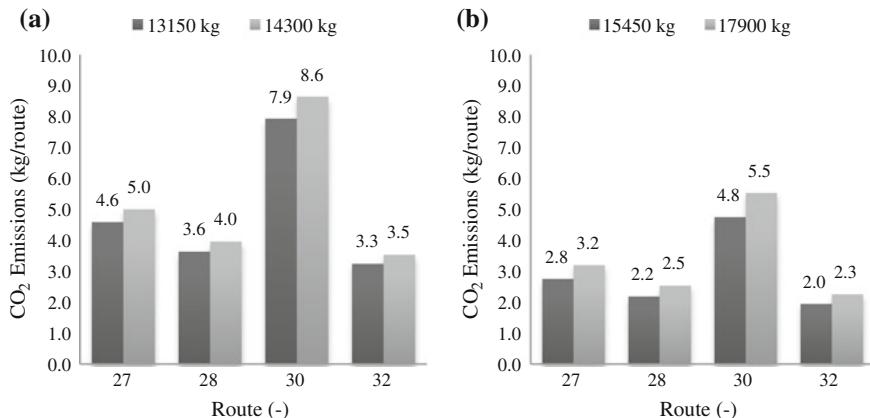
**Fig. 7.74** Total CO_2 emissions on the simulated routes: **a** classic bus, **b** hybrid bus

Due to the thermal engine which functions throughout the entire time the classic bus moves, the emissions are lower for the hybrid bus with a percentage of 65 % when the two bus models are loaded to half the maximum capacity of passengers to be transported (13,150 kg for the classic bus, 15,450 kg for the hybrid bus), respectively lower with a 55 % percentage when the two bus models are loaded to full capacity of passengers to be transported (14,300 kg for the classic bus, 17,900 kg for the hybrid bus).

The energy consumed based on the traveled distance on the simulated routes for the classic bus as compared to the hybrid bus are presented in the graphic from Fig. 7.75.

Due to the thermal engine which supplements the electric motor in hybrid bus movement, the values for consumed energy are greater for the electric bus with a
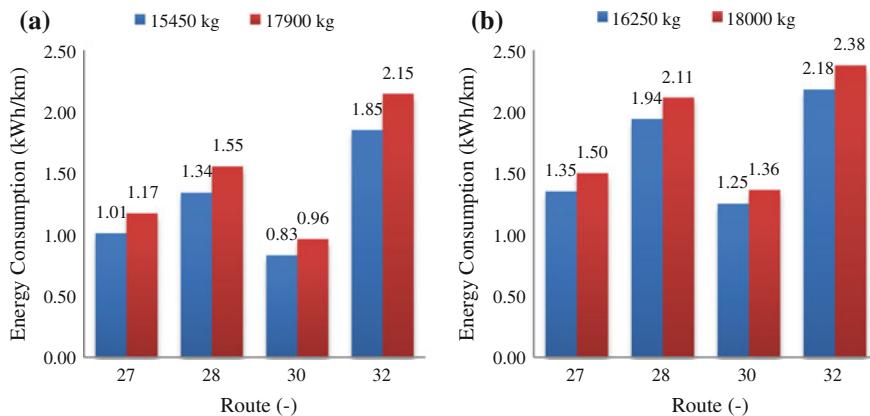
Fig. 7.75 Energy consumed based on distance traveled: **a** hybrid bus, **b** electric bus

20 % percentage when the two bus models are loaded to half the maximum capacity of passengers to be transported (15,450 kg for the hybrid bus, 16,250 kg for the electric bus), respectively higher with a 10 % when the two bus models are loaded to full capacity of passengers to be transported (17,900 kg for the hybrid bus, 18,000 kg for the electric bus).

The energy consumed based on the time traveled on the simulated routes for the hybrid bus as compared to the electric bus are presented in the graphic from Fig. 7.76.

Due to the thermal engine which supplements the electric motor in hybrid bus movement, the values for consumed energy are greater for the electric bus with a 35 % percentage when the two bus models are loaded to half the maximum capacity of passengers to be transported, respectively higher with a 30 %
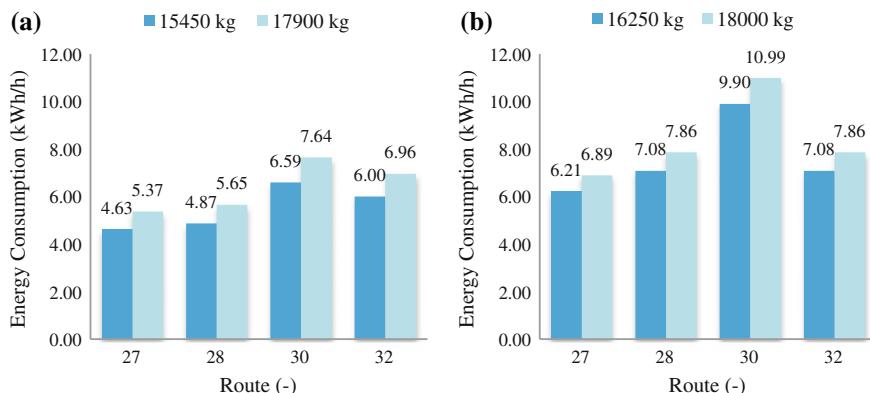

Fig. 7.76 Energy consumed based on the time traveled: **a** hybrid bus, **b** electric bus

percentage when the two bus models are loaded to full capacity of passengers to be transported.

As far as operation and exploitation costs go, it can be stated that numerous options for acquiring alternative technologies based on ecological drive systems imply higher initial costs, but these can generate costs savings for the life span of hybrid and electric buses due to lower fuel prices and consumptions, respectively a longer life span and lower maintenance costs.

To evaluate from the point of view of costs over the environmental and energetic impact typical for each studied bus model (classic, hybrid, electric), one must take into account the methodology provided in the Directive for Ecological Vehicles, respectively Directive 2009/33/CE of the European Parliament and the Council of Europe from 23rd of April 2009 regarding the promotion of transportation vehicles which are non-pollutant and energetically efficient [9].

The purpose of the present directive is to stimulate the market of transportation vehicles which are non-pollutant and energetically efficient and especially to influence the market of standardized vehicles produced in large quantities, like buses, thus assuring a level of demand for non-pollutant and energetically efficient transportation vehicles high enough to encourage the manufacturers and the industry to invest and to further develop vehicles with a lower energy consumption and reduced CO_2 emissions [2].

Although initially non-pollutant and energetically efficient vehicles cost more than conventional vehicles, the savings which can be made on the long-term by reducing the operating and maintenance costs encourages the acquisition of these bus models.

The calculus model for operating costs for the life span of ecological vehicles, based on pollutant emissions with the purpose of applying vehicle acquisition decisions, including the numerical values defined in the Directive 2009/33/CE, are presented in Table 7.9.

The methodology used for calculating the operating costs for the life span of vehicles comprises the operating costs for energetic consumption and the costs for CO_2 emissions and the pollutant emissions established in Table 7.9, afferent to vehicle operation which are subject of the evaluation. Thus the fuel consumption of a vehicle per kilometer is monitored in units of energetic consumption per kilometer (including in the case of electric vehicles). The operating cost of the energetic consumption for a vehicle, estimated for its entire life span, is calculated as being the result for the distance traveled during its entire life span.

The operating cost during the life span for CO_2 emissions generated by an operating vehicle are calculated by multiplying the distance traveled during its life span with the CO_2 emissions in kilograms per kilometer, and with the cost of a kilogram taken from the interval specified in Table 7.9.

Table 7.9 Operating costs based on pollutant emissions [9]	CO_2 (Euro/kg)	NO_x (Euro/g)	HC (Euro/g)	PM (Euro/g)
	0.03–0.04	0.0044	0.001	0.087

The maximum traveled distance during the life span of the buses is established by the Directive 2009/33/CE at 800,000 km.

The live cost cycle of a vehicle (LCC) comprises the following elements [10]:

- The acquisition costs of the vehicle, made of the acquisition price and the delivery price;
- Making the vehicle functional and implementing the infrastructure;
- The operating costs, respectively the fuel/energy consumptions and the pollutant emissions;
- The costs for periodical maintenance and occasional repairs;
- The taxes for the local budget and the state budget;
- The scrapping costs at the end of the payback period, respectively the resale value.

By replacing the classic buses with hybrid and electric buses, the following categories of expenses are affected:

- The fuel expenses are reduced due to a lower consumption in the case of hybrid buses;
- The maintenance expenses for hybrid and electric buses are reduced;
- The expenses assimilated with the costs for CO_2 emissions and pollutant emissions established in Table 7.9 are reduced;
- The acquisition prices are increased due to the higher price for hybrid and electric buses;
- The expenses for the infrastructure are increased due to the necessity of building charging stations for hybrid and electric buses;
- The electric energy expenses are increased due to the supply for hybrid and electric buses;
- The insurance expenses are increased due to the increase in value of the calculus base for hybrid and electric buses.

A distinct category of expenses for maintenance during the period of functioning of hybrid and electric buses is the replacement of electric batteries. According to the recommendations of manufacturers for hybrid and electric buses the life span of electric batteries equipping these models for an exploitation regime of 5000 km per month is of 5 years, thus for the forecast period of 10 years the batteries will only be replaced once, after the first 5 years, and the estimated cost for this operation is of 10 % from the acquisition value [2].

By correlating the acquisition prices of the three types of bus models with the annual distances traveled for each of the selected routes, respectively with the LCC elements, we can evaluate the values of operating costs (Table 7.10).

The operating costs based on fuel consumption, respectively energy, for the evaluated bus models on the selected routes according to the data from Table 7.10 are presented in Fig. 7.77, respectively the operating costs based on pollutant emissions (CO_2, NO_x, HC, PM) are presented in Fig. 7.78.

Table 7.10 Operating costs per life span LCC

Bus model		Classic				Hybrid				Electric			
Route	U.M.	27	28	30	32	27	28	30	32	27	28	30	32
Traveled distance	km/year	70,616	66,300	67,080	51,480	70,616	66,300	67,080	51,480	70,616	66,300	67,080	51,480
Total distance	km/10 years	706,160	663,000	670,800	514,800	706,160	663,000	670,800	514,800	706,160	663,000	670,800	514,800
CO_2 emissions	kg/km	1.00	1.00	1.00	1.00	0.60	0.60	0.60	0.60	0	0	0	0
CO_2 emissions cost	Euro/kg	0.003	0.003	0.003	0.003	0.003	0.003	0.003	0.003	–	–	–	–
Total CO_2 emissions	kg/year	70,616	66,300	67,080	51,480	42,370	39,780	40,248	30,888	0	0	0	0
CO_2 emissions cost	Euro/year	212	199	201	154	127	119	121	93	0	0	0	0
CO_2 emissions cost	Euro/10 years	2118	1989	2012	1544	1271	1193	1207	927	0	0	0	0
NO_x emissions	g/km	6.00	6.00	6.00	6.00	4.00	4.00	4.00	4.00	0	0	0	0
NO_x emissions cost	Euro/g	0.0044	0.0044	0.0044	0.0044	0.0044	0.0044	0.0044	0.0044	–	–	–	–
Total NO_x emissions	g/year	423,696	397,800	402,480	308,880	282,464	265,200	268,320	205,920	0	0	0	0
NO_x emissions cost	Euro/year	1864	1750	1771	1359	1243	1167	1181	906	0	0	0	0
NO_x emissions cost	Euro/10 years	18,643	17,503	17,709	13,591	12,428	11,669	11,806	9060	0	0	0	0
HC emissions	g/km	0.50	0.50	0.50	0.50	0.35	0.35	0.35	0.35	0	0	0	0
HC emissions cost	Euro/g	0.001	0.001	0.001	0.001	0.001	0.001	0.001	0.001	–	–	–	–
Total HC emissions	g/year	35,308	33,150	33,540	25,740	24,716	23,205	23,478	18,018	0	0	0	0
HC emissions cost	Euro/year	35	33	34	26	25	23	23	18	0	0	0	0
HC emissions cost	Euro/10 years	353	332	335	257	247	232	235	180	0	0	0	0
PM emissions	g/km	0.01	0.01	0.01	0.01	0.006	0.006	0.006	0.006	0	0	0	0
PM emissions cost	Euro/g	0.087	0.087	0.087	0.087	0.087	0.087	0.087	0.087	–	–	–	–
Total PM emissions	g/year	706	663	671	515	424	398	402	309	0	0	0	0
PM emissions cost	Euro/year	61	58	58	45	37	35	35	27	0	0	0	0
PM emissions cost	Euro/10 years	614	577	584	448	369	346	350	269	0	0	0	0
Fuel consumption	l/100 km	37	37	37	37	26	26	26	26	0	0	0	0

Table 7.10 (continued)

Bus model		Classic				Hybrid				Electric			
Route	U.M.	27	28	30	32	27	28	30	32	27	28	30	32
Total fuel	l/year	26,128	24,531	24,820	19,048	18,360	17,238	17,441	13,385	0	0	0	0
Total fuel	l/10 years	261,279	245,310	248,196	190,476	183,602	172,380	174,408	133,848	0	0	0	0
Ad Blue EURO 6	l/100 km	2	2	2	2	1.5	1.5	1.5	1.5	0	0	0	0
Ad Blue EURO 6	l/year	1412	1326	1342	1030	1059	995	1006	772	0	0	0	0
Ad Blue EURO 6	l/10 years	14,123	13,260	13,416	10,296	10,592	9945	10,062	7722	0	0	0	0
Fuel cost	Euro/l	1.30	1.30	1.30	1.30	1.30	1.30	1.30	1.30	–	–	–	–
Ad Blue cost	Euro/l	1.00	1.00	1.00	1.00	1.00	1.00	1.00	1.00	–	–	–	–
Fuel cost	Euro/year	35,379	33,216	33,607	25,791	24,927	23,404	23,679	18,172	0	0	0	0
Fuel cost	Euro/10 years	353,786	332,163	336,071	257,915	249,274	234,039	236,792	181,724	0	0	0	0
Energy consumption	kWh/100 km	0	0	0	0	98	129	81	173	132	190	123	206
Total energy	kWh/year	0	0	0	0	69,204	85,527	54,335	89,060	93,213	125,970	82,508	106,049
Total energy	kWh/10 years	0	0	0	0	692,037	855,270	543,348	890,604	932,131	1,259,700	825,084	1,060,488
Energy cost	Euro/kWh	–	–	–	–	0.10	0.10	0.10	0.10	0.10	0.10	0.10	0.10
Total energy cost	Euro/year	0	0	0	0	6920	8553	5433	8906	9321	12,597	8251	10,605
Total energy cost	Euro/10 years	0	0	0	0	69,204	85,527	54,335	89,060	93,213	125,970	82,508	106,049
Total operating cost	Euro/year	37,551	35,256	35,671	27,376	33,279	33,301	30,473	28,122	9321	12,597	8251	10,605
Total operating cost	Euro/10 years	375,515	352,564	356,711	273,755	332,793	333,006	304,726	281,221	93,213	125,970	82,508	106,049
Total operating cost	Euro/km	0.53	0.53	0.53	0.53	0.47	0.50	0.45	0.55	0.13	0.19	0.12	0.21
Medium operating cost	Euro/km	0.53				0.49				0.16			

Fig. 7.77 Operating costs based on energy/fuel consumption
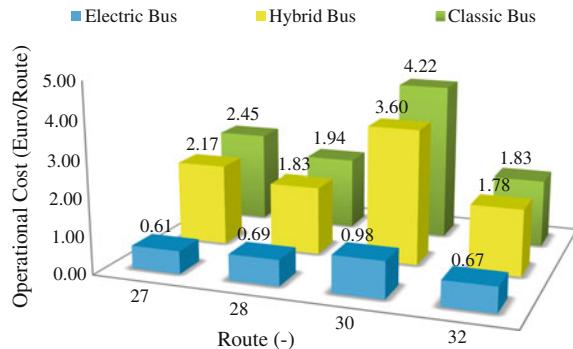
Fig. 7.78 Operating costs based on pollutant emissions
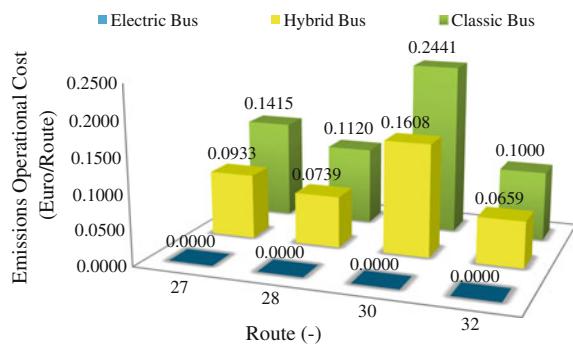
Fig. 7.79 Operating costs per passenger based on the nominal transport capacity
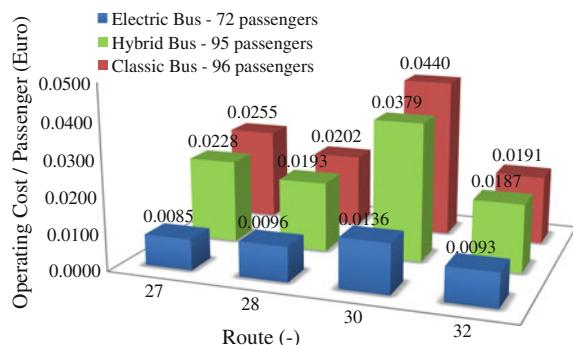
The operating costs per passenger based on the number of transported passengers for the bus models evaluated on the selected routes in the case in which the buses are loaded to a nominal transport capacity are presented in Fig. 7.79, and in the case in which the buses are loaded to half the transport capacity in Fig. 7.80.

Fig. 7.80 Operating costs per passenger based on half of nominal transport capacity
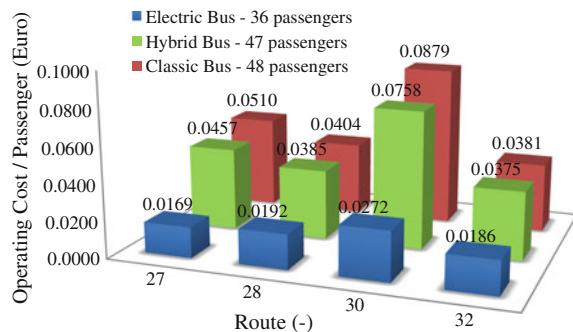
References

1. Varga, B. O., Mariașiu, F., Moldovanu, D., & Iclodean, C. (2015). *Electric and plug-in hybrid vehicles—advanced simulation methodologies, chapter 7* (pp. 477–524). Springer International Publishing. ISBN: 978-3-319-18638-2.
2. Varga, B. O. (2015). *Energy efficiency of vehicles equipped with hybrid or electrical powertrain for urban public transport (in Romanian), Habilitation thesis*, Technical University of Cluj-Napoca, Romania, 18 Sept 2015.
3. AVL CRUISE (2010). CRUISE—CarMaker/TruckMaker Co-Simulation, AVL List GmbH, Graz, Austria, Document no. 04.0115.2010, Edition 07.2010.
4. AVL CRUISE (2011). Users Guide, AVL List GmbH, Graz, Austria, Document no. 04.0104.2011, Edition 06.2011.
5. IPG CarMaker (2014). *User's guide version 4.5.2*. Germany: IPG Automotive, Karlsruhe.
6. IPG TruckMaker (2014). *Reference manual version 4.5, simulation solutions, test systems, engineering services*. Germany: IPG Automotive, Karlsruhe.
7. Racicovschi, V., Danciu, G., & Chefneux, M. (2007). *Automobile Electrice și Hibride, (in Roumanian)*. București: Editura Electra. ISBN 978-973-7728-98-2.
8. Surugiu, M. C., Barna, O. V., Obreja, L. G. (2015). *Considerations regarding the influence off traffic management system on pollutant emissions in congested urban areas*. UPB, Scientific Bulletin, Series C (Vol. 77(2), pp. 185–192) ISSN: 2286-3540.
9. Directive 2009/33/EC of the European Parliament and of the Council of 23 April 2009 on the promotion of clean and energy-efficient road transport vehicles. http://eur-lex.europa.eu/legal-content/EN/TXT/?uri=CELEX%3A32009L0033. Accessed 11 March 2015.
10. http://www.clean-fleets.eu/ro/main-navigation/despre-vehicule-ecologice/, (in Romanian). Accessed 20 Dec 2015.

Chapter 8
Comparative Evaluation for Using Hybrid and Electric Drive Systems in Urban Transportation with Buses

8.1 Analysis of the Developed Algorithm Related to Urban Routes

The identification of some optimal routes following the determinations made locally, in the current context, of reaching and applying the strategy objectives of Cluj-Napoca municipality authorities of promoting a common transport sustainable from the point of view of minimizing the pollutant emissions into the atmosphere by adopting some optimal solutions of partially replacing the existing bus fleet, needs creating an initial analysis of direct emissions of pollutants as compared to the EURO 0–EURO 6 pollution norms. The norms are regulated through the EC Regulation no. 595/2009 [1] and the EC Regulation no. 582/2011 [2], the EURO 6 pollution norm, which is taking effect from the year 2013, and its complete implementation to be realized in the year 2014.

The new regulation regarding the EURO 6 pollution norm brings significant modifications regarding the 50 % reduction of the emissions level measured for the following indicators: hydrocarbons (HC), methane (CH_4), nitrogen oxides (NO_x) and particulate matter (PM).

The analyzes realized and presented in the previous chapter regarding the comparative studies of pollutant emissions into the atmosphere, have taken into consideration and were related to the quantity of pollutants and are calculated according to the emission factor afferent to the used fuel, taking into consideration the pollution norm characteristic to the studied bus model, respectively the distanced traveled for each route.

By analyzing the data presented one can observe a considerable diminution of pollutant emissions concentration between the hybrid drive system and the classic drive system. In the case of electric propulsion, all emission indicators which were analyzed have had the value zero (locally).

Also, a comparative calculus of greenhouse gas emissions has been made, more specifically of CO_2 emissions, between the classic, hybrid and electric drive

systems, by using the afferent emission factors according to fuel consumption for a traveled distance of 100 km.

It is imposed to specify the fact that in the case of CO_2 emissions, these are zero only in the case where the electric energy used for charging the batteries comes exclusively from clean water, which does not pollute, such as hydroelectric energy, wind energy, photovoltaic energy.

The comparative study was also made for the noise and vibrations factor, from which resulted that in the case of buses classic and hybrid drive systems there is a level of noise generated while the buses function, of approximately 90 dB (A), as opposed to buses with electric drive systems, for which the level of noise pollution do not go over 55 dB (A) [3].

In conclusion, it can be asserted that following the detailed comparative analysis, the buses with electric drive systems are within the parameters of total reduction of CO_2 emissions, but also within the parameters of the other emission indicators, as opposed to the buses with classic and hybrid drive systems.

Also, as it was demonstrated above from the analysis of the noise level generated by a bus with electric drive system, it results that it is approximately 20 dB (A) lower than in the case of buses powered by thermal engine, fact which assures a higher level of comfort for the passengers.

In regards to the power supply system for electric buses, the batteries used in the case of an electric bus have a life span of up to 5 years, and they are 100 % recyclable.

The implementation of the algorithm developed as a solution for updating the urban routes studied for hybrid and electric buses through the analysis of the obtained results, indicates the bus with electric drive system as being the most economical from the point of view of fuel combustion and pollutant emissions, with the possibility of amortization of investments with infrastructure and acquisition costs on a medium and long term.

8.2 Results for Buses Equipped with a Classic Drive System

Presently most companies operating in the urban passenger transportation use buses with classic drive systems, buses which fit within the EURO 0–EURO 6 pollution norms, characterized by a high fuel consumption, equipped with compression ignition engine with a cylindrical capacity of 4–6 L, and having the following advantages: a great passenger transport capacity, the simplicity of systems composing the bus models and a high autonomy due to the equipment of high capacity fuel tanks, but with a lover comfort level in comparison with electric buses.

One of the most important advantages that classic buses equipped with thermal engines have as opposed to hybrid and electric buses is the low acquisition price, which is really an advantage only in the situation in which one chooses the

acquisition of buses from local budget personal financial means, without using non-refundable European funds, which allow the acquisition of non-pollutant buses for prices comparable to those of classic buses.

The classic buses now existing in urban traffic do not meet the more and more strict imposed criteria, namely:

- the reduction of noise levels and the improvement in air quality, according to the regulations imposed by EU directives;
- the reduction of CO_2 emissions produced by classic buses because of internal combustions engines;
- the reduction of exploitation of conventional energy resources obtained from fossil fuels.

Replacing the buses equipped with classic diesel engines with hybrid and electric buses is necessary on the strength of the legislation promoted by EU, more precisely the Regulation 443/23 April 2009 which targets the reduction of emissions coming from vehicles and which imposes the limit for CO_2 emission (130 g CO_2/km until 2015, respectively 95 g CO_2/km until 2020, as opposed to 150 g CO_2/km which is now) [4].

The vibration sources depend on the type of means of transport, thus for classic buses the level of vibrations is higher due to their equipment of thermal engines which generate vibrations while the bus runs. Because of this, to cushion the vibrations thermal engines they are fixed on elastic restraint systems. Also the exhaust systems for exhaust gases are fixed on bus chassis through elastic elements, and the connection between the engine and the exhaust system is also made through elements of elastic tubing. The more the fixation system of vibrant elements is more rigid, the more the vibrations made by the generating sources are amplified, thus generating supplementary noises and creating a major discomfort for both pedestrians and for passengers of common transportation means.

8.3 Results for Buses Equipped with a Hybrid Drive System

For hybrid buses, from start off, respectively until they reach a velocity of 30 km/h, only the electric motor functions. At velocities between 30–60 km/h, respectively in a regime of strong acceleration, the thermal engine also starts to function, thus assuring together with the electric motor the propulsion of the bus. Once the velocity increases, the power surplus developed by the thermal engine assures the battery is recharged, concomitantly with the energy flow used by the bus to travel.

While braking, the kinetic energy is recovered and the electric motor starts to function as a generator and recharges the battery. If the energy from the batteries runs below a certain level (30–40 %), while stationary, the thermal engine starts and trains the generator to charge the batteries.

This exact functional cycle for a hybrid bus corroborated with the Plug-in characteristic which allows the connection of the bus to a charging station makes the hybrid buses an advantageous alternative for replacing the classic buses, with the proviso that they are also equipped with thermal engines which produce a quantity of pollutant emissions and it consumes fuel.

The fact that hybrid buses have a thermal engine with a cylindrical capacity lower than that of a classic bus and being equipped also with an electric motor which can function independently or together with the thermal engine, makes this bus model 30 % more advantageous that the classic bus from the point of view of consumed energy resources, and the pollutant emissions can be diminished with up to 35 % [3].

The reductions of pollutant emissions of hybrid buses vary according to the limit to which the thermal engine is used. This depends on the selected route and is affected by aspects such as route topography, traffic and driver efficiency. Much greater savings can be reached in urban environments due to the frequent change of gears.

The advantages of buses equipped with hybrid drive systems are as follows [3]:

- the reduction of pollutant emissions (CO, NO_x, HC, PM, CO_2 etc.) compared to buses equipped with classic drive systems and the elimination of the exposure to these emissions of the passengers and pedestrians;
- the reduction of pollutant emissions which have a negative impact on the surfaces of historic buildings;
- the reduction of vibrations generated by classic engines which are harmful to the infrastructure and the historical buildings from the central areas;
- the assurance of a higher comfort for passengers and traffic participants by lack of vibrations generated by high capacity thermal engines;
- the possibility of creating new central zones in cities with a lower pollution level;
- lower maintenance costs due to the reduction of systems which are specific to classic engines;
- lower exploitations costs due to the price of electric energy which is lower compared to classic fuel, according to traveled distances.

The disadvantages of buses equipped with hybrid drive systems are as follows [3]:

- the lower temperatures during the cold season affect the storage capacities of batteries, but also their recharge time, fact which limits the traveled distance and extends the recharge time;
- hybrid drive systems have a superior autonomy, being independent in relation to the existence of electric recharge stations because of the possibility of recharge with the help of thermal engines, fact which leads to an increase of pollutant emissions;
- diminished transport capacity due to the mass of the batteries which equip these models of buses;

- the use of hybrid buses requires investments in acquiring new battery charging stations located at the ends of public transportation routes, through inductive recharge stations of multiple stations for fast recharge;
- the necessity of investments for new constructions;
- the necessity of special equipment to maintain hybrid buses;
- the necessity of instruction for technical personnel and drivers in order to adequately use the hybrid buses;
- the acquisition price for hybrid buses is higher than the price of classic buses.

8.4   Results for Buses Equipped with an Electric Drive System

Electric buses have a transport capacity of 70 passengers, as opposed to 95 passengers which is the capacity for classic and hybrid buses and they are the most expensive and they have a limited autonomy, because a fully recharged battery can make the bus run for a maximum distance of 250 km [3].

The advantage of electric buses is that they are non-polluting (zero local emissions) and are eligible to being financed by non-refundable European funds. The autonomy may be increased through intermediary charges at the ends of routes, assured by charging stations, and the cost for the life cycle is lower for an electric bus, finally resulting in a decrease in the initial investment cost.

The advantages of electric buses with fixed charging stations located at the ends of the route are as follows [3]:

- zero local pollution (zero locally produced emissions);
- superior efficiency of electric motors (>90 %) compared to the efficiency of thermal engines ($\sim$30 %);
- the capacity of electric motors of functioning as a generator in the braking periods and the energy produced being stocked in the batteries, thus increasing the total efficiency of the system;
- the possibility of fast charging the batteries with a capacity able to assure a minimal autonomy for traveling certain route;
- a reduced initial investment necessary for creating the fast charging stations due to the possibility of using the existing infrastructure and due to the fact that the autonomy can be extended limitlessly through partial charges between traveled tours;
- the flexibility of the system in relation to the adaptation to the existing public transport network.

The disadvantages of electric buses with fixed charging stations located at the ends of the route are as follows [3]:

- reduced autonomy in the case of any malfunctions in the intermediary charging stations;
- the complexity of the electric system of the bus due to the dual charging system composed of the fast charging system and the slow charging system;
- the necessity of assuring a temperature difference for the batteries within the limits −5 to +25 °C in order to assure an optimal functioning.

From the data presented from the public transportation companies which have tested this model [5], it result that electric buses are with approximately 20 % more economical in regards to energy consumption, compared to classic buses, and from the point of view of the cost per life cycle they are only approximately 5 % more expensive than buses using diesel fuel. Although as initial price the electric buses are twice more expensive than classic buses, their acquisition is justified as level of costs for the entire commercial exploitation period of 10 years, especially due to the fact that the acquisition of electric buses is possible through financing, based on non-refundable European funds using the environmental program.

The major advantages brought by electric buses as a solution for public transport, especially in major urban agglomerations, are from the point of view of the environment and the economy. The environmental advantages consist in the fact that electric busses are completely non-polluting, have zero local emissions of CO_2, but also a reduced noise level compared to buses equipped with thermal engines. The batteries equipping the electric buses are 100 % recyclable, without toxic electrolytes and heavy metals. The economy related advantages consist of the fact that the electric motor assures important savings from operational costs—both for fuel (the electric energy is much cheaper than classic fuels) and for periodic maintenance costs. The total savings, calculated for using an electric bus rather than a classic bus for a life span of 10 years, is of approximately 330,000 € for one single bus. After another 2 years of usage, the total saving increase to approximately 580,000 € for one bus. This sum results for gathering all costs (acquisitions price, periodic maintenance costs, respectively the fuel cost) [3].

In conclusion, following the detailed comparative analyses, the buses with electric drive stay within the parameters of total reduction of local CO_2 emissions, but also within the limits of other emission parameters, as opposed to the bus equipped with an internal combustion engine.

The increase in autonomy in the case of electric buses requires the installation of batteries with bigger energy capacity, but whom also have a corresponding volume. The diminution of this volume has as direct result the reduction of bus autonomy and implicitly the periodic recharge of its batteries.

The assurance of electric energy while in the work graphic requires a fast charge (5–10 min), and during the night a slow charge (4–6 h) of multiple electric buses at the same time.

For the bus routes studied in this book, it is necessary to use two charging stations located at the last station of the routes and having two charging systems, namely:

- fast charge during the day, for which will be used the infrastructure of the trolleybuses overlapping the studied routes, by utilizing the existing infrastructure and creating derivations from it to fast charge the buses with the help of a pantograph from the 750 V network;
- slow charge during the night, by arranging a system of three-phase outlets for connecting to the 400 V network;
- stations for complete charge from the 750 and 400 V networks.

The usage of all three types of charging stations overlapping the infrastructure specific to public transportation for Cluj-Napoca municipality has the following advantages:

- the use of the existing infrastructure (the trolleybus network) for charging during the day and during the night;
- the medium value of the electric power installed on the batteries and implicitly a reduced volume for the batteries as compared to the other alternatives, but without lowering the bus autonomy under 50–70 km, which represents a sufficient distance for traveling twice or three times the selected routes without needing to recharge the batteries;
- the reduced quantity of batteries contributing to the diminution of recharging times and to the diminution of replacements costs for them, at the end of their life cycle.

Another advantage of using all three types of charging stations exists due to the dual module of fast and slow recharge with the help of a pantograph or a three-phase outlet, a system which allows the adjustment of the charging module to the specifics of the existing infrastructure. This type of periodic charge for a short period of time allows the functioning of the bus permanently during the entire work period. By charging during the night, the buses can use electric energy at a lower price compared to the one for charging during the day, when signing a contract with the power supply provider for a differential price between day and night [3].

For the design and creation of a system with charging stations it is necessary to make an analysis based on the following parameters:

- the medium time of traveling the distance between two stations which for a bus varies between 2 and 5 min due to traffic conditions. This time interval can suffer modifications especially in a central zone of the city during intense traffic hours or in the case of unforeseen events (traffic jams, accidents etc.);
- the operating mode in the case of functioning during the day and being stationary for recharging during the night, in order to charge the batteries to full capacity during the night in the station from the end of the route to be able to assure the bus with an autonomy of 50–70 km;
- fast charge of the bus for approximately 5–10 min in order to avoid the situation in which it would run out of electric energy.

Thus, the bus travels the route with batteries loaded to maximum capacity, reducing the risks of running out of energy when it is stuck in traffic for a longer

period of time due to unforeseen situations. This type of operation correlated with successive charges allows the bus to function 24 h a day, 7 days a week.

While the bus functions, the energy flow is transmitted from the batteries to the control and command elements, and then towards the electric machinery which makes the conversion of electric energy to mechanical energy with an efficiency of over 90 %. The thus obtained mechanical energy is transmitted to the motor wheels via the mechanical transmission elements.

The bus autonomy of 50–70 km is assured by the energy stocked in the batteries to which is added the energy recovered during braking periods. The quantity of energy recovered through braking depends on many factors: route topography, braking period, the behavior of the bus driver etc.

The periodic charging and permanent functioning with batteries loaded to an almost maximum capacity allows the functioning of auxiliary systems (ventilation and heating) to optimum parameters in order to assure passenger comfort, no matter the traffic conditions.

For the charging during the day (fast charging) a pantograph system is used which is connected to the continuous current network assured either by a dedicated charging station, or by using the existing electric network for trolleybus lines.

On the other hand, during the night one can choose from the fast charging method using a pantograph or the slow charging method (for an interval of 4–6 h) by connecting the bus to a three-phase system of 400 V. The slow charging method allows a parallel charging of up to five buses in each charging station located at the end of the route.

To eliminate the risks of running out of electric energy in situations such as long period traffic jams when the auxiliary systems run (heating, ventilation, light etc.), the electric buses can be equipped with additional energy systems.

The first version implies the use of a group consisting of a classic engine and an electric generator of 30 kW which would assure the quantity of electric energy necessary for the bus to travel the distance from the end of the route to the charging zone. This solution transforms the bus into an electric vehicle with Range Extender, which is a superior travel autonomy, but it becomes a vehicle which pollutes while the classic engine is running.

A much simpler version and which completely eliminates any source of pollution, implies the use of additional batteries in two constructive options:

- The supplementary battery is separated from the main energy source and it is maintained at a maximum charge level. It is then introduced in the power supply circuit of the drive system of the bus in the case in which the main battery cannot assure the necessary electric energy due to a technical failure or a fast discharge. The supplementary battery needs an installed power of up to 15 kW in order to assure a bus autonomy of up to 10 km, necessary to arrive to a route end.
- The supplementary battery is integrated in the main battery. By using one single battery, the connection elements between the two distinct sources and the drive system, but also the operations necessary for maintaining the supplementary

battery (periodic charge/discharge) are eliminated. In this option the electric bus will have a superior autonomy without having the backup energy only in the case of damage. The technical efficiency indicates that this option is one of the best solutions for equipping an electric bus with an autonomy of 50–70 km, no matter the traffic and weather conditions.

The zone and placement of the proposed routes were selected from the routes of the local transport system of Cluj-Napoca municipality, which have been studied in this book. For the charging stations, the following places have been selected as emplacements for regular charging and daily use:

- the route end for 27, 28 and 30 in Grigorescu neighborhood;
- the route end for 30 on Aurel Vlaicu Street.

Regarding route 32, it is considered one with a reduced length and with a road configuration of great altitude differences, thus it was not opted to include a charging station at the end of this route in this book.

Considering a consumption of 1–1.5 kWh/km for a route with the length of approximately 15 km, the electric energy consumed by a bus will come to 20–25 kWh. Depending on the route length, it is possible to choose to charge the electric bus at the two ends of the route or just at one end, for the routes with a smaller length. For longer routes two charging stations may be necessary (at both ends of the route), which will assure the functioning of the buses during working hours (fast charge), but also during the night [3].

If the routes 27, 28 and 30 are taken into consideration in the exploitation of electric buses, two charging stations are requires, namely one in Grigorescu neighborhood at the end of the above listed routes and one at the end of route 30, in Mărăşti neighborhood, and for the maintenance activities one stations is required at the trolleybus depot.

Due to the fact that in Cluj-Napoca municipality there is an extended network as electric energy supply for trolleybuses, at a voltage of 750 V, the fast charging of 5–10 min of electric buses through a pantograph which can be connected to this supply system is considered feasible.

The connection of the electric bus to the pantograph supply system allows it to function as the trolleybus, in the case in which it adapts to the connecting system for the electric network identically to the system equipped on trolleybuses for the portions of route where the respective infrastructure exists. In this time interval the bus can absorb the electric energy necessary for travelling, but also for recharging the batteries, thus increasing the bus autonomy.

In the case of stations where there is trolleybus supply infrastructure, and in order to not influence their functioning, a derivation of the electric network will be made which will be used only for fast charging the electric buses.

The charging in a short time interval can also be made by using high power three-phase outlets (400 V–125 A, respectively 400 V–250 A). This solution has several advantages: it reduces the acquisition costs of the buses (lack of pantograph), it reduces the costs for arranging the charging stations (because the

connection to a cable with a three-phase outlet is enough), and the driver of the bus does not need to park within a certain perimeter because the charging can be made at a nominal voltage of the electric network without having to need converters and electrical transformers, but it also has a major disadvantage because the driver or another person has to connect the supply cable to the bus. The charging power of the electric bus batteries for the 125 A outlet is of 85 kW, which implies that a charging of the batteries at a value of 20 kWh can be made in an interval of 15 min [6].

The most feasible choice for fast charging is the pantograph charging option, which if overlapped over the specific of the public transportation of Cluj-Napoca municipality would become the option which offers an increased autonomy for electric buses in both kilometers and charging possibilities. The fast charging stations consist of derivations of existing trolleybus routes or of the building of one such conformation (which is for the charging stations from Grigorescu neighborhood). These charging stations must be located so as to not affect the circulation of the trolleybuses.

Fast charging with a pantograph system is made as follows: the electric bus will be redirected, with the help of visible driver demarcations, under the two electric supply lines. After the bus stops, the driver commands the rising of the pantograph which will make an electric connection with the two supply lines. After the contact was made, conditioned by the presence of voltage, then the battery charging starts automatically. When the driver wishes to interrupt the charging, he will push the decoupling button which will stop the charging process and the pantograph will be lowered, and the electric bus is ready for departure.

During the night when regularly the electric buses are not used, they can be fully charged via slow charging stations, equipped with three-phase outlets (400 V–32 A or 400 V–63 A) of lower power, which charge the batteries during a longer time interval (4–6 h).

Assuring the necessary conditions for maintenance operations implies creating a charging stations in the zone where these operations take place. Because this type of station is only used for periodical technical maintenance operations, it is sufficient for assuring the possibilities of slow charging the buses in a 4–6 h time intervals, but with the possibility of later upgrading it to a fast-charging regime also.

Slow charging stations consist of a reinforced concrete foundations arranged so as to assure the access of operating personnel around the buses and slow charging equipment.

The slow charging in route end charging stations is made as follows: the electric bus is redirected, with the help of visible driver demarcations, close to the three-phase charging outlet. The driver or another person instructed in using the charging station will connect the plug from the three-phase outlet mounted on the bus body and the charging process will start automatically. The plug will be retracted from the three-phase outlet after the battery of the electric bus is fully charged.

The charging with electric energy of the fast and slow charging stations is made using a three-phased system with the following parameters: phase voltage 230 V,

line voltage 400 V, voltage frequency 50 Hz. For slow charging a 750 V voltage is necessary, which is obtained from using a three-phase voltage amplifier transformer and uncontrolled diode rectifier. Slow charging is made via three-phase outlets connected to the supply system through cables.

A more energetically efficient solution can be made by connecting the charging station to a three-phase supply system of 6–20 kV, and then via a transformer with secondary windings (one with a 400 V nominal voltage and the other with a 560 V nominal voltage) the voltages necessary for the slow and fast charging system are obtained.

Another constructive option implies the elimination of the transformer and the charging of the electric bus with a continuous 560 V voltage. This option requires the use of an uncontrolled three-phase rectifier in the charging station. The electric bus must be equipped in this case with a power supply system (150 kW) which runs at supply voltage values between 500 and 1000 V.

According to European norms in effect all equipment used for charging the bus must meet the following standards in the field: IEC 61851-22 (for alternative current) and IEC 61851-23 (for continuous current) [7].

The charging time for an electric bus is of maximum 10 min for fast charging, taking into consideration that stocking the volume of necessary energy of 15–25 kWh, respectively of maximum 4–6 h for slow charging, depending on the state of charge of the batteries at the starting point of the charging process.

The fast charging system can serve one bus at once, but the slow charging system allows the charging of five buses simultaneously.

In order to assure the energy transfer necessary for fast charging the electric buses in a time interval which does not exceed 10 min, the power installed for each of the two fast charging stations must be lower than 150 kW (which allows the transfer of an energy volume of 25 kWh in 10 min).

The energy necessary for charging the batteries of an electric bus can also be obtained from renewable energy sources. Photovoltaic panels offer the fastest amortization of investment, especially if they are installed in urban areas.

In the case of using photovoltaic panels for a power installed of the fast charging station of 150 kW, it would be necessary to use photovoltaic panels with a surface of approximately 1000 m^2, because the energy conversion efficiency is around the value 15 %, and the solar energy per surface unit is approximately 1000 W/m^2. The flat surface on which the photovoltaic panels must be installed at an optimal angle of 45° in order to not provide shade to one another, is of approximately 3000–4000 m^2. If this surface has an inclination towards the south, with an angle as wide as possible (30–45 grade), the installation surface does not exceed 1500 m^2 [3].

In order to provide electric energy from photovoltaic sources to the charging stations in any moment, this energy must be stocked given the variability of periods with sunny weather and of the incidence angle of the solar radiation on the panels.

But the 150 kW power can only be obtained in ideal conditions when the weather is sunny and the solar radiation incidence is maximum on the panels. The

energy quantity estimated to be produced with photovoltaic panels for a 150 kW power is of 180 MWh during a calendar year.

The medium energy consumed by an electric bus during a year is of approximately 63 MWh (taking into consideration the daily necessary energy quantity of 200 kWh). Using this supply system, three electric buses can be powered from photovoltaic panels, considering there is an electric energy stocking capacity which can also be made using batteries.

For all the 10 electric buses to be fueled with renewable energy from photovoltaic panels, an installed power of approximately 600 kW is necessary. This implies a flat surface of 12,000–16,000 m^2 or an inclined surface of approximately 6000 m^2 [3].

References

1. Regulation (EC) No 595/2009 of the European Parliament and of the Council of 18 June 2009 on type-approval of motor vehicles and engines with respect to emissions from heavy duty vehicles (EURO 6) and on access to vehicle repair and maintenance information and amending Regulation (EC) No 715/2007 and Directive 2007/46/EC and repealing Directives 80/1269/EEC, 2005/55/EC and 2005/78/EC. Retrieved March 11, 2016, from http://eur-lex.europa.eu/legal-content/EN/ALL/?uri=CELEX%3A32009R0595.
2. Regulation (EU) No 582/2011 of 25 May 2011 implementing and amending Regulation (EC) No 595/2009 of the European Parliament and of the Council with respect to emissions from heavy duty vehicles (EURO 6) and amending Annexes I and III to Directive 2007/46/EC of the European Parliament and of the Council. Retrieved March 11, 2016, from http://eur-lex.europa.eu/legal-content/EN/TXT/?uri=CELEX%3A32011R0582.
3. Varga, B. O. (2015). Energy efficiency of vehicles equipped with hybrid or electrical powertrain for urban public transport (in Romanian). Habilitation thesis, Technical University of Cluj-Napoca, Romania, 18th of September 2015.
4. Regulation (EC) No 443/2009 of the European Parliament and of the Council of 23 April 2009 setting emission performance standards for new passenger cars as part of the Community's integrated approach to reduce CO_2 emissions from light-duty vehicles. Retrieved March 11, 2016, from http://eur-lex.europa.eu/legal-content/EN/TXT/?uri=URISERV%3Ami0046.
5. Retrieved December 21, 2015, from http://www.urtp.ro/library/2014-11/2/8._stefano-albarosa_aic_romania.pdf.
6. Retrieved December 21, 2015, from http://www.techandfacts.com/busbaar-v3-supercharger-station-for-city-bus/.
7. Economic Commission for Europe. (2014). Proposal for an Electric Vehicle Regulatory Reference Guide, ECE/TRANS/WP.29/GRPE/2014/13. Retrieved March 11, 2015, from https://www.unece.org/fileadmin/DAM/trans/doc/2014/wp29grpe/ECE-TRANS-WP29-GRPE-2014-13e.pdf.

Chapter 9
Conclusions

At the EU level, a great quantity of the greenhouse gases (GHG) come from internal combustion engines equipping vehicles within the general transport system (cargo and passengers). It is estimated that annually a vehicle emits into the atmosphere a CO_2 quantity with a mass four times larger than its own mass. The dependence of the transport sector on fossil fuels is the most acute compared to other domains, from which results the degree of pollution that this sector has.

The implementation and use of a public transport system based on hybrid and electric buses can directly and efficiently contribute to maintaining and improving the qualitative parameters of the environment, by reducing the air pollution and the level of noise and vibrations.

For the particular case described in this book (Cluj-Napoca municipality, Romania) the legal norms in force establish the evaluation and management of the environmental noise level at an afferent value for road traffic noise of 50 dB (A). The conducted studies place the noise level afferent to passenger transportation vehicle presently composing the local urban transport system to be at a level between 60 and 95 dB (A), well above the level established by the law.

The introduction of hybrid and electric drive systems has the particularity of respecting the regulations regarding the EURO 6 pollution norms which stipulate the reduction of up to 50 % of the pollutant emissions level measured for the following pollutants: carbon dioxide (CO_2), hydrocarbons (HC), methane (CH_4), nitrogen oxides (NO_x) and particulate matter (PM).

The hybrid drive systems respect these indicators and remain within the limitations imposed by the EURO 6 pollution norms, while for the electric drive systems all the indicators mentioned above have the value 0 (as local emission).

A major determinant factor in choosing a traction energy source equipping a transport vehicle is given by the priority regarding environmental performances. The transport by bus is a significant factor contributing to local pollution of the environment in European cities, mainly because of low velocities and inappropriate exploitation regimes of energetic sources (in the case of internal combustion engines). Where air pollution is a major issue, the city can prioritize by choosing the

bus based on emissions of de NO_x and particulates, as opposed to energetic efficiency or performances regarding specific CO_2 emissions. Some authorities can have/introduce some strict missions in reducing CO_2 emissions which would favor the options for alternative vehicles and others can target accomplishing an air pollution reduction, both locally and globally.

From the point of view of the research methodology presented in this book and with the help of IPG TruckMaker application options, some control actions were defined, similar to those of a human driver for a virtual vehicle (Virtual Driver) through a mathematical model. The IPG TruckMaker application has achieved the integration of a virtual vehicle on a virtual road and has assured its control by a virtual driver. Thus a VVE (Virtual Vehicle Environment) was created to test vehicles in real time.

As outcome results the following were pursued: improving the performances of hybrid and electric vehicles, optimizing the distribution of energetic flows, reducing fuel consumption and pollutant emissions, goals aimed by all great manufacturers in the automotive industry, having as main objective the reach of a working economic pole. These objectives can be reached through an efficient management of intelligent systems controlling and coordinating the processes and phenomena taking place in functioning vehicles with hybrid and electric drive. The management of energy provided by a running internal combustion engine, respectively an electric motor, but also by controlling the choice of type of propulsion was made by efficiently using the electronic control units, which compared to classic vehicles have the double role of controlling and coordinating the energy generated by the two drive systems.

In order to make a comparative evaluation of energetic flows for the three types of drive systems (classic, hybrid and electric), the four routes selected to be used by CTP Cluj-Napoca for urban passenger transport were generated through digitization.

The computer simulation through which the three studied bus models were evaluated offers a series of advantages, namely: the reduction of costs for building a model, the possibility of modifying the structure of the model in any step of the project, the possibility of evaluating the functioning of the models on the selected routes in real time and of adapting the model characteristics at the requests imposed in a short time interval.

The virtual roads used in parameterized computer simulations with the help of the AVL Road Importer application have been digitized in formats compatible with the applications used for computer simulations, and these routes have been implemented in the IPG TruckMaker application in order to define real traffic conditions, namely: atmospheric conditions, geometry of the routes, particularities of the routes, road particularities, respectively the particularities of road adjacent areas.

The simulation processes through which the studied bus models have been evaluated offer a series of advantages, namely: the reduction of costs for building a model, the possibility of modifying the structure of the model in any step of the project and the possibility of adapting the model characteristics at the requests imposed in a short time interval.

In order to achieve the evaluation of energetic flows for the three types of drive systems (classic, hybrid and electric) the four routes selected to be used by CTP Cluj-Napoca for urban passenger transport were generated through digitization.

The computer simulation through which the three studied bus models were evaluated offers a series of advantages, namely: the reduction of costs for building a model, the possibility of modifying the structure of the model in any step of the project, the possibility of evaluating the functioning of the models on the selected routes in real time and of adapting the model characteristics at the requests imposed in a short time interval.

As a result from the performed studies and researches, it was found that the reduction of emissions generated by electric vehicles depends on the way in which the electric energy is produced and it can be of 30 % in the case of using electricity from the national network, or of 100 % in the case of generating energy from renewable electricity sources.

The analysis of hybrid and electric vehicles from the point of view of energy consumption was made through the analysis of average operating point, a quasi-static method which involves a dynamic modeling of the studied model. For this method, the requests and restrictions of the model have been determined, and then the components of the system have been designed. The numerical simulation, through the used methodology, helped the optimization of performances of the studied hybrid and electric vehicles.

According to the results obtained from computer simulations, one can observe that from the point of view of the pollutant emissions of the studies bus models, the following particularities are drawn/exist:

- The elimination of pollutant emissions obtained from the combustion process of the internal combustion engines is made near the ground, fact which leads to high concentrations at low heights;
- The elimination of pollutant emissions in the atmosphere is made on the entire surface of the locality (urban areas crossed by routes of the transport system), the concentration differences depending mostly on the intensity of parameters and factors of characterizing the road traffic dynamics.

The introduction of hybrid and electric drive systems has the particularity of respecting the regulations regarding the EURO 6 pollution norms which stipulate the reduction of up to 50 % of the pollutant emissions level measured for the following pollutants: carbon dioxide (CO_2), hydrocarbons (HC), methane (CH_4), nitrogen oxides (NO_x) and particulate matter (PM).

The implementation of the new drive system proposed in this book offers a tendency of increase in common transportation dynamic, in comparison with the individual transport based on personal vehicles, which in an urban agglomeration contributes to maintaining and improving the qualitative parameters of the state of the environment, by reducing air pollution, respectively by minimizing the greenhouse gas emissions, especially CO_2 emissions.

From the perspective of diverse economic sectors of the European Union, the generation of electric energy is responsible for 37 % of the total CO_2 emissions, the transport activities for 28 %, household activities for 16 %, and services for 5 %.

In the case of urban passenger transport it is necessary that one of the solutions for reducing greenhouse gas emissions to be replacing the vehicles using conventional fuel with vehicles with hybrid and electric drive. The simulation of operation according to particular conditions within a virtual environment to offer immediate future premises, of some constructive adaptations which are intelligent and efficient from the point of view of acquisition and operating costs in the general and integrated system of the urban transportations system. The development of some advanced hybrid and electric drive systems, corroborated with the design, the development and/or the identification of a road infrastructure feasible for the proposed goal, increases the value of urban public transport and guides the society towards a modern and sustainable solution for mobility, compatible with the present demands regarding environment protection.